Development of Iron-Catalyzed Enantioselective Carbon–Carbon Bond Forming Reactions for Efficient Access to Bioactive Compounds and Their Derivatives

Masayoshi Jin

2021

CONTENTS

Abbreviations

acac	acetylacetonate
AFIR	artificial force induced reaction
BINAP	2,2'-bis(diphenylphosphino)-1,1'-binaphthyl
Bn	benzyl
Boc	*tert*-butoxycarbonyl
^{i}Bu	isobutyl
^{t}Bu	*tert*-butyl
cod	1,5-cyclooctadiene
DFT	density functional theory
DME	1,2-dimethoxyethane
DMPU	*N*,*N*'-dimethylpropyleneurea
dppbz	1,2-bis(diphenylphosphino)benzene
ee	enantiomeric excess
eq	equation
equiv	equivalent
er	enantiomer ratio
Et	ethyl
GC	gas chromatography
IR	infrared
KHMDS	potassium bis(trimethylsilyl)amide
LiHMDS	lithium bis(trimethylsilyl)amide
Me	methyl
MOM	methoxymethyl
MTBE	methyl *tert*-butyl ether
NaHMDS	sodium bis(trimethylsilyl)amide
NMP	*N*-methylpyrrolidinone
NMR	nuclear magnetic resonance
OMs	methanesulfonyl
OTf	trifluoromethanesulfonyl
OTs	*p*-toluenesulfonyl
^{i}Pr	isopropyl
Ph	phenyl
PMB	4-methoxybenzyl
TBAT	tetrabutylammonium difluorotriphenylsilicate
TBDPS	*tert*-butyldiphenylsilyl
TBS	*tert*-butyldimethylsilyl
TFA	trifluoroacetic acid
THF	tetrahydrofuran
TIPS	triisopropylsilyl
TMEDA	*N*,*N*,*N*',*N*'-tetramethylethane-1,2-diamine
tol-BINAP	2,2'-bis(di-*p*-tolylphosphino)-1,1'-binaphthyl
Z	benzyloxycarbonyl
9-BBN	9-borabicyclo[3.3.1]nonane

GENERAL INTRODUCTION

1. Synthesis of enantiopure compounds

All the lives on the earth consist of only one of the pairs of enantiomers, such as L-amino acids and D-sugars, known as "biological homochirality". Due to this biological homochirality, a pair of enantiomers can have different effects on lives including human beings. Figure 1 shows some examples of a severe adverse effect caused by the other enantiomer of the medicinal compound: (*S*)-naproxen is used as an anti-inflammatory drug, but (*R*)-naproxen is reported as a liver toxin;[1] While (*S*,*S*)-ethambutol is an antibiotic used for tuberculosis therapy, (*R*,*R*)-ethambutol causes blindness.[2]

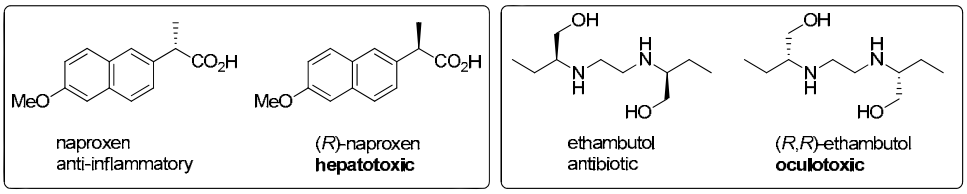

Figure 1. Difference of bioactivities between a pair of enantiomers.

In order to deliver an expected therapeutic effect, a number of enantiopure drugs are widely used for medication, such as rivaroxaban (anticoagulant), sitagliptin (antidiabetic), and pregabalin (analgesic), just to name a few as shown in Figure 2.

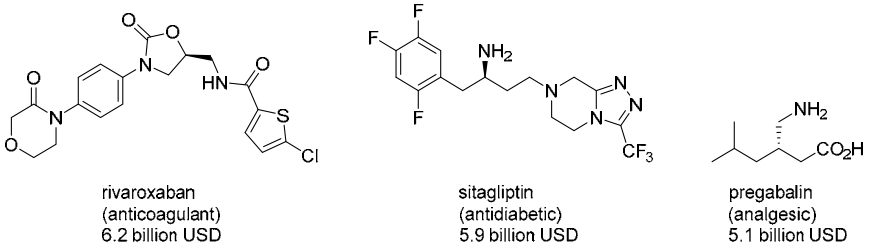

Figure 2. Top selling enantiopure drugs (2017).

The enantioselective manufacturing of these chiral medicines is essential from the patient protection perspective since the other enantiomer of these medicinal compounds has no medicinal effect or, what is worse, a severe adverse effect. Therefore, providing enantiopure medicinal compounds is not only the health authorities' demands but also the social demands, and hence the enantioselective manufacturing is now performed on a commercial scale. The methodologies to prepare enantiopure compounds are classified into three categories: (1) Chiral pool synthesis: using chiral building blocks,

which are generally sourced from natural products; (2) Chiral resolution: racemic products are separated by crystallization, chromatography, etc., and; (3) Enantioselective synthesis: a chiral center is constructed by the aid of a stoichiometric amount of a chiral auxiliary or a chiral catalyst. All the methodologies are practical and applied to the commercial productions, but one of the most efficient methods to construct the chiral center is the catalytic enantioselective synthesis because: a) a catalytic amount of chiral compounds is needed while other methods require a stoichiometric amount or an excess amount of chiral compounds, and b) both pair of enantiomers can be generally prepared with the catalytic enantioselective synthesis but other methods (especially the chiral pool synthesis) can provide only one of a pair of the enantiomers.

Catalytic enantioselective carbon-carbon bond formation reactions are not only of academic interest but also of industrial importance because simultaneous construction of molecular framework and chirality are possible. The catalytic enantioselective carbon-carbon bond formation reactions are, therefore, extensively examined to date, and a number of conjugate addition reactions,[3] allylic alkylation reactions,[4] arylation reactions,[5] carbometalation reactions, cross-coupling reactions, etc. are reported using palladium, rhodium and other transition metal catalysts.[6] Although these transition metal catalysts are a powerful tool to construct molecules in an enantioselective manner, disadvantages from the pharmaceutical industries' perspective are: (a) heavy metal toxicity,[7] (b) difficulties to remove those heavy metals from the desired product[8] and (c) high cost due to the rarity of those metals.

The use of the iron catalyst can solve these problems because of its low toxicity and low cost, but only one example is known as an enantioselective carbon-carbon bond formation reaction catalyzed by iron[9] due to the difficulty in controlling the reactivity. In this dissertation are described the iron-catalyzed enantioselective carbometalation reactions and cross-coupling reactions, and synthesis of optically active medicines and bioactive compounds with these reactions.

2. Transition Metal-Catalyzed Enantioselective Carbometalation

2-1. Transition Metal-Catalyzed Carbometalation

The carbometalation reactions of alkenes and alkynes are synthetically very useful transformations because simultaneous constructions of carbon-carbon bond and carbon-metal bond formation are achievable. The resulted organometallic compounds can be utilized to further transformations such as cross-coupling reactions, nucleophilic additions, halogenations, and other carbon-carbon or carbon-heteroatom bond formation reactions. Transition metal catalysts can accelerate these carbometalation reactions, and a variety of alkenes and alkynes including less reactive substrates are used for these reactions.[10]

2-2. Enantioselective Carbometalation Reactions Producing Non-Organometallic Products

The first enantioselective carbometalation reactions catalyzed by a transition metal was reported by Hoveyda.[11] Highly enantioselective carbometalation reactions of cyclic alkenes with alkyl Grignard reagents were achieved by the aid of chiral zirconocene catalyst **1**, giving ring-opening products (Figure 3). The limitation of this reaction lays in the quick β-oxygen (or β-nitrogen) elimination from the organomagnesium intermediate: no further transformations can be performed using the reactive carbon-metal bond.

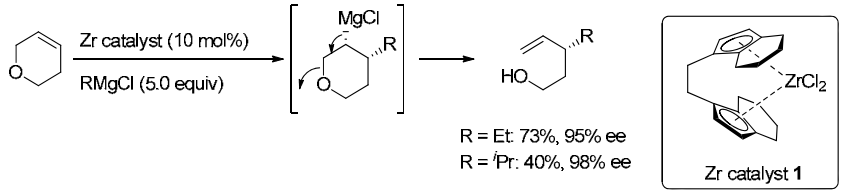

Figure 3. First example of the transition metal-catalyzed enantioselective carbometalation.

Lautens reported the first enantioselective carbometalation reactions of oxabicyclic alkenes by the aid of the catalytic amounts of palladium and tol-BINAP (Figure 4).[12] The addition of in situ generated ethylpalladium species to the cyclic alkene gives carbopalladation product, which is readily followed by the β-oxygen elimination, likely assisted by complexation to the Lewis acidic zinc, affording ring-opening products.

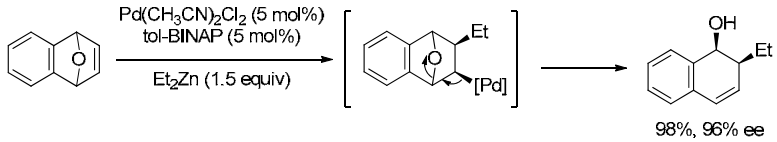

Figure 4. Palladium-catalyzed enantioselective carbometalation/ring-opening reaction.

The total synthesis of ionomycin was achieved with the help of this enantioselective carbometalation/ring-opening reaction (Figure 5).[13] The palladium-catalyzed enantioselective carbometalation of azabicyclic alkenes was also developed and applied to the total synthesis of (+)-homochelidonine (Figure 6).[14]

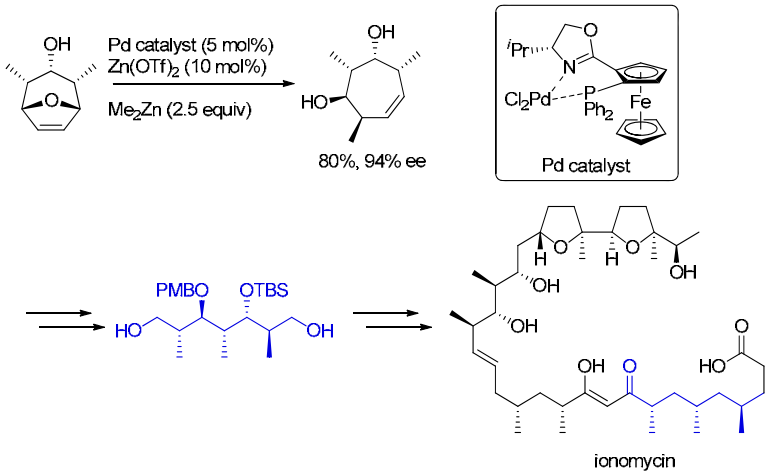

Figure 5. Total synthesis of ionomycin via palladium catalyzed enantioselective carbometalation.

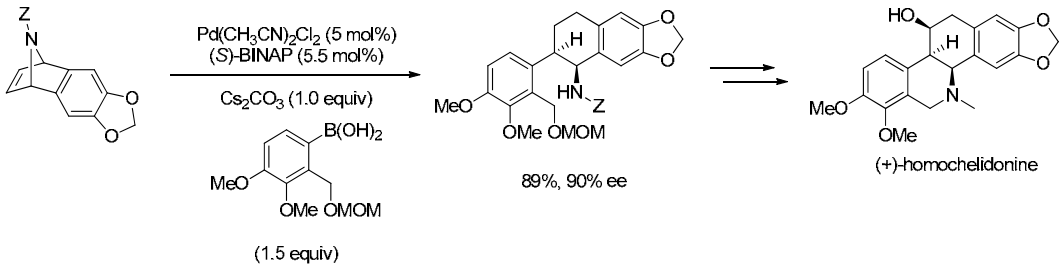

Figure 6. Total synthesis of (+)-homochelidonine via palladium catalyzed enantioselective carbometalation of azabicyclic alkene.

Rhodium-catalyzed carbometalation reactions of oxabicyclic alkenes with arylboronic acids are also reported by Lautens (Figure 7).[15] Again, ring-opening products that contain no carbon-metal bond are solely obtained.

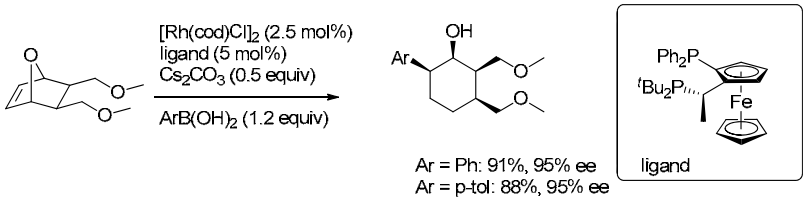

Figure 7. Rhodium-catalyzed enantioselective carbometalation.

Feringa reported copper-catalyzed reactions (Figure 8);[16] though the *syn*-products are solely obtained by the reactions with palladium and rhodium catalysts, the reactions with copper catalyst give the *anti*-products. This unique selectivity is discussed, being associated with the reaction mechanism: The initial step of these copper-catalyzed reactions is carbon-oxygen bond activation by the *anti*-attack of alkylcopper species to form the π-allyl-copper intermediate. The reductive elimination, with retention of configuration, from the intermediate gives *anti*-product.

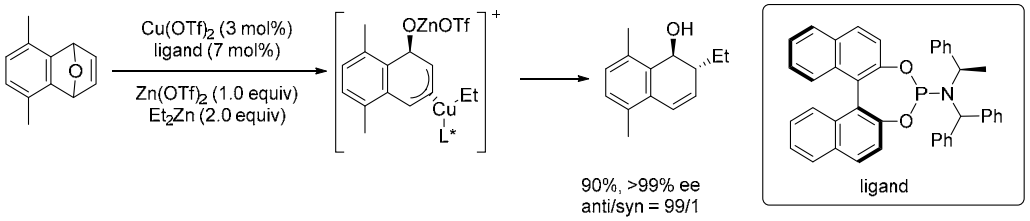

Figure 8. Copper-catalyzed enantioselective carbometalation giving *anti*-product.

2-3. Enantioselective Carbometalation Reactions Producing Organometallic Products

Negishi discovered that simple terminal alkenes can also be applied to the enantioselective carbometalation reactions by using alkylaluminum reagents instead of alkyl Grignard reagents in the presence of chiral zirconium catalyst **2**.[17] Figure 9 shows the zirconium-catalyzed asymmetric carboalumination reactions (*ZACA reaction*), which can take the full advantage of the enantioselective carbometalation reaction, that is, the formation of optically active organometallic compounds or reactive intermediates. A variety of natural products and medicinal compounds possessing multiple stereogenic carbon centers have thus been synthesized using ZACA reaction in an enantioselective manner: Figure 10 shows the examples of vitamin E,[18,19] siphonarienal,[20] siphnarienolone,[20] and fluvirucinnin A_1.[21] The total synthesis of phthioceranic acid was achieved by the combination of ZACA reaction and palladium-catalyzed cross-coupling

reaction:[22] organoaluminum intermediate **3** prepared by ZACA reaction was cross-coupled with vinyl bromide in the presence of the palladium catalyst. The resulted alkene was utilized to the second ZACA reaction, and finally, five stereogenic centers of phthioceranic acid were constructed by the ZACA reactions.

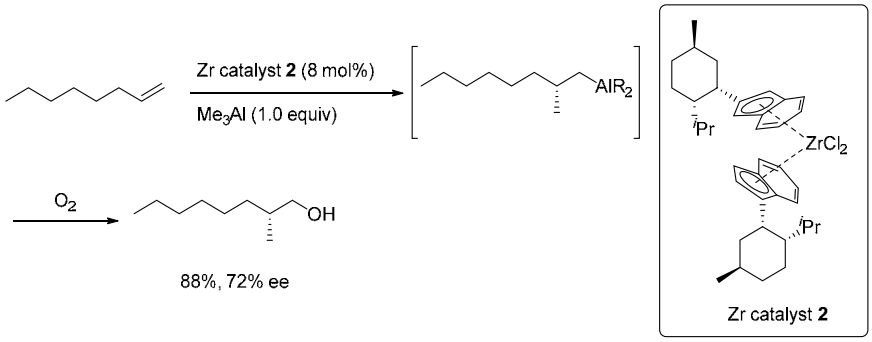

Figure 9. Zirconium-catalyzed asymmetric carboalumination reaction (ZACA reaction).

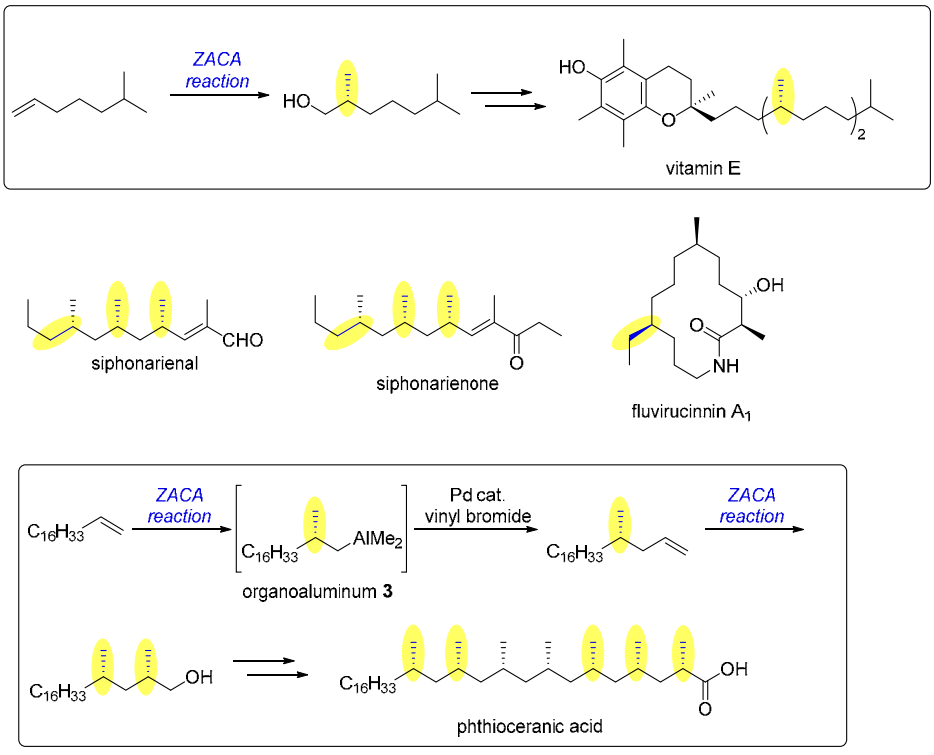

Figure 10. Bioactive compounds synthesized by using ZACA reaction (C–C bonds constructed by ZACA reaction are highlighted in yellow).

Nakamura reported the first example of the iron-catalyzed enantioselective carbometalation reactions of a dialkylzinc reagent to cyclopropene to give an optically active intermediate possessing carbon-zinc bond as shown in Figure 11.[23] It should be

noted that the presence of TMEDA, the achiral ligand, is essential for the enantioselective reactions: In the absence of TMEDA, the racemic product is obtained even though (*R*)-tol-BINAP is used as a ligand.

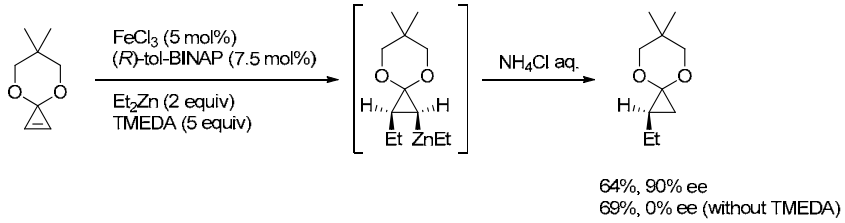

Figure 11. Iron-catalyzed enantioselective carbometalation.

3. Transition Metal-Catalyzed Enantioselective Cross-Coupling Reactions

3-1. Nickel-Catalyzed Enantioselective Cross-Coupling Reactions

Botteghi and Kumada independently reported the pioneering studies in early 1970s, where enantioselective cross-coupling reactions of alkyl Grignard reagents were performed in the presence of chiral phosphine ligand (DIOP) and nickel catalyst (Figure 12).[24] This enantioselective cross-coupling reaction proceeded along with the dynamic optical resolution of racemic secondary alkyl Grignard reagents.

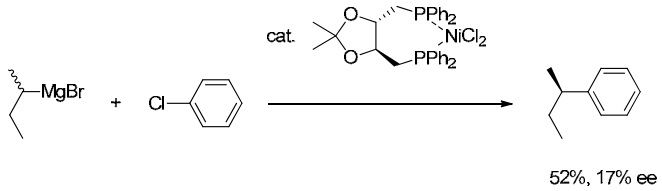

Figure 12. The first example of nickel-catalyzed enantioselective cross-coupling reaction.

After more than 30 years later since the pioneering study reported, a highly enantioselective cross-coupling reaction was developed by Fu in 2005. Using PyBOX as a chiral ligand, racemic α-bromoamides were cross-coupled with a varied alkylzinc reagents to give corresponding alkylated products with high enantioselectivity and in high yield (Figure 13).[25a–e]

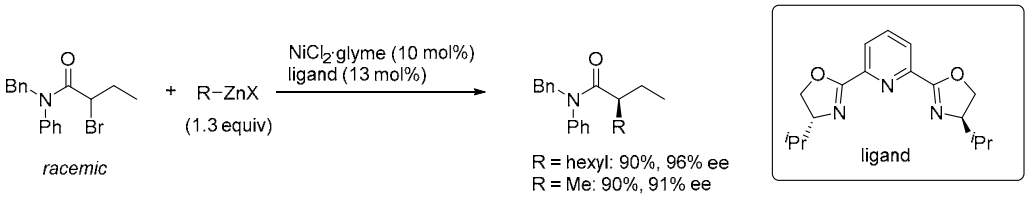

Figure 13. Highly enantioselective cross-coupling reaction catalyzed by nickel-PyBOX catalyst.

Fu and co-workers also reported a series of nickel-catalyzed asymmetric cross-coupling reactions of haloalkanes with various organometallics such as organosilicons,[25f] organoboranes[25g–i] and organomagnesiums (Figures 14, 15 and 16, respectively).[25j] The first enantioselective arylation/vinylation of alkyl halides were achieved by using organosilicons.[25f] In order to activate less-reactive organosilicons, an excess amount of TBAT, a fluoride source, is essential for the reaction. The phenolic ester of optically active products can be deprotected using cerium ammonium nitrate without losing the enantiopurity to give carboxylic acids.

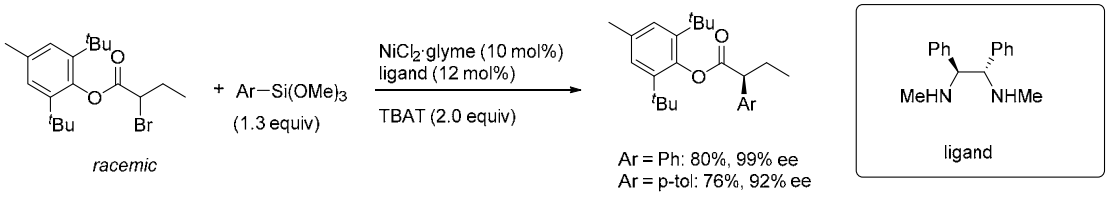

Figure 14. Enantioselective nickel-catalyzed cross-coupling reaction of organosilicons.

With the organoboranes, not only organobromides but also organochlorides can be used as an electrophile (Figure 15).[25g–i] This Suzuki-type cross-coupling requires a strong base (^{t}BuOK/^{i}BuOH) to activate the organoboranes, where base-sensitive substrates/products as shown in Figure 16 are not compatible.

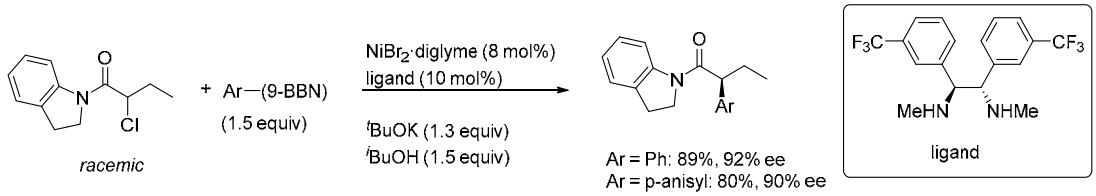

Figure 15. Enantioselective nickel-catalyzed cross-coupling reaction of organoboranes.

The cross-coupling reactions with organomagnesiums do not need any activation due to the high transmetalation ability of organomagnesiums.[25j] In addition, this enantioselective cross-coupling proceeded at low temperature (−40 °C or −60 °C), which enables the preparation of racemization-prone α-aryl ketones as shown in Figure 16.

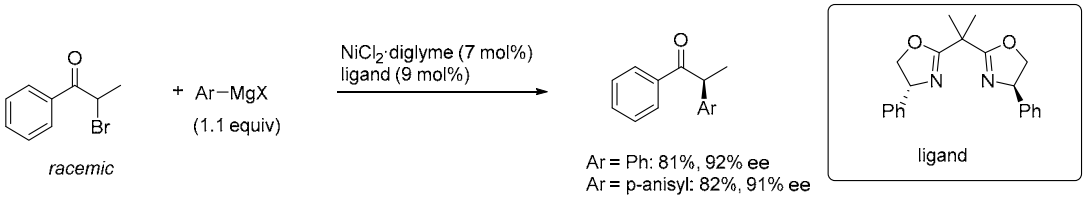

Figure 16. Enantioselective nickel-catalyzed cross-coupling reaction of organomagnesiums.

The electrophiles for these enantioselective nickel-catalyzed cross-coupling reactions are not limited to the α-halocarbonyl compounds. For instance, the bromoalkanes possessing a CF_3 group can be applied for the enantioselective cross-coupling reactions (Figure 17).[25e]

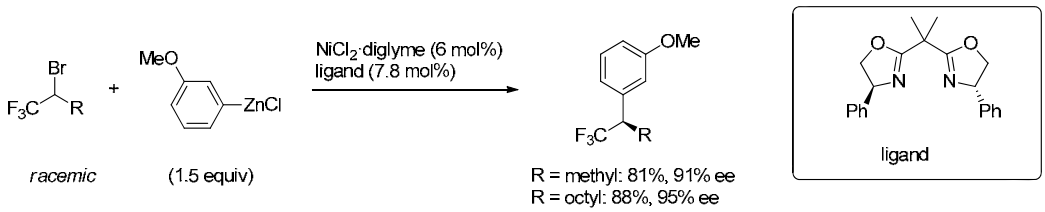

Figure 17. Enantioselective nickel-catalyzed cross-coupling reaction of bromoalkanes possessing a CF_3 group.

3-2. Cobalt-Catalyzed Enantioselective Cross-Coupling Reactions

Zhong and Bian reported the first cobalt-catalyzed enantioselective cross-coupling reactions of α-bromoesters with aryl Grignard reagents (Figure 18).[26]

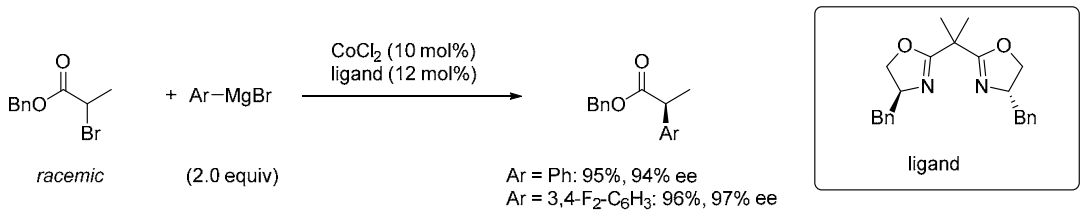

Figure 18. Enantioselective cobalt-catalyzed cross-coupling reaction of α-bromoesters.

The total synthesis of (*S*)-*ar*-turmerone, a natural product isolated from the rhizomes of *Curcuma longa*, has been accomplished with this cobalt-catalyzed reaction (Figure 19).

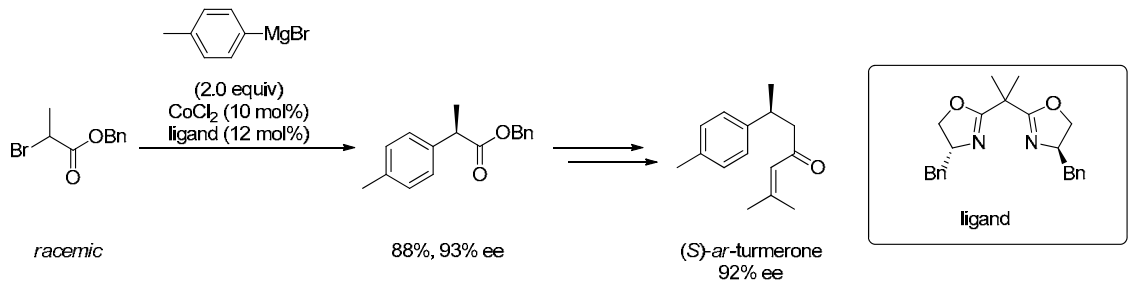

Figure 19. Total synthesis of (*S*)-*ar*-turmerone via cobalt catalyzed enantioselective cross-coupling reaction.

4. Outline of the Present Thesis

The iron-catalyzed enantioselective carbon-carbon bond formation reaction is one of the most useful reactions for the pharmaceutical and chemical industries because of the low toxicity and low cost of the iron catalysts. However, despite the remarkable progress of the cross-coupling reactions using an iron catalyst in the last decade,[27,28] only one example is known as an enantioselective carbon-carbon bond formation reaction catalyzed by iron[9] due to the difficulty in controlling the reactivity. The present thesis describes the development of novel iron-catalyzed carbon-carbon bond forming reactions (enantioselective carbometalation reactions and cross-coupling reactions) and the application of these reactions to the syntheses of optically active bioactive molecules and their derivatives.

The enantioselective carbometalation reactions are described in Chapters 1 and 2, Part 1. In Chapter 1, the iron-catalyzed enantioselective carbometalation reactions of azabicycloalkenes with arylzinc reagents with the aid of chiraphos as a chiral ligand are described. The synthesis of epibatidine derivatives (epibatidine is an alkaloid found from the frog *Epipedobates anthonyi*) is also reported. The synthesis of C_1 and C_2 symmetric chiraphos derivatives, some of which show higher enantioselectivity for the iron-catalyzed carbometalation reaction, are reported in Chapter 2. The author also reports the evaluation of these new chiraphos derivatives not only in the enantioselective iron-catalyzed carbometalation of diarylzincs to bicyclic alkenes but also in an asymmetric cationic palladium-catalyzed 1,4-addition reaction of arylboron compounds to an enone (Miyaura-Michael reaction).

The enantioselective cross-coupling reactions and related research works are described in Chapters 3–7, Part 2. The iron-catalyzed cross-coupling reactions of non-activated chloroalkanes with aryl Grignard reagents are described in Chapter 3. The method is also effective for arylating polychloroalkanes that would form byproducts under other conditions. The iron-catalyzed cross-coupling reactions of α-

bromocarboxylic acid derivatives with aryl Grignard reagents are reported in Chapter 4. This cross-coupling reaction requires a simple iron catalyst of $Fe(acac)_3$, and no ligand is necessary. In Chapter 5, the iron-catalyzed enantioselective cross-coupling reactions of α-chloroesters with aryl Grignard reagents using of BenzP* as a chiral ligand are described. The utilization of this reaction to synthesize dexibuprofen, an enantiopure nonsteroidal anti-inflammatory drug (NSAID), is also reported. The Suzuki-Miyaura variant of the enantioselective cross-coupling reactions is reported in Chapter 6. It is noteworthy that BenzP*, the best ligand for the cross-coupling reactions with aryl Grignard reagents, gave racemic product; QuinoxP* is the most suitable chiral ligand for the Suzuki-Miyaura coupling. This reaction also provides some optically active NSAIDs. The reaction mechanism of these enantioselective cross-coupling reactions is studied and reported in Chapter 7, by the help of the DFT and AFIR study.

References and notes

[1] Hart, H.; Hadad, C. M.; Craine, L. E.; Hart, D. J.; *Organic Chemistry: A Short Course 13th Edition*; Brooks Cole: Salt Lake City, **2011**. pp 147–181.
[2] Lim, S. A. *Ann. Acad. Med. Singapore* **2006**, *35*, 274–278.
[3] Córdova, A. Ed. *Catalytic Asymmetric Conjugate Reactions*; Wiley-VCH: Weinheim, **2010**.
[4] Trost, B. M.; Crawley, M. L. *Chem. Rev.* **2003**, *103*, 2921–2944.
[5] Bolm, C.; Hildebrand, J. P. *Angew. Chem. Int. Ed.* **2001**, *40*, 3284–3308.
[6] Organocatalysis is not the scope of this thesis. The enantioselective organocatalysis is described: Berkessel, A.; Gröger, H. *Asymmetric Organocatalysis*; Wiley-VCH: Weinheim, **2005**.
[7] *Guideline for elemental impurities, Q3D (R2), ICH*.
[8] The recent works to remove palladium from the medicinal compounds: (a) Affouard, C.; Crockett, R. D.; Diker, K.; Farrell, R. P.; Gorins, G.; Huckins, J. R.; Caille, S. *Org. Process Res. Dev.* **2015**, *19*, 476–485. (b) Recho, J.; Black, R. J.; North, C.; Ward, J. E.; Wilkes, R. D. *Org. Process Res. Dev.* **2014**, *18*, 626–635.
[9] Nakamura, M.; Hirai, A.; Nakamura, E. *J. Am. Chem. Soc.* **2000**, *122*, 978–979.
[10] Reviews for transition metal catalyzed carbometalation reactions: (a) Negishi, E. *Acc. Chem. Res.* **1987**, *20*, 65–72. (b) Murakami, K.; Yorimitsu, H. *Beilstein J. Org. Chem.* **2013**, *9*, 278–302.
[11] Morken, J. P.; Didiuk, M. T.; Hoveyda, A. H. *J. Am. Chem. Soc.* **1993**, *115*, 6997–6998.
[12] Lautens, M.; Renaud, J.-L.; Hiebert, S. *J. Am. Chem. Soc.* **2000**, *122*, 1804–1805.
[13] Lautens, M.; Colucci, J. T.; Hiebert, S. Smith, N. D.; Bouchain, G. *Org. Lett.* **2002**, *4*, 1879–1882.
[14] McManus, H. A.; Fleming, M. J.; Lautens, M. *Angew. Chem. Int. Ed.* **2007**, *46*, 433–436.
[15] Lautens, M.; Dockendorff, C.; Fagnou, K.; Malicki, A. *Org. Lett.* **2002**, *4*, 1311–1314.
[16] (a) Bertozzi, F.; Pineschi, M.; Macchia, F.; Arnold, L. A.; Minnaard, A. J.; Feringa, B. L. *Org. Lett.* **2002**, *4*, 2703–2705. (b) Zhang, W.; Wang, L.-X.; Shi, W.-J.; Zhou, Q.-L. *J. Org. Chem.* **2005**, *70*, 3734–3736.
[17] Kondakov, D. Y.; Negishi, E. *J. Am. Chem. Soc.* **1995**, *117*, 10771–10772.
[18] Huo, S.; Negishi, E. *Org. Lett.* **2001**, *3*, 3253–3256.
[19] Huo, S.; Shi, J.; Negishi, E. *Angew. Chem. Int. Ed.* **2002**, *41*, 2141–2143.
[20] Magnin-Lachaux, M.; Tan, Z.; Liang, B.; Negishi, E. *Org. Lett*. **2004**, *6*, 1425–1427.
[21] Liang, B.; Negishi, E. *Org. Lett*. **2008**, *10*, 193–195.
[22] Xu, S.; Oda, A.; Bobinski, T.; Li, H.; Matsueda, Y.; Negishi, E. *Angew. Chem. Int. Ed.* **2015**, *54*, 9319–9322.
[23] Nakamura, M.; Hirai, A.; Nakamura, E. *J. Am. Chem. Soc.* **2000**, *122*, 978–979.
[24] (a) Consiglio, G.; Botteghi, C. *Helv. Chim. Acta* **1973**, *56*, 460–461. (b) Kiso, Y.; Tamao, K.; Miyake, N.; Yamamoto, K.; Kumada, M. *Tetrahedron Lett.* **1974**, *15*, 3–6.
[25] For leading references: [coupling with organozincs] (a) Fischer, C.; Fu, G. C. *J. Am. Chem. Soc.* **2005**, *127*, 4594–4595. (b) Lundin, P. M.; Esquivias, J.; Fu, G. C. *Angew. Chem., Int. Ed.* **2009**, *48*, 154–156. (c) Oelke, A. J.; Sun, J.; Fu, G. C. *J. Am. Chem. Soc.* **2012**, *134*, 2966–2969. (d) Choi, J.; Fu, G. C. *J. Am. Chem. Soc.* **2012**, *134*, 9102–9105. (e) Liang, Y.; Fu, G.C. *J. Am. Chem. Soc.* **2015**, *137*, 9523–9526. [coupling with organosilicons] (f) Dai, X.; Strotman, N. A.; Fu, G. C. *J. Am. Chem. Soc.* **2008**, *130*, 3302–3303. [coupling with organoboranes] (g) Lundin, P. M.; Fu, G. C. *J. Am. Chem. Soc.* **2010**, *132*, 11027–11029. (h) Wilsily, A.; Tramutola, F.; Owston, N. A.; Fu, G. C. *J. Am. Chem. Soc.* **2012**, *134*, 5794–5797. (i) Binder, J. T.; Cordier, C. J.; Fu, G. C. *J. Am. Chem. Soc.* **2012**, *134*, 17003–17006. [coupling with organomagnesiums] (j) Lou, S.; Fu, G. C. *J. Am. Chem. Soc.* **2010**, *132*, 1264–1266.
[26] Mao, J.; Liu, F.; Wang, M.; Wu, L.; Zheng, B.; Liu, S.; Zhong, J.; Bian, Q.; Walsh, P. J. *J. Am. Chem. Soc*. **2014**, *136*, 17662–17668.
[27] Reviews: (a) Bolm, C.; Legros, J.; Le Paih, J.; Zani, L. *Chem. Rev.* **2004**, *104*, 6217–6254. (b) Fürstner, A.; Martin, R. *Chem. Lett.* **2005**, *34*, 624–629. (c) Czaplik, W. M.; Mayer, M.; Cvengroš, J.; von Wangelin, A. J. *ChemSusChem* **2009**, *2*, 396–417. (d) Plietker, B. *Synlett* **2010**, 2049–2058. (e) Sherry, B. D.; Fürstner, A. *Acc. Chem. Res.* **2008**, *41*, 1500–1511.
[28] Selected recent papers: [coupling with organozincs] (a) Bedford, R.B.; Huwe, M.; Wilkinson, M. C. *Chem. Commun.* **2009**, 600–602. (b) Hatakeyama, T.; Nakagawa, N.; Nakamura, M. *Org. Lett.* **2009**, *11*, 4496–4499. (c) Lin, X.; Zheng. L.; Qing, F.-L. *Organometallics* **2012**, *31*, 1578–1582. [coupling with organoboranes] (d) Hatakeyama, T.; Hashimoto, T.; Kondo, Y.; Fujiwara, Y.; Seike, H.; Takaya, H.; Tamada, Y.; Ono, T.; Nakamura, M. *J. Am. Chem. Soc.* **2010**, *132*, 10674–10676. (e) Hatakeyama, T.; Hashimoto,

T.; Kathriarachchi, K. K. A. D. S.; Zenmyo T.; Seike, H.; Nakamura, M. *Angew. Chem., Int. Ed.* **2012**, *51*, 8834–8837. [coupling with organomagnesiums] (f) Nakamura, M.; Matsuo, K.; Ito, S.; Nakamura, E. *J. Am. Chem. Soc.* **2004**, *126*, 3686–3687. (g) Nagano, T.; Hayashi, T. *Org. Lett.* **2004**, *6*, 1297–1299. (h) Martin, R.; Fürstner, A. *Angew. Chem., Int. Ed.* **2004**, *43*, 3955–3957. (i) Bedford, R. B.; Bruce, D. W.; Frost, R. M.; Goodby, J. W.; Hird, M. *Chem. Commun.* **2004**, 2822–2823. (j) Jin, M.; Nakamura, M. *Chem. Lett.* **2011**, *40*, 1012–1014. (k) Hatakeyama, T.; Fujiwara, Y.; Okada, Y.; Itoh, T.; Hashimoto, T.; Kawamura, S.; Ogata, K.; Takaya, H.; Nakamura, M. *Chem. Lett.* **2011**, *40*, 1030–1032.

PART 1

Iron-Catalyzed Enantioselective Carbometalation Reaction: Access to the Epibatidine Derivatives

CHAPTER 1

Iron-Catalyzed Enantioselective Carbometalation of Azabicycloalkenes

Abstract

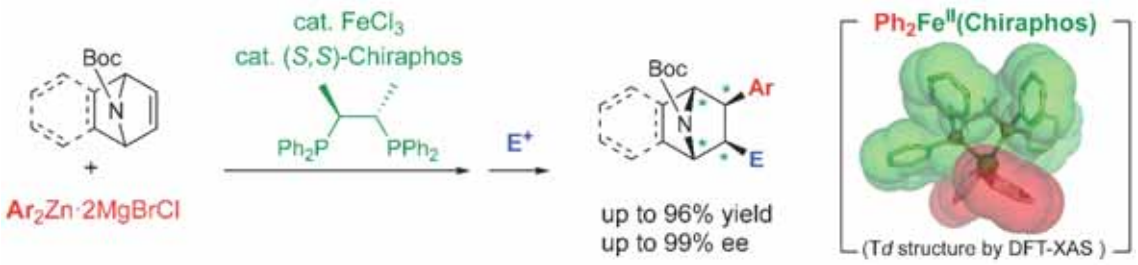

The first enantioselective carbometalation reaction of azabicycloalkenes has been achieved by iron catalysis to *in situ* form optically active organozinc intermediates, which are amenable to further synthetic elaborations. The observed chiral induction, along with the DFT and XAS analysis, reveals that the direct coordination of the chiral phosphine ligand to the iron center during the carbon–carbon and carbon–metal bonds forming step. The new class of iron-catalyzed asymmetric reaction will contribute to the synthesis and production of bioactive molecules.

Reproduced from *Chem. Commun.* **2021**, *57*, 6975–6978. with permission from the Royal Society of Chemistry.

Introduction

Carbometalation reactions, the 1,2-addition of organometallic species to alkenes or alkynes, are a powerful synthetic tool for carbon–carbon (C–C) bond formation.[1] In particular, the transition metal-catalyzed asymmetric carbometalation of oxa- and azabicyclic alkenes is an effective strategy for the enantioselective synthesis of chiral building blocks for various natural products.[2] Lautens and co-workers have extensively studied the asymmetric transformations of bicyclic alkenes catalyzed by rhodium[3] and palladium,[2b, 4] where the enantioselective carbometalation brings about desymmetrization of the *meso*-substrates.[5] Subsequent ring-opening reactions of the carbometalation intermediates give optically active products bearing multiple stereocenters. Copper [6] and iridium [7] catalysts can also affect the asymmetric transformations of oxa- and azabicyclic alkenes (Scheme 1a).

The enantioselective carbometalation of azabicyclic alkenes without the ring-opening is also of significant synthetic interest, as they can provide direct access to the azabicyclo[2.2.1]heptane skeleton of alkaloid derivatives, such as epibatidine and epiboxidine (Scheme 1b).[8] Nevertheless, the catalytic asymmetric addition of organometallic species (i.e., carbon nucleophiles) to azabicyclic alkenes without the ring-opening remains virtually unexplored.[9]

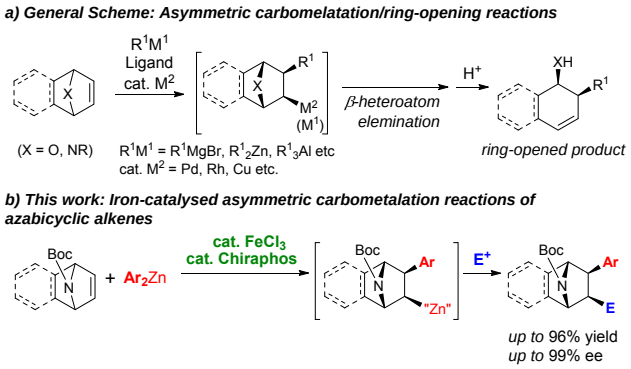

Scheme 1. Transition Metal-Catalyzed Asymmetric Carbometalation Reactions. E^+ = electrophile.

Asymmetric iron catalyses have emerged rapidly in organic synthesis,[10] while their use in enantioselective carbometalation remains limited to the highly strained cyclopropene substrates.[5b] This can be attributed to the unstable coordination of chiral ligands with the iron center, of which oxidation states often fluctuates during the catalytic cycle. Indeed, Bedford and coworkers discovered that phosphine ligands do not coordinate to the iron center in the iron-catalyzed Negishi coupling.[11] On the other hand,

the author has observed evident asymmetric induction in iron-bisphosphine-catalyzed enantioselective cross-coupling reactions,[12] and an acceleration effect of a chelate phosphine in the diastereoselective carbometalation of oxa- and azabicyclic alkenes with arylzinc reagents.[9b] These conflicting observations have led the author to attempt an enantioselective carbometalation under iron catalysis.

Results and Discussion

Based on Nakamura group's recent success in controlling iron-catalyzed enantioselective cross-coupling reactions,[12] the author began the study by exploring effective chiral ligands and conditions for the carbometalation of azabicyclic alkene **1a** with phenylzinc reagent **2a** in the presence of catalytic amounts of $FeCl_3$ and a ligand (Figure 1 and Table 1). Arene-1,2-bisphosphine ligands, bearing *P*-stereogenic centers, (*R,R*)-BenzP* (**L1**) which is effective for enantioselective cross-coupling reaction[12] did not show the similar reactivity and selectivity for this carbometalation reaction (entry 1). However, (*R,R*)-QuinoxP* (**L2**) provided the product **3a** with moderate yield (50%) and low selectivity (12% ee, entry 2). The use of a *P*-chiral ligand, (*S,S′,R,R′*)-Tangphos (**L3**), with a rigid and chiral aliphatic backbone provided the product with moderate selectivity (33% ee, entry 3). The axially chiral ligand (*R*)-BINAP (**L4**) gave the racemic product with negligible yield (entry 4).[13] The chiral alkylphosphine ligand (*R*)-PROPHOS (**L5**) provided the product with high yield (94%) and moderate selectivity (42% ee, enty 5). Whereas (*S,S*)-Chiraphos (**L6**) provided the product with the highest yield (>99%) and selectivity (77% ee, entry 6), suggesting that 1,2-bisphosphine containing chiral alkyl backbone is essential for achieving high enantioselectivity and high chemical yield. Other bisphosphine ligands having flexible alkane backbones such as (-)-DIOP (**L7**) and (*S,S*)-Skewphos (**L8**) showed moderate reactivity and selectivity (entries 7 and 8). Nitrogen containing chiral ligands such as (*S*)-*i*-Pr-Phox (**L9**) and (*S,S*)-PyBOX (**L10)** showed moderate or no chiral induction (entries 9 and 10). In the absence of ligand only 8% product was obtained (entry 11). The enantioselectivity of products increased by lowering temperature and the best selectivity (82% ee) was obtained when reaction was performed at –20 °C (entries 12 and 13).

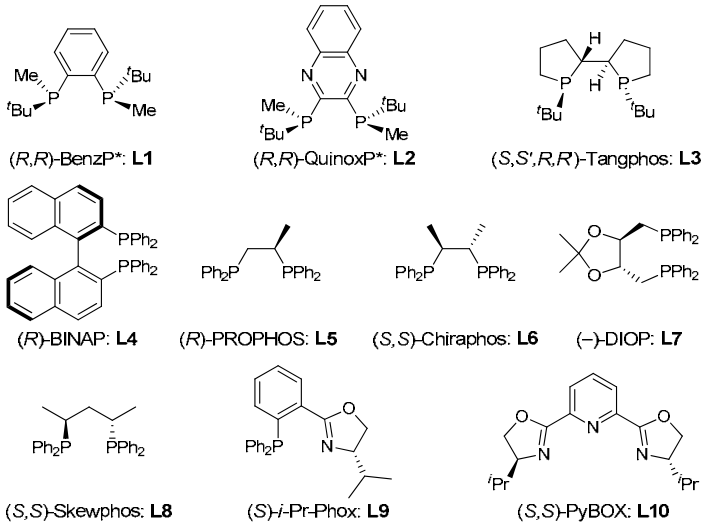

Figure 1. Chiral ligands used for screening (see Table 1).

Table 1. Screening of Reaction Conditions for Iron-Catalyzed Asymmetric Carbometalation Reactions.[a]

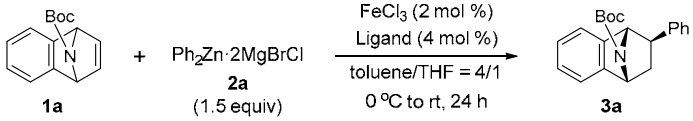

Entry	Ligand	Yield [%][b]	ee [%][c]	RSM [%][b,d]
1	(*R*,*R*)-BenzP*: **L1**	2	6	86
2	(*R*,*R*)-QuinoxP*: **L2**	50	12	41
3	(*S*,*S'*,*R*,*R'*)-Tangphos: **L3**	25	33	65
4	(*R*)-BINAP: **L4**	5	<1	88
5	(*R*)-PROPHOS: **L5**	94	42	0
6	(*S*,*S*)-Chiraphos: **L6**	99	77	0
7	(–)-DIOP: **L7**	62	7	5
8	(*S*,*S*)-Skewphos: **L8**	54	49	30
9	(*S*)-*i*-Pr-Phox: **L9**	27	17	65
10	(*S*,*S*)-PyBOX: **L10**	50	<1	40
11	none	8	—	86
12[e]	(*S*,*S*)-Chiraphos: **L6**	99	78	0
13[f]	(*S*,*S*)-Chiraphos: **L6**	94	82	0

[a] All reactions were performed on 0.5 mmol scale and reactions were quenched by using degassed MeOH/AcOH = 80/20 (1.0 mL). [b] Yields were determined by ^{1}H NMR analysis, using 1,1,2,2-tetrachloroethane as an internal standard. [c] The ee values were determined by chiral HPLC analysis. [d] Recovering of starting material. [e] This reaction was performed at 0 °C for 13 h. [f] Reaction was done at –20 °C for 17 h.

Table 2 shows the effects of the catalyst loading and other metal salts on the enantioselective carbometalation reaction of **1a** with **2a**. A 1:1 ratio of iron/ligand also

achieved comparable chiral induction to give the corresponding product in 74% ee, while higher yields and ee were observed by using excess amounts of ligand to iron (entries 1−3). In the absence of iron salt the reaction did not proceeds and the starting material was recovered in a quantitative amount (entry 4). The results achieved with $Fe(acac)_3$, $Fe(acac)_2$, and $FeBr_3$ were comparable to those with $FeCl_3$ (entries 5–7). Other transition metal chlorides did not afford the desired product under the present conditions (entries 8− 11).

Table 2. Effect of Catalyst Amount and Metal Salts on Iron-Catalyzed Asymmetric Carbometalation Reactions.[a]

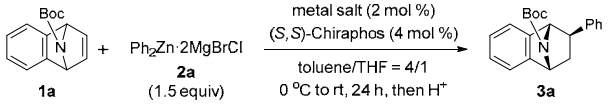

1a 3a

entry	metal salt (mol %)	(*S*,*S*)-Chiraphos (mol %)	yield (%)[b]	ee (%)[c]	RSM (%)[b]
1	$FeCl_3$ (2)	4	>99	77	N.D.
2	$FeCl_3$ (2)	2	86	74	7
3	$FeCl_3$ (1)	2	87	77	6
4	-	4	N.D.	-	>99
5	$Fe(acac)_3$ (2)	4	93[d]	72	N.D.
6	$Fe(acac)_2$ (2)	4	96[d]	74	N.D.
7	$FeBr_3$ (2)	4	95[d]	73	N.D.
8	$CoCl_2$ (2)	4	N.D.	-	86
9	$NiCl_2$ (2)	4	<1	-	85
10	$CuCl_2$ (2)	4	N.D.	-	>99
11	$Pd(CH_3CN)_2Cl_2$ (2)	4	N.D.	-	97

[a]All reactions were performed on 0.5 mmol scale and reactions were quenched by using degassed MeOH/AcOH = 80/20 (1.0 mL). [b]Yields were determined by ^{1}H NMR analysis, using 1,1,2,2-tetrachloroethane as an internal standard. [c]The ee values were determined by chiral HPLC analysis on a CHIRALCEL IC-3 column (0.46 cm i.d., 15 cm length) under the following conditions: Hexane:IPA = 99:1, 1.0 mL/min, 5 °C. [d]Isolated yield.

The standardized carbometalation protocol (entry 13, Table 1) was tested with various arylzinc reagents and azabicyclic alkenes; Table 3 illustrates the scope of the developed reaction. The reaction of **1a** with *para*- and *meta*-substituted arylzinc reagents gave corresponding products **3a**–**3f** in 85%–99% yield with good enantioselectivities (77%–85% ee).[14] When *o*-tolylzinc reagent was employed, the enantioselectivity increased dramatically to give **3g** in 93% yield with 99% ee. Other sterically hindered arylzinc reagents such as *o*-methoxyphenyl-, 1-naphthyl-, and 9-phenanthrylzinc reagents also provided the corresponding products (**3h**–**3j**) with high enantioselectivities (93%–97% ee). The heteroaromatic 4-chloro-3-pyridylzinc reagent can also participate in the carbometalation to give **3k** in 84% yield with relatively low enantioselectivity (45% ee). The steric factor of aryl nucleophiles had substantial impact on the enantioselectivity, suggesting that the spatial interaction of the aryl group and the alkene substrate leads to

mutual orientation of the two reactants in the stereochemistry-determining carbometalation step.

Table 3. Scope of Iron-Catalyzed Asymmetric Carbometalation Reactions.[a]

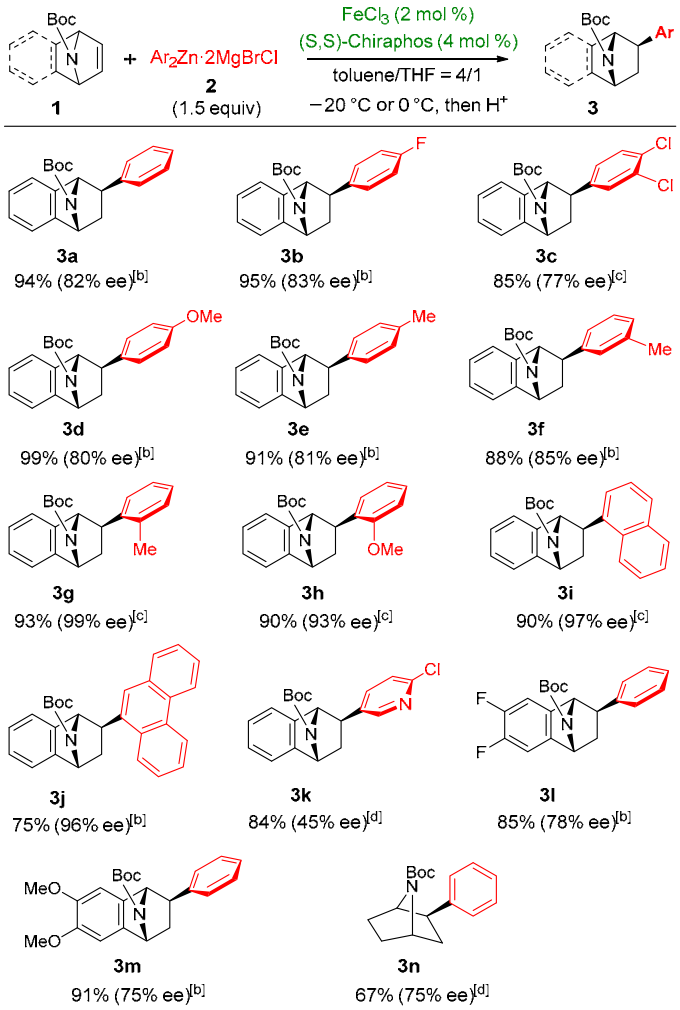

[a] Reactions were performed on a 0.5–1.0 mmol scale and reactions were quenched by using degassed MeOH/AcOH = 80/20 (1.0 mL) unless otherwise noted. [b] Reactions were carried out at –20 °C. [c] Reactions were performed at 0 °C. [d] Reactions were carried out at 30 °C. See the experimental section for details regarding the reaction conditions for each case.

The electronic factors of alkene substrates seemed not to affect this carbometalation reaction: substrates having electron-withdrawing fluoro groups or electron-donating methoxy groups provided corresponding products **3l** and **3m** in excellent yields (85% and 91%, respectively) and good enantioselectivities (78% and 75% ee, respectively). On the other hand, the reaction with an aliphatic azabicyclic alkene **1n** became sluggish and did not proceed at 0 °C: the expected product **3n** was obtained

in 67% with 75% ee at an elevated reaction temperature. As this reaction's enantioselectivity is comparable to that of other substrates, the fused benzene ring has no significant effect on the enantioselectivity.

Trapping of the carbometalation intermediate **4** with various electrophiles showed the stereospecific nature of the carbometalation/trapping sequence.[5,9b] The reaction of **1a** with *o*-tolylzinc reagent gave optically active organozinc intermediate, which underwent electrophilic trapping with CD_3CO_2D to give deuterated product **5a** in 96% yield with 99% ee and >99% *cis*-selectivity (entry 1, Table 4). Similarly, when trapped with iodine as the electrophile, product **5b** was obtained in 84% yield with 99% ee and a diastereomeric excess of 94% (entry 2, Table 4).[15]

Table 4. Electrophilic Trapping of Carbozincation Intermediate.

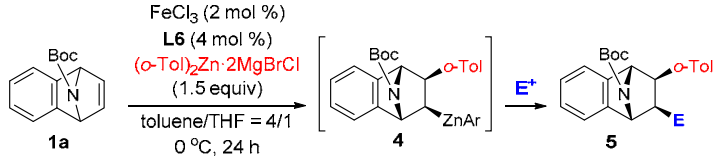

Entry	Electrophile	E	Yield of **5** [%][a]	ee [%]	de [%][b]
1	$CD_3OD/CD_3CO_2D = 80/20$	D	96 (**5a**)	99	>99
2	I_2	I	84 (**5b**)	99	94

[a] Isolated yield. [b] Diastereomeric excess was determined by ^{1}H NMR analysis.

In order to clarify the reaction mechanism, X-ray absorption near edge structure (XANES) and extended X-ray absorption fine structure (EXAFS) measurements were performed at BL14B2 beamline of SPring-8 under standard beamline conditions. At first, the complexation step between $FeBr_3$ and (*S*,*S*)-Chiraphos was investigated by in situ X-ray absorption spectroscopy (XAS) monitoring (Figure 2). The remarkable lower energy shift of the rising edge was observed by the addition of 1 equiv of (*S*,*S*)-Chiraphos to $FeBr_3$, indicating the increase of electron density of iron center due to the complexation with (*S*,*S*)-Chiraphos to form 1:1 complex of [$FeBr_3$(Chiraphos)]. The addition of 2 equiv of (*S*,*S*)-Chiraphos shows negligible change from that with 1 equiv, clarifying the nature of the bidentate complex of [$FeBr_3$(Chiraphos)], which does not accept the further coordination of (*S*,*S*)-Chiraphos in this concentration.

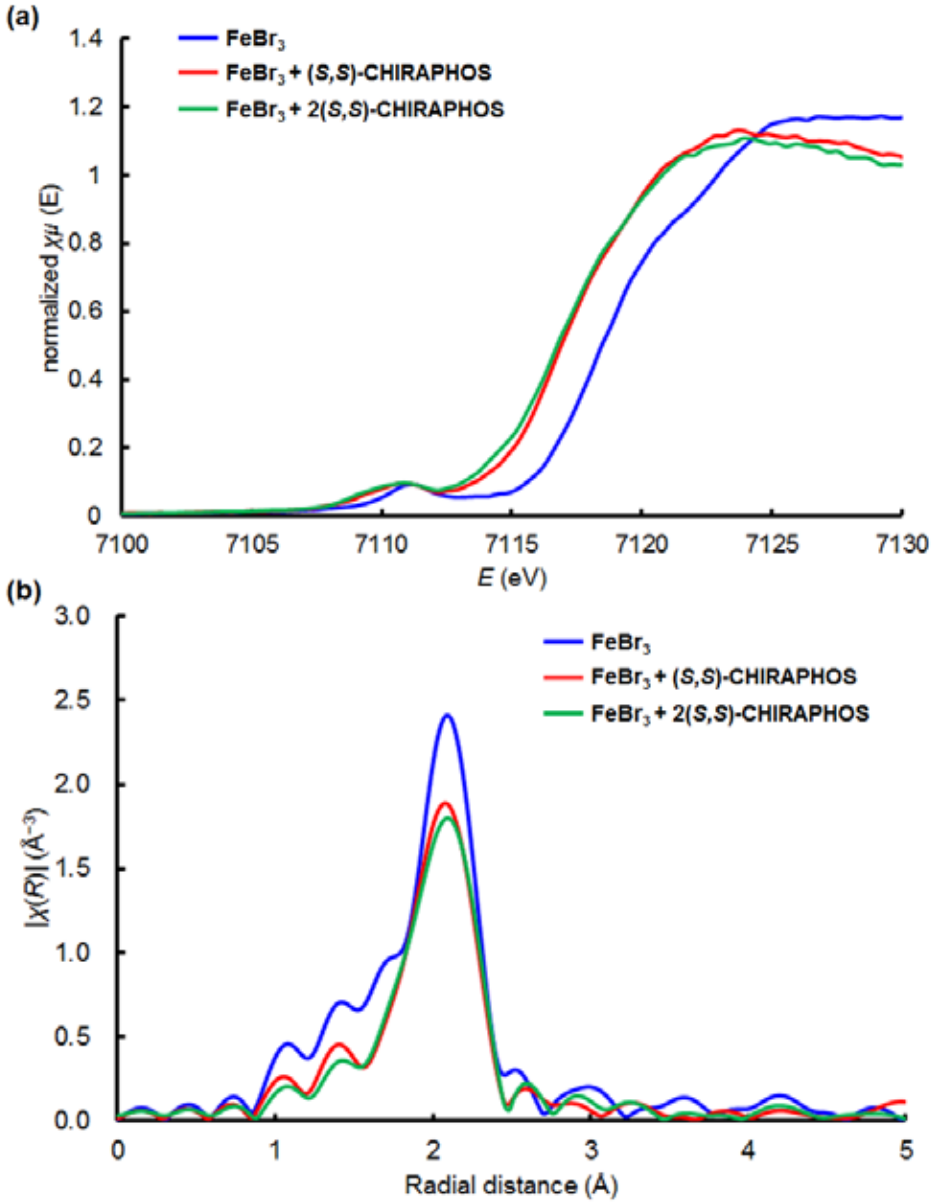

Figure 2. Fe K-edge (a) XANES and (b) EXAFS spectra for $FeBr_3$ solution (20 mM in THF/toluene) of $FeBr_3$ (blue line), with 1.0 equiv (red line), and 2.0 equiv (green line) of (*S*,*S*)-Chiraphos.

Next, the transmetalation-reductive elimination step forming aryliron intermediates was investigated by the stoichiometric reaction of $FeBr_3$, (*S*,*S*)-Chiraphos, and 1–3 equiv of $Ph_2Zn{\cdot}MgBrCl$ (Figure 3). By the addition of 1 and 2 equiv of $Ph_2Zn{\cdot}MgBrCl$, the rising edge gradually shifted to lower energy side, suggesting that the transmetalation between Fe–Br and Ph–Zn species takes place and following reductive elimination-comproportionation generates divalent Fe–Ph species,

[FeBr(Ph)(Chiraphos)]. The following 3 equiv addition of $Ph_2Zn{\cdot}2MgBrCl$ does not cause a significant shift of the rising energy, indicating the formation of diaryliron(II) species retaining the oxidation state of iron center. However, the remarkable change was observed at the pre-edge showing the intense peak at 7110.5 eV, together with the appearance of shoulder at 7116.6 eV. Previously, Nakamura group reported the XAS study on the diaryliron intermediates of the Grignard coupling reaction, in which [Fe(Mes)$_2$(SciOPP)] complex showed a 1s–4p_z transition at 7112.3 eV together with the pre-edge peak at 7109.5 eV.[16] The shoulder peak at 7112.3 eV originates from the 3d–4p orbital mixing of slightly distorted square planar geometry of [Fe(Mes)$_2$(SciOPP)] complex. The observed shoulder peak at 7116.6 eV with 3 equiv of $Ph_2Zn{\cdot}2MgBrCl$ is also considered to originate from the 1s–4p_z transition of diaryliron(II) species of [Fe(Ph)$_2$(Chiraphos)]. A little higher energy transition than that of [Fe(Mes)$_2$(Chiraphos)] suggests the tetrahedral geometry of [Fe(Ph)$_2$(Chiraphos)]. Relating to this energy shift, the author considered that the intense pre-edge peak originates from 1s–3d transition of the tetrahedral iron center.[16] EXAFS spectra also show the corresponding spectral change by the addition of $Ph_2Zn.2MgBrCl$ (Figure 4). The stepwise decreasing of the peak at 2.09 Å accompanied by the increasing of the peak at around 1.0–2.0 Å. These spectral changes can be attributed to the conversion of Fe–Br bonds to Fe–C bonds, resulting from the transmetalation-reductive elimination steps generating diaryliron species, [Fe(Ph)$_2$(Chiraphos)].

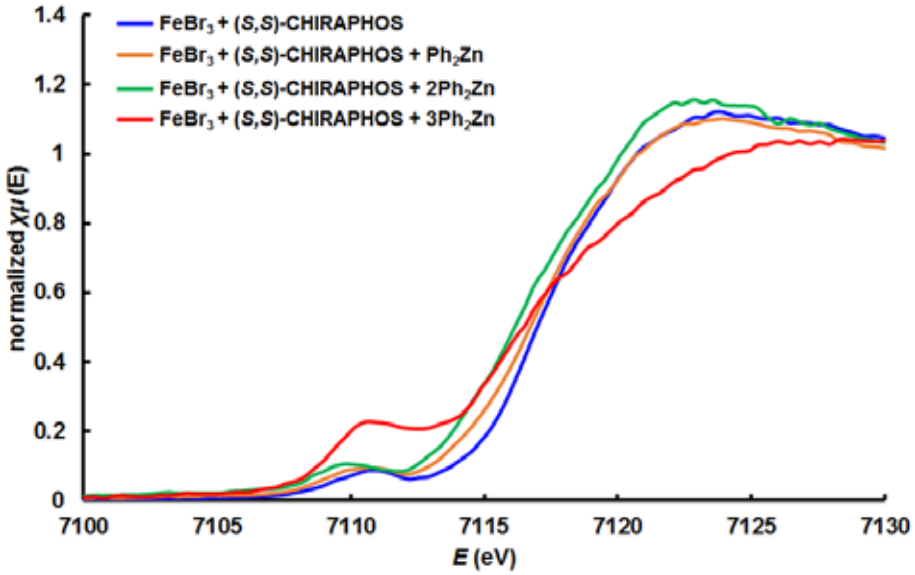

Figure 3. Fe K-edge XANES spectra for 1:1 mixture solution (20 mM in THF/toluene) of $FeBr_3$ and (*S*,*S*)-Chiraphos (blue line), with 1.0 equiv (orange line), 2.0 equiv (green line), and 3.0 equiv (red line) of $Ph_2Zn{\cdot}2MgBrCl$.

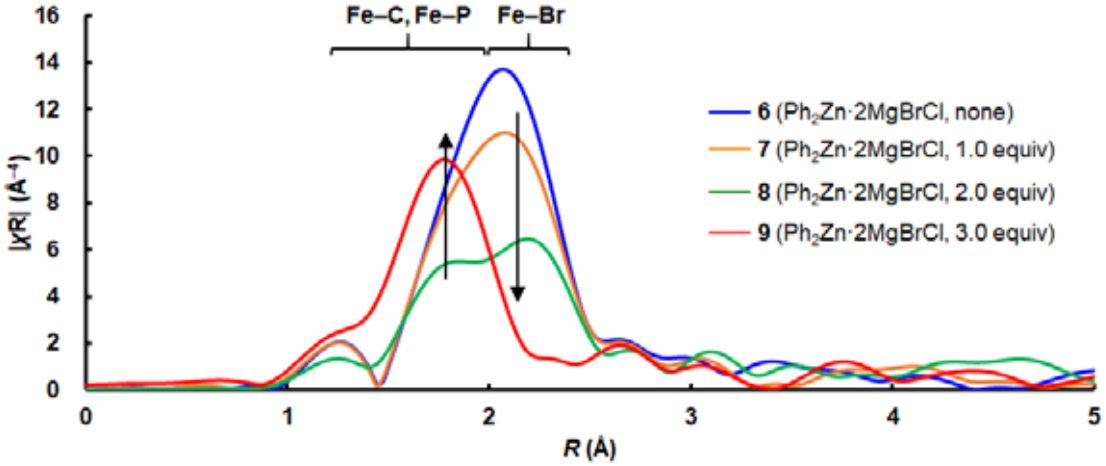

Figure 4. Fe K-edge EXAFS spectra for 1:1 mixture solution (20 mM in THF/toluene) of $FeBr_3$ and (*S*,*S*)-Chiraphos (blue line), with 1.0 equiv (orange line), 2.0 equiv (green line), and 3.0 equiv (red line) of $Ph_2Zn{\cdot}2MgBrCl$.

For structural analysis of the in situ prepared diaryliron intermediate of $[Fe(Ph)_2(Chiraphos)]$ by the reaction of $FeBr_3$, (*S*,*S*)-Chiraphos, and 3 equiv of $Ph_2Zn{\cdot}2MgBrCl$, FEFF fitting analyses on EXAFS spectrum was carried out using the atomic coordinates obtained from DFT-optimized geometries.[17] Energetically favorable

two possible structures with different spin states were provided by DFT calculation at the $PCM_{toluene}$/B3LYP-D2/SDD(Fe),6-31G*(C,H,O,P) level of theory (Table 5, **L1**). The FEFF fitting analysis based on the above DFT-calculated tetrahedral (Td) geometry with high spin state (S = 2) and square planar (SqP) geometry with intermediate spin state (S = 1) showed a good agreement with adequate R value and χ statics. These FEFF fitting results indicated that diaryliron intermediates [$Fe(Ph)_2$(Chiraphos)] with tetrahedral geometry is the predominant species.

Table 5. Relative Energies (kcal/mol) of Diaryliron Intermediates for Different Geometries and Spin States.

		L1[a]		**L2**[c]	
Spin State	Geometry	ΔE_{ZPE}	ΔG^a	$\Delta E_{ZPE}{}^a$	ΔG^a
		[$Fe(Ph)_2$(*S*,*S*-Chiraphos)]			
S=0	**Td**	23.2	26.2	23.2	26.1
S=0	**SqP**	15.4	16.3	14.3	15.1
S=1	**Td**	17.3	18.5	17.2	18.4
S=1	**SqP**	2.4	3.1	1.7	2.4
S=2	**Td**	**0.0**	**0.0**	**0.0**	**0.0**
S=2	**SqP**	12.5	12.7	16.6	16.7
		[$Fe(Ph)_2$(*S*,*S*-Chiraphos)(THF)]			
S=0	**TBPy**	-0.4	17.4	2.9	20.7
S=0	**SqPy**	-3.6	13.9	-0.6	16.8
S=1	**TBPy**	-8.7	6.8	-5.5	10.0
S=1	**SqPy**	-15.0	1.1	-11.9	4.3
S=2	**TBPy**	-13.9	**-0.7**	-10.7	2.6
S=2	**Td**[c]	-7.6	5.3	-5.0	7.9

[a]L1=$PCM_{Toluene}$/B3LYP-D2/SDD(Fe),6-31G*(C,H,O,P); [b]L2 = $PCM_{Toluene}$/B3LYP-D2/ECP10-MDF(Fe),6-311+G**(C,H,O,P)//$PCM_{Toluene}$/B3LYP-D2/SDD(Fe),6-31G*(C,H,O,P). [c]One phosphorus decoordinates from Fe.

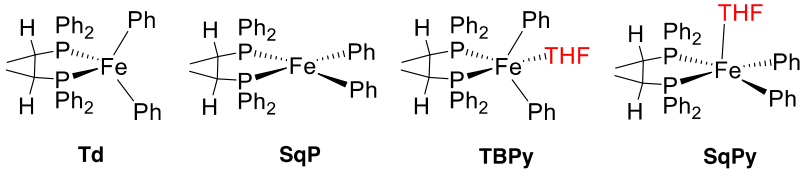

The corresponding XAFS data were processed using Athena by extracting

the EXAFS oscillations $\chi(k)$ as a function of photoelectron wave number k. Fourier transformation of the k^3-weighted χ from k space to r space was carried out to obtain the radial distribution function. The EXAFS fitting calculation was performed by FEFF6[1] program embedded with Artemis, where the theoretical scattering paths were generated from DFT-optimized structure as depicted in Figures 5, 7, and Table 5. The parameters for FEFF fitting analysis are as follows: Ab-Sc: the X-ray absorbing atom and the scattering atom; CN: coordination number; *DW*: Debye-Waller factor (Å^2); ΔE: energy shift (eV); *R*: atomic distance (Å). The parameter for the many-body effect of S_0^2 is fixed to 1.0 for all fitting calculations.

For fitting calculation of tetrahedral [Fe(Ph_2)((*S*,*S*)-Chiraphos)] (S = 2) based on DFT-optimized geometry, eight independent parameters (Fe–C1: S_0^2, e1, r1, σ1; Fe–P: S_0^2, e2, r2, σ1; Fe–C2/C3/C4: S_0^2, e2, r3, σ2) with three scattering paths (1st shell: Fe–C1, 2nd shell: Fe–P, 3rd shell: Fe–C2/C3/C4) give the fitting results with adequate accuracy as shown in Figures 5, where the many-body effect S_0^2 parameter was fixed with an appropriate values for Fe–C1 as S_0^2 = 1.1 and for Fe–CP/C2/C3/C4 as S_0^2 = 1.0, respectively.

For fitting calculation of square planar [Fe(Ph_2)((*S*,*S*)-Chiraphos]] (S = 1) based on DFT-optimized geometry, seven independent parameters (Fe–C1: S_0^2, e1, r1, σ1; Fe–P: S_0^2, e2, r2, σ1; Fe–C2/C3/C4: S_0^2, e2, r3, σ2) with three scattering paths (1st shell: Fe–C1, 2nd shell: Fe–P, 3rd shell: Fe–C2/C3/C4) give the fitting results with adequate accuracy as shown in Figures 7, where the many-body effect S_0^2 parameter was fixed with an appropriate value as S_0^2 = 1.0.

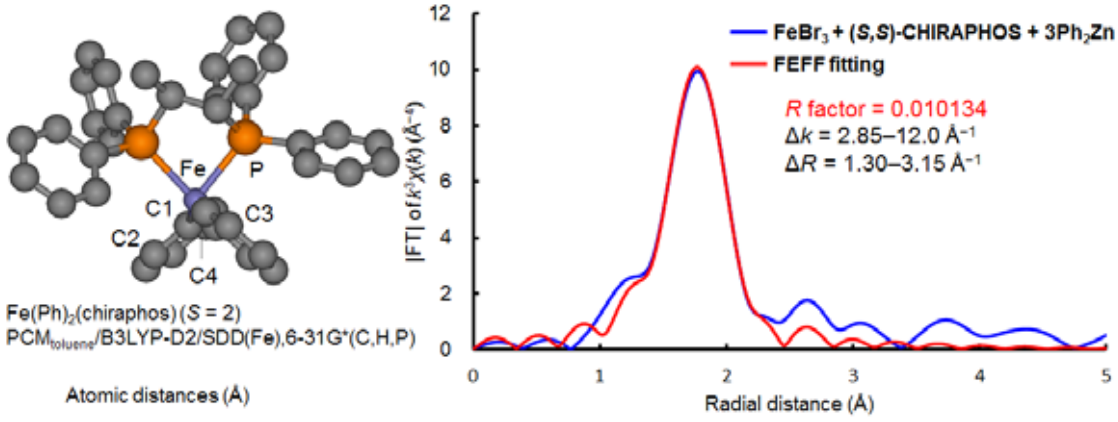

Ab–Sc	CN	Δ*E* (eV)	R (Å)	*DW* (Å^{-1})
Fe–C1	2.0	−3.984 ± 9.46	1.63 ± 0.05	0.00322 ± 0.0008
Fe–P	2.0	1.225 ± 3.86	2.05 ± 0.34	0.00322 ± 0.0008
Fe–C2	1.0	1.225 ± 3.86	2.41 ± 0.34	0.03697 ± 0.0272
Fe–C3	2.0	1.225 ± 3.86	2.41 ± 0.34	0.03697 ± 0.0272
Fe–C4	1.0	1.225 ± 3.86	2.41 ± 0.34	0.03697 ± 0.0272

Figure 5. FEFF fitting analysis on the EXAFS spectrum of the reaction mixture of $FeBr_3$, (*S*,*S*)-Chiraphos (1 equiv), and $Ph_2Zn{\cdot}MgBrCl$ (3 equiv) using the DFT-optimized tetrahedral geometry of $Fe(Ph_2)$[(*S*,*S*)-Chiraphos] (*S* = 2) (red line) at the $PCM_{toluene}$/B3LYP-D2/SDD(Fe),6-31G*(C,H,P) level of theory shown in Table 4, **L1**.

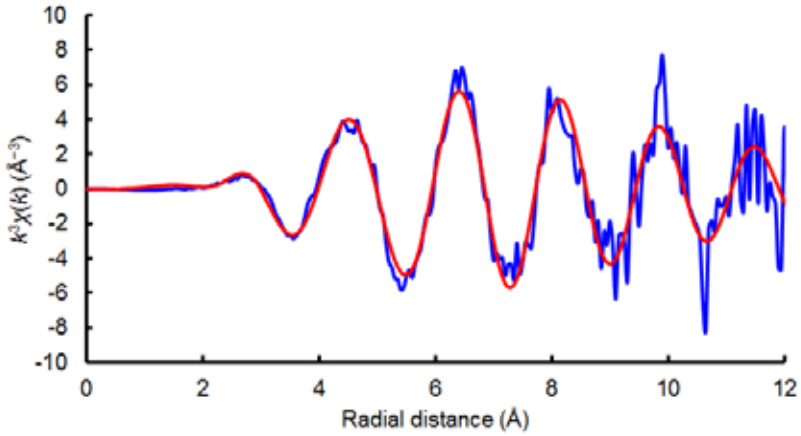

Figure 6. FEFF fitting in *K*-space.

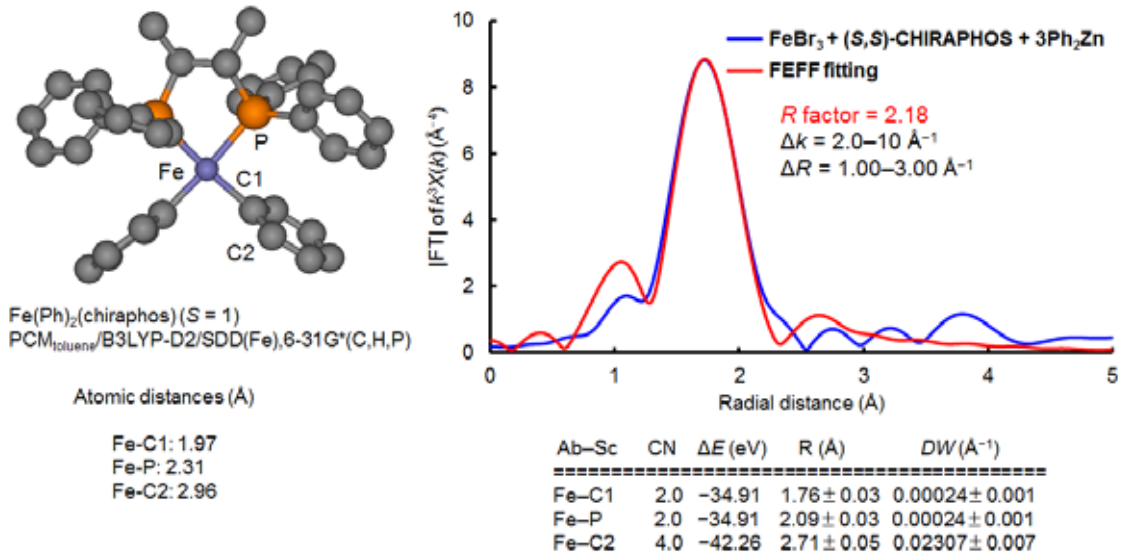

Figure 7. FEFF fitting analysis on the EXAFS spectrum of the reaction mixture of $FeBr_3$, (*S*,*S*)-Chiraphos (1 equiv), and $Ph_2Zn{\cdot}MgBrCl$ (3 equiv) using the DFT-optimized square planar geometry of $Fe(Ph_2)$[(*S*,*S*)-Chiraphos] (*S* = 1) (red line) at the $PCM_{toluene}$/B3LYP-D2/SDD(Fe),6-31G*(C,H,P) level of theory shown in Table 4, **L1**.

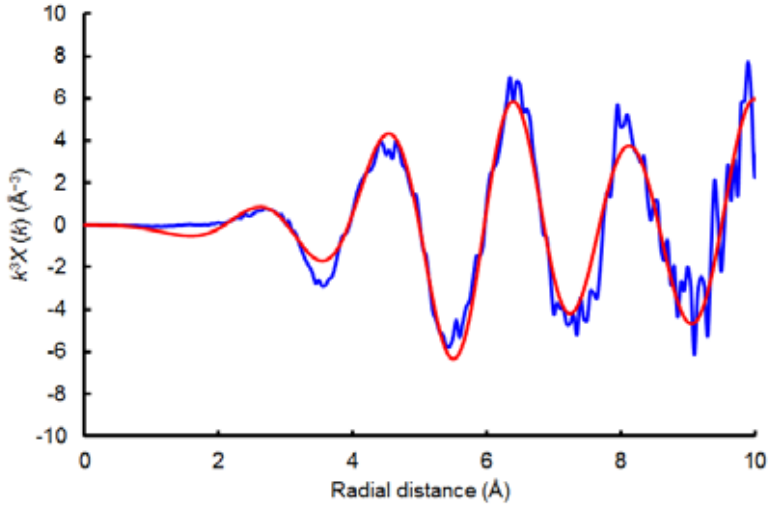

Figure 8. FEFF fitting in *K*-space.

Further insight into the reaction mechanism was obtained by the stoichiometric reaction of azabicycloalkene substrate and iron intermediates (Table 6). A series of iron intermediates were prepared as similar to the above-mentioned XAS experiments by the addition of 1–3 equiv of $Ph_2Zn{\cdot}MgBrCl$ to the mixture of $FeBr_3$ and (*S*,*S*)-Chiraphos. Then, 1 equiv of azabicycloalkene **1a** was added and stirred at room temperature. After 30 min, the reaction was quenched according to the general procedure and subjected to

GC analysis.

Table 6. Stoichiometric Carbometalation Reactions.

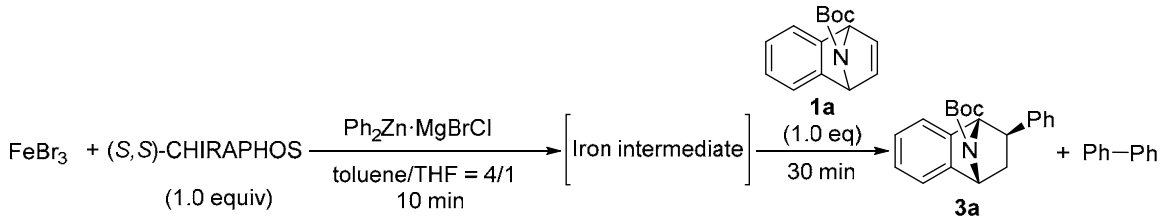

Entry	Ph_2Zn·MgBrCl (equiv)	estimated iron intermediate	**3a** (%)[a]	Ph-Ph[b]
1	1.0	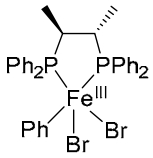	ND	ND
2	2.0	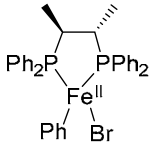	10	detected
3	3.0	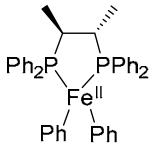	75	detected

[a]Calculated by the GC area ratio of starting material and product **3a**. [b]Ph-Ph was detected by GC.

The product **3a** and biphenyl (**BP**) were not formed with 1 equiv of Ph_2Zn·MgBrCl (entry 1), suggesting only the transmetalation takes place in this step. In the case of 2 and 3 equiv of Ph_2Zn·MgBrCl, the expected carbometalation product **3a** was obtained in 10% and 75% yield, respectively, together with the formation of **BP** (entries 2 and 3). The formation of **BP** indicates that the reductive elimination takes place when 2 equiv of Ph_2Zn·MgBrCl was added. Most importantly, the formation of the carbometalation product **3a** in 75% yield with 3 equiv of diarylzinc reagents clarifies that the catalytically active species is the diaryliron complex [$Fe(Ph)_2$(Chiraphos)] as characterized by XAS analysis. The lower product yield (10%) with 2 equiv of diarylzinc reagents suggests the formation of less reactive aryliron species which is considered to be [FeBr(Ph)(Chiraphos)]. The higher electrophilic reactivity of [$Fe(Ar)_2$(bisphosphine)] complex than [FeX(Ar)(bisphosphine)] complex was previously observed in iron-

catalyzed cross-coupling reaction,[20] which corresponds well with the current diaryliron intermediates showing higher electrophilic reactivity towards azabicycloalkene. From these results, the mechanism for the formation of diaryliron species is proposed as Figure 9.

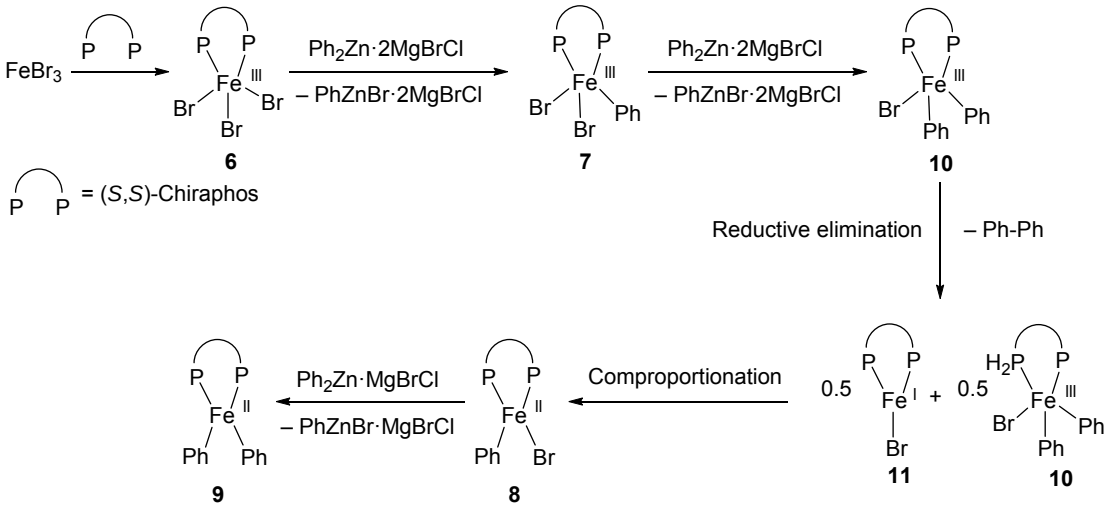

Figure 9. Proposed mechanism for formation of diaryl iron intermediates involving transmetalation-comproportionation steps.

Stepwise transmetalation of $FeBr_3$(Chiraphos) **6** with diarylzinc reagents generates trivalent diaryliron species **7** and **10** which facilitates the reductive elimination forming monovalent bromoiron species **11**. The comproportionation between **10** and **11** forms divalent aryliron species **8**. The additional arylzinc reagent generates the highly active diaryliron intermediate **9**, of which geometry is suggested to be tetrahedral with a high spin state by EXAFS analysis combined with DFT-calculation.

Scheme 2 shows a plausible mechanism for the present carbometalation reaction.[18] The catalytic cycle starts with diaryl iron(II)–(*S*,*S*)-Chiraphos complex **A**, which is generated by the reduction of $FeCl_3$ with excess organozinc reagent (>3.0 equivalents) in the presence of (*S*,*S*)-Chiraphos. The XAS and DFT analyses reveal that the geometry of **A** is tetrahedral. An azabicyclic alkene coordinates to the intermediate likely in an exo-fashion to give intermediate **B**. Enantioselective olefin insertion proceeds to form carboferration intermediate **C**. Subsequent transmetalation with the organozinc reagent leads to optically active organozinc intermediate **D** and regenerates iron(II) species **A**. Upon the sequential addition of electrophiles to the reaction mixture, intermediate **D** undergoes trapping to provide final product **E**. The sharp contrast between

Bedford's and the author's observations can be attributed to the difference of the redox behaviors of the iron center in cross-coupling and carbometalation; the latter reaction maintains iron(II) oxidation states during the catalytic cycle and the bisphosphine ligand predominantly coordinated to the iron center, rather than to the zinc center.[19,20]

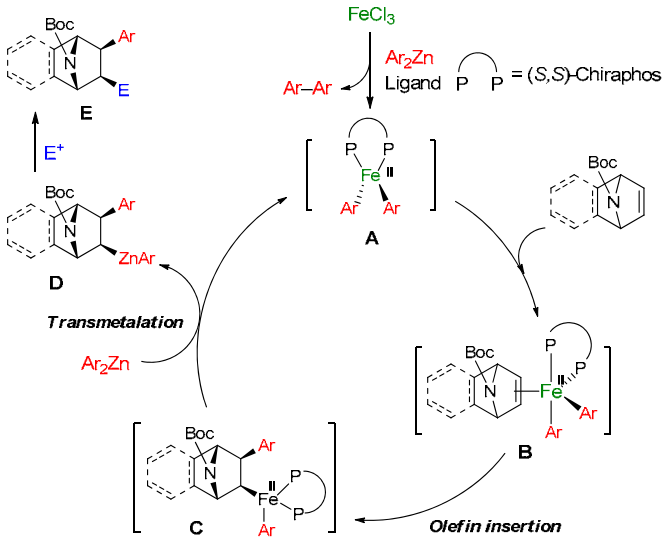

Scheme 2. Catalytic Cycle Based on the XAS and DFT Analyses of the Stoichiometric Reactions.

Conclusion

In summary, the author has developed the first enantioselective carbometalation reactions between various azabicycloalkenes and arylzinc reagents, which proceed under mild conditions by using a readily available $FeCl_3$ and (*S*,*S*)-Chiraphos catalytic system. Trapping experiments reveal the formation of a densely-functionalized optically active organozinc intermediate. XAS and DFT studies provided evidence for the direct coordination of the chiral phosphine ligand to the iron(II) center, even in the presence of excess zinc species that can undergo competitive coordination of the phosphine ligands. The present findings demonstrate the potential of iron-catalyzed stereoselective C–C bond formations for synthesizing complex chiral molecules of biological relevance. Further mechanistic studies on the detailed multi-spin reaction pathway and the origin of the asymmetric induction are currently underway.

Experimental Section

General Information

All reactions dealing with air- or moisture-sensitive compounds were carried out in a dry reaction vessel under a positive pressure of argon. The air- and moisture-sensitive liquids and solutions were transferred *via* syringes or a PTFE cannula. Analytical TLC was performed on glass plates coated with 0.25 mm 230–400 mesh silica gel containing a fluorescent indicator (Merck, #1.05715.0009). The TLC plates were visualized by exposure to UV light (254 nm) and by immersion in an acidic staining solution of *p*-anisaldehyde, followed by heating on a hot plate. The organic solutions were concentrated using rotary evaporation at *ca.* 40 hPa. Column chromatography was performed on prepacked silica gel cartridges (SNAP Ultra; Biotage, Uppsala, Sweden). Flash column chromatography was performed on Merck Silica Flash® 60 (spherical, neutral, 140–325 mesh), as described by Still *et* al.[21]

Instrumentation

NMR spectroscopy

^{1}H and ^{13}C NMR spectra were obtained using JEOL ECS-400 (391.8 MHz) NMR spectrometers. The proton chemical shift values are reported in parts per million (ppm, δ scale) downfield from tetramethylsilane (TMS) and are referenced to TMS (δ 0.0) and $CHCl_3$ (δ 7.26). The chemical shifts of the carbon atoms are reported in parts per million (ppm, δ scale) downfield from TMS and referenced to the carbon resonance of $CDCl_3$ (δ 77.16). The data are presented as chemical shift, multiplicity (s = singlet, d = doublet, t = triplet, q = quartet, quint = quintet, sext = sextet, sept = septet, m = multiplet and/or multiple resonances, and br = broad), coupling constant in hertz (Hz), and signal area integration in natural numbers.

GC, GPC and HPLC analysis

GC analyses were performed using a Shimadzu GC-2010 plus analyzer equipped with an FID detector and a ZB-1MS capillary column (10 m × 0.1 mm i.d., film thickness = 0.1 μm). Gel- permeation chromatography was performed using JAIGEL-1H and JAIGEL-2H (40 mm i.d.) columns with an LC-9104 system (Japan Analytical Industry Co., Ltd.). HPLC analysis was performed on a JASCO LC-2000 series HPLC with CHIRALCEL IC-3 column.

IR analysis

IR spectra were recorded using a Perkin Elmer Spectrum One FT-IR spectrometer;

characteristic IR absorptions are reported in cm^{-1}.

HRMS and melting point

High-resolution mass spectra (HRMS) were recorded using fast atom bombardment (FAB) ionization with a JEOL JMS-700 mass spectrometer or electron spray ionization (ESI) with a Bruker Daltonics GmbH SolariX FT-ICR-MS spectrometer. Melting points were recorded using a Yanaco MP-500D instrument.

Materials

Anhydrous THF was purchased from Wako Pure Chemical Industries, Ltd. and distilled from benzophenone ketyl under argon (at atmospheric pressure) immediately before use. The water content of the solvent was determined using a Karl Fischer moisture titrator (MKC-610, Kyoto Electronics Manufacturing Co., Ltd.), and found to be <15 ppm. Celite and Florisil(100–200 mesh) were purchased from Nacalai Tesque, Inc. (*S,S)*-Chiraphos was purchased from Wako Pure Chemical Industries, Ltd. and Stream Chemicals Inc. and $FeCl_3$ (>99.99%) from Sigma-Aldrich Co. $ZnCl_2$ (99.9%) was purchased from Wako Pure Chemical Industries, Ltd., 268-01022). The commercially available aryl Grignard reagents were purchased from Kanto Chemical Co. Inc. or Sigma-Aldrich Co., and used without purification. The author and coworkers prepared other aryl Grignard reagents according to standard procedure.[22] 2-Chloro-5-pyridylmagnesium bromide was prepared by direct insertion of magnesium into the C–Br bond in the presence of LiCl.[23] Other chemicals were purchased from Wako Pure Chemical Industries, Ltd., Tokyo Chemical Industry Co., Ltd., Sigma-Aldrich Co., and other commercial suppliers, and were used after appropriate purification, unless otherwise stated.

Preparation of Materials

***tert*-Butyl 1,4-dihydro-1,4-epiminonaphthalene-11-carboxylate (1a)**

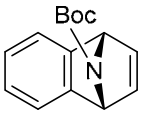

The title compound was prepared followed by the literature procedure.[4b] The spectral data matched to that previously reported in the literature; ^{1}H NMR ($CDCl_3$, 391.8 MHz) δ 1.37 (s, 9H), 5.48 (br, 2H), 6.94–7.00 (m, 4H), 7.25–7.26 (m, 2H).

***tert*-Butyl 6,7-dimethoxy-1,4-dihydro-1,4-epiminonaphthalene-11-carboxylate (1b)**

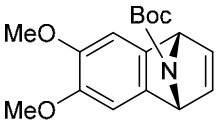

The title product was prepared followed by the literature.[4b] The spectral data matched to that previously reported in the literature; ^{1}H NMR ($CDCl_3$, 391.8 MHz) δ 1.38 (s, 9H), 3.84 (s, 6H), 5.44 (br, 2H), 6.97–7.02 (br, 4H).

***tert*-Butyl 6,7-difluoro-1,4-dihydro-1,4-epiminonaphthalene-11-carboxylate (1c)**

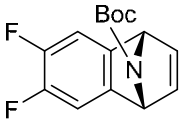

The title product was prepared followed by the literature.[4b] The spectral data matched to that previously reported in the literature; ^{1}H NMR ($CDCl_3$, 391.8 MHz) δ 1.37 (s, 9H), 5.44 (br, 2H), 6.97 (br, 2H), 7.09 (t, J = 7.4 Hz, 2H).

***tert*-Butyl 7-azabicyclo[2.2.1]hept-2-ene-7-carboxylate (1d)**

The title product was prepared followed by the literature.[24] The spectral data matched to that previously reported in the literature; ^{1}H NMR ($CDCl_3$, 391.8 MHz) δ 1.07 (d, J = 8.2 Hz, 2H), 1.38 (s, 9H), 1.82 (d, J = 8.6 Hz, 2H), 4.63 (br, 2H), 6.19 (br, 2H).

General Procedure: Iron-Catalyzed Asymmetric Carbometalation of Azabicyclic Alkenes with Arylzinc Reagents

$ZnCl_2$ (545.2 mg, 4.0 mmol) was dried by fusing *in vacuo* and cooled quickly followed by addition of 4.0 mL of THF to prepare a 1.0 M THF solution of $ZnCl_2$. After stirring for 20 minutes, the THF solution of $ZnCl_2$ (0.85 mL, 1.0 M) was transferred to the other Schlenk flask, and ArMgBr (3.2 equiv.) was added at 0 °C and stirred for 1.0 h to 2.0 h. Then, the solvent was removed and the resulting $Ar_2Zn{\cdot}2MgBrCl$ was dried for 10 minutes under vacuum. To the arylzinc powder, a mixture of (*S,S*)-Chiraphos (8.5 mg, 0.02 mmol), THF (0.70 mL), toluene (3.2 mL), and $FeCl_3$ (100 μL, 0.1 M solution in THF, 0.01 mmol) was added followed by the addition of azabicyclic alkene (**1a**, 122 mg, 0.50 mmol) and the reaction mixture was stirred at –20 °C or 0 °C for 12–20 h. Degassed

AcOH/MeOH (1:4) was added at 0 °C for quenching. The mixture was stirred for 10 minutes and then saturated aqueous NH_4Cl (1.0 mL) and MTBE were added. The separated aqueous layer was extracted with additional portions of MTBE (5 mL × 3). The combined organic extracts were passed through a pad of Florisil® and the filtrate was concentrated *in vacuo*. The residue was purified by silicagel column chromatography.

The corresponding racemic sample was synthesized by using 1,2-bis(diphenylphosphino)benzene instead of (*S,S*)-Chiraphos.

***tert*-Butyl (*1S,2R,4R*)-2-phenyl-1,2,3,4-tetrahydro-1,4-epiminonaphthalene-11-carboxylate (3a)** (Table 3)

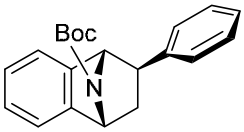

The reaction was carried out according to the general procedure using *tert*-butyl 1,4-dihydro-1,4-epiminonaphthalene-11-carboxylate (**1a**; 121.7 mg, 0.50 mmol), phenylmagnesium bromide (1.73 mL, 0.925 M in THF solution, 3.2 equiv.) and $ZnCl_2$ (0.85 mL of 1.0 M solution in THF, 1.7 equiv). The reaction was performed at –20 °C for 16 h. The crude product was purified by silica gel column chromatography (hexane/AcOEt = 95/5) to give the title product in 94% yield (151.5 mg, 82% ee) as a white solid.

The ee was determined by HPLC on a CHIRALCEL IC-3 column (4.6 mm i.d.; 150 mm length) with following conditions: hexane/IPA = 99/1, 1.0 mL/min, 4.4 °C. Retention times (t_r) = 6.69 min (major) and 7.29 min (minor).

M.p. 98.8–100.3 °C; IR (neat) ν 666, 703, 748, 761, 851, 908, 948, 980, 1077, 1088, 1157, 1173, 1265, 1363, 1459, 1695, 2971, 3027 cm^{-1}; ^1H NMR (391.8 MHz, $CDCl_3$) δ 1.32 (s, 9H), 1.93 (dd, *J* = 11.9, 8.9 Hz, 1H), 2.19 (dt, *J* = 11.7, 4.5 Hz, 1H), 2.84 (dd, *J* = 8.5, 4.5 Hz, 1H), 5.08 (br, 1H), 5.24 (br, 1H), 7.15–7.39 (m, 9H); ^{13}C NMR (98.5 MHz, $CDCl_3$) δ 28.3 (3C), 37.4 (br), 46.6 (br), 61.2 (br), 67.3 (br), 80.2, 120.1, 126.5, 126.6 (2C), 126.7, 127.6 (2C), 128.6 (3C), 144.4, 146.0, 155.5; HRMS (FAB): *m/z* $[M+H]^+$ calcd for $C_{21}H_{24}NO_2$ 322.1807, found 322.1804; Anal. Calcd for $C_{21}H_{23}NO_2$ C, 78.47; H, 7.21; N, 4.36. Found C, 78.22; H, 7.31; N, 4.20. $[\alpha]^{25}_D$ +63.7 (*c* 1.0, CH_2Cl_2). All analytical data are in good accordance with those reported in the literature.[9]

***tert*-Butyl (1*S*,2*R*,4*R*)-2-(4-fluorophenyl)-1,2,3,4-tetrahydro-1,4-epiminonaphthalene-11-carboxylate (3b)** (Table 3)

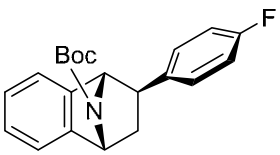

The reaction was carried out according to the general procedure using *tert*-butyl 1,4-dihydro-1,4-epiminonaphthalene-11-carboxylate (**1a**; 122.0 mg, 0.50 mmol), 4-fluorophenylmagnesium bromide (1.60 mL, 1.00 M in THF

solution, 3.2 equiv.) and $ZnCl_2$ (0.85 mL of 1.0 M solution in THF, 1.7 equiv). Reaction was run at –20 °C for 12 h. The crude product was purified by silica gel column chromatography (hexane/AcOEt = 95/5) to give the title product in 95% yield (161.9 mg, 83% ee) as a white solid. The ee was determined by HPLC on a CHIRALCEL IC-3 column (4.6 mm i.d.; 150 mm length) with following conditions: hexane/IPA = 99/1, 1.0 mL/min, 4.3 °C. Retention times (t_r) = 6.25 min (major) and 6.80 min (minor);

M.p. 78.3–80.9 °C; IR (neat) ν 568, 639, 754, 824, 900, 1087, 1138, 1164, 1230, 1281, 1363, 1419, 1509, 1606, 1692, 2977 cm^{-1}; ^1H NMR ($CDCl_3$, 391.8 MHz) δ 1.32 (s, 9H), 1.93 (dd, *J* = 11.9, 8.7 Hz, 1H), 2,13 (dt, *J* = 12.1, 4.5 Hz, 1H), 2.82 (dd, *J* = 8.6, 4.5 Hz, 1H), 5.02 (br, 1H), 5.23 (br, 1H), 7.00 (t, *J* = 8.7 Hz, 2H), 7.14–7.17 (m, 2H), 7.29–7.35 (m, 4H); ^{13}C NMR ($CDCl_3$, 98.5 MHz) δ 28.3 (3C), 37.8 (br), 45.8 (br), 61.3 (br), 67.5 (br), 80.3, 115.3 (d, $J_{C\text{-}F}$ = 20.7 Hz, 2C), 120.1, 126.6 (2C), 126.7 (2C), 129.0 (d, $J_{C\text{-}F}$ = 7.5 Hz, 2C), 140.2 (d, $J_{C\text{-}F}$ = 2.8 Hz, 1C), 146.0, 155.7, 161.7 (d, $J_{C\text{-}F}$ = 244.3 Hz, 1C); HRMS (FAB): *m/z* $[M+H]^+$ calcd for $C_{21}H_{23}FNO_2$ 340.1713, found 340.1714; Anal. Calcd for $C_{21}H_{22}FNO_2$ C, 74.31; H, 6.53; N, 4.13; F, 5.60. Found C, 74.30; H, 6.64; N, 4.07; F, 5.61. $[\alpha]^{25}_D$ +55.8 (*c* 1.0, CH_2Cl_2).

***tert*-Butyl (1*S*,2*R*,4*R*)-2-(3,4-dichlorophenyl)-1,2,3,4-tetrahydro-1,4-epiminonaphthalene-11-carboxylate (3c)** (Table 3)

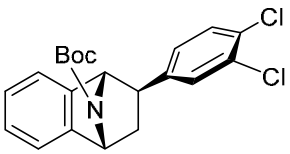

The reaction was carried out according to the general procedure using *tert*-butyl 1,4-dihydro-1,4-epiminonaphthalene-11-carboxylate (**1a**; 121.9 mg, 0.50 mmol), 3,4-dichlorophenylmagnesium bromide (3.2 mL, 0.50 M in THF solution, 3.2 equiv.) and $ZnCl_2$ (0.75 mL of 1.0 M solution in THF, 1.7 equiv). Reaction was run at 0 °C for 16 h. The crude product was purified by silica gel column chromatography (hexane/AcOEt = 95/5) to give the title product in 85% yield (166.2 mg, 77% ee) as a white solid.

The ee was determined by HPLC on a CHIRALCEL IC-3 column (4.6 mm i.d.; 150 mm length) with following conditions: hexane/IPA = 99/1, 1.0 mL/min, 5.3 °C. Retention times (t_r) = 7.56 min (major) and 8.07 min (minor);

M.p. 88.8–90.1 °C; IR (neat) ν 572, 705, 757, 792, 814, 949, 892, 905, 1027, 1075, 1089, 1140, 1153, 1169, 1288, 1259, 1273, 1290, 1328, 1366, 1392, 1461, 1476, 1560, 1679, 2974 cm^{-1}; ^1H NMR ($CDCl_3$, 391.8 MHz) δ 1.34 (s, 9H), 1.93 (dd, *J* = 11.9, 8.7 Hz, 1H), 2.13 (dt, *J* = 11.8, 4.5 Hz, 1H), 2.78 (dd, *J* = 8.6, 4.5 Hz, 1H), 5.02 (br, 1H), 5.24 (br, 1H), 7.15–7.18 (m, 2H), 7.21 (d, *J* = 9.0 Hz, 1H), 7.29 (t, *J* = 3.4 Hz, 2H), 7.36 (d, *J* = 8.5 Hz, 1H), 7.48 (s, 1H); ^{13}C NMR ($CDCl_3$, 98.5 MHz) δ 28.3 (3C), 37.9 (br), 45.5 (br), 61.1

(br), 67.1, 80.6, 120.2, 126.7 (2C), 126.9, 127.1, 129.5, 130.5 (2C), 132.5, 144.8 (2C), 145.9, 155.3; HRMS (FAB): *m/z* $[M+H]^+$ calcd for $C_{21}H_{22}Cl_2NO_2$ 390.1028, found 390.1029; Anal. Calcd for $C_{21}H_{21}Cl_2NO_2$ C, 64.62; H, 5.42; N, 3.59. Found C, 64.78; H, 5.53; N, 3.61. $[\alpha]^{25}_D$ +58.6 (*c* 1.0, CH_2Cl_2).

***tert*-Butyl (1*S*,2*R*,4*R*)-2-(4-methoxyphenyl)-1,2,3,4-tetrahydro-1,4-epiminonaphthalene-11-carboxylate (3d)** (Table 3)

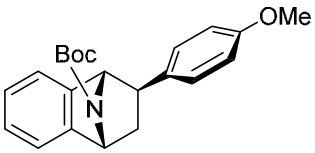

The reaction was carried out according to the general procedure using *tert*-butyl 1,4-dihydro-1,4-epiminonaphthalene-11-carboxylate (**1a**; 121.7 mg, 0.50 mmol), 4-methoxyphenylmagnesium bromide (1.52 mL, 1.05 M in THF solution, 3.2 equiv.) and $ZnCl_2$ (0.85 mL of 1.0 M solution in THF, 1.7 equiv). Reaction was run at –20 °C for 12 h. The crude product was purified by silica gel column chromatography (hexane/AcOEt = 95/5) to give the title product in 99% yield (173.9 mg, 80% ee) as a white solid.

The ee was determined by HPLC on a CHIRALCEL IC-3 column (4.6 mm i.d.; 150 mm length) with following conditions: hexane/IPA = 90/10, 1.0 mL/min, 4.5 °C. Retention times (t_r) = 6.08 min (major) and 6.78 min (minor);

M.p. 78.0–80.2 °C; IR (neat) ν 656, 762, 790, 819, 903, 1031, 1081, 1141, 1156, 1168, 1245, 1284, 1339, 1459, 1512, 1608, 1693, 2977, 3024cm^{-1}; ^1H NMR ($CDCl_3$, 391.8 MHz) δ 1.32 (s, 9H), 1.91 (dd, *J* = 11.9, 8.7 Hz, 1H), 2.14 (dt, *J* = 12.1, 4.5 Hz, 1H), 2.79, (dd, *J* = 8.6, 4.5 Hz, 1H), 3.80 (s, 3H), 5.01 (br, 1H), 5.24 (br, 1H), 6.86 (d, *J* = 8.9 Hz, 2H*),* 7.13–7.16 (m, 2H), 7.27–7.30 (m, 4H); ^{13}C NMR ($CDCl_3$, 98.5 MHz) δ 28.3 (3C), 37.4 (br), 45.8 (br), 55.4, 61.0 (br), 67.6 (br), 80.1, 113.9 (2C), 120.0, 126.4 (2C), 126.5 (2C), 128.5 (2C), 136.5, 146.0, 155.6, 158.3; HRMS (FAB): *m/z* $[M+H]^+$ calcd for $C_{22}H_{26}NO_3$ 352.1913, found 352.1912; Anal. Calcd for $C_{22}H_{25}NO_3$ C, 75.19; H, 7.17; N, 3.99. Found C, 75.08; H, 7.26; N, 3.98. $[\alpha]^{25}_D$ +71.6 (*c* 1.0, CH_2Cl_2).

***tert*-Butyl (1*S*,2*R*,4*R*)-2-(4-methylphenyl)-1,2,3,4-tetrahydro-1,4-epiminonaphthalene-11-carboxylate (3e)** (Table 3)

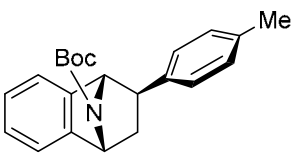

The reaction was carried out according to the general procedure using *tert*-butyl 1,4-dihydro-1,4-epiminonaphthalene-11-carboxylate (**1a**; 122.0 mg, 0.50 mmol), 4-methylphenylmagnesium bromide (1.53 mL, 1.04 M in THF solution, 3.2 equiv.) and $ZnCl_2$ (0.85 mL of 1.0 M solution in THF, 1.7 equiv). Rection was run at –20 °C for 24 h. The crude product was purified by silica gel column

chromatography (hexane/AcOEt = 95/5) to give the title product in 91% yield (160.6 mg, 81% ee) as a white solid.

The ee was determined by HPLC on a CHIRALCEL IC-3 column (4.6 mm i.d.; 150 mm length) with following conditions: hexane/IPA = 99/1, 1.0 mL/min, 5.3 °C. Retention times (t_r) = 8.10 min (major) and 9.10 min (minor);

M.p. 91.4–93.1 °C; IR (neat) ν 655, 718, 732, 778, 807, 825, 842, 854, 871, 909, 939, 1007, 1020, 1088, 1134, 1156, 1174, 1254, 1282, 1365, 1385, 1459, 1514, 1691, 2974 cm^{-1}; ^1H NMR ($CDCl_3$, 391.8 MHz) δ 1.32 (s, 9H), 1.92 (dd, *J* = 11.9, 8.7 Hz, 1H), 2.17 (dt, *J* = 11.9, 4.5 Hz, 1H), 2.34 (s, 3H), 2.80 (dd, *J* = 8.7, 4.5 Hz, 1H), 5.04 (br, 1H), 5.24 (br, 1H), 7.12–7.17 (m, 4H), 7.26 (d, *J* = 8.2 Hz, 4H*);* ^{13}C NMR ($CDCl_3$, 98.5 MHz) δ 20.9, 28.2 (3C), 37.3 (br), 46.0 (br), 61.0 (br), 67.4, 79.9, 119.9, 126.3, 126.4 (2C), 127.3 (2C), 128.9 (3C), 135.9, 141.2, 145.9, 155.4; HRMS (FAB): *m/z* $[M+H]^+$ calcd for $C_{22}H_{26}NO_2$ 336.1964, found 336.1962; Anal. Calcd for $C_{22}H_{25}NO_2$ C, 78.77; H, 7.51; N, 4.18. Found C, 78.74; H, 7.63; N, 4.07. $[\alpha]^{25}_D$ +73.0 (*c* 1.0, CH_2Cl_2).

***tert*-Butyl (1*S*,2*R*,4*R*)-2-(3-methylphenyl)-1,2,3,4-tetrahydro-1,4-epiminonaphthalene-11-carboxylate (3f)** (Table 3)

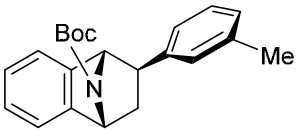

The reaction was carried out according to the general procedure using *tert*-butyl 1,4-dihydro-1,4-epiminonaphthalene-11-carboxylate (**1a**; 121.8 mg, 0.50 mmol), 3-methylphenylmagnesium bromide (2.05 mL, 0.78 M in THF solution, 3.2 equiv.) and $ZnCl_2$ (0.85 mL of 1.0 M solution in THF, 1.7 equiv). Reaction was run at –20 °C for 18 h. The crude product was purified by silica gel column chromatography (hexane/AcOEt = 95/5) to give the title product in 88% yield (147.6 mg, 85% ee) as a white solid.

The ee was determined by HPLC on a CHIRALCEL IC-3 column (4.6 mm i.d.; 150 mm length) with following conditions: hexane/IPA = 99/1, 1.0 mL/min, 5.3 °C. Retention times (t_r) = 7.02 min (major) and 7.48 min (minor);

M.p. 81.6–82.1 °C; IR (neat) ν 660, 781, 797, 821, 851, 872, 907, 1022, 1092, 1140, 1154, 1173, 1250, 1290, 1368, 1393, 1459, 1597, 1692, 2982 cm^{-1}; ^1H NMR ($CDCl_3$, 391.8 MHz) δ 1.32 (s, 9H), 1.91 (dd, *J* = 11.9, 8.7 Hz, 1H), 2.18 (dt, *J* = 11.8, 4.5 Hz, 1H), 2.35 (s, 3H), 2.80 (dd, *J* = 8.7, 4.5 Hz, 1H), 5.07 (br, 1H), 5.25 (br, 1H), 7.04 (d, *J* = 7.3 Hz, 1H), 7.13–7.23 (m, 5H), 7.25–7.29 (m, 2H); ^{13}C NMR ($CDCl_3$, 98.5 MHz) δ 21.6, 28.3 (3C), 37.4 (br), 46.5 (br), 60.9 (br), 67.3, 80.1, 119.8, 124.6, 126.5 (2C), 126.6, 127.3 (2C), 128.3, 128.5, 138.1, 144.4, 146.0, 155.4; HRMS (FAB): *m/z* $[M+Na]^+$ calcd for $C_{22}H_{25}NO_2Na$ 358.1783, found 358.1782; Anal. Calcd for $C_{22}H_{25}NO_2$ C, 78.77; H, 7.51; N, 4.18. Found C, 78.57; H, 7.59; N, 4.16. $[\alpha]^{25}_D$ +64.1 (*c* 1.0, CH_2Cl_2).

***tert*-Butyl (1*S*,2*R*,4*R*)-2-(2-methylphenyl)-1,2,3,4-tetrahydro-1,4-epiminonaphthalene-11-carboxylate (3g)** (Table 3)

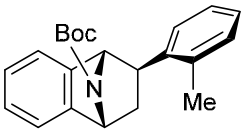

The reaction was carried out according to the general procedure using *tert*-butyl 1,4-dihydro-1,4-epiminonaphthalene-11-carboxylate (**1a**; 127.7 mg, 0.52 mmol), 2-methylphenylmagnesium bromide (1.48 mL, 1.08 M in THF solution, 3.2 equiv.) and $ZnCl_2$ (0.85 mL of 1.0 M solution in THF, 1.7 equiv). Reaction was run at 0 °C for 24 h. The crude product was purified by silica gel column chromatography (hexane/AcOEt = 95/5) to give the title product in 93% yield (163.8 mg, 99% ee) as a white solid.

The ee was determined by HPLC on a CHIRALCEL IC-3 column (4.6 mm i.d.; 150 mm length) with following conditions: hexane/IPA = 99/1, 1.0 mL/min, 4.4 °C. Retention times (t_r) = 7.31 min (major) and 7.56 min (minor);

M.p. 63.7–65.3 °C; IR (neat) ν 752, 762, 854, 908, 1086, 1138, 1157, 1175, 1265, 1364, 1376, 1459, 1693, 2954, 2972 cm^{-1}; ^1H NMR ($CDCl_3$, 391.8 MHz) δ 1.34 (s, 9H), 1.94–2.06 (m, 2H), 2.21 (s, 3H), 2.97 (dd, *J* = 8.5, 4.9 Hz, 1H), 5.22 (br, 2H), 7.13–7.18 (m, 4H), 7.19–7.25 (m, 1H), 7.30 (br, 2H), 7.55 (d, *J* = 8.0 Hz, 1H); ^{13}C NMR ($CDCl_3$, 98.5 MHz) δ 20.0, 28.3 (3C), 36.6 (br), 42.0 (br), 61.4 (br), 66.2 (br), 80.2, 120.2, 125.6, 126.2 (2C), 126.5 (2C), 126.6 (2C), 130.1, 135.9, 142.6, 146.3, 155.5; HRMS (FAB): *m/z* $[M+H]^+$ calcd for $C_{22}H_{26}NO_2$ 336.1964, found 336.1966; Anal. Calcd for $C_{22}H_{25}NO_2$ C, 78.77; H, 7.51; N, 4.18. Found C, 78.71; H, 7.43; N, 4.12. $[\alpha]^{25}_D$ +123.4 (*c* 1.0, CH_2Cl_2).

***tert*-Butyl (1*S*,2*R*,4*R*)-2-(2-methoxyphenyl)-1,2,3,4-tetrahydro-1,4-epiminonaphthalene-11-carboxylate (3h)** (Table 3)

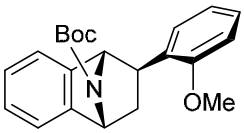

The reaction was carried out according to the general procedure using *tert*-butyl 1,4-dihydro-1,4-epiminonaphthalene-11-carboxylate (**1a**; 128.0 mg, 0.53 mmol), 2-methoxyphenylmagnesium bromide (1.68 mL, 0.95 M in THF solution, 3.2 equiv.) and $ZnCl_2$ (0.85 mL of 1.0 M solution in THF, 1.7 equiv). Reaction was run at 0 °C for 24 h. The crude product was purified by silica gel column chromatography (hexane/AcOEt = 95/5) to give the title product in 90% yield (165.0 mg, 93% ee) as a white solid.

The ee was determined by HPLC on a CHIRALCEL IC-3 column (4.6 mm i.d.; 150 mm length) with following conditions: hexane/IPA = 99/1, 1.0 mL/min, 5 °C. Retention times (t_r) = 10.02 min (major) and 11.23 min (minor);

M.p. 149.6–151.7 °C; IR (neat) ν 662, 753, 764, 902, 911, 1029, 1120, 1137, 1156, 1176, 1238, 1347, 1357, 1458, 1493, 1601, 1686, 2939, 2989 cm^{-1}; ^1H NMR ($CDCl_3$, 391.8

MHz) δ 1.32 (s, 9H), 1.91 (t, J = 10.1 Hz, 1H), 2.05 (br, 1H), 3.20 (dd, J = 8.1, 4.9 Hz, 1H), 3.78 (s, 3H), 5.18 (br, 2H), 6.84 (d, J = 8.1 Hz, 1H), 6.97 (t, J = 7.2 Hz, 1H), 7.13–7.30 (m, 5H), 7.51 (d, J = 7.2 Hz, 1H); ^{13}C NMR ($CDCl_3$, 98.5 MHz) δ 28.3 (3C), 35.6 (br), 39.3 (br), 55.4, 61.0 (br), 66.1 (br), 80.0, 110.0, 120.0, 120.8, 126.4, 126.5 (2C), 126.6, 127.3 (2C), 132.6, 146.2, 155.2, 157.2; HRMS (FAB): *m/z* $[M+H]^+$ calcd for $C_{22}H_{26}NO_3$ 352.1913, found 352.1913; Anal. Calcd for $C_{22}H_{25}NO_3$ C, 75.19; H, 7.17; N, 3.99. Found C, 75.09; H, 7.25; N, 3.95. $[\alpha]^{25}_D$ +92.6 (*c* 1.0, CH_2Cl_2).

***tert*-Butyl (1*S*,2*R*,4*R*)-2-(naphthalen-1-yl)-1,2,3,4-tetrahydro-1,4-epiminonaphthalene-11-carboxylate (3i)** (Table 3)

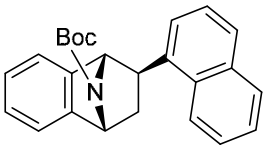

The reaction was carried out according to the general procedure using *tert*-butyl 1,4-dihydro-1,4-epiminonaphthalene-11-carboxylate (**1a**; 126.3 mg, 0.52 mmol), 1-naphtyhlmagnesium bromide (4.95 mL, 0.323 M in THF solution, 3.2 equiv.) and $ZnCl_2$ (0.85 mL of 1.0 M solution in THF, 1.7 equiv). Reaction was run at 0 °C for 24 h. The crude product was purified by silica gel column chromatography (hexane/AcOEt = 95/5) to give the title product in 90% yield (168.1 mg, 97% ee) as a white solid.

The ee was determined by HPLC on a CHIRALCEL IC-3 column (4.6 mm i.d.; 150 mm length) with following conditions: hexane/IPA = 99/1, 1.0 mL/min, 4.3 °C. Retention times (t_r) = 11.50 min (major) and 15.75 min (minor);

M.p. 120.4–121.1 °C; IR (neat) ν 600, 756, 775, 795, 904, 1089, 1140, 1156, 1168, 1251, 1334, 1364, 1459, 1597, 1689, 2952, 2976 cm^{-1}; ^{1}H NMR ($CDCl_3$, 391.8 MHz) δ 1.34 (s, 9H), 2.15 (br, 2H), 3.55 (t, J = 5.8 Hz, 1H), 5.29 (br, 2H), 7.19–7.21 (m, 2H), 7.32–7.45 (m, 4H), 7.49 (t, J = 7.8 Hz, 1H), 7.73 (d, J = 8.0 Hz 2H), 7.79–7.86 (m, 2H); ^{13}C NMR ($CDCl_3$, 98.5 MHz) δ 28.4 (3C), 37.4 (br), 41.6 (br), 61.5 (br), 65.9 (br), 80.2, 120.2 (br), 122.6, 123.3 (2C), 125.5, 126.0, 126.7 (2C), 126.8, 126.9, 129.0 (2C), 131.9, 133.9, 140.0, 146.4, 155.5; HRMS (FAB): *m/z* $[M+H]^+$ calcd for $C_{25}H_{26}NO_2$ 372.1964, found 372.1965. Anal. Calcd for $C_{25}H_{25}NO_2$ C, 80.83; H, 6.78; N, 3.77. Found C, 80.85; H, 6.97; N, 3.68. $[\alpha]^{25}_D$ +139.9 (*c* 1.0, CH_2Cl_2).

***tert*-Butyl (1*S*,2*R*,4*R*)-9-(phenanthrene-1-yl)-1,2,3,4-tetrahydro-1,4-epiminonaphthalene-11-carboxylate (3j)** (Table 3)

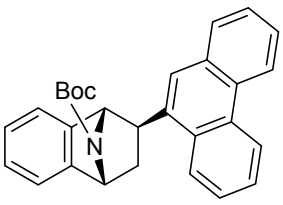

The reaction was carried out according to the general procedure using *tert*-butyl 1,4-dihydro-1,4-epiminonaphthalene-11-carboxylate (**1a**; 122.0 mg, 0.50 mmol), 9-phenanthryhlmagnesium bromide (3.01 mL, 0.53 M in THF

solution, 3.2 equiv.) and $ZnCl_2$ (0.85 mL of 1.0 M solution in THF, 1.7 equiv). Reaction was run at –20 °C for 21 h. The crude product was purified by silica gel column chromatography (hexane/AcOEt = 95/5) to give the title product in 75% yield (158.1 mg, 96% ee) as a white solid.

The ee was determined by HPLC on a CHIRALCEL IC-3 column (4.6 mm i.d.; 150 mm length) with following conditions: hexane/IPA = 95/5, 1.0 mL/min, 5 °C. Retention times (t_r) = 6.16 min (major) and 6.95 min (minor);

M.p. 100.4–102.1 °C; IR (neat) ν 660, 781, 797, 821, 851, 872, 907, 1022, 1092, 1140, 1155, 1173, 1250, 1290, 1368, 1393, 1459, 1597, 1692, 2982 cm^{-1}; ^1H NMR ($CDCl_3$, 391.8 MHz) δ 1.37 (s, 9H), 2.19 (br, 2H), 3.55 (t, *J* = 6.7 Hz, 1H), 5.32 (br, 1H), 5.50 (br, 1H), 7.22–7.25 (m, 2H), 7.37–7.41 (m, 2H), 7.57–7.65 (m, 4H), 7.87–7.96 (m, 3H), 8.66 (d, *J* = 7.6 Hz, 1H), 8.75 (d, *J* = 7.7 Hz, 1H); ^{13}C NMR ($CDCl_3$, 98.5 MHz) δ 28.5 (3C), 36.6 (br), 42.4 (br), 60.9 (br), 65.9 (br), 80.3, 120.3 (br), 122.4, 123.4, 123.5 (2C), 124.0, 126.3, 126.4, 126.7 (2C), 126.8 (2C), 128.9, 129.6, 130.8, 131.3, 132.0, 138.0 (2C), 146.5, 155.1; HRMS (FAB): *m/z* $[M]^+$ calcd for $C_{29}H_{27}NO_2$ 421.2042, found 421.2040. $[\alpha]^{25}_D$ +187.7 (*c* 1.0, CH_2Cl_2).

***tert*-Butyl (1*S*,2*R*,4*R*)-2-(6-chloropyridin-3-yl)-1,2,3,4-tetrahydro-1,4-epiminonaphthalene-9-carboxylate (3k)** (Table 3)

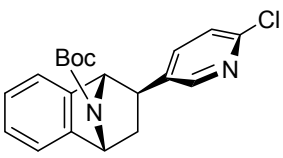

In a Schlenk tube under inert atmosphere, 5-bromo-2-chloropyridine (308 mg, 1.6 mmol) was dissolved in THF (2.0 mL). After cooling to 0 °C, *i*-PrMgCl·LiCl (1.24 mL, 1.6 mmol, 1.292 M in THF) was added dropwise to the reaction mixture and it was stirred for 4 h at 0 °C. A THF solution of $ZnCl_2$ (0.84 mL, 1.0 M) was added to the reaction mixture and stirred for 1.5 h. Then, the solvent was removed and the resulting $Ar_2Zn{\cdot}2MgCl_2$ was dried for 45 minutes under vacuum. To the arylzinc, a mixture of (*S,S*)-CHIRAPHOS (17.1 mg, 0.04 mmol), THF (0.80 mL), toluene (3.0 mL), and $FeCl_3$(200 μL, 0.1 M solution in THF, 0.02mmol) was added followed by the addition of azabicyclic alkene (**1a**, 97 mg, 0.40 mmol) and the reaction mixture was stirred at 30 ºC for 36 h. Degassed AcOH/MeOH (1:4) was added at 0 °C for quenching. The mixture was stirred for 10 minutes and then saturated aqueous NH_4Cl (1.0 mL) and MTBE were added. The separated aqueous layer was extracted with additional portions of MTBE (5 mL × 3). The combined organic extracts were passed through a pad of Florisil® and the filtrate was concentrated *in vacuo*. The residue was purified by silica gel column chromatography (hexane/AcOEt = 80/20) to give the title product in 84% yield (119.9 mg, 45% ee) as a white solid.

The ee was determined by HPLC on a CHIRALCEL IC-3 column (4.6 mm i.d.; 150 mm length).

M.p. 102.8–105.3 °C; IR (neat) ν 553, 633, 684, 736, 761, 830, 899, 1084, 1099, 1128, 1141, 1155, 1168, 1269, 1286, 1364, 1388, 1458, 1698, 2980 cm^{-1}; ^1H NMR ($CDCl_3$, 391.8 MHz) δ 1.32 (s, 9H), 1.97 (dd, *J* = 11.9, 8.7 Hz, 1H), 2.12 (dt, *J* = 11.9, 4.5 Hz, 1H), 2.84 (dd, *J* = 8.6, 4.5 Hz, 1H), 5.00 (br, 1H), 5.25 (br, 1H), 7.17–7.20 (m, 2H), 7.27–7.33 (m, 3H),7.76 (dd, *J* = 8.5, 1.8 Hz, 1H), 8.32 (d, *J* = 1.8 Hz, 1H); ^{13}C NMR ($CDCl_3$, 98.5 MHz) δ 28.3 (3C), 37.8 (br), 43.0 (br), 61.6 (br), 67.2, 80.7, 120.2, 124.3, 126.8 (2C), 127.0, 137.6, 139.0, 145.1, 145.8, 149.1, 149.8, 155.7; HRMS (ESI-FT-ICR): *m/z* $[M+H]^+$ calcd for $C_{20}H_{21}ClN_2O_2$ 357.13643, found 357.13895. Anal. Calcd for $C_{20}H_{21}ClN_2O_2 \cdot (H_2O)_{0.25}$ C, 66.48; H, 6.00; N, 7.75. Found C, 66.64; H, 5.94; N, 7.73. $[\alpha]^{25}_D$ +37.9 (*c* 1.0, CH_2Cl_2).

***tert*-Butyl (1*S*,2*R*,4*R*)-6,7-difluoro-2-phenyl-1,2,3,4-tetrahydro-1,4-epiminonaphthalene-11-carboxylate (3l)** (Table 3)

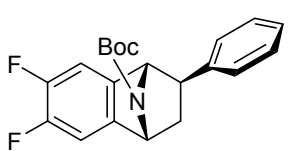

The reaction was carried out according to the general procedure using *tert*-butyl 6,7-difluoro-1,4-dihydro-1,4-epiminonaphthalene-11-carboxylate (**1c**; 134 mg, 0.48mmol), phenylmagnesium bromide (1.73 mL, 0.92 M in THF solution, 3.2 equiv.) and $ZnCl_2$ (0.85 mL of 1.0 M solution in THF, 1.7 equiv). Reaction was run at –20 °C for 24 h. The crude product was purified by silica gel column chromatography (hexane/AcOEt = 95/5) to give the title product in 85% yield (132.9 mg, 78% ee) as a white solid.

The ee was determined by HPLC on a CHIRALCEL IC-3 column (4.6 mm i.d.; 150 mm length) with following conditions: hexane/IPA = 99/1, 1.0 mL/min, 5 °C. Retention times (t_r) = 5.93min (major) and 8.02 min (minor);

M.p. 103.4–105.1 °C; IR (neat) ν 702, 733, 772, 805, 858, 891, 911, 1052, 1082, 1132, 1149, 1162, 1264, 1285, 1296, 1368, 1477, 1612, 1694, 2975 cm^{-1}; ^1H NMR ($CDCl_3$, 391.8 MHz) δ 1.34 (s, 9H), 1.90 (dd, *J* = 12.1, 8.9 Hz, 1H), 2.19 (dt, *J* = 12.1, 4.5 Hz, 1H), 2.78 (dd, *J* = 8.9, 4.5 Hz, 1H), 5.04 (br, 1H), 5.21 (br, 1H), 7.13 (t, *J* = 8.3 Hz, 2H), 7.23–7.37 (m, 5H); ^{13}C NMR ($CDCl_3$, 98.5 MHz) δ 28.3 (3C), 37.6 (br), 46.2 (br), 61.3 (br), 67.1, 80.8, 110.1,126.8 (2C), 127.5 (2C), 128.7 (3C), 142.1, 143.8, 149.2 (ddd, *J* = 248.5, 15.5, 10.7 Hz, 2C), 155.6; HRMS (FAB): *m/z* $[M+Na]^+$calcd for $C_{21}H_{21}F_2NO_2Na$ 380.1438, found 380.1439; Anal. Calcd for $C_{21}H_{21}F_2NO_2$ C, 70.57; H, 5.92; N, 3.92. Found C, 70.29; H, 6.06; N, 3.74. $[\alpha]^{25}_D$ +56.6 (*c* 1.0, CH_2Cl_2).

***tert*-Butyl (1*S*,2*R*,4*R*)-6,7-dimethoxy-2-phenyl-1,2,3,4-tetrahydro-1,4-epiminonaphthalene-11-carboxylate (3m)** (Table 3)

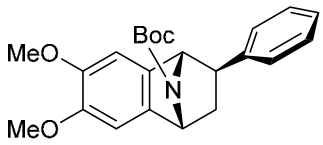

The reaction was carried out according to the general procedure using *tert*-butyl 6,7-dimethoxy-1,4-dihydro-1,4-epiminonaphthalene-11-carboxylate(**1b**; 141.2 mg, 0.465 mmol), phenylmagnesium bromide (1.74 mL, 0.92 M in THF solution, 3.2 equiv.) and $ZnCl_2$ (0.85 mL of 1.0 M solution in THF, 1.7 equiv). Reaction was run at –20 °C for 24 h. The crude product was purified by silica gel column chromatography (hexane/AcOEt = 90/10) to give the title product in 91% yield (161.5 mg, 75% ee) as a white solid.

The ee was determined by HPLC on a CHIRALCEL IC-3 column (4.6 mm i.d.; 150 mm length) with following conditions: hexane/IPA = 30/70, 1.0 mL/min, 5 °C. Retention times (t_r) = 5.93 min (major) and 7.08 min (minor);

M.p. 111.6–112.9 °C; IR (neat) ν 675, 702, 755, 801, 827, 882, 899, 915, 1071, 1174, 1216, 1247, 1260, 1283, 1303, 1375, 1453, 1469, 1490, 1606, 1684, 2945 cm^{-1}; ^1H NMR ($CDCl_3$, 391.8 MHz) δ 1.34 (s, 9H), 1.89 (dd, *J* = 11.7, 8.9 Hz, 1H), 2.15 (dt, *J* = 11.7, 4.5 Hz, 1H), 2.77 (dd, *J* = 8.8, 4.5 Hz, 1H), 3.89 (s, 6H), 5.01 (br, 1H), 5.21 (br, 1H), 6.92 (s, 2H), 7.21–7.25 (m, 1H), 7.31 (t, *J* = 7.6 Hz, 2H), 7.37 (d, *J* = 7.8 Hz, 2H); ^{13}C NMR ($CDCl_3$, 98.5 MHz) δ 28.4 (3C), 37.8 (br), 47.1 (br), 56.3 (2C), 61.5 (br), 67.5 (br), 80.2, 105.0 (br), 126.5 (2C), 127.5 (2C), 128.6 (3C), 138.2, 144.5, 147.7, 147.8, 155.6; HRMS (FAB): *m/z* $[M+H]^+$ calcd for $C_{23}H_{28}NO_4$ 382.2018, found 382.2019; Anal. Calcd for $C_{23}H_{27}NO_4$ C, 72.42; H, 7.13; N, 3.67. Found C, 72.36; H, 7.22; N, 3.67. $[\alpha]^{25}_D$ +67.4 (*c* 1.0, CH_2Cl_2).

***tert*-Butyl (1*R*,2*R*,4*S*)-2-phenyl-7-azabicyclo[2.2.1]heptane-7-carboxylate (3n)** (Table 3)

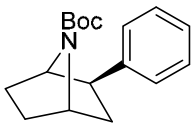

The reaction was carried out according to the general procedure using azabicyclic alkene (**1d**; 92 μL, 0.50 mmol), phenylmagnesium bromide (1.73 mL, 0.92 M in THF solution, 3.2 equiv.) and $ZnCl_2$ (0.85 mL of 1.0 M solution in THF, 1.7 equiv). Reaction was run at 30 °C for 16 h. The crude product was purified by silica gel column chromatography (hexane/AcOEt = 95/5) to give the title product in 67% yield (92.1 mg, 75% ee) as a white solid.

The ee was determined by HPLC on a CHIRALCEL IC-3 column (4.6 mm i.d.; 150 mm length) with following conditions: hexane/IPA = 90/10, 1.0 mL/min, 5.3 °C. Retention times (t_r) = 4.33 min (minor) and 5.36 min (major);

M.p. 61.6–63.3°C; IR (neat) ν 530, 707, 761, 856, 891, 902, 1087, 1128, 1150, 1182, 1251,

1319, 1364, 1383, 1455, 1686, 2878, 2929, 2973, 3012 cm^{-1}; ^1H NMR ($CDCl_3$, 391.8 MHz) δ 1.41 (s, 9H), 1.48–1.59 (m, 2H), 1.82–1.98 (m, 4H), 2.86 (dd, *J* = 8.5, 5.8 Hz, 1H), 4.23 (br, 1H), 4.36 (br, 1H), 7.15–7.20 (m, 1H), 7.25–7.28 (m, 4H); ^{13}C NMR ($CDCl_3$, 98.5 MHz) δ 28.4 (3C), 28.9 (br), 30.4 (br), 40.3 (br), 48.4 (br), 55.7 (br), 62.2 (br), 79.5, 126.2 (2C), 127.2, 128.5 (2C), 145.9, 155.2; Anal. Calcd for $C_{17}H_{23}NO_2$ C, 74.69; H, 8.48; N, 5.12. Found C, 74.42; H, 8.51; N, 5.12. $[\alpha]^{25}_D$ +18.0 (*c* 1.0, CH_2Cl_2).

***tert*-Butyl (1*S*,2*R*,3*R*,4*R*)-2-(2-methylphenyl)-1,2,3,4-tetrahydro-1,4-epiminonaphthalene-11-carboxylate-3-*d* (5a)** (Table 4)

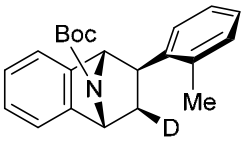

$ZnCl_2$ (545.2 mg, 4.0 mmol) was dried by fusing *in vacuo* and cooled quickly followed by addition of 4.0 mL of THF to prepare a 1.0 M THF solution of $ZnCl_2$. After stirring for 20 minutes, the THF solution of $ZnCl_2$ (0.85 mL, 1.0 M) was transferred to the other Schlenk flask, and 2-methylphenylmagnesium bromide (1.48 mL, 1.08 M solution in THF, 3.2 equiv.) was added at 0 °C and stirred for 2.0 hours. Then, the solvent was removed and the resulting arylzinc reagent was dried for 10 minutes under vacuum. To the arylzinc powder, a mixture of (*S,S*)-Chiraphos (8.5 mg, 0.020 mmol), THF (0.70 mL), toluene (3.2 mL), and $FeCl_3$ (1.62 mg, 0.01mmol) in THF (0.1 M, 100 μL) was added, followed by the addition of azabicyclic alkene (**1a**, 127.7 mg, 0.52 mmol) and the reaction mixture was stirred for 24 h at 0 °C. Degassed CD_3COOD/CD_3OD (1:4) was added at –78 °C for quenching. The mixture was stirred overnight at rt and then saturated aqueous NH_4Cl (1.0 mL) and MTBE were added. The separated aqueous layer was extracted with additional portions of MTBE (5 mL × 3). The combined organic extracts were passed through a pad of Florisil® and the filtrate was concentrated *in vacuo*. The product was purified by flash chromatography on silica gel (hexane/AcOEt = 95/5) to give the title compound in 96% yield (172.8 mg, 99% ee) as white solid.

The ee was determined by HPLC on a CHIRALCEL IC-3 column (4.6 mm i.d.; 150 mm length) with following conditions: hexane/IPA = 99/1, 1.0 mL/min, 4.3 °C. Retention times (t_r) = 7.08 min (major) and 7.72 min (minor);

M.p. 149.7–152.9 °C; IR (neat) ν 564, 588, 659, 744, 760, 847, 905, 1086, 1157, 1276, 1364, 1376, 1458, 1692, 2964 cm^{-1}; ^1H NMR ($CDCl_3$, 391.8 MHz) δ 1.34 (s, 9H), 1.95 (d, *J* = 8.5 Hz, 1H), 2.21 (s, 3H), 2.97 (d, *J* = 8.9 Hz, 1H), 5.22 (br, 2H), 7.14 (d, *J* = 4.9 Hz, 2H), 7.16–7.18 (m, 2H), 7.20–7.24 (m, 1H), 7.30 (br, 2H), 7.55 (d, *J* = 7.6 Hz, 1H); ^{13}C NMR ($CDCl_3$, 98.5 MHz) δ 20.1, 28.4 (3C), 36.3 (br), 42.1 (br), 61.6 (br), 66.0 (br), 80.2, 119.9 (br), 125.6, 126.3 (2C), 126.6 (2C), 126.7, 130.2 (2C), 135.9, 142.6, 146.3, 155.4; Anal. Calcd for $C_{22}H_{24}NO_2$ C, 78.54; H, 7.51; N, 4.16. Found C, 78.40; H, 7.56;

N, 4.05. $[\alpha]^{25}_{D}$ +125.2 (*c* 1.0, CH_2Cl_2).

***tert*-Butyl (1*S*,2*R*,3*R*,4*S*)-2-iodo-3-(2-methylphenyl)-1,2,3,4-tetrahydro-1,4-epiminonaphthalene-11-carboxylate (5b)** (Table 4)

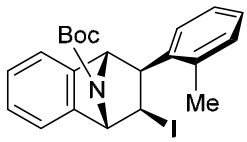

$ZnCl_2$ (545.2 mg, 4.0 mmol) was dried by fusing *in vacuo* and cooled quickly followed by addition of 4.0 mL of THF to prepare a 1.0 M THF solution of $ZnCl_2$. After stirring for 20 minutes, the THF solution of $ZnCl_2$ (0.85 mL, 1.0 M) was transferred to the other Schlenk flask, and 2-methylphenylmagnesium bromide (1.48 mL, 1.08 M solution in THF, 3.2 equiv.) was added at 0 °C and stirred for 2.0 hours. Then, the solvent was removed and the resulting arylzinc reagent was dried for 10 minutes under vacuum. To the arylzinc powder, a mixture of (*S,S*)-Chiraphos (8.5 mg, 0.020 mmol), THF (0.70 mL), toluene (3.2 mL), and $FeCl_3$ (1.62 mg, 0.01mmol) in THF (0.1 M, 100 μL) was added, followed by the addition of azabicyclic alkene (**1a**, 127.7 mg, 0.52 mmol) and the reaction mixture was stirred for 24 h at 0 °C. THF solution of I_2 (2.00 mL, 1.0 M, 2.00 mmol) was added at –78 °C. The mixture was stirred overnight at rt and then saturated aqueous NH_4Cl (1.0 mL) and MTBE were added. The separated aqueous layer was extracted with additional portions of MTBE (5 mL × 3). The combined organic extracts were passed through a pad of Florisil® and the filtrate was concentrated *in vacuo*. The product was purified by flash chromatography on silica gel (hexane/AcOEt = 95/5) to give the title compound in 84% yield (202.1 mg, 99% ee) as white solid.

The ee was determined by HPLC on a CHIRALCEL IC-3 column (4.6 mm i.d.; 150 mm length) with following conditions: Hexane/IPA = 99/1, 1.0 mL/min, 5 °C. Retention times (t_r) = 7.77 min (minor) and 8.43 min (major);

M.p. 65.3–66.9 °C; IR (neat) ν 592, 656, 739, 751, 829, 902, 915, 1087, 1150, 1255, 1275, 1335, 1366, 1458, 1702, 2953, 2973 cm^{-1}; ^1H NMR ($CDCl_3$, 391.8 MHz) δ 1.39 (s, 9H), 2.07 (s, 3H), 2.97 (d, *J* = 7.6 Hz, 1H), 4.46 (d, *J* = 7.6 Hz, 1H), 5.39–5.45 (br, 2H), 7.15 (d, *J* = 7.2 Hz, 1H), 7.20–7.23 (m, 3H), 7.28–7.32 (m, 2H), 7.39 (br, 1H), 7.58 (d, *J* = 7.6 Hz, 1H); ^{13}C NMR ($CDCl_3$, 98.5 MHz) δ 20.6, 28.4 (3C), 34.1, 46.8, 65.4, 72.2, 80.9, 120.7, 126.3, 127.0, 127.2 (2C), 127.3, 127.7 (2C), 130.0, 136.7, 143.4, 147.0, 155.1; HRMS (FAB): *m/z* $[M+Na]^+$ calcd for $C_{22}H_{24}NO_2NaI$ 484.0750, found 484.0752; Anal. Calcd for $C_{22}H_{24}INO_2$ C, 57.28; H, 5.24; N, 3.04; I, 27.51. Found C, 57.13; H, 5.27; N, 3.09; I, 27.33. $[\alpha]^{25}_{D}$ +105.0 (*c* 1.0, CH_2Cl_2).

Crystallographic Data

Single-crystal X-ray structure determination for 3c and 5b

Single crystals of **3c** and **5b** suitable for X-ray diffraction studies were analyzed by using a Rigaku AFC-10R diffractometer with Saturn 724 CCD detector using graphite-monochromated Mo-*Kα* radiation (λ = 0.71070 Å) and synchrotron radiation at beam line BL02B1 (λ = 0.70090 Å) of SPring-8 (Hyogo, Japan) with Rigaku Mercury II detector. The structures of **3c** and **5b** were solved by direct methods and refined by the full-matrix least squares method by using SHELX-97. The position of all non-hydrogen atoms was found from difference Fourier electron density maps and refined anisotropically. All calculations were performed using the Rigaku Crystal Structure ver 4.0 crystallographic software packages and illustrations were drawn by using ORTEP.

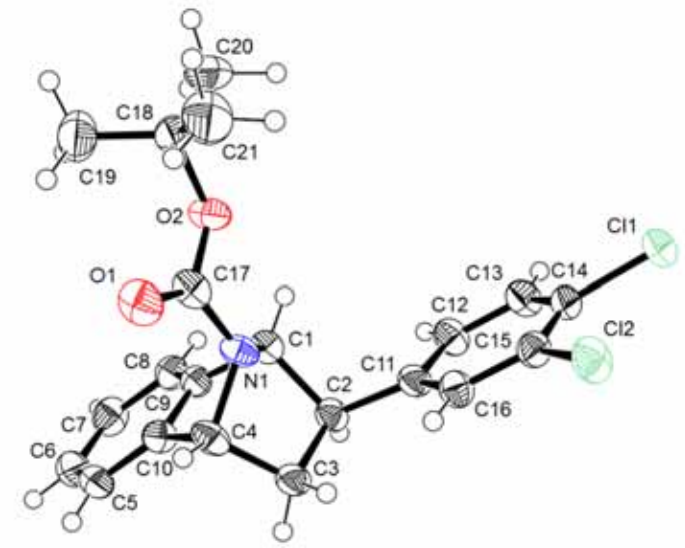

Figure 13. ORTEP drawing for **3c**. Thermal ellipsoids are drawn at 50% probability level.

Table 7. Crystallographic Data for **3c** Obtained from EtOH–H_2O.

Molecular Formula	$C_{21}H_{21}Cl_2NO_2$
Formula Weight	390.31
Crystal Dimensions (mm)	0.40 × 0.30 × 0.10
Crystal Color, Habit	colorless, block
Crystal System	monoclinic
Lattice Type	primitive
Space Group	$P2_1$(#4)
a (Å)	9.168(3)
b (Å)	6.287(2)
c (Å)	17.508(5)
β (°)	104.478(4)
Cell Volume (Å^3)	977.1(5)
Z Value	2
F (000)	408.00
D_{calc} (g/cm^{-3})	1.327
Temperature (°C)	−99.8
Radiation	graphite monochromated Mo-*K*α (λ = 0.71075 Å)
μ(Mo-*K*α) (cm^{-1})	3.465
$2\theta_{max}$ (°)	62.9
Total Number of Reflections	11150
Number of Unique Reflections	4030
Number of Variables	319
Reflection / Parameter Ratio	12.63
Final R_{all} and $_wR_2$	0.0478; 0.1128
Goodness of Fit	1.121
Max Shift / Error	0.000
Flack parameter	0.000
Method of phase determination	Direct Methods (SIR-2008)

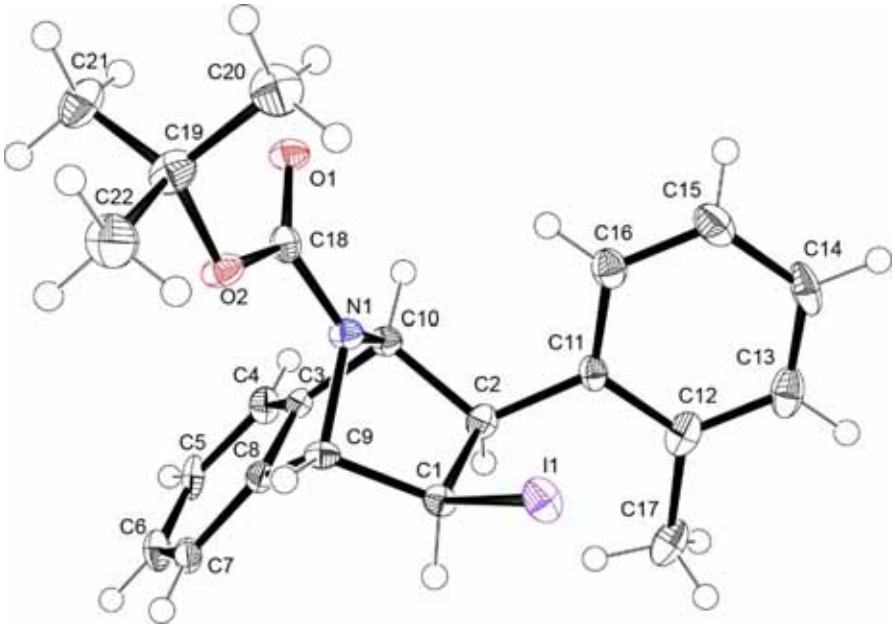

Figure 14. ORTEP drawing for **5b**. Thermal ellipsoids are drawn at 50% probability level.

Table 8. Crystallographic Data for **5b** Obtained from EtOH–H_2O.

Molecular Formula	$C_{22}H_{24}INO_2$
Formula Weight	461.34
Crystal Dimensions (mm)	0.10 × 0.10 × 0.50
Crystal Color, Habit	colorless, needle
Crystal System	monoclinic
Lattice Type	primitive
Space Group	$P2_1$(#4)
a (Å)	6.4237(9)
b (Å)	10.1859(14)
c (Å)	15.326(2)
β (°)	91.632(7)
Cell Volume (Å^3)	1002.4(2)
Z Value	2
F (000)	464.00
D_{calc} (g/cm^{-3})	1.528
Temperature (°C)	23.0
Radiation	synchrotron (λ = 0.70090 Å)
μ (cm^{-1})	0.000
$2\theta_{max}$ (º)	54.1
Total Number of Reflections	13303
Number of Unique Reflections	4570
Number of Variables	235
Reflection / Parameter Ratio	19.45
Final R_{all} and $_wR_2$	0.0368; 0.0777
Goodness of Fit	1.010
Max Shift / Error	0.001
Flack parameter	0.00(3)
Method of phase determination	Direct Methods (SIR2004)

X-ray Absorption Spectroscopy (XAS) Measurements

X-ray absorption near edge structure (XANES) and extended X-ray absorption fine structure (EXAFS) measurements were performed at BL14B2 beamline of SPring-8 under standard beamline conditions. The Fe K-edge (7.11 keV) XAS data were collected by transmission mode using N_2/Ar mixed gas-filled ionization chambers with optimized gas ratio and pressure with Si(111) double-crystal monochromator. For solution phase XAS, air- and moisture-sensitive sample solutions were transferred into a specially designed quarts-made solution cell with ultrafine Teflon windows in the glovebox. All the process for sample preparation were performed under an argon-filled glovebox.

Typical Procedure for XAS Analysis of Stoichiometric Reactions of $FeBr_3$ and (*S*,*S*)-Chiraphos with Phenylzinc reagent

In the argon-filled glovebox, a THF solution of $FeBr_3$ (8.9 mg, 0.03 mmol) in THF (0.375 mL) was diluted by toluene (1.125 mL) to prepare $FeBr_3$ solution in toluene:THF=4:1 mixture solvent. To the solution was added equimolar amounts of (*S*,*S*)-Chiraphos (1.0 M, 30 μL, 0.03 mmol) followed by $Ph_2Zn{\cdot}MgBrCl$ (1.0 M, 30 μL, 0.03 mmol for 1 equiv; 60 μL, 0.06 mmol for 2 equiv) at rt. The resulting reaction mixture was stirred for 10 min at rt, then filtered and transferred into the solution XAS cell to measure Fe K-edge XANES and EXAFS spectra according to the above method at the BL14B2, beamline of SPring-8. After 30 min, the sample solution was quenched and analyzed by GC.

References and Notes

[1] a) D. S. Müller, I, Marek, *Chem. Soc. Rev*. **2016**, *45*, 4552–4566; b) D. Didier, P.-O. Delaye, M. Simaan, B. Island, G. Eppe, H. Eijsberg, A. Kleiner, P. Knochel, I. Marek, *Chem. Eur. J.* **2014**, *20*, 1038–1048; c) K. Murakami, H. Yorimitsu, *Beilstein J. Org. Chem*. **2013**, *9*, 278–302; d) A. Pérez-Luna, C. Botuha, F. Ferreira, F. Chemla, *New J. Chem*. **2008**, *32*, 594–606.

[2] a) K. Fagnou in *Modern Rhodium-Catalyzed Organic Reactions* (Ed.: P. A. Evans), Wiley-VCH, Weinheim, **2005**, pp. 173–190; b) M. Lautens, K. Fagnou, S. Hiebert, *Acc. Chem. Res*. **2003**, *36*, 48–58; c) M. Lautens, K. Fagnou, M. Taylor, T. Rovis, *J. Organomet. Chem*. **2001**, *624*, 259–270; d) S. V. Kumar, A. Yen, M. Lautens, P. J. Guiry, *Chem. Soc. Rev.* **2021**, *50*, 3013–3093.

[3] a) L. Zhang, C. M. Le, M. Lautens, *Angew. Chem. Int. Ed.* **2014**, *53*, 5951–5954; b) G. C. Tsui, M. Lautens, *Angew. Chem. Int. Ed*. **2012**, *51*, 5400–5404; c) J. Zhu, G. C. Tsui, M. Lautens, *Angew. Chem. Int. Ed*. **2012**, *51*, 12353–12356; d) Y. Cho, V. Zunic, H. Senboku, M. Olsen, M. Lautens, *J. Am. Chem. Soc*. **2006**, *128*, 6837–6846; e) M. Lautens, K. Fagnou, *Proc. Natl. Acad. Sci. USA* **2004**, *101*, 5455–5460; f) F. Menard, M. Lautens, *Angew. Chem. Int. Ed*. **2008**, *47*, 2085–2088; g) J. Panteleev, F. Menard, M. Lautens, *Adv. Synth. Catal.* **2008**, *350*, 2893–2902; h) J. Bexrud, M. Lautens, *Org. Lett.* **2010**, *12*, 3160–3163.

[4] a) M. Lautens, S. Hiebert, J.-L. Renaud, *J. Am. Chem. Soc.* **2001**, *123*, 6834–6839; b) M. Lautens, C. Dockendorff, *Org. Lett.* **2003**, *5*, 3695–3698; c) S. Cabrera, R. Gómez Arrayás, J. C. Carretero, *Angew. Chem. Int. Ed.* **2004**, *43*, 3944–3947; d) S. Cabrera, R. Gómez Arrayás, I. Alonso, J. C. Carretero, *J. Am. Chem. Soc.* **2005**, *127*, 17938–17947; e) H. A. McManus, M. J. Fleming, M. Lautens, *Angew. Chem. Int. Ed.* **2007**, *46*, 433–436; f) T. Ogura, K. Yoshida, A. Yanagisawa, T. Imamoto, *Org. Lett.* **2009**, *11*, 2245–2248; g) X.-J. Huang, D.-L. Mo, C.-H. Ding, X.-L. Hou, *Synlett* **2011**, *2011*, 943–946; h) B. Fan, S. Li, H. Chen, Z. Lu, S. Liu, Q. Yang, L. Yu, J. Xu, Y. Zhou, J. Wang, *Adv. Synth. Catal.* **2013**, *355*, 2827–2832; i) K.-L. Huang, C. Guo, L.-J. Cheng, L.-G. Xie, Q.-L. Zhou, X.-H. Xu, S.-F. Zhu, *Adv. Synth. Catal.* **2013**, *355*, 2833–2838.

[5] a) M. Nakamura, M. Arai, E. Nakamura, *J. Am. Chem. Soc.* **1995,** *117,* 1179–1180; b) M. Nakamura, A. Hirai, E. Nakamura, *J. Am. Chem. Soc.* **2000**, *122*, 978–979.

[6] a) F. Bertozzi, M. Pineschi, F. Macchia, L. A. Arnold, A. J. Minnaard, B. L. Feringa, *Org. Lett.* **2002**, *4*, 2703–2705; b) W. Zhang, L.-X. Wang, W.-J. Shi, Q.-L. Zhou, *J. Org. Chem.* **2005**, *70*, 3734–3736.

[7] a) R. Lou, J. Liao, L. Xie, W. Tang, A. S. C. Chan, *Chem. Commun.* **2013**, *49*, 9959–9961; b) Y. Long, D. Yang, Z. Zhang, Y. Wu, H. Zeng, Y. Chen, *J. Org. Chem*. **2010**, *75*, 7291–7299.

[8] a) T. F. Spande, H. M. Garraffo, M. W. Edwards, H. J. C. Yeh, L. Pannell, J. W. Daly, *J. Am. Chem. Soc.* **1992**, *114*, 3475–3478; b) C. Qian, T. Li, T. Y. Shen, L. Libertine-Garahan, J. Eckman, T. Biftu, S. Ip, *Eur. J. Pharmacol.* **1993**, *250*, R13–R14; c) B. Badio, H. M. Garraffo, C. V. Plummer, W. L. Padgett, J. W. Daly, *Eur. J. Pharmacol.* **1997**, *321*, 189–194; d) J. C. Namyslo, D. E. Kaufmann, *Synlett* **1999**, 804–806.

[9] a) Only one example of a cobalt-catalyzed asymmetric addition of silylacetylenes to azabicyclic alkenes has been reported recently, see: T. Sawano, K. Ou, T. Nishimura, T. Hayashi, *Chem. Commun.* **2012**, *48*, 6106–6108. b) Nakamura group has reported a racemic carbozincation of oxa- and aza-bicycloalkenes under iron catalysis: S. Ito, T. Itoh, M. Nakamura, *Angew. Chem. Int. Ed.* **2011**, *50*, 454–457.

[10] Selected books and reviews: a) A. Casnati, M. Lanzi, G. Cera, *Molecules* **2020**, *25*, 3889; b) A. Piontek, E. Bisz, M. Szostak, *Angew. Chem. Int. Ed.* **2018**, *57,* 11116–11128; c) A. Fürstner, *ACS Cent. Sci.* **2016,** *2,* 778–789; d) I. Bauer, H.-J. Knölker, *Chem. Rev.* **2015,** *115,* 3170–3387; e) J. Legros, B. Figadere, *Nat. Prod. Rep*. **2015**, *32,* 1541–1555; f) E. Nakamura, T. Hatakeyama, S. Ito, K. Ishizuka, L. Ilies, M. Nakamura, *Org. React.* **2014**, *83*, 1–209; g) K. Gopalaiah, *Chem. Rev.* **2013,** *113,* 3248–3296; h) C. Bolm, J. Legros, J. Le Paih, L. Zani, *Chem. Rev.* **2004**, *104*, 6217–6254.

[11] A. M. Messinis, S. L. J. Luckham, P. P. Wells, D. Gianolio, E. K. Gibson, H. M. O'Brien, H. A. Sparkes, S. A. Davis, J. Callison, D. Elorriaga, O. Hernandez-Fajardo, R. B. Bedford, *Nature Catal.* **2019,** *2,* 123–133.

[12] The author reported the iron-catalyzed enantioselective Kumada–Tamao–Corriu and Suzuki–Miyaura coupling reactions of α-haloesters. see: a) T. Iwamoto, C. Okuzono, L. Adak, M. Jin, M. Nakamura, *Chem. Commun.* **2019,** *55,* 1128–1131; b) M. Jin, L. Adak, M. Nakamura, *J. Am. Chem. Soc.* **2015**, *137*, 7128–7134.

[13] Axial chiral ligand is effective in the iron-catalyzed enantioselective carbozincation of cyclopropenone acetal, see: ref 5b.

[14] The absolute configuration of 3,4-dichlorophenyl-substituted product **3c** was determined by X-ray single crystal analysis (Figure 13). Similar configurations are expected for the other products owing to the

similarity of the ^{1}H NMR coupling constants and the chiral HPLC retention times.

[15] The absolute configuration of iodo-substituted product **5b** was determined by X-ray single crystal analysis (Figure 14).

[16] Recently, Nakamura group reported the similar X-ray absorption spectral feature of tetrahedral alkyliron intermediate showing an intense pre-edge peak at 7110 eV, see: R. Agata, H. Takaya, H. Matsuda, N. Nakatani, K. Takeuchi, T. Iwamoto, T. Hatakeyama, M. Nakamura, *Bull. Chem. Soc. Jpn.* **2019,** *92,* 381–390.

[17] The fitting calculation was performed by the FEFF6 program (revision 9.6.4) embedded with Artemis. For the FEFF6 program, see: a) J. J. Rehr, J. J. Kas, F. D. Vila, M. P. Prange, K. Jorissen *Phys. Chem. Chem. Phys.* **2010,** *12,* 5503–5513. b) J. J. Rehr, R. C. Albers, *Rev. Mod. Phys.* **2000,** *72,* 621–654. For Artemis software, see: c) M. Newville, *J. Synchrotron Radiat.* **2001,** *8,* 322–324. (d) B. Ravel, M. Newville, *J. Synchrotron Radiat.* **2005,** *12,* 537–541.

[18] The formation of diaryl iron(II) species with the bisphosphine ligand is confirmed by various methods: by Mössbauer spectroscopy: a) S. L. Daifuku, M. H. Al-Afyouni, B. E. R. Snyder, J. L. Kneebone, M. L. Neidig, *J. Am. Chem. Soc.* **2014**, *136*, 9132–9143; b) S. L. Daifuku, J. L. Kneebone, B. E. R. Snyder, M. L. Neidig, *J. Am. Chem. Soc.* **2015**, *137*, 11432–11444; by XAS and DFT: ref 16; by XRD: c) E. J. Hawrelak, W. H. Bernskoetter, E. Lobkovsky, G. T. Yee, E. Bill, P. J. Chirik, *Inorg. Chem.* **2005**, *44*, 3103–3111; d) J. M. Hoyt, M. Shevlin, G. W. Margulieux, S. W. Krska, M. T. Tudge, P. J. Chirik, *Organometallics* **2014**, *33*, 5781–5790; e) C.-L. Sun, H. Krause, A. Fürstner, *Adv. Synth. Catal.* **2014**, *356*, 1281–1291.

[19] a) L. Adak, S. Kawamura, G. Toma, T. Takenaka, K. Isozaki, H. Takaya, A. Orita, H. C. Li, T. K. M. Shing, M. Nakamura, *J. Am. Chem. Soc.* **2017**, *139*, 10693–10701; b) T. Hatakeyama, T. Hashimoto, K. K. A. D. S. Kathriarachchi, T. Zenmyo, H. Seike, M. Nakamura, *Angew. Chem. Int. Ed*. **2012**, *51*, 8834–8837; c) S. Kawamura, T. Kawabata, K. Ishizuka, M. Nakamura, *Chem. Commun*. **2012**, *48*, 9376–9378; d) T. Hatakeyama, Y. Okada, Y. Yoshimoto, M. Nakamura, *Angew. Chem. Int. Ed.* **2011**, *50*, 10973–10976; e) T. Hatakeyama, T. Hashimoto, Y. Kondo, Y. Fujiwara, H. Seike, H. Takaya, Y. Tamada, T. Ono, M. Nakamura, *J. Am. Chem. Soc.* **2010**, *132*, 10674–10676.

[20] Computational DFT studies show certain bulky bisphosphines coordinate to the iron centre even when the oxidation state of the iron fluctuates in the catalytic cycle: a) A. K. Sharma, M. Nakamura, *Molecules* **2020**, *25*, 3612. b) A. K. Sharma, W. M. C. Sameera, M. Jin, L. Adak, C. Okuzono, T. Iwamoto, M. Kato, M. Nakamura, K. Morokuma, *J. Am. Chem. Soc.* **2017**, *139*, 16117–16125; c) H. Takaya, S. Nakajima, N. Nakagawa, K. Isozaki, T. Iwamoto, R. Imayoshi, N. J. Gower, L. Adak, T. Hatakeyama, T. Honma, M. Takagi, Y. Sunada, H. Nagashima, D. Hashizume, O, Takahashi, M. Nakamura, *Bull . Chem Soc. Jpn.* **2015**, *88*, 410–418.

[21] W. C. Still, M. Kahn, A. Mitra, *J. Org. Chem.* **1978**, *43,* 2923–2925.

[22] a) *Handbook of Grignard Reagents;* G. S. Silverman, P. E. Rakita, Eds.; Marcel Dekker, Inc.: New York, 1996. b) D. J. amEnde, P. J. Clifford, D. M. DeAntonis, C. SantaMaria, S. J. Brenek, *Org. Proc. Res. Dev.* **1999**, *3,* 319–329.

[23] T. Leermann, F. R. Leroux, F. Colobert, *Org. Lett.* **2011**, *13,* 4479–4481.

[24] F. I. Carroll, F. Liang, H. A. Navarro, L. E. Brieaddy, P. Abraham, M. I. Damaj, B. R. Martin, *J. Med. Chem.* **2001**, *44,* 2229–2237.

CHAPTER 2

Synthesis of Novel C_1 and C_2 Symmetric Chiraphos Derivatives and Their Application in Iron Catalyzed Enantioselective Carbometalation

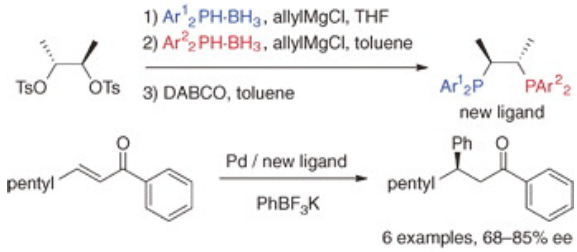

Abstract

A new method for the synthesis of C_2 and C_1 symmetric chiraphos derivatives and their application in Pd-catalyzed 1,4-addition reaction of an aryl boron compound to an α,β-unsaturated carbonyl compound (Miyaura–Michael reaction) are described. Six chiraphos congeners are prepared by substitution reactions of (2*R*,3*R*)-butane-2,3-diyl ditosylate with metalated phosphine-borane adducts and subsequent deprotection of the resulting borane-protected bisphosphines. In the asymmetric Miyaura–Michael reaction, the chiraphos derivative containing 4-tolyl groups showed higher enantioselectivity than the others including parent chiraphos. 3,5-Xylyl derivative showed slightly higher enantioselectivity in the iron-catalyzed enantioselective carbometalation reactions of oxabicycloalkenes.

Reproduced from *Chem. Lett.* **2013**, *42*, 1035–1037. with permission from the Chemical Society of Japan.

Introduction

Transition metal-catalyzed enantioselective synthesis is a powerful tool for the preparation of optically active compounds, and consequently, it is widely used in the industrial production of bioactive compounds or their intermediates.[1] Because chiral ligands can have a pivotal role in the catalytic activity and the enantioselectivity of metal-based catalysts, a variety of optically active chiral phosphorus compounds have been synthesized and studied.[2] Chiraphos [butane-2,3-diylbis(diphenylphosphine)] was synthesized by Bosnich in 1977,[3a] and it is now recognized as the first member of the group of C_2-symmetrical chiral bisphosphine ligands. Although chiraphos has been used successfully in a number of transition metal-catalyzed enantioselective reactions, such as hydrogenations,[4] allylic alkylations,[5] and 1,4-additions,[6] improvements in the selectivity of such reactions through the elaboration of the parent chiraphos have been hampered by a lack of suitable and efficient methods for synthesizing congeners of the ligand. Here, the author reports a new synthetic method based on a substitution reaction of (2*R*,3*R*)-butane-2,3-diyl ditosylate with metalated arylphosphine–borane adducts, which provides easy access to C_2 and C_1 symmetrical chiraphos derivatives. The author also describes the evaluation of these new ligands in an asymmetric cationic palladium-catalyzed 1,4-addition reaction of arylboron compounds to an enone (Miyaura-Michael reaction) and a diastereo- and enantioselective iron-catalyzed carbometalation of a diarylzinc to a bicyclic olefin.

Results and Discussion

The preparation of chiraphos derivatives by Bosnich's original method needs the use of a stoichiometric amount of the nickel salt to isolate the product by crystallization, and the handling and purification of the intermediates and products have to be carried out under an inert atmosphere.[3a,b] The author surmised that substitution of (2*R*,3*R*)-butane-2,3-diyl ditosylate **3** with a diarylphosphine-borane adduct **1** might provide a simpler and more synthetically viable route to chiraphos derivatives because the resulting bis(phosphine-borane) should be stable to air and moisture and, in addition, they are isolable by standard column chromatography on silica gel. The borane moieties would then be readily removed from bis(phosphine-borane) ligands by treatment with 1,4-diazabicyclo[2.2.2]octane (DABCO) to give the free phosphine ligands.[7] The resulting free ligands may then be used directly without further purification in asymmetric reactions unless DABCO does not facilitate the corresponding racemic reaction nor affect the enantioselectivity.

The author initially optimized the synthetic conditions of chiraphos derivatives

using a diphenylphosphine-borane adduct as a nucleophile. Table 1 shows the effect of the leaving groups on the product distributions of chiraphos synthesis. While a dimesylate or a bis(4-fluorobenzenesulfonate) resulted in low yields of 7% and 8%, respectively, a ditosylate gave a higher yield of 15%.

Table 1. The Product Distributions of the Chiraphos Synthesis Using Various Leaving Groups

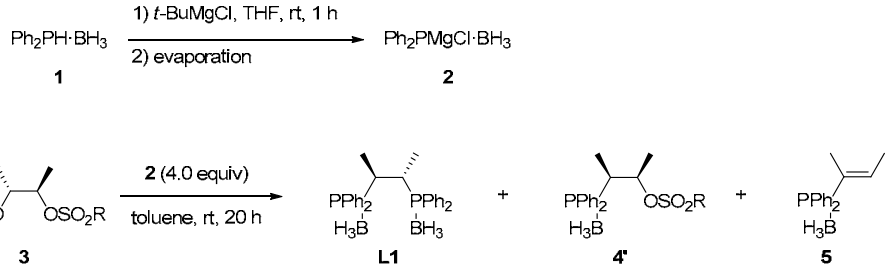

entry	-OSO_2R	NMR yields[a] /%			
		L1	**3**	**4'**	**5**
1	-OMs	7	5	6	79
2	-OTs	15	8	4	68
3	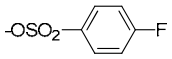	8	11	6	47

[a]NMR yields were calculated using 1,1,2,2-tetrachloroethane as an internal standard.

Table 2 illustrates the results of chiraphos synthesis using various metalated phosphine-borane reagents. The relatively less basic lithium salt[8] provided desired product **L1** in 18% yield, but sodium[9] or potassium salts gave low yields along with a large amount of the elimination byproduct **5** (entries 1–3). The magnesium salt, which was prepared by the reaction of the phosphine-borane complex and allylmagnesium chloride, gave the highest yield of 22% probably due to its lower basicity than the corresponding alkali metal salts. Although the difference between the lithium salt and the magnesium salt was subtle, the magnesium salt was selected in the following experiments because the mono-substituted product did not remain in the reaction mixture. The author eventually concluded that the substitution reaction of butane-2,3-diyl ditosylate **3** with magnesiated diphenylphosphine-borane gave the highest yield.

Table 2. The Effect of the Bases on the Product Distributions of the Chiraphos Synthesis

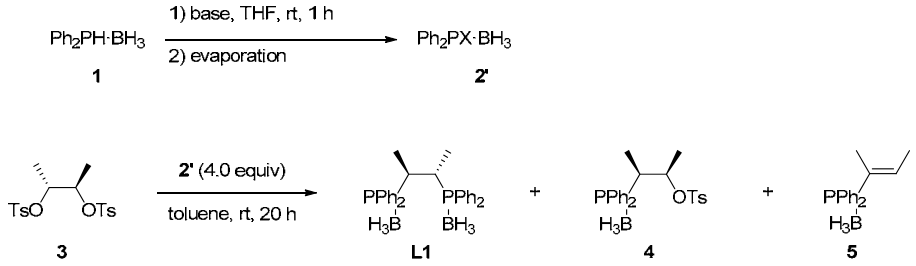

entry	base	NMR yields[a] /%			
		L1	**3**	**4**	**5**
1	LiHMDS	18	<1	10	57
2	NaHMDS	7	<1	4	69
3	KHMDS	1	<1	1	86
4	allylMgCl	22	<1	1	68

[a]NMR yields were calculated using 1,1,2,2-tetrachloroethane as an internal standard.

The optimal method for synthesizing the chiraphos derivatives is shown in Scheme 1. The diphenylphosphine-borane adduct **1a** was treated with an equimolar amount of allylmagnesium chloride at room temperature to give the magnesiated phosphine **2**. The reaction between four equivalents of the metalated phosphine **2** and tosylate **3** in toluene at room temperature for 20 hours gave optically pure (*S*,*S*)-chiraphos·2BH_3 (**L1**) in 22% isolated yield (Table 3, entry 1). Stereoisomers, such as the (*R*,*R*)- or *meso*-ligands, were not observed, suggesting that the substitution reaction proceeds exclusively by an S_N2 mechanism and no S_N1 pathway is involved. The major byproduct was the olefin **5**, and its formation could not be suppressed even under the optimal reaction conditions.

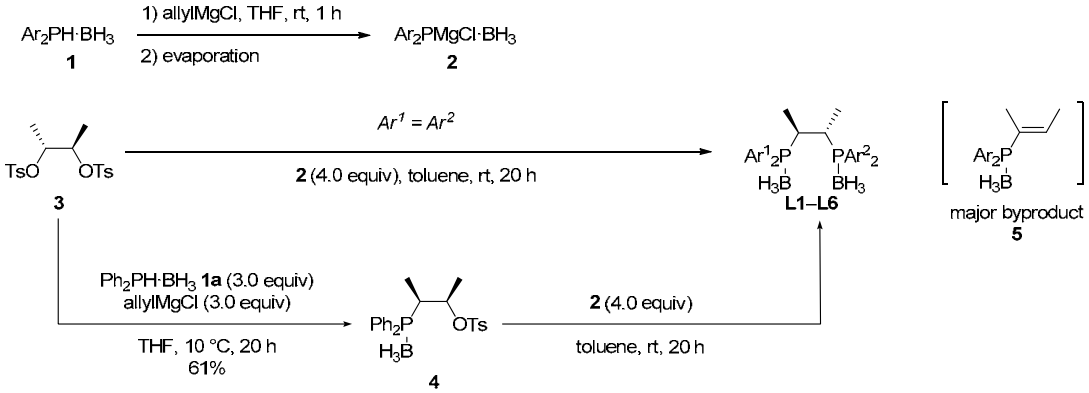

Scheme 1. Synthesis of C_2 and C_1 Symmetrical Chiraphos Derivatives

By using various substituted diarylphosphine-borane adducts instead of **1a**, the corresponding optically pure C_2 symmetrical chiraphos derivatives were synthesized (Table 3). The 4-fluorophenyl (**L2**, 13% yield),[3c] 4-methoxyphenyl **(L3**, 15% yield), 4-tolyl (**L4**, 20% yield),[3c] and 3,5-dimethylphenyl analogs (**L5**, 21% yield) were synthesized and isolated in this manner (entries 2–5). Sterically demanding aryl groups such as 2-methylphenyl or 3,5-di-*tert*-butylphenyl group could not be introduced by this method (entries 8 and 9). The C_1 symmetrical chiraphos derivatives, which have not previously been reported, were synthesized by means of the stepwise substitution reaction depicted in Scheme 1. First, the ditosylate **3** was treated with three equivalents of adduct **1a** and allylmagnesium chloride in tetrahydrofuran at 10 °C to give the monosubstituted ligand **4** in 61% isolated yield. Ligand **4** was then treated with bis(4-fluorophenyl)phosphine-borane or bis(3,5-methylphenyl)phosphine-borane to give the C_1 symmetrical chiraphos derivatives **L6** and **L7** in 16% and 17% yield (for two steps), respectively, in an optically pure form (entries 6 and 7). Although the formation of byproduct **5** decreased the chemical yield of the target molecules, the simple procedure and purification make the present method preparative.

Table 3. Synthesis of C_2 and C_1 Symmetrical Chiraphos Derivatives

entry[a]	product	Ar^1	Ar^2	yield[b] /%	ee[c] /%
1	**L1** (H, H)	Ph	Ph	22	>99
2	**L2** (F, F)	4-F-C_6H_4	4-F-C_6H_4	13	>99
3	**L3** (ani, ani)	4-MeO-C_6H_4	4-MeO-C_6H_4	15	–[d]
4	**L4** (tol, tol)	4-Me-C_6H_4	4-Me-C_6H_4	20	>99
5	**L5** (xyl, xyl)	3,5-Me_2-C_6H_3	3,5-Me_2-C_6H_3	21	–[d]
6	**L6** (F, H)	Ph	4-F-C_6H_4	16	>99
7	**L7** (xyl, H)	Ph	3,5-Me_2-C_6H_3	17	>99
8	**L8**	2-Me-C_6H_4	2-Me-C_6H_4	0	NA
9	**L9**	3,5-^{t}Bu$_2$-C_6H_3	3,5-^{t}Bu$_2$-C_6H_3	0	NA

[a]Reactions were conducted on a 3–8 mmol scale. [b]Isolated yield by silica gel column chromatography. [c]By chiral HPLC analysis. [d]Not determined.

Having various chiraphos derivatives in hands, the author evaluated the newly synthesized ligands **L1**–**L7** in an asymmetric cationic palladium-catalyzed 1,4-addition reaction.[6c] While Miyaura and Yamamoto originally reported this reaction by using an isolated cationic chiraphos complex of palladium, the author performed the reaction by using a catalyst generated *in situ* according to their preceding report on the 1,4-addition of organosilicon compounds.[10] The catalyst was prepared by mixing

bis(dibenzylideneacetone)palladium(0) [$Pd(dba)_2$], the appropriate ligand, and copper(II) bis(tetrafluoroborate) hexahydrate in 10:1 v/v methanol-water at 25 °C for 30 minutes (Scheme 2). When ligands **L1**–**L7** were used in this reaction, the boranes on the phosphorus were deprotected by treatment with an excess of DABCO immediately before the preparation of the catalyst, and the resulting free ligands were used directly without further purification. The resulting catalyst solution was treated with potassium trifluoro(phenyl)borate and enone **6** at 10 °C,[11] and the mixture was then stirred at 10 °C for 20 hours to give the 1,4-adduct **7**.[12]

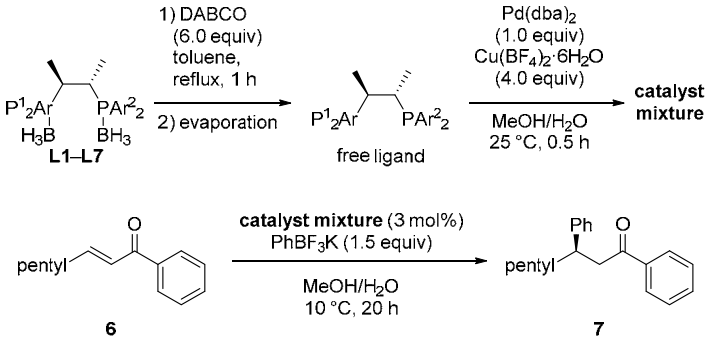

Scheme 2. Asymmetric 1,4-Addition to Enone **6** Using the *in situ*-Generated Cationic Palladium Catalyst and Chiraphos Derivatives

Table 4 summarizes the result of asymmetric 1,4-addition reactions using the various palladium chiraphos catalysts generated *in situ* from the corresponding ligands **L1**–**L7**. The free chiraphos and the deprotected ligand **L1** gave comparable yields (98% and 97%, respectively) and enantiomeric excesses (79% and 80% ee, respectively), confirming that residual DABCO and its borate salt have no effect on the chemical yield or the enantioselectivity (entries 1 and 2). Note that ligand **L4**, which contains a 4-tolyl group (entry 5), showed the highest stereoselectivity of 85% ee and gave an excellent yield (98%), whereas use of the electron-deficient ligand **L2** or the sterically demanding ligand **L5** resulted in lower enantiomeric excesses of 68% and 74%, respectively (entries 3 and 6). The C_1 symmetric ligands **L6** and **L7** gave the product **7** with fair enantioselectivity, but one that was slightly lower than produced by the parent chiraphos (entries 7 and 8).

Table 4. Asymmetric 1,4-Addition to Enone **6** in the Presence of the *in situ*-Generated Cationic Palladium Catalyst and Various Chiraphos Derivatives

entry[a]	ligand	yield[b] /%	ee[c] /%
1	CHIRAPHOS	98	79
2	**L1** (H, H)	97	80
3	**L2** (F, F)	95	68
4	**L3** (ani, ani)	97	77
5	**L4** (tol, tol)	98[d]	85
6	**L5** (xyl, xyl)	97	74
7	**L6** (ani, H)	99	78
8	**L7** (xyl, H)	96	77

[a]Reactions were conducted on a 0.5–2.0 mmol scale. [b]GC yield with undecane as an internal standard unless otherwise noted. [c]The ee was determined by chiral HPLC analysis. [d]Isolated yield (silica gel column chromatography).

The author also applied newly synthesized chiraphos derivatives to the diastereo- and enantioselective iron-catalyzed carobometalation of oxabicycloalkenes with diarylzinc reagents. This iron-catalyzed reaction was highly sensitive to the residue of DABCO or the DABCO-borane adduct, thereby removing the excess DABCO before the carbometalation reaction was essential. The reaction procedure is as follows: After deprotection of chiraphos-borane derivatives with DABCO, the reaction mixture was washed with 0.20 M aqueous solution of TFA under oxygen-free atmosphere to remove DABCO completely. The borane and amine free ligand was obtained after drying under reduced pressure. These ligands **L1**–**L7** were applied to the carbometalation reaction, and the results are shown in Table 5. The electron deficient phosphine ligand **L2** gave racemic ring-opening product **10** in 70% yield and a small amount of product **9** with 68% ee (entry 2). This result indicates that ligand **L2** hardly coordinated with iron due to its low Lewis basicity, and thus the iron catalysis without ligand dominantly proceeded to give the racemic ring-opening product **10**. On the other hand, electron donating ligand **L3** and **L4** provided a high yield of product **9** with 69% ee and 78% ee, respectively (entries 3 and 4). These ligands clearly controlled the iron-catalyzed carbometalation by strong coordination to iron. Fine tuning of phosphine basicity seemed to be required for obtaining good enantioselectivity: ligand **L1** and **L4**, which have medium phosphine basicity, afforded higher ee's of 78%, but less basic ligand **L2** or more basic ligand **L3** gave lower ee's of 68% or 69%, respectively. Sterically demanding ligand **L5** gave the highest ee of 81% (entry 6). C_1 symmetrical ligand **L6** possessing 4-fluorophenyl gave

ring-opening product **10** in 57% yield with only 3% ee, suggesting this ligand cannot coordinate with iron like **L2** (entry 6). Since the ligand **L7** gave a comparable yield and ee with ligand **L1** (entries 1, 7), the carbometalation reaction may proceed at the diphenylphosphanyl-side, albeit not at dixylylphosphanyl-side when the C_1 ligand having enough Lewis basicity was applied (entry 7).

Table 5. Application of Various Chiraphos Type Ligands **L1**–**L7** to Iron-Catalyzed Carbometalation

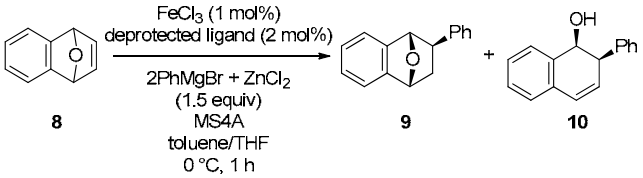

8 **9** **10**

entry[a]	ligand[b]	time /h	NMR yield[c] (ee)[d] /%		
			9	**10**	**8**
1	**L1** (H, H)	1	87 (78)	9 (9)	0
2	**L2** (F, F)	4	3 (68)	70 (0)	23
3	**L3** (ani, ani)	1	93 (69)	6 (9)	0
4	**L4** (tol, tol)	1	93 (78)	3 (39)	0
5	**L5** (xyl, xyl)	3	81 (81)	13 (16)	0
6	**L6** (F, H)	4	12 (70)	57 (3)	0
7	**L7** (xyl, H)	1	85 (75)	9 (14)	0

[a]Reactions were carried out on a 0.5 mmol scale. [b]Substituents on aromatic rings were shown in the parenthesis.[c]1,1,2,2-Tetrachloroethane was used as an internal standard. [d]Enantiomeric excess was determined by HPLC analysis.

Di(3,5-xylyl)zinc was applied for the carbometalation reaction (Table 6). The ligand **L5** showed clear superiority over ligand **L1** in this carbometalation reaction as expected: the ligand **L5** provided desired product **11** in 98% yield with 90% ee (entry 2), but the ligand **L1** gave a lower yield of 63% and a lower ee of 84% (entry 1).

Table 6. Racemic Carbometalation Reaction of Olefin **8** with Di(3,5-xylyl)zinc

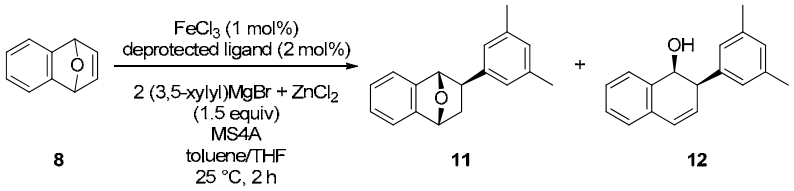

entry[a]	ligand	time /h	NMR yield[b] (ee)[c] /%		
			11	**12**	**8**
1	**L1** (H, H)	4	63 (84)	ND	18
2	**L5** (xyl, xyl)	1	98 (90)	ND	ND

[a]Reactions were carried out on a 0.5 mmol scale. [b]1,1,2,2-Tetrachloroethane was used as an internal standard. [c]Enantiomeric excess was determined by HPLC analysis.

Conclusion

In summary, the author has developed a new synthetic approach to chiraphos derivatives, based on the substitution reaction of (2*R*,3*R*)-butane-2,3-diyl ditosylate with metalated phosphine–borane adducts. This approach provides ready access to C_2 as well as C_1 symmetrical derivatives. Although there remains room for improvement in the chemical yield of the subsequent substitution reactions, the reaction does not need any expensive chemicals and is therefore scalable for multi-gram-scale preparations of the readily handled borane-protected precursors. These phosphine-borane complexes are easily deprotected with DABCO and the resulting ligands can be used directly in asymmetric cationic palladium-catalyzed 1,4-addition reactions. Among the ligands the author prepared, the chiraphos analog containing 4-tolyl groups showed higher enantioselectivity than the parent chiraphos in the 1,4-addition reaction. On the other hand, the chiraphos congener possessing 3,5-xylyl groups gave the highest enantioselectivity in the iron-catalyzed carbometalation reaction. Fine-tuning of chiraphos becomes available and the author hopes that the results will facilitate the further application of chiraphos congeners in various asymmetric transition metal-catalyzed reactions.

Experimental Section

General Information

All the reactions were carried out in dry reaction vessels under a positive pressure of nitrogen. Column chromatography was performed on prepacked silica gel cartridges (SNAP Ultra; Biotage, Uppsala, Sweden). Commercial reagents and solvents were purchased from Kanto Chemical Co., Sigma-Aldrich Co., and other commercial suppliers, and used as received. NMR spectra were recorded on a JEOL ECS-500 spectrometer. GC analyses were performed on an Agilent 7890A instrument equipped with an FID detector and a capillary column, DB-1 (20 m length, 0.18 mm i.d., 0.18 μm film). IR spectra were recorded on a JASCO FT/IR-6100 Type A spectrometer. Enantiomeric excesses were determined by HPLC analysis with a chiral stationary column (details below).

Chiral HPLC Conditions

For chiraphos derivatives

Column: Daicel Chiralpak AD-3 (150 mm length, 4.6 mm i.d., 3 μm p.s.), eluent: hexane–*i*-PrOH (95:5) (unless otherwise noted), flow: 1.0 mL/min; temp: 25 °C; detector: UV 254 nm.

For 1,3-diphenyloctan-1-one (7)

Column: Daicel Chiralpak AD-3 (150 mm length, 4.6 mm i.d., 3 μm p.s.), eluent: hexane–*i*-PrOH (99:1), flow: 1.0 mL/min; temp.: 25 °C; detector: UV 220 nm.

Preparation of Materials

Bis(3,5-dimethylphenyl)phosphine oxide

1-Bromo-3,5-dimethylbenzene (129.5 g, 3.5 equiv) was slowly added to a suspension of Mg turnings (17.0 g, 3.5 equiv) in THF (770 mL) while the internal temperature was maintained at 40–50 °C. The mixture was stirred at 40–50 °C for 1 h then cooled to 0 °C. $(EtO)_2POH$ (27.7 g, 0.200 mol) was added over 30 min, and the mixture was stirred at 0 °C for 1 h. The reaction was quenched with 6 M aq HCl (260 mL) and the mixture was extracted with CH_2Cl_2 (260 × 3 mL) and washed with H_2O (130 × 2 mL). After concentration *in vacuo*, the residue was purified by chromatography on silica gel to give the title compound (49.7 g, 96%) as a pale yellow solid.

IR (KBr, cm^{-1}) ν 3427, 2949, 2916, 2859, 2321, 1602, 1456, 1379, 1274, 1184, 1128, 965, 933, 852, 697, 569, 556, 524, 459, 423; ^1H NMR (500 MHz, $CDCl_3$) δ 2.35 (s, 12H), 7.19 (s, 2H), 7.29 (s, 2H), 7.327 (s, 2H), 7.95 (d, J = 477 Hz, 1H); ^{13}C NMR (125 MHz,

$CDCl_3$) δ 21.2, 128.1 (d, *J* = 11.0 Hz), 131.3 (d, *J* = 101 Hz), 134.2 (d, *J* = 2.9 Hz), 138.6 (d, *J* = 13.3 Hz); ^{31}P NMR (202 MHz, $CDCl_3$) δ 22.8; HRMS (ES^+) *m/z* $[M + H]^+$ Calcd for $C_{16}H_{20}OP$, 259.1252; Found, 259.1264.

Bis(3,5-dimethylphenyl)phosphine-borane adduct

A solution of bis(3,5-dimethylphenyl)phosphine oxide (18.1 g, 70.0 mmol) in THF (360 mL) at 0 °C was treated by slow addition of a 1.02 M solution of DIBAL-H in toluene (206 mL, 3.0 equiv). The mixture was stirred at room temperature for 1 h, cooled to 0 °C, and a 1.06 M solution of BH_3·THF in THF (132 mL, 2.0 mmol) was added. The resulting mixture was stirred at 0 °C for 1 h and then the reaction was then quenched with 2 M aq KOH (270 mL). The mixture was extracted with toluene (270 × 2 mL) and washed successively washed with 2 M aq KOH (90 mL) and H_2O (90 mL). After concentration *in vacuo*, the residue was purified by chromatography on silica gel to give the title compound (14.0 g, 78%) as a white solid.

IR (KBr, cm^{-1}) ν 2949, 2415, 2857, 2388, 2347, 1603, 1446, 1377, 1136, 1058, 947, 916, 906, 850, 695, 602, 419; ^{1}H NMR (500 MHz, $CDCl_3$) δ 0.56–1.47 (m, 3H), 2.33 (s, 12H), 6.17 (dq, *J* = 378, 6.9 Hz, 1H), 7.12 (s, 2H), 7.24 (s, 2H), 7.27 (s, 2H); ^{13}C NMR (125 MHz, $CDCl_3$) δ 21.2, 126.1 (d, *J* = 56.3 Hz), 130.4 (d, *J* = 9.1 Hz), 133.3 (d, *J* = 2.3 Hz), 138.7 (d, *J* = 10.9 Hz); ^{31}P NMR (202 MHz, $CDCl_3$) δ 1.6 (d, *J* = 57.1 Hz); HRMS (ES^+) *m/z* M^+ Calcd for $C_{16}H_{22}BP$, 256.1552; Found, 256.1541.

Borane-(2*S*,3*S*)-butane-2,3-diylbis[bis(3,5-dimethylphenyl)phosphine] adduct (2:1) (L5); Typical Procedure for a chiraphos derivative

A solution of bis(3,5-dimethylphenyl)phosphine–borane adduct (8.20 g, 4.0 equiv) in THF (32 mL) was treated with a 1.97 M solution of CH_2=$CHCH_2MgCl$ in THF (16.2 mL, 4.0 equiv) at room temperature for 1 h. The solvent was removed *in vacuo*, (2*R*,3*R*)-butane-2,3-diyl ditosylate (3.19 g, 8.0 mmol) and toluene (32 mL) were added, and the mixture was sonicated to dissolve the gummy magnesiated phosphide, then stirred at room temperature for 20 h. The reaction was quenched with 20% aq NH_4Cl (90 mL), the mixture was extracted with EtOAc (60 mL), and the extracts were washed with H_2O (30 mL). After concentration *in vacuo*, the residue was purified by chromatography on silica gel to give the title compound as a white amorphous powder (1.01 g, 21%). IR (KBr, cm^{-1}) ν 3429, 2978, 2919, 2859, 2388, 1601, 1454, 1417, 1380, 1131, 1065, 992, 849, 744, 694, 607, 464, 440; ^{1}H NMR (500 MHz, $CDCl_3$) δ 0.65–1.40 (m, 6H), 1.12 (d, *J* = 7.2 Hz, 3H), 1.15 (d, *J* = 7.2 Hz, 3H), 2.29 (s, 12H), 2.32 (s, 12H), 3.11 (q, *J* = 7.2 Hz, 2H), 7.09 (s, 2H), 7.11 (s, 2H), 7.14–7.18 (m, 4H), 7.29–7.33 (m, 4H); ^{13}C NMR (125

MHz, $CDCl_3$) δ 10.4, 21.29, 21.30, 28.5 (d, *J* = 35.6 Hz), 127.2 (d, *J* = 52.5 Hz), 128.5 (d, *J* = 52.5 Hz), 130.0 (m), 130.7 (m), 132.8, 133.2, 138.3 (m); ^{31}P NMR (202 MHz, $CDCl_3$) δ 26.1; HRMS (ES^-) *m/z* $[M + AcO]^-$ Calcd for $C_{38}H_{53}B_2O_2P_2$, 625.3707; Found, 625.3700. $[\alpha]^{28}_D$ –70 (*c* 1.0, $CHCl_3$).

Borane-(2*S*,3*S*)-butane-2,3-diylbis(diphenylphosphine) adduct (2:1) (L1)

A white amorphous powder; Yield: 22%; >99% ee ($t_{S,S}$ = 8.9 min, $t_{R,R}$ = 4.8 min).
IR (KBr, cm^{-1}) ν 3058, 2983, 2948, 2882, 2390, 1482, 1436, 1105, 1066, 998, 740, 701, 692, 599, 589, 499, 483; ^{1}H NMR (500 MHz, $CDCl_3$) δ 0.60–1.75 (m, 6H), 1.18 (d, *J* = 7.2 Hz, 3H), 1.21 (d, *J* = 7.2 Hz, 3H), 3.09 (q, *J* = 7.2 Hz, 2H), 7.34–7.40 (m, 4H), 7.41–7.46 (m, 4H), 7.47–7.58 (m, 8H), 7.69–7.75 (m, 4H); ^{13}C NMR (125 MHz, $CDCl_3$) δ 10.4, 28.3 (d, *J* = 36.1 Hz), 127.3 (d, *J* = 53.4 Hz), 128.2 (d, *J* = 53.4 Hz), 128.7 (m), 128.9 (m), 131.2, 131.5, 132.5 (m), 133.0 (m); ^{31}P NMR (202 MHz, $CDCl_3$) δ 26.3; HRMS (ES^-) *m/z* $[M + AcO]^-$ Calcd for $C_{30}H_{37}B_2O_2P_2$, 513.2455; Found, 513.2466. $[\alpha]^{28}_D$ –74 (*c* 1.0, $CHCl_3$).

Borane-(2*S*,3*S*)-butane-2,3-diylbis[bis(4-fluorophenyl)phosphine] adduct (2:1) (L2)

A white amorphous powder; Yield: 13%; >99% ee ($t_{S,S}$ = 7.1 min, $t_{R,R}$ = 4.8 min).
IR (KBr, cm^{-1}) ν 3099, 3068, 2985, 2947, 2880, 2387, 1592, 1498, 1467, 1396, 1306, 1236, 1163, 1103, 1062, 1013, 835, 748, 689, 574, 540, 517, 443; ^{1}H NMR (500 MHz, $CDCl_3$) δ 0.65–1.40 (m, 6H), 1.12 (d, *J* = 7.2 Hz, 3H), 1.15 (d, *J* = 7.2 Hz, 3H), 3.03 (q, *J* = 7.2 Hz, 2H), 7.07–7.12 (m, 4H), 7.15–7.20 (m, 4H), 7.50–7.56 (m, 4H), 7.70–7.76 (m, 4H); ^{13}C NMR (125 MHz, $CDCl_3$) δ 10.5, 28.4, 28.7, 116.4 (m), 116.5 (m), 122.7 (dd, *J* = 55.1, 3.5 Hz), 123.6 (dd, *J* = 55.1, 3.5 Hz), 134.8 (m), 135.5 (m), 163.8 (m), 165.8 (m); ^{31}P NMR (202 MHz, $CDCl_3$) δ 25.4; HRMS (ES^-) *m/z* $[M + AcO]^-$ Calcd for $C_{30}H_{33}B_2O_2F_4P_2$, 585.2078; Found, 585.2083. $[\alpha]^{28}_D$ –52 (*c* 1.0, $CHCl_3$).

Borane-(2*S*,3*S*)-butane-2,3-diylbis[bis(4-methoxyphenyl)phosphine] adduct (2:1) (L3)

A white amorphous powder; Yield: 15%.
^{1}H NMR (500 MHz, $CDCl_3$) δ 0.73–1.38 (m, 6H), 1.13 (d, *J* = 7.2 Hz, 3H), 1.16 (d, *J* = 7.2 Hz, 3H), 2.99 (q, *J* = 7.2 Hz, 2H), 3.82 (s, 6H), 3.84 (s, 6H), 6.87 (d, *J* = 8.2 Hz, 4H), 6.94 (d, *J* = 8.2 Hz, 4H), 7.42–7.47 (m, 4H), 7.61–7.65 (m, 4H); ^{13}C NMR (125 MHz, $CDCl_3$) δ 10.4, 28.3, 28.6, 55.27, 55.29, 114.4 (m), 119.0 (m), 134.2 (m), 134.7 (m), 161.7 (m), 162.0; ^{31}P NMR (202 MHz, $CDCl_3$) δ 23.1; HRMS (ES^-) *m/z* HRMS (ES^-) *m/z* $[M + AcO]^-$ Calcd for $C_{34}H_{45}B_2O_6P_2$, 633.2877; Found, 633.2878.

Borane-(2*S*,3*S*)-butane-2,3-diylbis(di-4-tolylphosphine) adduct (2:1) (L4)

a white amorphous powder; Yield: 20%; >99% ee (hexane:*i*-PrOH = 80:20, $t_{S,S}$ = 24.3 min, $t_{R,R}$ = 14.5 min).

IR (KBr, cm^{-1}) ν 3433, 3023, 2980, 2921, 2881, 2386, 1601, 1499, 1449, 1398, 1313, 1190, 1104, 1064, 1020, 807, 748, 710, 691, 646, 633, 575, 507, 495, 439; ^{1}H NMR (500 MHz, $CDCl_3$) δ 0.62–1.38 (m, 6H), 1.13 (d, *J* = 7.2 Hz, 3H), 1.16 (d, *J* = 7.2 Hz, 3H), 2.37 (s, 6H), 2.39 (s, 6H), 3.05 (q, *J* = 7.2 Hz, 2H), 7.16 (d, *J* = 7.5 Hz, 4H), 7.23 (d, *J* = 7.5 Hz, 4H), 7.37–7.42 (m, 4H), 7.56–7.62 (m, 4H); ^{13}C NMR (125 MHz, $CDCl_3$) δ 10.4, 21.42, 21.45, 28.3 (d, *J* = 36.8 Hz), 124.2 (d, *J* = 55.1 Hz), 125.1 (d, *J* = 55.1 Hz), 129.5 (m), 132.5 (m), 133.0 (m), 141.4, 141.8; ^{31}P NMR (202 MHz, $CDCl_3$) δ 24.8; HRMS (ES^-) *m/z* $[M + AcO]^-$ Calcd for $C_{34}H_{45}B_2O_2P_2$, 569.3081; Found, 569.3075. $[\alpha]^{28}_D$ –73 (*c* 1.0, $CHCl_3$).

Borane-(1*R*,2*S*)-2-(Diphenylphosphino)-1-methylpropyl tosylate adduct (1:1) (4)

A solution of $Ph_2PH{\cdot}BH_3$ (9.60 g, 3.0 equiv) in THF (38 mL) was treated with a 1.97 M solution of CH_2=$CHCH_2MgCl$ in THF (24.4 mL, 3.0 equiv). The mixture was stirred at room temperature for 1 h then cooled to 10 °C. (2*R*,3*R*)-butane-2,3-diyl ditosylate (6.38 g, 16.0 mmol) was added, and the mixture was stirred at the 10 °C for 20 h. The reaction was quenched with 20% aq NH_4Cl (300 mL), and the mixture was extracted with EtOAc (200 mL) and washed with H_2O (100 mL). After concentration *in vacuo*, the residue was purified by chromatography on silica gel to give the title compound as a white solid (4.16 g, 61%); >99% ee [hexane–*i*-PrOH (80:20); $t_{2S,3R}$ = 8.0 min, $t_{2R,3S}$ = 7.4 min].

IR (KBr, cm^{-1}) ν 3056, 2983, 2944, 2428, 2398, 2364, 1435, 1355, 1174, 1096, 1073, 1029, 972, 905, 861, 752, 716, 699, 672, 610, 560, 504, 480; ^{1}H NMR (500 MHz, $CDCl_3$) δ 0.54–1.28 (m, 3H), 0.98 (dd, *J* = 14.9, 6.9 Hz, 3H), 1.12 (d, *J* = 6.4 Hz, 3H), 2.43 (s, 3H), 2.80–2.90 (m, 1H), 4.88–4.96 (m, 1H), 7.27–7.32 (m, 2H), 7.36–7.50 (m, 6H), 7.67–7.75 (m, 4H), 7.78–7.84 (m, 2H); ^{13}C NMR (125 MHz, $CDCl_3$) δ 12.4, 21.5 (d, *J* = 3.5 Hz), 21.6, 35.4 (d, *J* = 32.9 Hz), 81.1 (d, *J* = 11.0 Hz), 127.8, 128.4 (d, *J* = 35.8 Hz), 128.8 (d, *J* = 9.8 Hz), 128.9 (m), 129.7, 131.3 (d, *J* = 2.3 Hz), 131.5 (d, *J* = 2.3 Hz), 132.5 (d, *J* = 8.7 Hz), 132.7 (d, *J* = 8.7 Hz), 134.1, 144.7; ^{31}P NMR (202 MHz, $CDCl_3$) δ 20.2 (d, *J* = 58.8 Hz); HRMS (ES^+) *m/z* $[M + NH_4]^+$ Calcd for $C_{23}H_{32}BNO_3PS$, 444.1934; Found, 444.1928; Anal. Calcd for $C_{23}H_{28}BO_3PS$: C, 64.80; H, 6.62%. Found: C, 64.56; H, 6.71%. $[\alpha]^{28}_D$ +47 (*c* 1.0, $CHCl_3$);

Borane-{(1*S*,2*S*)-2-[bis(4-fluorophenyl)phosphino]-1-methylpropyl}
-(diphenyl)phosphine adduct (2:1) (L6)

A white amorphous powder; Yield: 16%; >99% ee ($t_{S,S}$ = 7.8 min, $t_{R,R}$ = 5.2 min).
IR (KBr, cm^{-1}) ν 3060, 2978, 2943, 2881, 2390, 2355, 1591, 1498, 1436, 1396, 1238, 1161, 1104, 1067, 1012, 996, 829, 744, 695, 591, 572, 524, 496, 487, 449, 437; ^{1}H NMR (500 MHz, $CDCl_3$) δ 0.65–1.41 (m, 6H), 1.14 (dd, *J* = 16.9, 7.4 Hz, 3H), 1.21 (dd, *J* = 15.9, 6.9 Hz, 3H), 2.93–3.04 (m, 1H), 3.06–3.18 (m, 1H), 7.04–7.10 (m, 2H), 7.12–7.18 (m, 2H), 7.37–7.58 (m, 10H) , 7.68–7.77 (m, 4H); ^{13}C NMR (125 MHz, $CDCl_3$) δ 10.4, 10.5, 21.3, 28.3 (dd, *J* = 30.6, 5.8 Hz), 28.4 (dd, *J* = 31.8, 6.4 Hz), 116.3 (dd, *J* = 21.4, 5.2 Hz), 116.4 (dd, *J* = 21.6, 4.6 Hz), 123.4 (m), 126.9 (d, *J* = 52.6 Hz), 128.3 (d, *J* = 53.8 Hz), 129.9 (m), 131.3 (d, *J* = 2.3 Hz), 131.7 (d, *J* = 2.3 Hz), 132.5 (d, *J* = 8.7 Hz), 133.3 (d, *J* = 8.7 Hz), 134.1 (m), 135.3 (m), 164.6 (dd, *J* = 257, 2.3 Hz), 164.8 (dd, *J* = 254, 2.3 Hz); ^{31}P NMR (202 MHz, $CDCl_3$) δ 23.5, 25.6; HRMS (ES^-) *m/z* $[M + AcO]^-$ Calcd for $C_{30}H_{35}B_2F_2O_2P_2$, 549.2267; Found, 549.2272. $[\alpha]^{28}_D$ –62 (*c* 1.0, $CHCl_3$);

Borane-{(1*S*,2*S*)-2-[bis(3,5-dimethylphenyl)phosphino]-1-methylpropyl}
-(diphenyl)phosphine (2:1) (L7)

A white amorphous powder ; Yield: 16%, >99% ee (hexane:*i*-PrOH = 98:2, $t_{S,S}$ = 9.7 min, $t_{R,R}$ = 3.9 min).
IR (KBr, cm^{-1}) ν 3453, 3059, 2978, 2940, 2910, 2881, 2394, 2382, 1600, 1586, 1456, 1436, 1387, 1129, 1104, 1059, 1035, 992, 861, 851, 740, 716, 697, 659, 621, 604, 568, 499, 461, 442; ^{1}H NMR (500 MHz, $CDCl_3$) δ 0.57–1.74 (m, 12H), 2.30 (s, 6H), 2.31 (s, 6H), 2.95–3.08 (m, 1H), 3.10–3.21 (m, 1H), 7.07–7.20 (m, 4H), 7.23–7.57 (m, 10H), 7.68–7.77 (m, 2H); ^{13}C NMR (125 MHz, $CDCl_3$) δ 10.4, 21.3, 28.3 (dd, *J* = 31.2, 5.2 Hz), 28.5 (dd, *J* = 30.6, 5.2 Hz), 126.7 (d, *J* = 52.0 Hz), 126.9 (d, *J* = 51.4 Hz), 128.3 (d, *J* = 52.6 Hz), 128.5 (m), 128.7 (d, *J* = 9.2 Hz), 130.2 (d, *J* = 8.1 Hz), 130.7 (d, *J* = 8.7 Hz), 131.0 (d, *J* = 2.3 Hz), 131.5 (d, *J* = 2.3 Hz), 132.5 (d, *J* = 8.1 Hz), 138.3 (d, *J* = 10.4 Hz), 138.4 (d, *J* = 10.4 Hz); ^{31}P NMR (202 MHz, $CDCl_3$) δ 24.4, 25.7; HRMS (ES^-) *m/z* $[M + AcO]^-$ Calcd for $C_{34}H_{45}B_2O_2P_2$, 569.3081; Found, 569.3071 $[\alpha]^{28}_D$ –81 (*c* 1.0, $CHCl_3$);.

Borane-[(1*E*)-1-Methylprop-1-en-1-yl](diphenyl)phosphine adduct (1:1) (5)

A white amorphous powder; Yield: 45%.
IR (KBr, cm^{-1}) ν 3434, 3074, 3054, 2920, 2851, 2381, 2345, 2253, 1633, 1480, 1436, 1382, 1312, 1137, 1106, 1061, 1029, 998 742, 695, 682, 625, 608, 508, 494, 473, 441, 432; ^{1}H NMR (500 MHz, $CDCl_3$) δ 0.64–1.47 (m, 3H), 1.78–1.87 (m, 6H), 6.12 (ddq, *J* = 19.8, 1.0, 6.0 Hz, 1H), 7.41–7.54 (m, 6H), 7.58–7.66 (m, 4H); ^{13}C NMR (125 MHz,

$CDCl_3$) δ 14.1 (d, *J* = 11.0 Hz), 15.0 (d, *J* = 13.9 Hz), 125.9 (d, *J* = 54.3 Hz), 128.4 (d, *J* = 57.2 Hz), 128.7 (d, *J* = 10.4 Hz), 131.0 (d, *J* = 2.3 Hz), 133.1 (d, *J* = 9.2 Hz), 141.21 (d, *J* = 10.4 Hz); ^{31}P NMR (202 MHz, $CDCl_3$) δ 26.4 (d, *J* = 69.2 Hz); HRMS (ES^+) *m/z* [M – H]$^+$ Calcd for $C_{14}H_{19}BP$, 253.1317; Found, 253.1311.

(3*R*)-1,3-diphenyloctan-1-one (7); representative procedure for asymmetric 1,4-addition catalyzed by *in situ*-generated palladium catalyst

DABCO (40.4 mg, 18 mol%) was added to a solution of ligand **L3** (34.5 mg, 3 mol%) in toluene (4.0 mL) and the mixture was heated to 110 °C with stirring for 1 h. The solvent was removed *in vacuo*, $Pd(dba)_2$ (34.5 mg, 3 mol%), $Cu(BF_4)_2 \cdot 6H_2O$ (82.9 mg, 12 mol%), $KPhBF_3$ (552 mg, 1.5 equiv), and 10:1 MeOH–H_2O (10.0 mL) were added, and the resulting mixture was stirred at 25 °C for 30 min. (*E*)-1-Phenyloct-2-en-1-one (**6**; 405 mg, 2.00 mmol) was added at 10 °C, and the mixture was stirred at 10 °C for 20 h. The resulting mixture was washed with 20% aq K_2CO_3 (2.0 mL) and extracted with MTBE (4.0 × 2 mL). The combined extracts were dried (Na_2SO_4) and concentrated *in vacuo* to give a residue that was purified by chromatography (silica gel) to give the title compound as a white solid [551 mg, 98%; 85% ee (t_{major} = 7.2 min, t_{minor} = 6.7 min)].

IR (KBr, cm^{-1}) ν 3333, 3082, 3062, 3027, 3005, 2950, 2923, 2855, 1672, 1595, 1495, 1966, 1448, 1414, 1375, 1353, 1275, 1239, 1211, 1072, 1004, 973, 763, 747, 699, 685, 593, 571; ^{1}H NMR (500 MHz, $CDCl_3$) δ 0.82 (t, *J* = 6.4 Hz, 3H), 1.05–1.29 (m, 6H), 1.59–1.75 (m, 2H), 3.20–3.36 (m, 3H), 7.18 (t, *J* = 7.6 Hz, 1H), 7.22 (d, *J* = 7.6 Hz, 2H), 7.27 (dd, *J* = 7.6, 7.6 Hz, 2H) , 7.43 (dd, *J* = 7.6, 7.6 Hz, 2H), 7.53 (t, *J* = 7.6 Hz, 1H), 7.89 (d, *J* = 7.6 Hz, 2H); ^{13}C NMR (125 MHz, $CDCl_3$) δ 14.0, 22.5, 27.1, 31.8, 36.3, 41.3, 46.0, 126.2, 127.6, 128.0, 128.4, 128.5, 132.9, 137.3, 145.0, 199.2; HRMS (ES^+) *m/z* [M + H]$^+$ Calcd for $C_{20}H_{25}O$, 281.1905; Found, 281.1896. $[\alpha]^{25}_D$ +2.1 (*c* 1.0, $CHCl_3$); lit. $[\alpha]^{25}_D$ +1.3 (55% ee, *c* 1.1, $CHCl_3$).[12]

<Typical procedure for carbometalation>

To a solution of ligand **L5** (5.7 mg, 0.010 mmol) of toluene (1.7 mL) was added DABCO (6.7 mg, 0.060 mmol) and stirred at 110 °C for 1 hour. After cooling to 25 °C, the resulting mixture was washed with 0.20 M aqueous solution of TFA (0.60 mL), concentrated *in vacuo*, and added toluene (1.7 mL) to give a ligand solution. To another flask was added activated MS4A (36 mg) and $ZnCl_2$ solution (1.0 M in THF, 0.75 mL, 0.75 mmol), then transferred supernatant of the ligand solution. To the mixture was added PhMgBr solution (1.04 M in THF, 1.40 mL, 1.50 mmol) at 0 °C and stirred at the same temperature for 30 minutes. After addition of $FeCl_3$ solution (0.05 M in THF, 0.10 mL,

0.050 mmol) and stirring for 5 minutes, a solution of 1,4-epoxy-1,4-dihydronaphthalene **8** (72 mg, 0.50 mmol) in toluene (0.50 mL) was added and stirred at 0 °C for 4 hours. The reaction was quenched with degassed 20% methanolic solution of acetic acid (0.60 mL) at the same temperature and stirred for 10 minutes. The mixture was added a saturated aqueous solution of NH_4Cl, extracted with MTBE, dried over Na_2SO_4, and concentrated *in vacuo*. The residue was analyzed by ^1H NMR and HPLC (81% yield, 81% ee).

Enantiomeric excesses of compound **3** and **4** were determined by HPLC analysis: Daicel Chiralcel OD-3R column, acetonitrile/0.01 M phosphate buffer (pH 6.8) = 60/40, 1.0 mL/min, 25 °C, UV 220 nm.

References and Notes

[1] Complete issue: *Organometallics in Process Chemistry* in *Topics in Organometallic Chemistry*, Springer, **2004,** Vol. 6, pp. 1–301.

[2] (a) *Phosphorus Ligands in Asymmetric Catalysis: Synthesis and Applications*, Vol. 1; A. Börner, Ed.; Wiley-VCH: Weinheim, 2008; pp. 73–113. (b) J. M. Whitesell, *Chem. Rev.* **1989**, *89*, 1581–1590.

[3] (a) M. D. Fryzuk, B. Bosnich, *J. Am. Chem. Soc.* **1977**, *99*, 6262–6267. (b) C. Bianchini, H. M. Lee, A. Meli, W. Oberhauser, M. Peruzzini, F. Vizza, *Organometallics* **2002**, *21*. 16–33. (c) S. –K. Kim, T. –J. Kim, J. –H. Chung, T. –K. Hahn, S. –S. Chae, H. –S. Lee, M. Cheong, S. O. Kang, *Organometallics* **2010**, *29*, 5805–5811.

[4] (a) I. Ojima, N. Clos, C. Bastos, *Tetrahedron* **1989**, *45*, 6901–6939. (b) R. Kadyrov, T. H. Riermeier, U. Dingerdissen, V. Tararov, A. Börner, *J. Org. Chem.* **2003**, *68*, 4067–4070. (c) *Asymmetric Catalysis on Industrial Scale: Challenges, Approaches and Solutions*, 2nd ed.; H.-U. Blaser, H.-J. Federsel, Eds.; Wiley-VCH: Weinheim, 2010; pp. 187–205.

[5] (a) M. Yamaguchi, T. Shima, T. Yamagishi, M. Hida, *Tetrahedron: Asymmetry* **1991**, *2*, 663–666. (b) E. Gomez-Bengoa, N. M. Heron, M. T. Didiuk, C. A. Luchaco, A. H. Hoveyda, *J. Am. Chem. Soc.* **1998,** *120*, 7649–7650.

[6] (a) P. Mauleon, J.C. Carretero, *Org. Lett.* **2004**, *6*, 3195–3198. (b) T. Nishikata, Y. Yamamoto, N. Miyaura, *Chem. Commun. (Cambridge, U. K.)* **2004**, 1822–1823. (c) T. Nishikata, Y. Yamamoto, N. Miyaura, *Chem. Lett.* **2005**, *34*, 720–721. (d) T. Nishikata, Y. Yamamoto, N. Miyaura, *Adv. Synth. Catal.* **2007**, *349*, 1759–1764. (e) T. Nishikata, Y. Yamamoto, N. Miyaura, *Tetrahedron Lett.* **2007**, *48*, 4007–4010. (f) T. Nishikata, Y. Kobayashi, K. Kobayshi, Y. Yamamoto, N. Miyaura, *Synlett* **2007**, 3055–3057. (g) T. Nishikata, Y. Yamamoto, N. Miyaura, *Chem. Lett.* **2007**, *36*, 1442–1443. (h) T. Nishikata, S. Kiyomura, Y. Yamamoto, N. Miyaura, N. *Synlett* **2008**, 2487–2490. (i) K. Kobayashi, Y. Yamamoto, N. Miyaura, T. Nishikata, *Bull. Chem. Soc. Jpn.* **2008**, *81*, 1019–1025. (j) T. Nishikata, Y. Yamamoto, N. Miyaura, *Adv. Synth. Catal.* **2007**, *349*, 1759–1764. (k) X.-Q. Yu, T. Shirai, Y. Yamamoto, N. Miyaura, *Chem. Asian J.* **2011**, *6*, 932–937.

[7] H. Brisset, Y. Gourdel, P. Pellon, M. Le Corre, *Tetrahedron Lett.* **1993**, *34*, 4523–4526.

[8] G. B. Consiglio, P. Queval, A. Harrison-Marchand, A. Mordini, J.-F. Lohier, O. Delacroix, A.-C. Gaumont, H. Gérard, J. Maddaluno, H. Oulyadi, *J. Am. Chem. Soc.* **2011**, *133*, 6472–6480.

[9] C. A. Busacca, E. Farber, J. DeYoung, S. Campbell, N. C. Gonnella, N. Grinberg, N. Haddad, H. Lee, S. Ma, D. Reeves, S. Shen, C. H. Senanayake, *Org. Lett.* **2009**, *11*, 5594–5597.

[10] (a) T. Nishikata, Y. Yamamoto, N. Miyaura, *Chem. Lett.* **2003**, 32, 752–753. (b) Personal correspondence from Prof. Yasunori Yamamoto.

[11] Miyaura performed the same 1,4-addition reaction by using the isolated cationic palladium catalyst at –15 °C and obtained the desired product with a slightly higher enantioselectivity (89% ee). The *in situ*-generated catalyst, however, showed <5% conversion at temperatures below –15 °C. See also ref 6c.

[12] The absolute configuration of compound **7** was assigned as *R* by comparison with the reported chiral HPLC analysis and the optical rotation. Q. Chen, M. Kuriyama, X. Hao, T. Soeta, Y. Yamamoto, K. Yamada, K. Tomioka, *Chem. Pharm. Bull.* **2009**, *57*, 1024–1027.

PART 2

Iron-Catalyzed Enantioselective Cross-Coupling Reaction: Access to the NSAIDs

CHAPTER 3

Cross-Coupling of Non-activated Chloroalkanes with Aryl Grignard Reagents in the Presence of Iron/*N*-Heterocyclic Carbene Catalysts

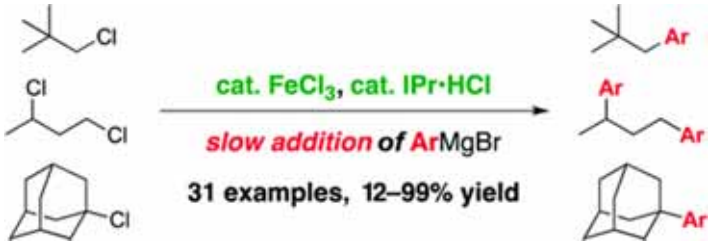

Abstract

An efficient and high-yielding cross-coupling reaction of various primary, secondary, and tertiary alkyl chlorides with aryl Grignard reagents was achieved by using catalytic amounts of *N*-heterocyclic carbene ligands and iron salts. This reaction is a simple and efficient arylation method having applicability to a wide range of industrially abundant chloroalkanes, including polychloroalkanes, which are challenging substrates under conventional cross-coupling conditions.

Introduction

Aryl and alkyl chlorides are abundant industrial feedstocks with annual global production on the order of millions of tons.[1] Significant progress has been made in the development of synthetically valuable cross-coupling reactions with aryl chlorides. These transformations are extremely important for preparing aromatic compounds in academic and industrial settings.[2] However, alkyl chlorides remain challenging substrates in cross-coupling reactions, and they are not commonly used as electrophilic coupling partners[3] because the kinetic and thermodynamic stability of unactivated sp^3 carbon-chlorine bonds toward transition-metal catalysts hampers efficient bond reorganizations between the coupling partners.[4] Recently, considerable effort has been devoted to achieving useful cross-coupling reactions with non-activated alkyl chlorides. Several catalysts have been reported,[5] but they are mostly limited to primary alkyl electrophiles, and only one method is applicable to secondary alkyl chlorides.[5f] Besides these other metal catalysts, iron catalysts have recently proved to be remarkably effective for coupling reactions of non-activated alkyl halides.[6,7,8] Nonetheless, these iron-catalyzed reactions are mainly applied to alkyl bromides and iodides. Alkyl chlorides, especially primary and tertiary ones, remain poor substrates with iron catalysts. This is partly, but critically, owing to the reaction mechanism of the iron-catalyzed cross-couplings of alkyl halides, which are most likely radical-mediated.[9] Herein, the author reports a versatile metal-catalyzed cross-coupling method applicable to a variety of alkyl chlorides with aryl Grignard reagents. The reactions are easily carried out with catalytic amounts of $FeCl_3$ and *N*-heterocyclic carbene (NHC) ligands[10,11] by the *slow addition* technique developed by Nakamura previously[8a,m,n] (Figure 1).

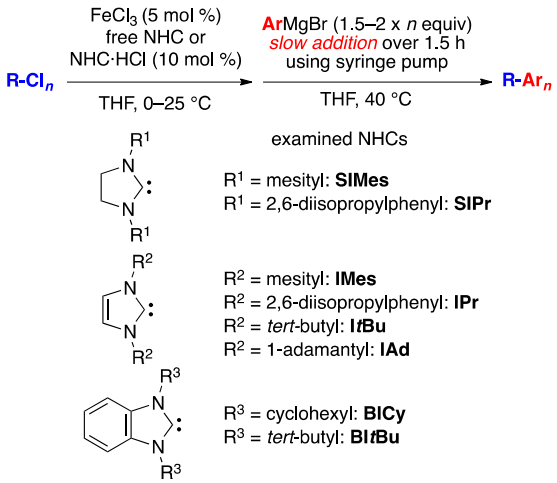

Figure 1. Coupling reaction between alkyl chlorides and aryl Grignard reagents in the presence of $FeCl_3$ and NHC ligands.

Results and Discussion

The author began by studying coupling reactions between 1-chlorodecane and phenylmagnesium bromide in the presence of an iron salt[12] and an NHC ligand. Table 1 summarizes the outcomes of the reactions with various ligands and conditions.[13] Use of the IPr ligand and the slow addition technique were the keys to obtaining the cross-coupling product in high yield. In the absence of a ligand, the desired coupling product **2** was obtained in 20% yield along with significant amounts of alkene and alkane byproducts; thus, the product selectivity was quite low at 32% (entry 1). While the widely used IMes did not work well (entry 2), bulkier NHCs such as I*t*Bu, IAd, and IPr improved the product selectivity to as high as 80% and caused efficient conversion of **1** (entries 3–5). A superior result was obtained when IPr·HCl was used as the NHC precursor (entry 6). Furthermore, the author found that without the slow addition technique, the reaction provided 1-decene as the major product in 47% yield and gave the desired product with only 25% selectivity (entry 7). The author tried to improve the reaction further with the NHC ligand SIPr, but it proved to be less effective than its unsaturated congener IPr (entry 8). Based on these results, the author selected IPr·HCl with the slow addition technique as the conditions for the rest of this study.

Table 1. Iron-Catalyzed Cross-Coupling Reaction of 1-Chlorodecane with Phenylmagnesium Bromide

entry[a]	ligand	GC yield[b] /% (er)				coupling selectivity[c]
		2	**3**	**4**	**1**	
1	none	20	18	24	31	32
2	IMes	31	18	31	0	39
3	I*t*Bu	78	6	11	0	82
4	IAd	72	3	14	0	81
5	IPr	78	3	16	0	80
6	IPr[d]	85	7	8	0	85
7	IPr[d,e]	23	47	21	0	25
8	SIPr	59	7	21	0	68
9	SIMes	13	19	13	42	29
10	IBCy[d]	10	6	13	65	32
11	BI*t*Bu[d]	24	13	40	0	31
12	cyclohexyl JohnPhos[f]	16	19	31	27	24
13	TMEDA[g] (2.0 equiv)	40	18	24	11	49

[a]Reactions were carried out on a 0.5–1.0 mmol scale under the conditions described in Figure 1. [b]Yields were determined by GC analysis using undecane as an internal standard. [c]% Selectivity of the coupling product **2** in all the products. [d]NHC free carbene was prepared in situ by mixing equimolar amounts of NHC·HCl and PhMgBr at 0 °C for 5 min. [e]PhMgBr was added at 0 °C in a single aliquot and heated to 40 °C for 1.5 h. [f]Biphenyl-2-yl(dicyclohexyl)phosphine. [g]1,1,2,2-Tetramethylethylenediamine.

Screening of some transition metal salts as a catalyst precursor was carried out according to the typical procedure (Table 2). The desired cross-coupling reaction proceeded smoothly when iron salts were used except citrate salts (entries 1–5). On the other hand, a trace amount of the desired product was obtained with cobalt salt or nickel salt (entries 6 and 7), and no cross-coupling product was attained when copper or palladium salt was used as a catalyst precursor (entries 8 and 9). These results strongly suggest that this cross-coupling reaction was accelerated by the iron catalyst, not the trace amount of other transition metals.[12]

Table 2. The Cross-Coupling Reaction of 1-Chlorodecane with Various Metal Catalyst Precursors

entry[a]	metal catalyst	GC yield[b] /% (er)				coupling selectivity[c]
		2	**3**	**4**	**1**	
1	$FeCl_3$	85	7	8	0	85
2	$FeCl_2$	79	7	9	1	82
3	iron(III) citrate	0	0	0	99	NA
4	$Fe(acac)_3$	81	3	8	0	88
5	$Fe(acac)_2$	78	7	8	2	84
6	$Co(acac)_2$	9	6	39	19	17
7	$Ni(acac)_2$	4	5	6	85	27
8	$Cu(acac)_2$	0	0	0	>99	NA
9	$Pd(acac)_2$	0	0	0	>99	NA

[a]Reactions were carried out on a 0.5–1.0 mmol scale under the conditions described in Figure 1. [b]Yields were determined by GC analysis using undecane as an internal standard. [c]% Selectivity of the coupling product **2** in all the products.

Table 3 presents the scope of the coupling reaction with a variety of alkyl chlorides. Primary alkyl chlorides were coupled with various aryl Grignard reagents to give the corresponding products in good to excellent yields. Phenyl and *para*-substituted aryl Grignard reagents gave the coupling products in 83–92% yields (Table 3, entries 1–6). Excellent yields were obtained with the moderately sterically demanding 2-tolyl- and 1-naphthylmagnesium bromides (entries 7, 8, and 13). Only the bulky mesityl Grignard failed to yield the product (entry 9). Sterics appear to hinder the reaction in cases of extreme crowding. As in entries 10 and 11, the steric hindrance at the beta position to the reaction site did not affect much on the chemical yield, suggesting that the substitution proceeded via a non-S_N2 mechanism.

Table 3. Cross-Coupling Reaction of Various Alkyl Chlorides with Arylmagnesium Halides

entry[b]	alkyl chloride	ArMgBr	yield[c] (%)
1[d]	decyl—Cl	Ar = Ph	84
2[d]		Ar = Ph[e]	84[f]
3[d]		Ar = 4-tolyl	85
4[d]		Ar = 4-MeO-C_6H_4	83
5[d]		Ar = 4-F-C_6H_4	92
6[d]		Ar = 2-naphthyl	84
7[d]		Ar = 1-naphthyl	98
8[d]		Ar = 2-tolyl	97
9[d]		Ar = mesityl	0[g]
10[d]		4-MeO-C_6H_4	69[h]
11[d]		4-MeO-C_6H_4	67[h]
12[d]	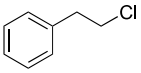	Ar = 4-MeO-C_6H_4	53[h]
13[d]		Ar = 1-naphthyl	95[h]
14		Ar = Ph	99
15		Ar = Ph[e]	96[h]
16		Ar = 4-MeO-C_6H_4	98
17		Ar = 4-F-C_6H_4	98
18		Ar = 2-tolyl	99
19		Ar = 2-naphthyl	98[h]
20[i]		Ar = 1-naphthyl	97[h]
21[i]		Ar = mesityl	trace[g]
22		Ph	99
23		Ph	96
24		4-MeO-C_6H_4	72
25[d]		4-MeO-C_6H_4	12[h]
26[d]	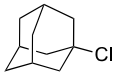	Ar = Ph	88
27[d]		Ar = 4-MeO-C_6H_4	90
28[d]		Ar = 4-F-C_6H_4	87
29	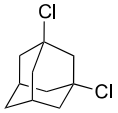	Ph	68
30	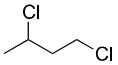	Ph	85
31	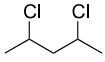	Ph	86
32[d]	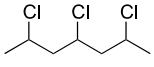	Ph	61

[a]The reactions were carried out on a 1–3 mmol scale for monochloro compounds, 0.5 mmol scale for dichloro compounds, and 0.33 mmol scale for trichloro compounds under slow addition conditions. [b]1.5 equiv of Grignard reagent was used per atom of chlorine present in the molecule unless otherwise noted. [c]Isolated yield. [d]2.0 equiv of Grignard was used per atom of chlorine present in the molecule. [e]PhMgCl was used instead of PhMgBr. [f]GC yield with undecane as an internal standard. [g]*ca.* 99% of recovery of the starting material. [h]NMR yield determined with 1,1,2,2-tetrachloroethane as an internal standard. [i]1.6 equiv of Grignard reagent was used.

Entries 14–24 show that the cross-coupling of secondary alkyl chlorides proceeded smoothly to give the corresponding coupling products in excellent yields. The only poor reaction was again with the mesityl nucleophile. Otherwise, steric or electronic factors did not significantly affect the selectivity, probably because a secondary carbon-chlorine bond is more susceptible to homolytic cleavage than a primary one. Phenylmagnesium chloride also gave the desired products in good yields, showing that the bromide ion derived from the Grignard reagent had no role in the coupling reactions (Table 3, entries 2 and 15). While reactions with tertiary alkyl chlorides were somewhat inconsistent, cross-couplings with adamantyl chloride gave the corresponding products in high yields (entries 26–28). Again, the electronic effects of the aryl substituents were negligible. Unfortunately, *tert*-butyl chloride gave the cross-coupling product in only 12% yield although the chloride substrate was consumed smoothly (entry 25).

The present method could be further applied to polychlorinated alkanes such as 1,3-dihalogenated compounds (entries 29–31). In the presence of the iron catalyst and the Grignard reagents, these polychlorinated alkanes usually provide elimination and cyclization products.[14] It is interesting to note that the coupling reaction of 2,4,6-trichloroheptane, a model compound of polyvinyl chloride (PVC),[15] gave the triply arylated product in good yield, suggesting a role of this reaction in polymer functionalization.

To gain mechanistic insight into the cross-coupling reaction, the author conducted a stereochemical study using diastereomerically pure α,β-[D_2]-β-adamantylethyl chloride **5**[5h] with PhMgBr under the standard conditions (Scheme 1). ^{1}H NMR analysis revealed that the reaction center completely epimerized to give a 1:1 mixture of diastereomers, suggesting a radical intermediate. This was in stark contrast with the Cu-catalyzed cross-coupling reactions between alkyl chlorides and Grignard reagents reported by Kambe and Terao, where the reactions proceeded with almost complete inversion of the stereochemistry at the reaction center, inferring an S_N2 mechanism.[5h]

Scheme 1. Cross-Coupling Reaction of Diastereomerically Pure Alkyl Chloride to Study the Mechanism

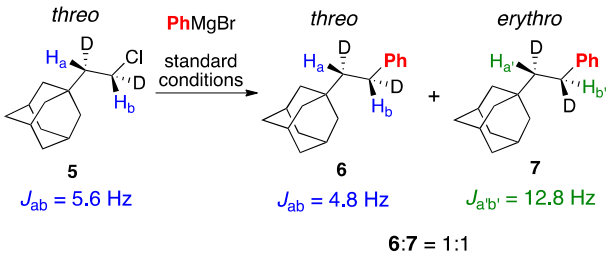

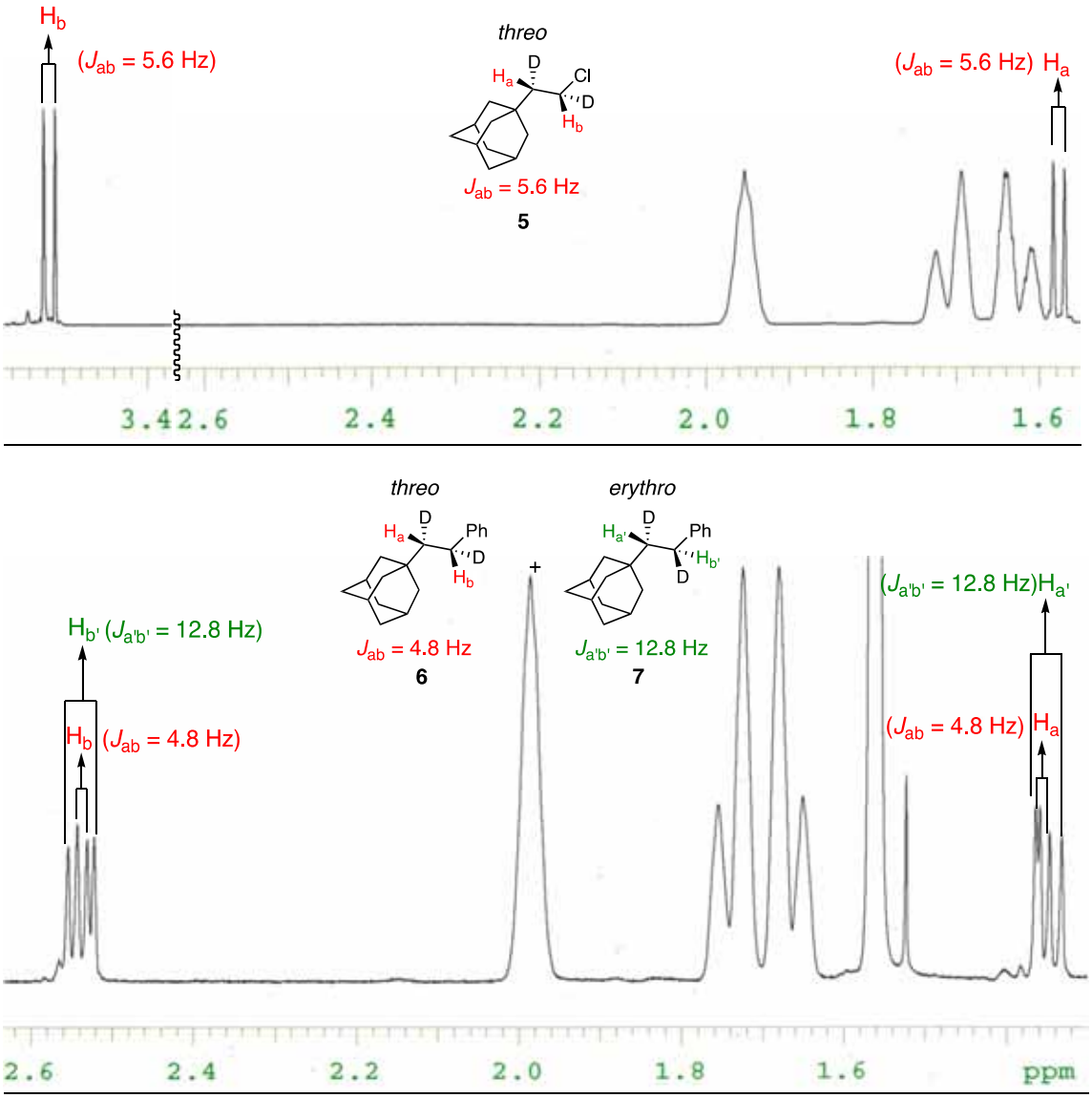

Figure 2. $^1H\{^2H\}$ NMR spectra of the starting *threo*-α,β-d_2-β-adamantylethyl chloride (top) and products (bottom) from $FeCl_2$ catalyzed cross-coupling reaction (1:1 mixture of *erythro* & *threo* diastereomers).

The time course analysis was carried out for the coupling reaction under standard conditions: aliquots were taken from the reaction mixture and analyzed by GC at different time points. The results are summarized in Figure 3. No reaction of 1-chlorodecane was observed during the addition of the initial 0.25 equiv. (i.e., 5 equiv. to $FeCl_3$) of PhMgBr and biphenyl was obtained in 3 % yield as an exclusive product (i.e., 60% yield based on the partial reduction of Fe(+III) to Fe(+II)). This result suggests that 0.1 euqiv of the PhMgBr was used to generate free IPr form IPr·HCl by deprotonation and the other 0.15 equiv was used to reduce $FeCl_3$ to a divalent iron species. After the addition of this supplemental amount of PhMgBr, the coupling reaction was initiated and the conversion of the substrate to the coupling product was observed, suggesting that diaryliron(II) species bearing one or two IPr ligands was converted to the catalytically active species in the presence of an excess amount of PhMgBr.

(a)

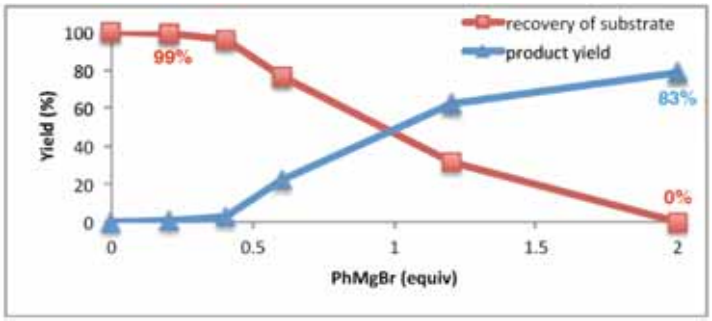

(b)

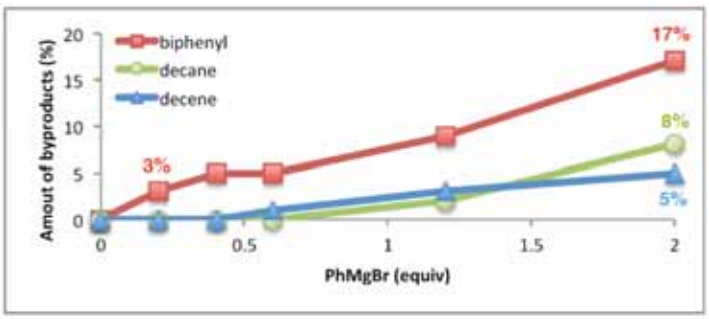

Figure 3: GC traces of the cross-coupling reactions of **1** with PhMgBr (a) Red and blue lines show the recovery of the substrate and the yield of the product, respectively. (b) Red, blue, and green lines show the yield of biphenyl, decane, and decene, respectively.

Based on these observations and results reported previously by Nakamura and the other researchers, a plausible mechanism is postulated in Scheme 2. The initial

reduction of $FeCl_3$ with an aryl Grignard reagent gives an iron(II) intermediate.[8h] The author actually observed an induction period for the coupling reaction during the addition of ca. 5 equiv of ArMgBr to $FeCl_3$, in which 3 equiv were used for the partial reduction of $FeCl_3$ to generate the biaryl and the other 2 equiv were used to generate two NHC ligands from the corresponding imidazolium salt. As shown in Scheme 2, the iron(II) intermediate can be best described as a neutral diaryliron possessing two NHC ligands,[16] such as **A**. While **A** may or may not be a reactive intermediate, the author is currently assuming that a ferrate(II) intermediate **B** is the catalytically active species because of its higher reducing potential than the neutral species.[17] Thus, homolytic cleavage of the sp^3 carbon-chlorine bond and recombination of the resulting elusive radical with an aryl ligand occur in a solvent cage to give the coupling product while regenerating **A**.

Scheme 2. A Plausible Mechanism for the Iron-Catalyzed Cross-Coupling Reaction

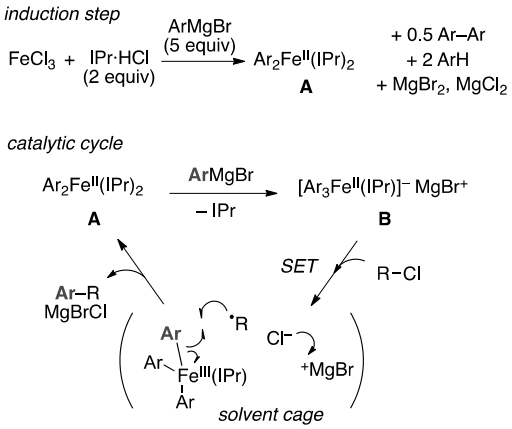

Conclusion

In summary, the author has developed an efficient iron-catalyzed cross-coupling reaction and demonstrated its scope with various primary, secondary, and tertiary alkyl chlorides and aryl Grignard reagents. The method was also effective for arylating polychloalkanes that would form byproducts under other conditions. This direct arylation uses catalytic amounts of IPr and $FeCl_3$ with the slow addition method. Instead of requiring more costly bromo- and iodoalkanes, the technique works with less costly alkyl chlorides, extending the utility of the catalytic cross-coupling of non-activated alkyl halides.

Experimental Section

General Information

All the reactions dealing with air or moisture sensitive compounds were carried out in a dry reaction vessel under a positive pressure of argon. Air- and moisture-sensitive liquids and solutions were transferred via syringe or stainless steel cannula. Analytical thin-layer chromatography was performed using glass plates pre-coated with 0.25-mm-thick 230–400-mesh silica gel impregnated with a fluorescent indicator (254 nm). Thin layer chromatography plates were visualized by exposure to ultraviolet light (UV) and/or by immersion in an ethanol solution of PMA (phosphomolybdic acid) followed by heating on a hot plate. Organic solutions were concentrated by a rotary evaporator at c.a. 15 Torr (evacuated with a diaphragm pump). Flash column chromatography was performed as described by Still et al.[18] employing Sigma-Aldrich Silica gel, Merck grade 9385, 230–400 mesh, 60 Å.

Materials

Commercial reagents were purchased from Tokyo Kasei Co., Aldrich Inc., and other commercial suppliers and were used either distilled or recrystallized before use. Anhydrous tetrahydrofuran (THF) was purchased from Kanto Chemical Co. and distilled from benzophenone ketyl at 760 Torr under an argon atmosphere immediately before use. The water content of the solvent was confirmed with a Karl-Fischer moisture titrator to be less than 20 ppm. $FeCl_3$ (powder, 99.99+%) purchased from Aldrich Inc. was used without further purification and was handled under an inert atmosphere. A 0.1 M THF solution of $FeCl_3$ tends to form polyether compounds upon room-temperature storage, and thus was prepared immediately before use or stored at –20 °C for a few days.

Instrumentation

Proton nuclear magnetic resonance (^{1}H NMR) and carbon nuclear magnetic resonance (^{13}C NMR) spectra were recorded on JEOL ECS-400 (392 MHz) and ECA-500 (500 MHz), Varian, Mercury 300 and 400 (300 MHz and 400 MHz, respectively) NMR spectrometers. Chemical shifts for protons are reported in parts per million (ppm, δ scale) downfield from tetramethylsilane and are referenced to residual protium in the NMR solvent ($CDCl_3$: δ 7.26). Carbon nuclear magnetic resonance spectra (^{13}C NMR) spectra were recorded at 75 MHz and 98.5 MHz: chemical shifts for carbons are reported in parts per million (ppm, δ scale) downfield from tetramethylsilane and are referenced to the carbon resonance of $CDCl_3$ (δ 77.0). Data

are presented as: chemical shift, multiplicity (s = singlet, d = doublet, t = triplet, q = quartet, quint = quintet, sext = sextet, sept = septet, m = multiplet and/or multiple resonances, br = broad), coupling constant in hertz (Hz), and signal area integration in natural numbers. Gas chromatographic (GC) analyses were performed on Shimadzu GC-14B, GC-17 and GC-2010 instruments equipped with an FID detector and a capillary column, HR-1 (25 m × 0.25 mm i.d., 0.25 μm film) or a CYCLOSILB (Agilent, 30 m × 0.25 mm i.d., 0.25 μm film) or a CHIRALDEX G-TA (ASTEC, 20 m × 0.25 mm i.d., 0.125 μm film). IR spectra recorded on a PerkinElmer Spectrum One FT-IR Spectrometer and characteristic IR absorptions are reported in cm^{-1}. NMR yield was determined for a crude product by ^{1}H NMR analyses by using dibromomethane as an internal standard. GC yield was determined upon calibration by using undecane as an internal standard. The purity of isolated compounds was determined by the above-described GC analysis.

Decylbenzene (Table 3, entry 1): (i) *Using TMEDA*: To a mixture of 1-chlorodecane (177 mg, 1.00 mmol), $FeCl_3$ (0.50 mL of a 0.1 M THF solution, 5 mol%) was added a mixture of PhMgBr (2.1 mL of a 0.96 M THF solution, 2.0 mmol) and TMEDA (0.30 mL, 2.0 mmol) via syringe pump over a period of 90 min at 40 °C. The reaction mixture was stirred at that temperature for 10 min after completion of the addition of the mixture of the Grignard reagent and TMEDA. After aqueous workup, the reaction mixture was filtered through a pad of Florisil® and concentrated *in vacuo*. GC Analysis showed that the yield of *n*-decylbenzene was 40%. (ii) *Using IPr·HCl*: To stirred solid powder IPr·HCl (42.5 mg, 10 mol%) at 0 °C was added small portion of PhMgBr (0.27 mL of a 0.94 M THF solution, 0.25 equiv) and allowed to stir for 5 min, then 0.1 M THF solution of $FeCl_3$ (0.50 mL, 5 mol%) was added followed by the addition of 1-chlorodecane (181 mg, 1.02 mmol). PhMgBr (1.87 mL of 0.94 M THF solution, 1.75 equiv) was then added slowly using syringe pump over a period of 90 min at 40 °C. The reaction mixture was stirred at that temperature for 10 min after completion of the addition of the Grignard reagent. After aqueous workup, the reaction mixture was filtered through a pad of Florisil® and concentrated *in vacuo*. GC Analysis showed that the yield of *n*-decylbenzene was 85%. Purification of the crude product with silica gel chromatography afforded the desired product as a colorless oil (188 mg, 84% yield); FTIR (neat, cm^{-1}) ν 2922, 2853, 1496, 1454, 1073, 744, 693; ^{1}H NMR (300 MHz, $CDCl_3$) δ 0.90 (t, J = 7.0 Hz, 3H), 1.22–1.40 (m, 14H), 1.58–1.68 (m, 2H), 2.62 (t, J = 7.8 Hz, 2H), 7.15–7.22 (m, 3H), 7.25–7.32 (m, 2H); ^{13}C NMR (75 MHz, $CDCl_3$) δ 14.3, 22.9, 29.5, 29.7, 29.8, 31.7, 32.1, 36.2, 125.7, 128.4, 128.6,143.2; HRMS (EI, 70

eV) *m*/*z* $[M]^+$ calcd for $C_{16}H_{26}$, 218.2035 ; found, 218.2037. Anal. Calcd for $C_{16}H_{26}$: C, 88.00; H, 12.00. Found: C, 88.15; H, 11.95. All analytical data are in good accordance with those reported in the literature.[19]

A typical procedure for the cross-coupling reactions using IPr·HCl: To stirred solid powder IPr·HCl (0.1 equiv) at 0 °C was added a small portion of Grignard reagent solution (0.25 equiv) and allowed to stir for 5 min, then 0.1 M THF solution of $FeCl_3$ (0.05 equiv) was added followed by the addition of alkyl chloride (1 equiv of chlorine). Grignard reagent solution (1.25 equiv) was then added slowly using a syringe pump over a period of 90 min at 40 °C. The reaction mixture was stirred at that temperature for 10 min after completion of the addition of the Grignard reagent. After aqueous workup, the reaction mixture was filtered through a pad of Florisil® and concentrated *in vacuo*. The crude product was finally purified by column chromatography over silica gel (230-400 mesh).

1-Decyl-4-methylbenzene (Table 3, entry 3): The titled compound was prepared from 1-chlorodecane (529 mg, 2.99 mmol) and 4-tolylmagnesium bromide (5.41 mL of a 1.11 M THF solution, 2.0 equiv) following the procedure described for synthesis of 1-decyl-2-methylbenzene. Purification of crude product with silica gel chromatography afforded the desired product as a colorless oil (591 mg, 85% yield); FTIR (neat, cm^{-1}) ν 2923, 2852, 1515, 1465, 806; ^1H NMR (400 MHz, $CDCl_3$) δ 0.88 (t, *J* = 7.0 Hz, 3H), 1.18–1.36 (m, 14H), 1.52–1.63 (m, 2H), 2.31 (s, 3H), 2.55 (t, *J* = 7.9 Hz, 2H), 7.03–7.11 (m, 4H); ^{13}C NMR (100 MHz, $CDCl_3$) δ 14.1, 21.0, 22.7, 29.4, 29.5, 29.61, 29.64, 31.7, 31.9, 35.5, 128.3, 128.9, 134.9, 139.9; HRMS (EI, 70 eV) *m*/*z* $[M]^+$ calcd for $C_{17}H_{28}$, 232.2191; found, 232.2194. Anal. Calcd for $C_{17}H_{28}$: C, 87.86; H, 12.14. Found: C, 87.90; H, 12.19. All analytical data are in good accordance with those reported in the literature.[5c]

1-Decyl-4-methoxybenzene (Table 3, entry 4): The titled compound was prepared from 1-chlorodecane (527 mg, 2.98 mmol) and 4-methoxyphenylmagnesium bromide (5.51 mL of a 1.09 M THF solution, 2.0 equiv) following the procedure described for synthesis of 1-decyl-2-methylbenzene. Purification of crude product with silica gel chromatography afforded the desired product as a colorless oil (617 mg, 83% yield); FTIR (neat, cm^{-1}) ν 2923, 2853, 1654, 1612, 1560, 1512, 1465, 1300, 1243, 1175, 1039, 819; ^1H NMR (400 MHz, $CDCl_3$) δ 0.88 (t, *J* = 6.8 Hz, 3H), 1.20–1.35 (m, 14H), 1.54–1.62 (m, 2H), 2.54 (t, *J* = 7.6 Hz, 2H), 3.78 (s, 3H), 6.78–6.85 (m, 2H), 7.05–7.12 (m,

2H); ^{13}C NMR (100 MHz, $CDCl_3$) δ 14.1, 22.7, 29.29, 29.34, 29.5, 29.6, 31.8, 31.9, 35.1, 55.2, 113.6, 129.2, 135.1, 157.6; HRMS (EI, 70 eV) *m*/*z* $[M]^+$ calcd for $C_{17}H_{28}O$, 248.2140; found, 248.2139. Anal. Calcd for $C_{17}H_{28}O$: C, 82.20; H, 11.36. Found: C, 82.09; H, 11.44. All analytical data are in good accordance with those reported in the literature.[5f]

1-Fluoro-4-decylbenzene (Table 3, entry 5): The titled compound was prepared from 1-chlorodecane (528 mg, 2.99 mmol) and 4-fluorophenylmagnesium bromide (6.32 mL of a 0.95 M THF solution, 2.0 equiv) following the procedure described for synthesis of 1-decyl-2-methylbenzene. Purification of crude product with silica gel chromatography afforded the desired product as a colorless oil (653 mg, 92% yield); FTIR (neat, cm^{-1}) ν 2924, 2854, 1600, 1509, 1465, 1221, 1156, 822; ^{1}H NMR (400 MHz, $CDCl_3$) δ 0.88 (t, *J* = 6.9 Hz, 3H), 1.17–1.34 (m, 14H), 1.52–1.63 (m, 2H), 2.56 (t, *J* = 7.8 Hz, 2H), 6.90–6.99 (m, 2H), 7.07–7.15 (m, 2H); ^{13}C NMR (100 MHz, $CDCl_3$) δ 14.1, 22.7, 29.2, 29.3, 29.5, 29.59, 29.62, 31.6, 31.9, 35.1, 114.8 (d, *J* = 20.6 Hz), 129.6 (d, *J* = 7.5 Hz), 138.5 (d, *J* = 1.8 Hz), 161.1 (d, *J* = 241 Hz); HRMS (EI, 70 eV) *m*/*z* $[M]^+$ calcd for $C_{16}H_{25}F$, 236.1940; found, 236.1945.Anal. Calcd for $C_{16}H_{25}F$: C, 81.30; H, 11.66. Found: C, 81.34; H, 10.67.

2-Decylnaphthalene (Table 3, entry 6): The titled compound was prepared from 1-chlorodecane (527 mg, 2.98 mmol) and naphth-2-ylmagnesium bromide (12.46 mL of a 0.48 M THF solution, 2.0 equiv) following the procedure described for synthesis of 1-decyl-2-methylbenzene. Purification of crude product with silica gel chromatography afforded the desired product as a colorless oil (784 mg, 98% yield); FTIR (neat, cm^{-1}) ν 2923, 2852, 1598, 1510, 1466, 774, 724; ^{1}H NMR (400 MHz, $CDCl_3$) δ 0.88 (t, *J* = 6.7 Hz, 3H), 1.16–1.44 (m, 14H), 1.68–1.77 (m, 2H), 3.05 (t, *J* = 7.8 Hz, 2H), 7.30 (d, *J* = 6.7 Hz, 1H), 7.38 (dd, *J* = 8.5, 6.7 Hz, 1H), 7.42–7.52 (m, 2H), 7.68 (d, *J* = 8.5 Hz, 1H), 7.83 (d, *J* = 7.1 Hz, 1H), 8.03 (d, *J* = 8.5 Hz, 1H); ^{13}C NMR (100 MHz, $CDCl_3$) δ 14.1, 22.7, 29.4, 29.6, 29.7, 29.9, 30.9, 31.9, 33.1, 123.9, 125.3, 125.5, 125.6, 125.8, 126.4, 128.7, 131.9, 133.9, 139.0; HRMS (EI, 70 eV) *m*/*z* $[M]^+$ calcd for $C_{20}H_{28}$, 268.2191; found, 268.2191. Anal. Calcd for $C_{20}H_{28}$: C, 89.49; H, 10.51. Found: C, 89.59; H, 10.54.

1-Decylnaphthalene (Table 3, entry 7): The titled compound was prepared from 1-chlorodecane (527 mg, 2.98 mmol) and naphth-2-ylmagnesium bromide (6.97 mL of a 0.86 M THF solution, 2.0 equiv) following the procedure described for synthesis of 1-decyl-2-methylbenzene. Purification of crude product with silica gel chromatography

afforded the desired product as a colorless oil (674 mg, 84% yield); FTIR (neat, cm^{-1}) ν 2923, 2852, 1669, 1601, 1508, 1465, 852, 813, 743; ^1H NMR (400 MHz, $CDCl_3$) δ 0.88 (t, *J* = 6.9 Hz, 3H), 1.17–1.40 (m, 14H), 1.66–1.78 (m, 2H), 2.76 (t, *J* = 7.6 Hz, 2H), 7.32 (dd, *J* = 1.8, 8.5 Hz, 1H), 7.36–7.47 (m, 2H), 7.60 (s, 1H), 7.72–7.82 (m, 3H); ^{13}C NMR (100 MHz, $CDCl_3$) δ 14.1, 22.7, 29.3, 29.4, 29.5, 29.60, 29.63, 31.4, 31.9, 36.1, 125.0, 125.8, 126.3, 127.38, 127.44, 127.6, 127.7, 131.9, 133.6, 140.5; HRMS (EI, 70 eV) *m*/*z* $[M]^+$ calcd for $C_{20}H_{28}$, 268.2191; found, 268.2191. Anal. Calcd for $C_{20}H_{28}$: C, 89.49; H, 10.51. Found: C, 89.48; H, 10.40.

1-Decyl-2-methylbenzene (Table 3, entry 8). To stirred solid powder IPr·HCl (850 mg, 10 mol%) at 0 °C was added small portion of 2-tolylMgBr (4.85 mL of a 1.03 M THF solution, 0.25 equiv) and allowed to stir for 5 min, then 0.1 M THF solution of $FeCl_3$ (10.0 mL, 5 mol%) was added followed by the addition of 1-chlorodecane (3.53 g, 20.0 mmol). 2-TolylMgBr (34.0 mL of 1.03 M THF solution, 1.75 equiv) was then added slowly using syringe pump over a period of 90 min at 40 °C. The reaction mixture was stirred at that temperature for 10 min after completion of the addition of the Grignard reagent. After aqueous workup, the reaction mixture was filtered through a pad of Florisil® and concentrated *in vacuo*. Purification of the crude product with silica gel chromatography afforded the desired product as a colorless oil (4.50 g, 97% yield); FTIR (neat, cm^{-1}) ν 2993, 2852, 1560, 1466, 739; ^1H NMR (400 MHz, $CDCl_3$) δ 0.88 (t, *J* = 7.0 Hz, 3H), 1.18–1.42 (m, 14H), 1.53–1.63 (m, 2H), 2.30 (s, 3H), 2.58 (t, *J* = 7.8 Hz, 2H), 7.04–7.13 (m, 4H); ^{13}C NMR (100 MHz, $CDCl_3$) δ 14.1, 19.3, 22.7, 29.4, 29.57, 29.64, 29.7, 30.3, 31.9, 33.4, 125.7, 125.8, 128.8, 130.1, 135.8, 141.1; HRMS (EI, 70 eV) *m*/*z* $[M]^+$ calcd for $C_{17}H_{28}$, 232.2191; found, 232.2191. Anal. Calcd for $C_{17}H_{28}$: C, 87.86; H, 12.14. Found: C, 87.65; H, 12.33.

1-Methoxy-4-(2-methylpropyl)benzene (Table 3, entry 10): The titled compound was prepared from 1-chloro-2-methylpropane (90.2 mg, 0.975 mmol) and 4-methoxyphenylmagnesium bromide (1.43 mL of a 1.05 M THF solution, 1.5 equiv) following the procedure described for synthesis of cycloheptylbenzene. The crude product was obtained as a white solid (610 mg). To this crude product was added 1,1,2,2-tetrachloroethane (55.9 mg, 0.333 mmol) and the yield was determined by ^1H NMR analysis (69%). Purification of crude product with silica gel chromatography afforded the desired product as a colorless oil (105 mg, 65% yield). NMR spectra are are in good accordance with those reported in the literature.[20]

1-(2,2-Dimethylpropyl)-4-methoxybenzene (Table 3, entry 11): The titled compound was prepared from 1-chloro-2,2-dimethylpropane (106 mg, 0.991 mmol) and 4-methoxyphenylmagnesium bromide (1.43 mL of a 1.05 M THF solution, 1.5 equiv) following the procedure described for synthesis of cycloheptylbenzene. The crude product was obtained as a white solid (294 mg). To this crude product was added 1,1,2,2-tetrachloroethane (55.8 mg, 0.332 mmol) and the yield was determined by ^{1}H NMR analysis (67%). Purification of crude product with silica gel chromatography afforded the desired product as a colorless oil (95.8 mg, 54% yield). NMR spectra are in good accordance with those reported in the literature.[21]

1-Methoxy-4-(2-phenylethyl)benzene (Table 3, entry 12): The titled compound was prepared from 1-chloro-2-phenylethane (141 mg, 1.00 mmol) and 4-methoxyphenylmagnesium bromide (2.16 mL of a 0.927 M THF solution, 2.0 equiv) following the procedure described for synthesis of 1-(1,1-dimethylethyl)-4-methoxybenzene. The crude product was obtained as a white solid (280 mg). To this crude product was added 1,1,2,2-tetrachloroethane (45.0 mg, 0.268 mmol) and the yield was determined by ^{1}H NMR analysis (53%). NMR spectra are in good accordance with those reported in the literature.[22]

1-(2-Phenylethyl)naphthalene (Table 3, entry 13): The titled compound was prepared from 1-chloro-2-phenylethane (141 mg, 1.00 mmol) and 1-naphthylmagnesium bromide (7.30 mL of a 0.274 M THF solution, 2.0 equiv) following the procedure described for synthesis of 1-(1,1-dimethylethyl)-4-methoxybenzene. The crude product was obtained as a white solid (346 mg). To this crude product was added 1,1,2,2-tetrachloroethane (60.2 mg, 0.359 mmol) and the yield was determined by ^{1}H NMR analysis (95%). NMR spectra are in good accordance with those reported in the literature.[22]

1-Cyclohexyl-4-methoxybenzene (Table 3, entry 16): The titled compound was prepared from chlorocyclohexane (118 mg, 0.994 mmol) following the procedure described for synthesis of cycloheptylbenzene. Purification of crude product with silica gel chromatography afforded the desired product as a white solid (185 mg, 98% yield); FTIR (neat, cm^{-1}) ν 2920, 1512, 1456, 1250, 1176, 1031, 815, 536; ^{1}H NMR (300 MHz, $CDCl_3$) δ 1.16–1.43 (m, 5H), 1.68–1.78 (m, 1H), 1.78–1.92 (m, 4H), 2.39–2.50 (m, 1H), 3.78 (s, 3H), 6.83 (d, J = 8.7 Hz, 2H), 7.13 (d, J = 8.7 Hz, 2H); ^{13}C NMR (75 MHz, $CDCl_3$) δ 26.4, 27.2 (2C), 34.9 (2C), 43.9, 55.5, 113.9 (2C), 127.8 (2C), 140.6, 157.9; HRMS (EI, 70 eV) m/z $[M]^+$ calcd for $C_{13}H_{18}O$, 190.1358; found, 190.1359; Anal.

Calcd for $C_{13}H_{18}O$: C, 82.06; H, 9.53. Found: C, 81.11; H, 9.57. All analytical data are in good accordance with those reported in the literature.[23]

1-Cyclohexyl-4-fluorobenzene (Table 3, entry 17): The titled compound was prepared from chlorocyclohexane (119 mg, 1.00 mmol) following the procedure described for synthesis of cycloheptylbenzene. Purification of crude product with silica gel chromatography afforded the desired product as a white solid (167 mg, 95% yield); FTIR (neat, cm^{-1}) ν 2923, 2851, 1508, 1222, 1158, 825, 806, 755, 565, 531; ^1H NMR (300 MHz, $CDCl_3$) δ 1.19–1.45 (m, 5H), 1.69–1.90 (m, 5H), 2.42–2.52 (m, 1H), 6.92–6.99 (m, 2H), 7.11–7.18 (m, 2H); ^{13}C NMR (75 MHz, $CDCl_3$) δ 26.3, 27.1, 34.9, 44.1, 115.1 (d, J = 6.9 Hz), 128.2 (d, J = 7.4 Hz), 143.9 (d, J = 3.2 Hz), 161.4 (d, J = 242 Hz); HRMS (EI, 70 eV) m/z $[M]^+$ calcd for $C_{12}H_{15}F$, 178.1158; found, 178.1153. Similarly all other cyclohexyl derivatives of Table 3; entries 15, 19, 20, and 21 were characterized and all the data are in good accordance with those reported in the literature.[8a]

Cyclopentylbenzene (Table 3, entry 22): The titled compound was prepared from chlorocyclopentane (106 mg, 1.01 mmol) following the procedure described for synthesis of cycloheptylbenzene. Purification of crude product with silica gel chromatography afforded the desired product as a colorless oil (146 mg, 99% yield); FTIR (neat, cm^{-1}) ν 2949, 2867, 1602, 1491, 1451, 753, 696, 524, ^1H NMR (300 MHz, $CDCl_3$) δ 1.52–1.74 (m, 4H), 1.75–1.84 (m, 2H), 2.01–2.11 (m, 2H), 2.92–3.05 (m, 1H), 7.14–7.20 (m, 1H), 7.22–7.31 (m, 4H); ^{13}C NMR (75 MHz, $CDCl_3$) δ 25.8, 34.8, 46.2, 125.9, 127.3, 128.4,146.7; HRMS (EI, 70 eV) m/z $[M]^+$ calcd for $C_{11}H_{14}$, 146.1096; found, 146.1094. All analytical data are in good accordance with those reported in the literature.[24]

Cycloheptylbenzene (Table 3, entry 23): To stirred solid powder IPr·HCl (42.5 mg, 10 mol%) at 0 °C was added small portion of PhMgBr (0.27 mL of a 0.94 M THF solution, 0.25 equiv) and allowed to stir for 5 min, then 0.1 M THF solution of $FeCl_3$ (0.50 mL, 5 mol%) was added followed by the addition of chlorocycloheptane (132 mg, 0.992 mmol). PhMgBr (1.32 mL of a 0.94 M THF solution, 1.25 equiv) was then added slowly using syringe pump over a period of 90 min at 40 °C. The reaction mixture was stirred at that temperature for 10 min after completion of the addition of the Grignard reagent. After aqueous workup, the reaction mixture was filtered through a pad of Florisil® and concentrated *in vacuo*. Purification of the crude product with silica gel chromatography afforded the desired product as a colorless oil (168 mg, 96% yield);

FTIR (neat, cm^{-1}) ν 3025, 2919, 2852, 1600, 1491, 1450, 1073, 1031, 752, 697; ^1H NMR (300 MHz, $CDCl_3$) δ 1.48–1.72 (m, 8H), 1.75–1.83 (m, 2H), 1.87–1.96 (m, 2H), 2.61–2.70 (m, 1H), 7.13–7.20 (m, 3H), 7.25–7.29 (m, 2H); ^{13}C NMR (75 MHz, $CDCl_3$) δ 27.5 (2C), 28.2 (2C), 37.0 (2C), 47.3, 125.7, 126.9 (2C), 128.5 (2C), 150.2; HRMS (EI, 70 eV) *m*/*z* $[M]^+$ calcd for $C_{13}H_{18}$, 174.1409; found, 174.1403. Anal. Calcd for $C_{13}H_{18}$: C, 89.59; H, 10.41. Found: C, 89.37; H, 10.34. All analytical data are in good accordance with those reported in the literature.[8a]

1-Methoxy-4-(1-methylpropyl)benzene (Table 3, entry 24): The titled compound was prepared from 2-chlorobutane (455 mg, 4.92 mmol) and 4-methoxyphenylmagnesium bromide (8.09 mL of a 0.927 M THF solution, 1.5 equiv) following the procedure described for synthesis of cycloheptylbenzene. Purification of crude product with silica gel chromatography afforded the desired product as a colorless oil (581 mg, 72% yield); ^1H NMR (500 MHz, $CDCl_3$) δ 0.81 (t, *J* = 7.4 Hz, 3H), 1.21 (d, *J* = 6.9 Hz, 3H), 1.56 (dq, *J* = 7.4, 7.4 Hz, 2H), 2.54 (tq, *J* = 7.4, 6.9 Hz, 1 H), 3.78 (s, 3H), 6.84 (d, *J* = 8.4 Hz, 2H), 7.09 (d, *J* = 8.4 Hz, 2H); ^{13}C NMR (125 MHz, $CDCl_3$) δ 12.2, 22.0, 31.3, 40.8, 55.2, 113.6, 127.8, 139.8, 157.6. All analytical data are in good accordance with those reported in the literature.[25]

1-(1,1-Dimethylethyl)-4-methoxybenzene (Table 3, entry 25): To stirred solid powder IPr·HCl (42.5 mg, 10 mol%) at 0 °C was added small portion of 4-methoxyphenylmagnesium bromide (0.27 mL of a 0.927 M THF solution, 0.25 equiv) and allowed to stir for 5 min, then 0.1 M THF solution of $FeCl_3$ (0.50 mL, 5 mol%) was added followed by the addition of 2-chloro-2-methylpropane (92.8 mg, 1.00 mmol). 4-Methoxyphenylmagnesium bromide (1.89 mL of a 0.927 M THF solution, 1.75 equiv) was then added slowly using syringe pump over a period of 90 min at 40 °C. The reaction mixture was stirred at that temperature for 10 min after completion of the addition of the Grignard reagent. After aqueous workup, the reaction mixture was filtered through a pad of Florisil® and concentrated *in vacuo*. The crude product was obtained as a white solid (144 mg). To this crude product was added 1,1,2,2-tetrachloroethane (44.1 mg, 0.263 mmol) and the yield was determined by ^1H NMR analysis (12%). NMR spectra are in good accordance with those reported in the literature.[26]

1,3-Diphenyladamantane (Table 3, entry 29): The titled compound was prepared from 1,3-dichloroadamantane[27] (102 mg, 0.499 mmol, prepared from adamantane with the

treatment of chlorosulphonic acid) and PhMgBr (1.60 mL of a 0.94 M THF solution, 3.0 equiv) following the procedure described for synthesis of cycloheptylbenzene. Purification of crude product with silica gel chromatography afforded the desired product as a white solid (98 mg, 68% yield); FTIR (neat, cm^{-1}) ν 2930, 1494, 1444, 1018, 770, 753, 735, 545, 533; ^{1}H NMR (300 MHz, CDCl3) δ 1.81 (t, *J* = 3.0 Hz, 2H), 1.98 (d, *J* = 3.0 Hz, 8H), 2.07 (s, 2H), 2.31–2.36 (m, 2H), 7.17–7.25 (m, 2H), 7.31–7.37 (m, 4H), 7.40–7.45 (m, 4H); ^{13}C NMR (75 MHz, $CDCl_3$) δ 29.9, 36.2, 37.5, 42.6, 49.2, 125.1, 125.9, 128.4,150.8; HRMS (EI, 70 eV) *m*/*z* $[M]^+$ calcd for $C_{22}H_{24}$, 288.1878; found, 288.1877. Anal. Calcd for $C_{22}H_{24}$: C, 91.61; H, 8.39. Found: C, 91,38; H, 8.44. All analytical data are in good accordance with those reported in the literature.[28]
Similarly, all other adamantane derivatives of Table 3; entries 26, 27, and 28 were characterized and all the data are in good accordance with those reported in the literature.[29]

1,3-Diphenylbutane (Table 3, entry 30): The titled compound was prepared from 1,3-dichlorobutane (64 mg, 0.503 mmol) and PhMgBr (1.60 mL of a 0.94 M THF solution, 3.0 equiv) following the procedure described for synthesis of cycloheptylbenzene. Purification of crude product with silica gel chromatography afforded the desired product as a colorless oil (89 mg, 85% yield); ^{1}H NMR (300 MHz, $CDCl_3$) δ 1.30 (d, *J* = 6.9 Hz, 3H), 1.85–2.03 (m, 2H), 2.54 (t, *J* = 9 Hz, 2H), 2.75 (st, *J* = 6.9 Hz, 1H), 7.12–7.36 (m, 10H); ^{13}C NMR (75 MHz, $CDCl_3$) δ 22.6, 34.2, 39.7, 40.2, 125.8, 126.1, 127.3, 128.5, 128.56, 128.59, 142.8, 147.5; HRMS (EI, 70 eV) *m*/*z* $[M]^+$ calcd for $C_{16}H_{19}$, 210.1409; found, 210.1412. Anal. Calcd for $C_{16}H_{19}$: C, 91.37; H, 8.63. Found: C, 91.47; H, 8.64. All analytical data are in good accordance with those reported in the literature.[30]

2,4-Diphenylpentane (Table 3, entry 31): The titled compound was prepared from 2,4-dichloropentane (83 mg, 0.58 mmol, 1:1 mixture of diastereomers) and PhMgBr (1.85 mL of a 0.94 M THF solution, 3.0 equiv) following the procedure described for synthesis of cycloheptylbenzene. Purification of crude product with silica gel chromatography afforded the desired product as a colorless oil as 1:1 diastereomeric (measured from crude NMR) mixture (112 mg, 85% yield). A small fraction of each pure isomer was obtained during column chromatography, which was sufficient for characterization.

***racemic* 2,4-Diphenylpentane**: ^{1}H NMR (300 MHz, $CDCl_3$) δ 1.17 (d, *J* = 6.9 Hz,

6H), 1.87 (t, *J* = 7.2 Hz, 2H), 2.50 (st, *J* = 6.9 Hz, 2H), 7.09–7.15 (m, 4H), 7.16–7.24 (m, 2H), 7.25–7.33 (m, 4H),; ^{13}C NMR (75 MHz, $CDCl_3$) δ 23.4, 38.0, 47.1, 126.1, 127.4, 128.5, 147.6; HRMS (EI, 70 eV) *m*/*z* $[M]^+$ calcd for $C_{17}H_{20}$, 224.1565; found, 224.1558. Anal. Calcd for $C_{17}H_{20}$: C, 91.01; H, 8.99. Found: C, 90.77; H, 9.07. All analytical data are in good accordance with those reported in the literature.[31]

***meso* 2,4-Diphenylpentane**: ^{1}H NMR (300 MHz, $CDCl_3$) δ 1.23 (d, *J* = 6.9 Hz, 6H), 1.75(dt, *J* = 7.2, 13.8 Hz, 1H), 1.94 (dt, *J* = 7.2, 13.8 Hz, 1H), 2.64 (st, *J* = 6.9 Hz, 2H), 7.12–7.20 (m, 6H), 7.25–7.31 (m, 4H),; ^{13}C NMR (75 MHz, $CDCl_3$) δ 22.3, 37.6, 47.3, 126.0, 127.1, 128.5, 147.9; HRMS (EI, 70 eV) *m*/*z* $[M]^+$ calcd for $C_{17}H_{20}$, 224.1565; found, 224.1567. Anal. Calcd for $C_{17}H_{20}$: C, 91.01; H, 8.99. Found: C, 90.83; H, 8.99. All analytical data are in good accordance with those reported in the literature.[31]

2,4,6-Triphenylheptane (Table 3, entry 32): The titled compound was prepared from 2,4,6-trichloroheptane (67 mg, 0.329 mmol) and PhMgBr (2.10 mL of a 0.94 M THF solution, 6.0 equiv) following the procedure described for synthesis of cycloheptylbenzene. Purification of crude product with silica gel chromatography afforded the desired product as a colorless oil (66 mg, 61% yield) which consists of mixture of three isomers of following ratio, (2R*,4r*, 6S*):(2R*,6R*):(2R*,4s*,6S*) = 1.0:1.38:0.56; determined from GC analysis. During the chromatographic separation, sufficiently pure fraction of all the isomers were obtained, ^{1}H NMR of which were distinguishable. All analytical data are in good accordance with those reported in the literature.[11] The starting 2,4,6-trichloroheptane, was prepared from corresponding alcohol with treatment of carbontetrachloride/triphenylphosphine,[32] and obtained as a mixture of two isomers with the following ratio, (2R*,4r*,6S*):(2R*,6R*): (2R*,4s*,6S*) = 1.0:0.0:1.23.

Stereochemical study on the cross-coupling reaction between a labeled β-adamantylethyl chloride and PhMgBr catalyzed by $FeCl_3$/NHC (Scheme 1).

(*threo*-α,β-*d*$_2$-β-Adamantylethyl) chloride (compound **5**): To a stirred solution of *erythro*-α,β-*d*$_2$-β-adamantylethanol[33] (300 mg, 1.64 mmol) and triphenylphosphine (863 mg, 3.29 mmol) in dry CH_2Cl_2 (3.2 mL) was added Cl_3CCONH_2 (534 mg, 3.29 mmol) at 30 °C under an argon atmosphere.[34] After 15 hours, the reaction mixture was quenched with cold water and organic layer was separated. Aqueous layer was extracted with CH_2Cl_2 and combined organic layers were washed with brine, dried over Na_2SO_4

and concentrated *in vacuo*. Purification of the crude product with silica gel (230–400 mesh) chromatography with pentane afforded *threo*-α,β-d_2-β-adamantylethyl chloride (250 mg, 76% yield). $^1H\{^2H\}$ NMR (400 MHz, $CDCl_3$) δ 1.51 (brd, J = 2.8 Hz, 6H), 1.58 (d, $J_{H\text{-}H}$ = 5.6 Hz, 1H), 1.60–1.74 (m, 6H), 1.95 (brs, 3H), 3.52 (d, $J_{H\text{-}H}$ = 5.6 Hz, 1H); ^{13}C NMR (75 MHz, $CDCl_3$) δ 28.7 (3C), 33.0, 37.2(3C), 40.6 (t, $J_{C\text{-}D}$ = 22.5 Hz), 42.5 (3C), 47.2 (t, $J_{C\text{-}D}$ = 19.5 Hz); HRMS (EI, 70 eV) *m*/*z* $[M]^+$ calcd for $C_{12}H_{17}D_2Cl$, 200.1301; found, 200.1308. All analytical data are in good accordance with those reported in the literature.[33]

(α,β-*d*$_2$-β-Adamantylethyl)benzene (*erythro: compound **7** & threo: compound **6**)*: To a mixture of IPr·HCl (10.9 mg, 10 mol%) and (*threo*-α,β-d_2-β-2-adamantylethyl) chloride (51.8 mg, 0.257 mmol) was added at 0 °C a small portion of PhMgBr (0.06 mL of a 1.07 M THF solution, 0.25 equiv) and allowed to be stirred for 5 min. To the resulting mixture, a suspension of $FeCl_2$ (0.13 mL, 5 mol%) in THF was added. PhMgBr (0.42 mL of a 1.07 M THF solution, 1.75 equiv) was then slowly added at 40 °C by using a syringe pump over a period of 2 hours. The reaction mixture was stirred at that temperature for 10 min after completion of the addition of PhMgBr. After aqueous workup, the reaction mixture was filtered through a pad of Florisil® and concentrated *in vacuo*. Purification of the crude product with silica gel (230–400 mesh) chromatography with pentane afforded the corresponding cross-coupling products (42 mg, 67% yield, 97% pure in ^1H NMR) as 1:1 mixture of *erythro:threo* diastereomers. $^1H\{^2H\}$ NMR (400 MHz, $CDCl_3$) (1:1 mixture of *erythro:threo* diastereomers): δ 1.34 (d, J = 12.8 Hz for *erythro,* 1H), 1.35 (d, J = 4.8 Hz for *threo*, 1H), 1.55 (s, 12H), 1.63–1.77 (m, 12H), 1.98 (s, 6H), 2.53 (d, J = 12.8 Hz for *erythro;* d, J = 4.8 Hz for *threo*, 2H), 7.14–7.19 (m, 6H), 7.21–7.29 (m, 4H); ^{13}C NMR (75 MHz, $CDCl_3$): δ 29.0 (t, $J_{C\text{-}D}$ = 18.9 Hz), 29.0 (3C, overlapped with triplet at δ 29.0), 32.6, 37.5 (3C), 42.6 (3C), 46.6 (t, $J_{C\text{-}D}$ = 19.1 Hz), 125.3, 128.5 (2C), 128.6 (2C), 144.1; HRMS (EI, 70 eV) *m*/*z* $[M]^+$ calcd for $C_{18}H_{22}D_2$, 242.2004; found, 242.2003. All analytical data are in good accordance with those reported in the literature.[35]

References and Notes

[1] Weissermel, K.; Arpe, H.-J. *Industrial Organic Chemistry*; VCH: New York, 2003.

[2] (a) Grushin, V. V.; Alper, H. *Top. Organomet. Chem*. **1999,** *3*, 193–226. (b) Fu, G. C. *Acc. Chem. Res.* **2008,** *41*, 1555–1564.

[3] (a) Review: Netherton, M. R.; Fu, G. C. *Adv. Synth. Catal*. **2004,** *346*, 1525–1532. (b) Frisch, A. C.; Beller, M. *Angew. Chem., Int. Ed.* **2005,** *44*, 674–688. (c) Terao, J.; Kambe, N. *Bull. Chem. Soc. Jpn.* **2006,** *79*, 663–672. (d) Rudolph, A.; Lautens, M. *Angew. Chem., Int. Ed.* **2009,** *48*, 2656–2670.

[4] Luh, T.-Y.; Leung, M.-K.; Wong, K.-T. *Chem. Rev*. **2000,** *100*, 3187–3204.

[5] Examples of cross-coupling of alkyl chlorides under transition metal catalysis other than iron. [Pd] (a) Frisch, A. C.; Shaikh, N.; Zapf, A.; Beller, M. *Angew. Chem., Int. Ed.* **2002,** *41*, 4056–4059. (b) Frisch, A. C.; Rataboul, F.; Zapf, A.; Beller, M. *J. Organomet. Chem.* **2003,** *683*, 403–409. (c) Ackermann, L.; Kapdi, A.; Schulzke, C. *Org. Lett.* **2010,** *12*, 2298–2301. [Ni] (d) Terao, J.; Watanabe, H.; Ikumi, A.; Kuniyasu, H.; Kambe, N. *J. Am. Chem. Soc.* **2002,** *124*, 4222–4223. (e) Vechorkin, O.; Proust, V.; Hu, X. *J. Am. Chem. Soc.* **2009,** *131*, 9756–9766. (f) González-Bobes, F.; Fu, G. C. *J. Am. Chem. Soc.* **2006,** *128*, 5360–5361. [Co] (g) Ohmiya, H.; Yorimitsu, H.; Oshima, K. *J. Am. Chem. Soc.* **2006,** *128*, 1886–1889. [Cu] (h) Terao, J.; Todo, H.; Begum, S. A.; Kuniyasu, H.; Kambe, N. *Angew. Chem., Int. Ed.* **2007,** *46*, 2086–2089.

[6] Reviews: (a) Bolm, C.; Legros, J.; Le Paih, J.; Zani, L. *Chem. Rev.* **2004,** *104*, 6217–6254. (b) Fürstner, A.; Martin, R. *Chem. Lett.* **2005,** *34*, 624–629. (c) Czaplik, W. M.; Mayer, M.; Cvengroš, J.; von Wangelin, A. J. *ChemSusChem* **2009,** *2*, 396–417. (d) Plietker, B. *Synlett* **2010,** 2049–2058. (e) Sherry, B. D.; Fürstner, A. *Acc. Chem. Res.* **2008**, *41*, 1500–1511.

[7] Seminal early studies on Fe-catalyzed cross-coupling reaction: (a) Tamura, M.; Kochi, J. K. *J. Am. Chem. Soc.* **1971,** *93*, 1487–1489. (b) Molander, G. A.; Rahn, B. J.; Shubert, D. C.; Bonde, S. E. *Tetrahedron Lett.* **1983,** *24*, 5449–5452. (c) Yanagisawa, A.; Nomura, N.; Yamamoto, H. *Tetrahedron* **1994,** *50*, 6017–6028. (d) Reddy, C. K.; Knochel, P. *Angew. Chem., Int. Ed. Engl.* **1996,** *35*, 1700–1701. (e) Cahiez, G.; Avedissian, H. *Synthesis* **1998,** 1199–1205. (f) Fürstner, A.; Leitner, A.; Méndez, M.; Krause, H. *J. Am. Chem. Soc*. **2002,** *124*, 13856–13863.

[8] Selected papers. Fe-catalyzed cross-coupling reactions of alkyl halides: (a) Nakamura, M.; Matsuo, K.; Ito, S.; Nakamura, E. *J. Am. Chem. Soc.* **2004,** *126*, 3686–3687. (b) Nagano, T.; Hayashi, T. *Org. Lett.* **2004,** *6*, 1297–1299. (c) Martin, R.; Fürstner, A. *Angew. Chem., Int. Ed.* **2004,** *43*, 3955–3957. (d) Bedford, R. B.; Bruce, D. W.; Frost, R. M.; Goodby, J. W.; Hird, M. *Chem. Commun.* **2004,** 2822–2823. (e) Bedford, R. B.; Betham, M.; Bruce, D. W.; Danopoulos, A. A.; Frost, R. M.; Hird, M. *J. Org. Chem.* **2006,** *71*, 1104–1110. (f) Dongol, K. G.; Koh, H.; Sau, M.; Chai, C. L. L. *Adv. Synth. Catal.* **2007,** *349*, 1015–1018. (g) Cahiez, G.; Habiak, V.; Duplais, C.; Moyeux, A. *Angew. Chem., Int. Ed.* **2007,** *46*, 4364–4366. (h) Fürstner, A.; Martin, R.; Krause, H.; Seidel, G.; Goddard, R.; Lehmann, C. W. *J. Am. Chem. Soc.* **2008,** *130*, 8773–8787. (i) Hatakeyama, T.; Nakagawa, N.; Nakamura, M. *Org. Lett*. **2009,** *11*, 4496–4499. (j) Kawamura, S.; Ishizuka, K.; Takaya, H.; Nakamura, M *Chem. Commun*. **2010,** *46*, 6054–6056. (k) Hatakeyama, T.; Hashimoto, T.; Kondo, Y.; Fujiwara, Y.; Seike, H.; Takaya, H.; Tamada, Y.; Ono, T.; Nakamura, M. *J. Am. Chem. Soc*. **2010,** *132*, 10674–10676. (l) Jin, M.; Nakamura, M. *Chem. Lett*. **2011,** *40*, 1012–1014. (m) Hatakeyama, T.; Fujiwara, Y.; Okada, Y.; Itoh, T.; Hashimoto, T.; Kawamura, S.; Ogata, K.; Takaya, H.; Nakamura, M. *Chem. Lett*. **2011,** *40*, 1030–1032. (n) Hatakeyama, T.; Okada, Y.; Yoshimoto, Y.; Nakamura, M. *Angew. Chem., Int. Ed*. **2011,** *50*, 10973–10976.

[9] Noda, D.; Sunada, Y.; Hatakeyama, T.; Nakamura, M.; Nagashima, H. *J. Am. Chem. Soc*. **2009,** *131*, 6078–6079.

[10] *N-Heterocyclic Carbenes in Transition Metal Catalysis and Organocatalysis, Catalysis by Metal Complexes Vo. 32*; Cazin, C. S. J., Ed.: Springer: UK, 2010.

[11] Favorable effects of NHC ligands in iron-catalyzed cross-couplings of haloalkanes were reported previously. (a) Bica, K.; Gaertner, P. *Org. Lett*. **2006,** *8*, 733–735. (b) Plietker, B.; Dieskau, A.; Möws, K.; Jatsch, A. *Angew. Chem., Int. Ed.* **2007,** *47*, 198–201. See also ref 8e.

[12] To avoid the risk of trace metal contamination, the author used pure anhydrous $FeCl_3$ (99.99% from Aldrich), even though other iron salts, such as $Fe(acac)_3$ and $FeCl_2$, were found to be effective. For the trace metal contamination in iron-catalyzed cross-couplings, see: (a) Buchwald, S. L.; Bolm, C. *Angew. Chem., Int. Ed.* **2009,** *48*, 5586–5588. (b) Bedford, R. B.; Nakamura, M.; Gower, N. J.; Haddow, M. F.;

Hall, M. A.; Huwe, M.; Hashimoto, T.; Okopie, R. A. *Tetrahedron Lett*. **2009,** *50*, 6110–6111.

[13] Other NHC or phosphine ligands as well as an excess amount of TMEDA were not effective.

[14] (a) Kharasch, M. S.; Weiner, M.; Nudenberg, W.; Bhattacharya, A.; Wang, T.-I.; Yang, N. C. *J. Am. Chem. Soc*. **1961,** *83*, 3232–3234. (b) Rollick, K. L.; Nugent, W. A.; Kochi, J. K. *J. Organomet. Chem*. **1982,** *225*, 279–299.

[15] Schilling, F. C.; Schilling, M. L. *Macromolecules* **1988,** *21*, 1530–1532.

[16] Xiang, L.; Xiao, J.; Deng, L. *Organometallics* **2011**, *30*, 2018–2025.

[17] Uchiyama, M.; Matsumoto, Y.; Nakamura, S.; Ohwada, T.; Kobayashi, N.; Yamashita, N.; Matsumiya, A.; Sakamoto, T. *J. Am. Chem. Soc.* **2004,** *126*, 8755–8759. See also ref 8h. Bedford proposed an SET/radical mechanism for cross-coupling of alkyl halides with aryl Grignard reagents in the presence of monodentate phosphine ligands as well as NHC ligands: see ref 8e.

[18] Still, W. C.; Kahn, M.; Mitra, A. *J. Org. Ch*em. **1978**, *43*, 2923–2924.

[19] Zhou, J.; Fu. G. C. *J. Am. Chem. Soc.* **2003**, *125*, 12527–12530.

[20] Limmert, M. E.; Roy, A. H.; Hartwig. J. F. *J. Org. Chem.* **2005**, *70*, 9364–9370.

[21] Li. M.-B.; Tang, X.-L.; Tian, S.-K. *Adv. Synth. Cat.* **2011**, *353*, 1980–1984.

[22] Molander, G. A.; Yun. C.-S. *Tetrahedron* **2002**, *58*, 1465–1470.

[23] Singh, R. P.; Kamble, R. M.; Chandra, K. L.; Saravanan, C. P.; Singh, V. K. *Tetrahedron* **2001**, *57*, 241–247.

[24] Wilt, J. W.; Kosturik, J. M.; Orlowski, R. C. *J. Org. Chem.* **1965**, *30*, 1052–1057.

[25] Joshi-Pangu, A.; Ganesh M.; Biscoe, M. R. *Org. Lett.* **2011**, *13*, 1218–1221.

[26] Joshi-Pangu, A.; Wang, C.-Y.; Biscoe, M. R. *J. Am. Chem. Soc.* **2011**, *133*, 8478–8481.

[27] Tanaka, T.; Yamaguchi, S. *Jpn. Kokai Tokyo Koho*, **2003**, 146916.

[28] Chalais, S.; Cornelis, A.; Gerstmans, A.; Kolodziejski, W.; Laszlo, P.; Mathy, A.; Metra, P. *Helv. Chim. Act* **1985**, *68*, 1196–1203.

[29] Brase, S.; Waegell, B.; de Meijere, A. *Synthesis* **1998**, 148–152.

[30] Hall, S. S. *J. Org. Chem*. **1973**, *38*, 1738–1740.

[31] Fujishige, S.; Ando, I. *Makromol. Chem.* **1976**, *177*, 2195–2200.

[32] Hoffmann, R. W.; Stemkamp, D. *Tetrahedron* **1999**, *55*, 7169–7176.

[33] Terao, J.; Begum. S. A.; Shinohara, Y.; Tomita, M.; Naitoh, Y.; Kambe, N. *Chem. Commun.* **2007**, 855–857.

[34] Pluempanupat, W.; Chavasiri, W. *Tetrahedron Lett.* **2006**, *47*, 6821–6823. (*threo*-α,β-d_2-β -Adamantylethyl) chloride was prepared directly from ery*thro*-α,β-d_2-β-adamantylethanol according to the procedure described for other materials.

[35] Terao, J.; Todo, H.; Begum. S. A.; Kuniyasu, H.; Kambe, N. *Angew. Chem. Int. Ed.* **2007**, *46*, 2086–2089.

CHAPTER 4

Iron-Catalyzed Chemoselective Cross-Coupling of α-Bromocarboxylic Acid Derivatives with Aryl Grignard Reagents

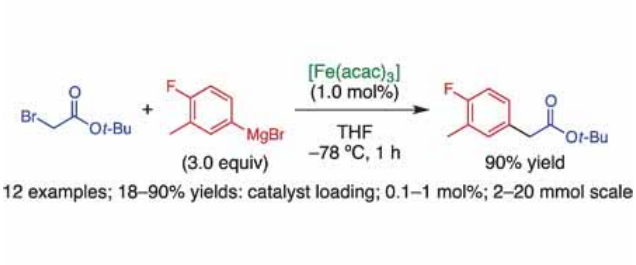

Abstract

The author has developed a simple and effective synthetic method of α-arylcarboxylic acid derivatives based on the iron-catalyzed cross-coupling reaction of α-bromocarboxylic acid derivatives with aryl Grignard reagents. The reaction proceeds smoothly at −78 °C in a chemoselective manner to produce the coupling product in good to excellent yields.

Reproduced from *Chem. Lett.* **2011**, *40*, 1012–1014. with permission from the Chemical Society of Japan.

Introduction

α-Arylcarboxylic acids and their derivatives are useful synthetic intermediates of pharmaceuticals, or important bioactive compounds themselves, such as loxoprofen or lumiracoxib.[1] Due to their significance, a number of synthetic methods for this class of compounds have been already developed;[2] however, there still needs further effort to establish more practical methods to overcome several drawbacks associated with the classical methods: for example, the use of toxic reagents such as NaCN, the requirement of multi-step transformations and/or harsh reaction conditions, just to name a few. Catalytic cross-coupling reactions have been recognized as a straightforward strategy to synthesize α-aryl carboxylic acid derivatives from aryl halides with preformed or *in situ* generated enolates by a single-step operation. The most popular metal catalysts utilized are palladium[3] and nickel.[3a,4] However, the disadvantages are the usage of toxic and expensive catalysts, the need for the preparation of the enolate substrate, undesired side reactions such as multiple arylations, and racemization at the α-carbon atom of the carbonyl group. The author envisioned that iron catalysts can solve the above problems since iron makes low-toxic, economical, and environmentally friendly catalysts. In addition, the author anticipated that the easily-available α-bromocarboxylic acid derivatives[5] could be used as the electrophilic substrate due to the distinctive reactivity of the iron catalyst toward alkyl halide electrophiles.[5,6] Herein the author reports the cross-coupling reaction of α-bromocarboxylic acid derivatives with aryl Grignard reagents in the presence of a catalytic amount of $Fe(acac)_3$.

Results and Discussion

The author firstly examined cross-coupling reactions of *tert*-butyl bromoacetate **1a** with arylzinc reagents in the presence of the catalytic amount of $FeCl_2(dppbz)_2$ since low nucleophilicity of arylzinc reagents, the coupling partner, would avoid the nucleophilic attack to the carbonyl group (Table 1). Although the coupling product was obtained in low yield when a mono- or diarylzinc reagent was used as a nucleophile, the fair yield was observed by using a diarylzinc-tmeda reagent (entries 1–3). These results suggest that high transferability of diarylzinc-tmeda is essential for proceeding this cross-coupling reaction. The cross-coupling reaction with diarylzinc-tmeda complex proceeded in moderate yield even at a low temperature of −40 °C (entry 4). The author estimated that the aryl Grignard reagent was a more suitable reagent for this reaction because the magnesium reagent has higher transmetalation ability than the zinc reagent and problematic nucleophilic attack to the carbonyl group can be suppressed by carrying out the reaction at low temperature. The cross-coupling reaction of **1b** with the

p-tolMgBr instead of the zinc reagents gave the desired product in a good yield of 61%, and furthermore, higher yield of 74% was obtained by conducting the reaction at −78 °C (entries 5 and 6).

Table 1. Cross-Coupling of Bromoacetate **1a** with Aryl Grignard Reagents

entry[a]	nucleophile (equiv)	temp., time	NMR yield[b] /%		
			3	**4**[c]	**1a**
1	*p*-tolZnX[d] (1.2)	25 °C, 16 h	3	12	33
2	*p*-tol$_2$Zn[d] (1.2)	0 °C, 3 h	13	25	<1
3	*p*-tol$_2$Zn(temda)[d] (1.2)	0 °C, 1 h	47	26	<1
4	*p*-tol$_2$Zn(temda)[d] (1.2)	–40 °C, 24 h	38	15	1
5	*p*-tolMgBr (2.0)	–40 °C, 1 h	61	10	<1
6[e]	*p*-tolMgBr (2.0)	–78 °C, 1 h	74	8	<1

[a]2.0 mol% $FeCl_2(dppbz)_2$ was used as a catalyst unless otherwise noted [b]Yields were determined by NMR using 1,1,2,2-tetrachloroethane as an internal standard [c]Based on the amount of the ArMgBr **2** used. [d]Arylzinc reagents were prepared *in-situ* by mixing $ZnCl_2$ and *p*-tolMgBr. [e]1.0 mol% $FeCl_2(dppbz)_2$ was used as a catalyst.

For the purpose of catalyst screening, *tert*-butyl bromoacetate **1a** was coupled with *p*-tolylmagnesium bromide in the presence of various metal catalysts (Table 2). To minimize the undesired nucleophilic attack of the Grignard reagent to the carbonyl group, the author chose the bulky *tert*-butyl ester, and the reactions were carried out at –78 °C. In the absence of a transition metal catalyst, the desired product **3** was formed in 15% yield along with 42% recovery of **1a** after 1 hour; it is noteworthy that, after 24 hours, the coupling product **3** was obtained in a decreased yield (5%) despite the further consumption of **1a** (entries 1 and 2). Conceivably, side-reactions including a nucleophilic attack to the ester group and halogen-metal exchange reaction competed with the coupling reaction, and several unidentified byproducts were obtained under the reaction conditions. On the other hand, the desired cross-coupling reaction proceeded smoothly in the presence of 1-mol% iron catalyst regardless of the forms of the precatalyst used (entries 3–7): *p*-tolylacetate **3** was obtained in 74–85% yield, accompanied by the formation of the byproduct 4,4'-dimethylbiphenyl **4** in 8–12% yield. $Fe(acac)_3$ gave the coupling product in the highest yield (85%) with the minimum amount of byproduct **4** (entry 7).[7] The coupling product was obtained in 84% even when the amount of the Grignard reagent was reduced to 1.5 equivalents (entry 8). The reaction proceeded in a chemoselective manner, and none of the alcohol or ketone by-products, potentially formed by the Grignard addition reaction, was detected by GC and ^{1}H NMR. The yield of the cross-coupling product significantly depends on the experimental procedure,[8] and the

best result was obtained by the slow addition of the THF solution of the iron catalyst to the precooled mixture of the Grignard reagent and bromoacetate.

Table 2. Cross-Coupling of Bromoacetate **1a** with Aryl Grignard Reagents

entry[a]	ArMgBr (equiv)	catalyst	NMR yield[b] /%		
			3	**4**[c]	**1a**
1	*p*-tolMgBr (2.0)	none	15	<1	42
2[d]	*p*-tolMgBr (2.0)	none	5	<1	21
3	*p*-tolMgBr (2.0)	$FeCl_2(dppbz)_2$[e]	74	8	<1
4	*p*-tolMgBr (2.0)	Fe complex **5**[e]	77	8	<1
5	*p*-tolMgBr (2.0)	Fe complex **6**[e]	84	11	<1
6	*p*-tolMgBr (2.0)	$FeCl_3$	77	11	<1
7	*p*-tolMgBr (2.0)	$Fe(acac)_3$	85	8	<1
8	*p*-tolMgBr (1.5)	$Fe(acac)_3$	84	9	<1
9	*p*-tolMgBr (1.2)	$Fe(acac)_3$	62	9	10
10	*p*-tolMgBr (2.0)	$Co(acac)_2$	82	8	<1
11	*p*-tolMgBr (2.0)	$Ni(acac)_2$	84	5	<1
12	*p*-tolMgBr (2.0)	$Cu(acac)_2$	5	5	47
13	*p*-tolMgBr (2.0)	$Pd(acac)_2$	5	<1	49
14	*p*-anisylMgBr (1.5)	$Fe(acac)_3$ (0.1 mol%)	85	4	<1
15	*p*-anisylMgBr (1.5)	$Co(acac)_2$ (0.1 mol%)	32	1	36
16	*p*-anisylMgBr (1.5)	$Ni(acac)_2$ (0.1 mol%)	34	1	37

[a]1.0 mol% catalyst was used unless otherwise noted [b]Yields were determined by NMR using 1,1,2,2-tetrachloroethane as an internal standard [c]Based on the amount of the ArMgBr **2** used. [d]The reaction was carried out for 24 h. [e]Structures of iron complexes are shown below.

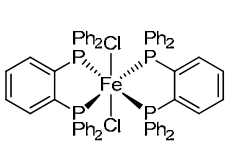

$FeCl_2(dppbz)_2$

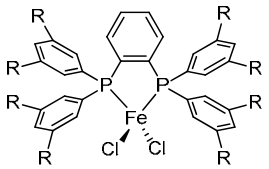

R = ^{t}Bu: complex **5**
R = TMS: complex **6**

The catalytic activities of the other transition metals were also studied by using the corresponding acetylacetonato complexes as in entries 10–13:[9] $Co(acac)_2$ and $Ni(acac)_2$ showed a comparable catalytic activity with $Fe(acac)_3$ to give the product in 82% and 84% yields, respectively (entries 10 and 11). The yields were substantially lower with the $Cu(acac)_2$ or $Pd(acac)_2$ catalyst (entries 12 and 13). The reaction of **1a** with *p*-tolylmagnesium bromide was equally catalyzed by the acetylacetonato complexes of iron, cobalt, and nickel. On the other hand, a clear difference among these metals was

observed in the cross-coupling of **1a** with *p*-anisylmagnesium bromide at a lower catalyst loading; only 0.1 mol% of $Fe(acac)_3$ gave the coupling product in 85% yield (entry 14), while 0.1 mol% of $Co(acac)_2$ and $Ni(acac)_2$ gave the product in 32% and 34% yields, respectively (entries 15 and 16). The results of the side-by-side experiments with various transition metals suggest that a trace metal contaminant, if any, is not likely to be acting as the true effective catalyst for the present iron-catalyzed coupling reaction.[9] Because of the high catalytic activity as well as the economical and operational advantages of the iron complex, the author chose $Fe(acac)_3$ as the precatalyst for the following studies.

Table 3 summarizes the scope of the present arylation reaction of α-bromocarboxylic acid derivatives. The size of the ester alkoxy substituent is critical for maximizing the yield of the desired coupling products. The larger substituents gave the better yields: the reaction with methyl bromoacetate **1b** did not give the coupling product due to the competitive nucleophilic addition of the Grignard reagent to the ester group, only to afford a mixture of the alcohol and ketone byproducts (entry 2). When isopropyl bromoacetate **1c** was subjected to the same reaction conditions, the coupling product was obtained in 15% yield along with the formation of several byproducts (entry 3). *tert*-Butyl α-bromopropionate **1d**, a secondary alkyl bromide, gave low yield even when the reaction was carried out according to the Fürstner's conditions (entry 4). It should be noted that Fürstner reported the reaction of ethyl α-bromobutyrate with phenylmagnesium bromide gave the coupling product in 87% yield in the presence of $[Li(tmeda)]_2[Fe(C_2H_4)_4]$.[5] The result suggests the low-valent iron species proposed in Fürstner's report are not likely to be involved as the catalytically active species in the present coupling reaction.

Table 3. Cross-Coupling of α-Bromocarboxylic Acid Derivatives with Aryl Grignard Reagents

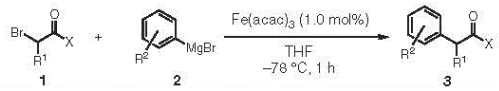

1 2 3

Entry	Electrophile	ArMgBr[a]	Coupling product	Yield[b]/%
1	**1a** (R^1 = H, X = O*t*-Bu)	**2a**	**3a**	78
2	**1b** (R^1 = H, X = OMe)	**2a**	**3b**	<1[c]
3	**1c** (R^1 = H, X = O*i*-Pr)	**2a**	**3c**	15[c]
4	**1d** (R^1 = Me, X = O*t*-Bu)	**2a**	**3d**	16[c], 26[c,d]
5	**1e** (R^1 = H, X = NEt_2)	**2a**	**3e**	44
6[e,f]	**1a**	**2b**	**3f**	84
7	**1a**	**2c**	**3g**	90
8	**1a**	**2d**	**3h**	81
9	**1a**	**2e**	**3i**	70
10	**1a**	**2f**	**3j**	41
11	**1a**	**2g**	**3k**	90
12	**1a**	**2h**	**3l**	70
13	**1a**	**2i**	**3m**	53
14	**1a**	**2j**	**3n**	18[c]
15	**1a**	**2k**	**3o**	37[c]
16	**1a**	**2l**	**3p**	82

[a]1.5 equivalents of Grignard reagents were used in entries 1–6, and 3.0 equivalents of Grignard reagents were used in entries 9–16. [b]Isolated yield unless otherwise noted. [c]NMR yields. [d]Reaction was carried out according to the Fürstner's conditions (see note 5): $Fe(acac)_3$ (5 mol %), ArMgBr (1.2 equiv), THF −20 °C, 0.5 h, [e]0.1 mol% of $Fe(acac)_3$ was used. [f]20 mmol scale.

A moderate yield was obtained when *N*,*N*-diethyl bromoacetamide **1e** was used as a substrate (entry 5). Reactions of **1a** with a variety of arylmagnesium bromides were studied next: *p*-substituted aryl Grignard reagents such as *p*-tolyl (**2a**), *p*-anisyl (**2b**), *p*-fluorophenyl (**2c**), and *p*-chlorophenyl (**2d**) Grignard reagents gave the desired products in high yields (entries 1, 6−8). *m*-Tolyl (**2e**) and *o*-tolyl (**2f**) Grignard reagent gave the corresponding arylation products in fair to modest yields (entries 9 and 10). Di-substituted aryl Grignard reagents including 4-fluoro-3-methylphenyl (**2g**), 3,4-difluorophenyl (**2h**), and 3,5-xylyl (**2i**) Grignard reagents afforded the coupling products in moderate to high yields (entries 11−13). In contrast, a low yield (18%) was obtained when mesitylmagnesium bromide **2j**, a tri-substituted aryl Grignard reagent, was used (entry 14). This result suggests that the present reaction is sensitive to the steric hindrance of aryl Grignard reagents. The reactions of **1a** with 1-naphthylmagnesium bromide **2k** and 2-naphthylmagnesium bromide **2l** further support this conclusion: the more sterically demanding reagent **2k** gave the product in 37% yield, while the less demanding reagent **2l** gave the product in 82% yield (entries 15 and 16).

Although the reaction mechanism remains unclear at the current stage of the study, the author supposes that bare ferrate species, which do not bear any auxiliary ligand, are responsible for the coupling reaction based on the observation that all the iron complexes examined in this study gave comparable results despite the ligands on the precatalyst, and also that extra additives did not affect the coupling reactions.[10] In order to expand the substrate scope of the present reaction and also to develop an asymmetric variant of the α-arylation reaction, detailed mechanistic studies will be needed to clarify the catalytically active species. Further investigation along this line is ongoing in our laboratory and will be reported in due course.

Conclusion

In summary, the author has developed a simple and effective synthetic method of α-arylacetic acid derivatives based on the iron-catalyzed chemoselective cross-coupling reactions of α-bromoacetic acid derivatives with aryl Grignard reagents. The reaction proceeds smoothly at –78 °C in a chemoselective manner to produce the coupling product in good to excellent yield.

Experimental Section

General Information

All the reactions were carried out in dry reaction vessels under a positive pressure of nitrogen. The following reagents and solvent were purchased and used as received: $Fe(acac)_3$ (≥99.9%) from Sigma-Aldrich Co.; THF (deoxidized, stabilizer free) from Wako Pure Chemical Industries Ltd. Other commercial reagents and solvents were purchased from Wako Pure Chemical Industries Ltd., Sigma-Aldrich Co., and other commercial suppliers, and used without further purification. Column chromatography was performed on prepacked silica gel cartridges (SNAP Ultra; Biotage, Uppsala, Sweden).

NMR spectra were recorded on a JEOL ECS-400 (392 MHz) and a JEOL ECS-500 spectrometer. GC analyses were performed on an Agilent 7890A instrument equipped with an FID detector and a capillary column, DB-1 (20 m length, 0.18 mm i.d., 0.18 μm film). IR spectra were recorded on a JASCO FT/IR-6100 Type A spectrometer. Enantiomer ratio (er) was determined by GC or HPLC analysis with a chiral stationary column.

General procedure

Under a positive pressure of argon, to a 0.50 M solution of *tert*-butyl bromoacetate in dry THF was dropwise added an arylmagnesium bromide solution (ca. 1.0 M in THF, 1.5–3.0 equiv) at –78 °C. To the mixture was slowly added a 0.005 M solution of $Fe(acac)_3$ (0.1–1.0 mol%) in dry THF over 1 h, and the resulting mixture was stirred at –78 °C for 1 h. After quenching with 3 M aqueous solution of hydrochloric acid, the mixture was extracted with EtOAc, passed through a pad of Florisil®, concentrated *in vacuo*. The residue was chromatographed on silica gel (*n*-hexane/toluene = 4/1, 2/1, 1/1) to give the desired product.

Iron-catalyzed chemoselective cross-coupling

tert-butyl (4-methylphenyl)acetate (3a)

The reaction was carried out according to the General Procedure using *tert*-butyl bromoacetate (389 mg, 1.99 mmol), $Fe(acac)_3$ (7.1 mg, 1.0 mol%), and *p*-tolylmagnesium bromide solution (1.1 M in THF, 2.7 mL, 1.5 equiv). The title compound (319 mg, 78%) was obtained as a colorless oil after silica gel column chromatography.

FTIR (neat, cm^{-1}) ν 2978, 1728, 1516, 1367, 1255, 1132, 955, 837, 783, 760, 511, 482; ^1H NMR (500 MHz, $CDCl_3$) δ 1.43 (s, 9H), 2.33 (s, 3H), 3.48 (s, 2H), 7.12–7.16 (m, 4H);

^{13}C NMR (125 MHz, $CDCl_3$) δ 21.1, 28.0 (3C), 42.2, 80.7, 129.0 (2C), 129.1 (2C), 131.6, 136.3, 171.2; HRMS for $C_{13}H_{19}O_2$ 207.1385, found 207.1385; Anal. Calcd for $C_{13}H_{18}O_2$: C, 75.69; H, 8.79. Found: C, 75.39; H, 8.79.

_N,N_-diethyl(4-methylphenyl)acetamide (3e)

The reaction was carried out according to the General Procedure using *N,N*-diethylbromoacetamide (388 mg, 2.00 mmol), $Fe(acac)_3$ (7.1 mg, 1.0 mol%), and *p*-tolylmagnesium bromide solution (1.1 M in THF, 2.7 mL, 1.5 equiv). The title compound (183 mg, 44%) was obtained as a colorless oil after silica gel column chromatography.

^{1}H NMR (500 MHz, $CDCl_3$) δ 1.09 (t, *J* = 6.9 Hz, 3H), 1.12 (t, *J* = 6.9 Hz, 3H), 2.32 (s, 3H), 3.29 (q, *J* = 6.9 Hz, 2H), 3.38 (q, *J* = 6.9 Hz, 2H), 3.65 (s, 2H), 7.11–7.15 (m, 4H); ^{13}C NMR (125 MHz, $CDCl_3$) δ 12.9, 14.2, 21.0, 40.1, 40.5, 42.3, 128.5 (2C), 129.3 (2C), 132.4, 136.1, 170.3; FTIR (neat, cm^{-1}) ν 2972, 2933, 1632, 1514, 1456, 1427, 1379, 1281, 1219, 1128, 1097, 949, 789, 588, 492; ^{1}H NMR (500 MHz, $CDCl_3$) δ 1.43 (s, 9H) HRMS for $C_{13}H_{20}NO_2$ 206.1545, found 206.1533.

***tert*-butyl (4-methoxyphenyl)acetate (3f)**

The reaction was carried out according to the General Procedure using *tert*-butyl bromoacetate (3.89 g, 19.9 mmol), $Fe(acac)_3$ (7.1 mg, 0.1 mol%), and *p*-anisylmagnesium bromide solution (1.0 M in THF, 30.0 mL, 1.5 equiv). The title compound (3.74 g, 84%) was obtained as a colorless oil after silica gel column chromatography.

FTIR (neat, cm^{-1}) ν 2978, 1726, 1612, 1512, 1367, 1300, 1134, 1034, 955, 820, 791, 758, 534, 515; ^{1}H NMR (500 MHz, $CDCl_3$) δ 1.43 (s, 9H), 3.46 (s, 2H), 3.80 (s, 3H), 6.84–6.86 (m, 2H), 7.17–7.19 (m, 2H); ^{13}C NMR (125 MHz, $CDCl_3$) δ 28.0 (3C), 41.7, 55.2, 80.7, 113.9 (2C), 126.8, 130.2 (2C), 158.5, 171.3; HRMS for $C_{13}H_{19}O_3$ 223.1334, found 223.1312.

***tert*-butyl (4-fluorophenyl)acetate (3g)**

The reaction was carried out according to the General Procedure using *tert*-butyl bromoacetate (389 mg, 1.99 mmol), $Fe(acac)_3$ (7.1 mg, 1.0 mol%), and *p*-fluoromagnesium bromide solution (0.95 M in THF, 3.2 mL, 1.5 equiv). The title compound (319 mg, 78%) was obtained as a colorless oil after silica gel column chromatography.

FTIR (neat, cm^{-1}) ν 2980, 1728, 1510, 1367, 1223, 1136, 955, 874, 825, 797, 521; ^1H NMR (500 MHz, $CDCl_3$) δ 1.43 (s, 9H), 3.49 (s, 2H), 6.98–7.02 (m, 2H), 7.21–7.24 (m, 2H); ^{13}C NMR (125 MHz, $CDCl_3$) δ 28.0 (3C), 41.7, 55.2, 81.0, 115.3 (d, *J* = 20.8 Hz, 2C), 130.4 (d, *J* = 3.5 Hz), 130.7 (d, *J* = 8.1 Hz, 2C), 158.5 (d, *J* = 245 Hz), 170.8; HRMS for $C_{12}H_{16}FO_2$ 211.1134, found 211.1152.

tert-butyl (4-chlorophenyl)acetate (3h)

The reaction was carried out according to the General Procedure using *tert*-butyl bromoacetate (389 mg, 1.99 mmol), $Fe(acac)_3$ (7.1 mg, 1.0 mol%), and *p*-fluoromagnesium bromide solution (1.0 M in THF, 3.0 mL, 1.5 equiv). The title compound (364 mg, 81%) was obtained as a colorless oil after silica gel column chromatography.

FTIR (neat, cm^{-1}) ν 2978, 1728, 1493, 1367, 1255, 1136, 1090, 1016, 808, 775, 584, 501; ^1H NMR (500 MHz, $CDCl_3$) δ 1.43 (s, 9H), 3.49 (s, 2H), 7.19–7.21 (m, 2H), 7.27–7.30 (m, 2H); ^{13}C NMR (125 MHz, $CDCl_3$) δ 28.0 (3C), 41.9, 81.1, 128.6 (2C), 130.6 (2C), 132.8, 133.1, 170.5; HRMS for $C_{12}H_{16}ClO_2$ 227.0839, found 227.0858.

tert-butyl (3-methylphenyl)acetate (3i)

The reaction was carried out according to the General Procedure using *tert*-butyl bromoacetate (389 mg, 1.99 mmol), $Fe(acac)_3$ (7.1 mg, 1.0 mol%), and *m*-tolylmagnesium bromide solution (0.78 M in THF, 6.6 mL, 7.7 equiv). The title compound (288 mg, 70%) was obtained as a colorless oil after silica gel column chromatography.

FTIR (neat, cm^{-1}) ν 2978, 1730, 1367, 1255, 1134, 957, 843, 766, 692, 436; ^1H NMR (500 MHz, $CDCl_3$) δ 1.44 (s, 9H), 2.34 (s, 3H), 3.49 (s, 2H), 7.05–7.08 (m, 3H), 7.18–7.22 (m, 1H); ^{13}C NMR (125 MHz, $CDCl_3$) δ 21.4, 28.0 (3C), 42.5, 80.7, 126.2, 127.6, 128.3, 130.0, 134.5, 138.0, 171.1; HRMS for $C_{13}H_{19}O_2$ 207.1385, found 207.1378.

tert-butyl (2-methylphenyl)acetate (3j)

The reaction was carried out according to the General Procedure using *tert*-butyl bromoacetate (389 mg, 1.99 mmol), $Fe(acac)_3$ (7.1 mg, 1.0 mol%), and *o*-tolylmagnesium bromide solution (0.91 M in THF, 6.6 mL, 3.0 equiv). The title compound (167 mg, 41%) was obtained as a colorless oil after silica gel column chromatography.

FTIR (neat, cm^{-1}) ν 2978, 1730, 1367, 1255, 1140, 955, 835, 739, 579, 446; ^1H NMR

(500 MHz, $CDCl_3$) δ 1.44 (s, 9H), 2.31 (s, 3H), 3.54 (s, 2H), 7.15–7.1719 (m, 4H); ^{13}C NMR (125 MHz, $CDCl_3$) δ 19.5, 28.0 (3C), 40.5, 55.2, 80.7, 126.0, 127.1, 130.1, 130.2, 133.5, 136.7, 170.9; HRMS for $C_{13}H_{19}O_2$ 207.1385, found 207.1372.

***tert*-butyl (4-fluoro-3-methylphenyl)acetate (3k)**

The reaction was carried out according to the General Procedure using *tert*-butyl bromoacetate (391 mg, 2.01 mmol), $Fe(acac)_3$ (7.1 mg, 1.0 mol%), and 4-fluoro-3methylphenylmagnesium bromide solution (0.75 M in THF, 8.0 mL, 3.0 equiv). The title compound (405 mg, 90%) was obtained as a colorless oil after silica gel column chromatography.

FTIR (neat, cm^{-1}) ν 2978, 1728, 1607, 1367, 1295, 1254, 1136, 1038, 954, 851, 796, 753, 688; ^1H NMR (392 MHz, $CDCl_3$) δ 1.44 (s, 9H), 2.25 (d, J = 1.8 Hz, 3H), 3.45 (s, 2H), 6.89–6.99 (m, 1H), 7.00–7.11 (m, 2H); ^{13}C NMR (99 MHz, $CDCl_3$) δ 14.5 (d, J = 3.8 Hz), 28.0 (3C), 41.7, 80.9, 114.9 (d, J = 22.5 Hz), 124.7 (d, J = 16.9 Hz), 127.9 (d, J = 7.5 Hz), 130.0 (d, J = 3.8 Hz), 132.3 (d, J = 4.7 Hz), 160.4 (d, J = 244 Hz), 171.0; HRMS for $C_{13}H_{17}FO_2$ 224.1213, found 224.1213; Anal. Calcd for $C_{13}H_{17}FO_2$: C, 69.62; H, 7.64; F, 8.47. Found: C, 69.66; H, 7.69; F, 8.38.

***tert*-butyl (3,4-difluorophenyl)acetate (3l)**

The reaction was carried out according to the General Procedure using *tert*-butyl bromoacetate (389 mg, 1.99 mmol), $Fe(acac)_3$ (7.1 mg, 1.0 mol%), and 3,4-difluorophenylmagnesium bromide solution (0.49 M in THF, 12.2 mL, 3.0 equiv). The title compound (317 mg, 70%) was obtained as a colorless oil after silica gel column chromatography.

FTIR (neat, cm^{-1}) ν 2978, 1731, 1501, 1367, 1252, 1209, 1136, 957, 884, 799, 753, 711; ^1H NMR (392 MHz, $CDCl_3$) δ 1.44 (s, 9H), 3.48 (s, 2H), 6.95-7.02 (m, 1H), 7.09–7.15 (m, 2H); ^{13}C NMR (99 MHz, $CDCl_3$) δ 28.0 (3C), 41.7, 81.3, 117.1 (d, J = 16.9 Hz), 118.2 (d, J = 17.8 Hz), 125.3 (dd, J = 5.6, 3.8 Hz), 131.5 (dd, J = 5.6, 3.8 Hz), 149.4 (dd, J = 247, 12.2 Hz), 150.2 (dd, J = 248, 12.2 Hz), 171.2; HRMS for $C_{12}H_{14}F_2O_2$ 228.0962, found 228.0957; Anal. Calcd for $C_{12}H_{14}F_2O_2$: C, 63.15; H, 6.18; F, 16.65. Found: C, 63.12; H, 6.23; F, 16.68.

***tert*-butyl (3,5-dimethylphenyl)acetate (3m)**

The reaction was carried out according to the General Procedure using *tert*-butyl bromoacetate (388 mg, 1.99 mmol), $Fe(acac)_3$ (7.1 mg, 1.0 mol%), and *p*-fluoromagnesium bromide solution (0.88 M in THF, 6.8 mL, 3.0 equiv). The title

compound (232 mg, 53%) was obtained as a yellow oil after silica gel column chromatography.

FTIR (neat, cm^{-1}) ν 2979, 1728, 1610, 1517, 1437, 1368, 1283, 1208, 1136, 968, 873, 791, 767, 753, 710; ^{1}H NMR (392 MHz, $CDCl_3$) δ 1.44 (s, 9H), 2.30 (s, 6H), 3.45 (s, 2H), 6.88 (s, 3H); ^{13}C NMR (99 MHz, $CDCl_3$) δ 21.5 (2C), 28.1 (3C), 42.4, 80.7, 127.0 (2C), 128.5, 134.4, 137.9 (2C), 171.2; HRMS for $C_{14}H_{20}O_2$ 220.1463, found 220.1468; Anal. Calcd for $C_{14}H_{20}O_2$: C, 76.33; H, 9.15; O, 14.52. Found: C, 76.25; H, 9.23; O, 14.78.

tert-butyl naphth-2-ylacetate (3p)

The reaction was carried out according to the General Procedure using *tert*-butyl bromoacetate (390 mg, 2.00 mmol), $Fe(acac)_3$ (7.1 mg, 1.0 mol%), and 2-naphthyl bromide solution (0.86 M in THF, 7.0 mL, 3.0 equiv). The title compound (397 mg, 82%) was obtained as a colorless oil after silica gel column chromatography.

FTIR (neat, cm^{-1}) ν 2978, 1713, 1365, 1269, 1161, 1126, 966, 949, 866, 829, 798, 746, 636, 474; ^{1}H NMR (500 MHz, $CDCl_3$) δ 1.44 (s, 9H), 3.69 (s, 2H), 7.41–7.46 (m, 3H), 7.71 (brs, 1H), 7.79–7.82 (m, 3H); ^{13}C NMR (125 MHz, $CDCl_3$) δ 28.0 (3C), 42.8, 80.9, 125.6, 126.0, 127.4, 127.6, 127.7, 127.8, 128.0, 132.2, 132.4, 133.5, 170.9; HRMS for $C_{16}H_{19}O_2$ 243.1385, found 243.1364; Anal. Calcd for $C_{16}H_{18}O_2$: C, 79.30; H, 7.49. Found: C, 79.02; H, 7.53.

References and Notes

[1] a) A. Terada, K. Wachi, H. Mitsusaka (Sankyo, co., ltd.) Jpn. Kokai Tokkyo Koho JP 53135958 A, 1978. b) M. Acemoglu, T. Allmendinger, J. Calienni, J. Cercus, O. Loiseleur, G. H. Sedelmeier, D. Xu, *Tetrahedron* **2004**, *60*, 11571–11586.

[2] a) Th. Zincke, *Ber. Dtsch. Chem. Ges.* **1869**, *2*, 737–740. b) R. Quelet, J. Gavarret, *Bull. Soc. Chim. Fr.* **1950**, 1075–1078. c) J. B. Woell, H. Alper, *Tetrahedron Lett.* **1984**, *25*, 3791–3794.

[3] a) J. F. Fauvarque, A. Jutand, *J. Organomet. Chem.* **1979**, *177*, 273–281. b) M. Kosugi, I. Hagiwara, T. Sumiya, T. Migita, *Bull. Chem. Soc. Jpn.* **1984**, *57*, 242–246. c) C. Carfagna, A. Musco, G. Sallese, R. Santi, T. Fiorani, *J. Org. Chem.* **1991**, *56*, 261–263. d) T. Sakamoto, Y. Kondo, K. Masumoto, H. Yamanaka, *Heterocycles* **1993**, *36*, 2509–2512. e) T. Sakamoto, Y. Kondo, K. Masumoto, H. Yamanaka, *J. Chem. Soc., Perkin Trans 1* **1994**, 235–236. f) F. Agnelli, G. A. Sulikowski, *Tetrahedron Lett.* **1998**, *39*, 8807–8810. g) W. A. Moradi, S. L. Buchwald, *J. Am. Chem. Soc.* **2001**, *123*, 7996–8002. h) S. Lee, N. A. Beare, J. F. Hartwig, *J. Am. Chem. Soc.* **2001**, *123*, 8410–8411. i) T. Hama, J. F. Hartwig, *Org. Lett.* **2008**, *10*, 1545–1548. j) T. Hama, J. F. Hartwig, *Org. Lett.* **2008**, *10*, 1549–1552. k) M. R. Biscoe, S. L. Buchwald, *Org. Lett.* **2009**, *11*, 1773–1775.

[4] K. Tamao, M. Zembayashi, M. Kumada, *Chem. Lett.* **1976**, 1239–1242.

[5] There is only sporadic reported literature example of utilizing α-bromocarboxylic acid derivatives and arylmetal reagents as the coupling partners under iron catalysis: R. Martin, A. Fürstner, *Angew. Chem. Int. Ed.* **2004**, *43*, 3955–3957.

[6] a) T. Nagano, T. Hayashi, *Org. Lett.* **2004**, *6*, 1297–1299. b) R. B. Bedford, D. W. Bruce, R. M. Frost, J. W. Goodby, M. Hird, *Chem. Commun.* **2004**, 2822–2823. c) M. Nakamura, K. Matsuo, S. Ito, E. Nakamura, *J. Am. Chem. Soc.* **2004**, *126*, 3686–3687. d) R. B. Bedford, D. W. Bruce, R. M. Frost, M. Hird, *Chem. Commun.* **2005**, 4161–4163. e) R. B. Bedford, M. Betham, D. W. Bruce, A. A. Danopoulos, R. M. Frost, M. Hird, *J. Org. Chem*. **2006**, *71*, 1104–1110. f) G. Gahiez, V. Habiak, C. Duplais, A. Moyeux, *Angew. Chem. Int. Ed.* **2007**, *46*, 4364–4366.

[7] $Fe(acac)_3$ was purchased from Aldrich Chemical co. and readily applied to the coupling reaction without purification.

[8] The yields of the desired coupling products decreased dramatically when the reaction was carried out under the procedure described as follows: to the pre-cooled mixture of a bromoacetate and an iron catalyst was slowly added a THF solution of a Grignard reagent, the corresponding α-arylated ester was obtained in less than 30% yield.

[9] a) S. L. Buchwald, C. Bolm, *Angew. Chem. Int. Ed.* **2009**, *48*, 5586–5587. b) R. B. Bedford, M. Nakamura, N. J. Gower, M. F. Haddow, M. A. Hall, M. Huwe, T. Hashimoto, R. A. Okopie, *Tetrahedron Lett*. **2009**, *50*, 6110–6111.

[10] The iron-catalyzed coupling reaction of *tert*-butyl bromoacetate with *o*-tolylmagnesium bromide was carried out in the presence of the following additives: the α-arylated ester was obtained in 42%, 6%, and 1% yield in the presence of 1,4-dioxane (10 equiv), *N*-methylpyrrolidone (NMP, 10 equiv), and *N*,*N*,*N*',*N*'-tetramethylethylenediamine (TMEDA, 3.0 equiv), respectively.

CHAPTER 5

Iron-Catalyzed Enantioselective Cross-Coupling Reactions of α-Chloroesters with Aryl Grignard Reagents

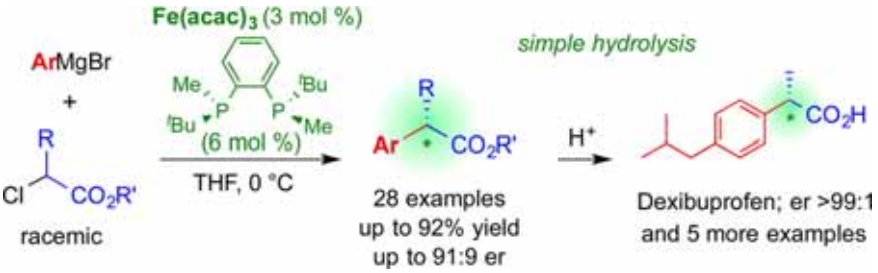

Abstract

The first iron-catalyzed enantioselective cross-coupling reaction between an organometallic compound and an organic electrophile is reported. Synthetically versatile racemic α-chloro- and α-bromoalkanoates were coupled with aryl Grignard reagents in the presence of catalytic amounts of an iron salt and a chiral bisphosphine ligand, giving the products in high yields with acceptable and synthetically useful enantioselectivities (er up to 91:9). The produced α-arylalkanoates were readily converted to the corresponding α-arylalkanoic acids with high optical enrichment (er up to >99:1) via simple deprotections/recrystallizations. The results of radical probe experiments are consistent with a mechanism that involves the formation of an alkyl radical intermediate, which undergoes subsequent enantioconvergent arylation in an intermolecular manner. The developed asymmetric coupling offers not only facile and practical access to various chiral α-arylalkanoic acid derivatives, which are of significant pharmaceutical importance, but also a basis of controlling enantioselectivity in an iron-catalyzed organometallic transformation.

Introduction

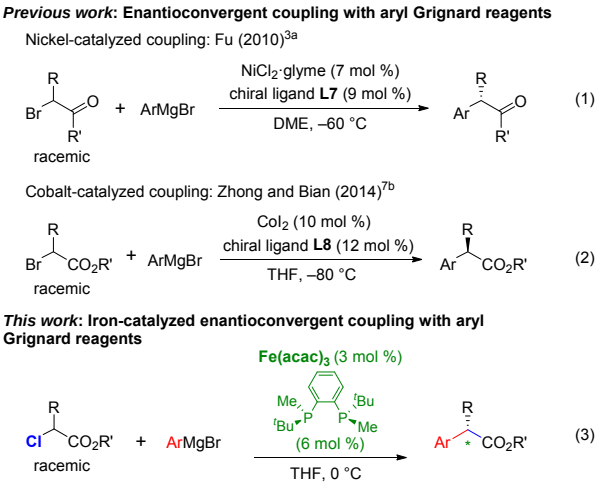

Transition-metal-catalyzed enantioselective cross-coupling reactions are powerful tools in the asymmetric synthesis of functional chiral molecules.[1] Recent progress in the cross coupling of various alkyl halides[2] has led to the development of a new class of enantioconvergent cross-coupling reactions, which enable the construction of various molecular frameworks and the catalytic installation of asymmetric carbon centers in one operation from racemic substrates. During the past decade, significant success has been achieved by Fu and co-workers using nickel catalysts (e.g., eq 1).[3] However, despite the rapid and notable development of iron,[4] cobalt,[5] and copper[6] catalysts for the coupling reactions of alkyl halides, the viability of these metal catalysts in the enantioconvergent cross coupling of alkyl halides remains virtually unexplored; only one example of a Co-catalyzed asymmetric cross coupling between α-bromoesters and aryl Grignard reagents was reported recently (eq 2).[7] In particular, iron has never been used in the catalytic, enantioselective coupling of organometallic compounds,[8] while its toxicologically benign nature and cost-effectiveness present clear practical advantages in the production of optically active fine chemicals, such as pharmaceutical and agricultural compounds. Furthermore, the application of iron catalysts to asymmetric organometallic transformation has proven to be challenging based on the fact that there is the one precedent in literature for such a reaction.[8b] In line with the research regarding the precise control of iron catalysis in C−C bond formation,[8b,9] the author presents the first example of iron-catalyzed enantioselective cross coupling facilitated by an easily accessible P-chiral bisphosphine ligand, BenzP*.[10] Specifically, synthetically versatile racemic α-chloroalkanoates were cross-coupled with aryl Grignard reagents to afford optically active α-arylalkanoates (eq 3) and the related alkanoic acids, upon simple deprotection, which are of particular pharmaceutical and biological importance as

nonsteroidal anti-inflammatory analgesics or cyclooxygenase inhibitors.[11]

Results and Discussion

Upon examining the combination of electrophiles and nucleophiles, the author found that alkyl 2-haloalkanoates **1** and the aryl Grignard reagents **2** cross-coupled to give desired product **3** in good yield with certain enantioselectivity in the presence of catalytic amounts of an iron salt and a bisphosphine ligand (Scheme 1).

Scheme 1. Enantioselective Iron-Catalyzed Cross-Coupling of **1** with **2**

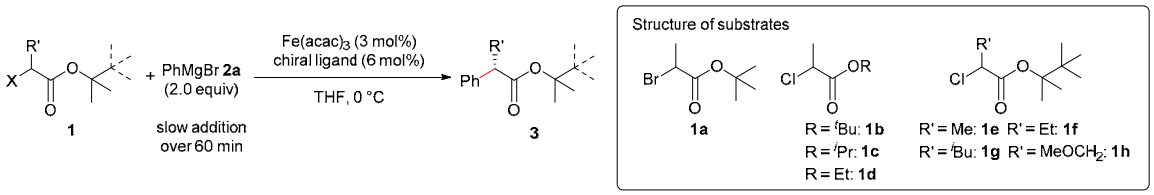

Table 1. Chiral Ligand Screening for the Asymmetric Iron-Catalyzed Cross-Coupling Reaction (Structures of Ligands are Shown in Right-Hand Side)

entry[a]	ligand	GC yield[b] /% (er, *S*:*R*)[c]		
		3	**1a**	**Ph-Ph**[d]
1	(*R*)-BINAP	33 (50:50)	0	48
2	(*R*)-T-BINAP	39 (50:50)	0	49
3	(*R*)-DM-BINAP	35 (50:50)	0	49
4	(*R*)-H_8-BINAP	34 (50:50)	0	49
5	(*R*)-SEGPHOS	32 (50:50)	0	51
6	(*R*)-MeO-BIPHEP	35 (50:50)	0	51
7	(*R*)-P-Phos	35 (55:45)	0	46
8	(*R*)-C_3-TunePhos	34 (50:50)	0	50
9	(*R*)-PHANEPHOS	35 (50:50)	0	48
10	(*S*,*S*)-Et-Ferrocelane	39 (53:47)	0	44
11	(*R*)-PROPHOS	33 (51:49)	0	50
12	(*S*,*S*)-CHIRAPHOS	33 (48:52)	0	53
13	(*R*,*R*)-DIPAMP	41 (48:52)	0	43
14	(*S*,*S*) -*i*-Pr-BPE	48 (50:50)	0	36
15	(*S*,*S*) -Ph-BPE	53 (50:50)	0	41
16	(*S*,*S*)-BDPP	49 (49:51)	0	36
17	(*S*,*S*)-DIOP	40 (50:50)	0	43
18	(*R*,*R*)-NORPHOS	35 (45:55)	0	44
19	(*R*)-SDP	32 (50:50)	0	50
20	**(*S*,*S*',*R*,*R*')-TangPhos**	**69 (79:21)**	**0**	**23**
21	(*R*)-BINAPINE	27 (50:50)	0	51
22	(*R*)-BINAPHANE	36 (49:51)	0	43
23	**(*R*,*R*)-QuinoxP***	**66 (83:17)**	**0**	**33**
24	**(*R*,*R*)-BenzP***	**85 (85:15)**	**0**	**15**
25	(*R*,*R*)-*t*-Bu-BisP*	51 (51:49)	0	38
26	(*R*,*R*)-PyridineP*	51 (53:47)	0	38
27	(*R*,*R*)-Me-DuPhos	39 (50:50)	0	44
28	(*R*,*R*)-*i*-Pr-DuPhos	75 (38:62)	0	23
29	(*R*)-(*S*)-Josiphos **A**	49 (50:50)	0	42
30	(*R*)-(*S*)-Josiphos **B**	68 (52:48)	0	19
31	(*R*)-(*S*)-Josiphos **C**	51 (48:52)	0	38

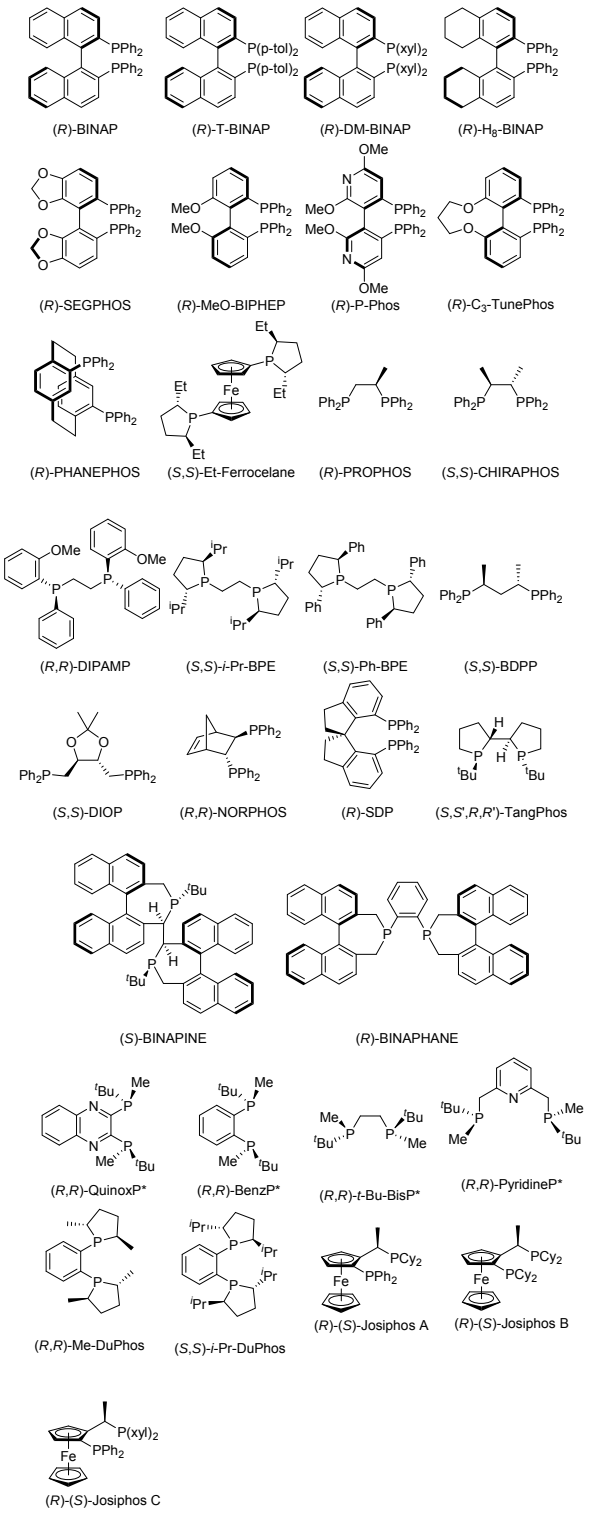

entry[a]	ligand	GC yield[b] /% (er, *S*:*R*)[c]		
		3	**1a**	**Ph-Ph**[d]
32	(*R*)-(*S*)-Mandyphos **A**	34 (49:51)	0	47
33	(*R*)-(*S*)-Mandyphos **B**	35 (51:49)	0	47
34	(*R*)-(*S*)-Taniaphos **A**	33 (52:48)	0	48
35	(*R*)-(*S*)-Taniaphos **B**	31 (50:50)	0	51
36	(*R*)-(*R*)-Walphos **A**	34 (50:50)	0	54
37	(*R*)-(*R*)-Walphos **B**	35 (50:50)	0	46
38	(*R*)-(*R*)-Walphos **C**	39 (50:50)	0	46
39	**(*S*,*S*)-Box A**	**80 (76:24)**	**0**	**16**
40	(*S*,*S*)-Box **B**	41 (52:48)	0	45
41	**(*R*,*R*)-Box C**	**78 (23:77)**	**0**	**22**
42	(*S*,*S*)-Box **D**	68 (75:25)	0	27
43	**(*S*,*S*)-Box E**	**80 (77:23)**	**0**	**20**
44	(*S*,*S*)-Box **F**	22 (51:49)	0	59
45	(*S*,*S*)-Box **G**	43 (79:21)	0	44
46	(*R*,*R*)-Box **H**	31 (26:74)	0	58
47	(*S*,*S*)-Box **I**	21 (53:47)	0	61
48	(*S*,*S*)-Box **J**	39 (52:48)	0	54
49	(*S*,*S*)-Box **K**	31 (52:48)	0	52
50	(*S*,*S*)-Box **L**	28 (50:50)	0	55
51	(*R*,*R*)-PyBox **A**	28 (51:49)	0	56
52	(*R*,*R*)-PyBox **B**	24 (50:50)	0	57
53	(*R*)-PHOX **A**	66 (40:60)	0	33
54	(*R*)-PHOX **B**	55 (39:61)	0	42
55	ip-FOXAP	86 (37:63)	0	15
56	(*S*)-QUINAP	36 (51:49)	0	46
57	(*R*)-MOP	35 (50:50)	0	48
58[e]	(*R*)-MOP	34 (50:50)	0	49
59[e]	(*R*)-Monophos	40 (50:50)	0	45
60[e]	(*R*)-Ship	38 (50:50)	0	41
61	Salen **A**	45 (50:50)	0	51
62	Trost **A**	41 (50:50)	0	38
63	aminophosphine **A**	36 (44:56)	0	50
64	(*R*,*R*)-DACH	21 (49:51)	0	61

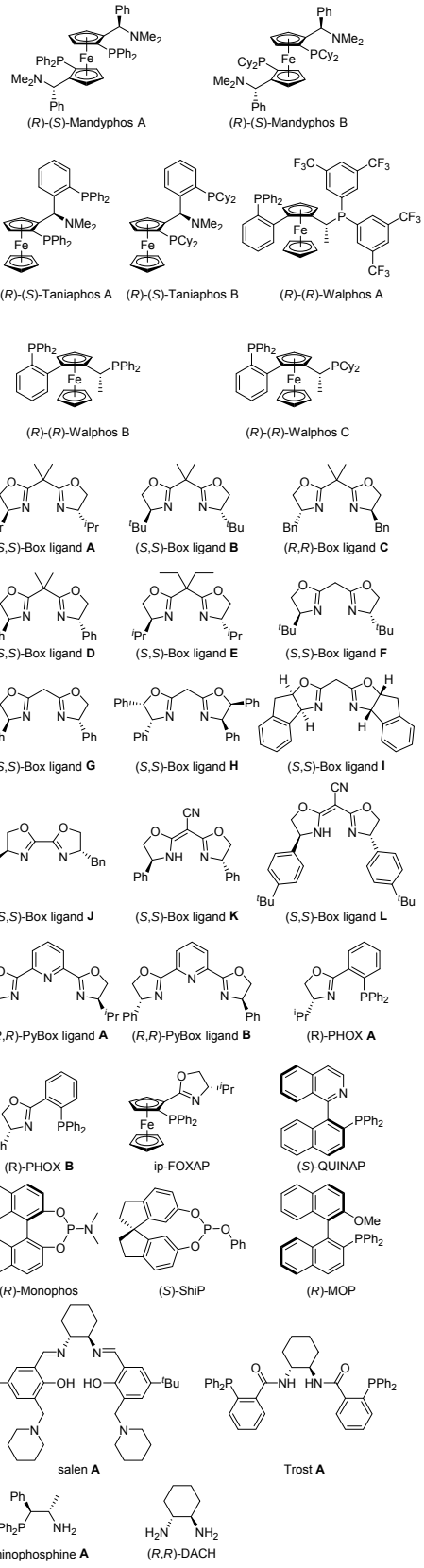

entry[a]	ligand	GC yield[b] /% (er, *S*:*R*)[c]		
		3	**1a**	**Ph-Ph**[d]
65	(*R*,*R*)-Me_2DACH	33 (65:35)	0	58
66	(*R*,*R*)-*tert*-DACH	59 (51:49)	0	24
67	(*S*,*S*)-DPEN	29 (50:50)	0	52
68	(*S*)-DABN	29 (50:50)	0	50
69	(*S*)-DMDBN	33 (50:50)	0	53
70	(*S*,*S*)-bipyrrolidine	27 (72:28)	0	62
71	(*S*)-*t*-Bu-BIMAH	44 (52:48)	0	45
72	(*S*,*S*)-Me_2DPEN	10 (50:50)	0	65
73	(*R*,*R*)-SciPROP*	82 (59:41)	0	7
74	(*R*,*R*)-SciPROP-TB*	81 (67:33)	0	6

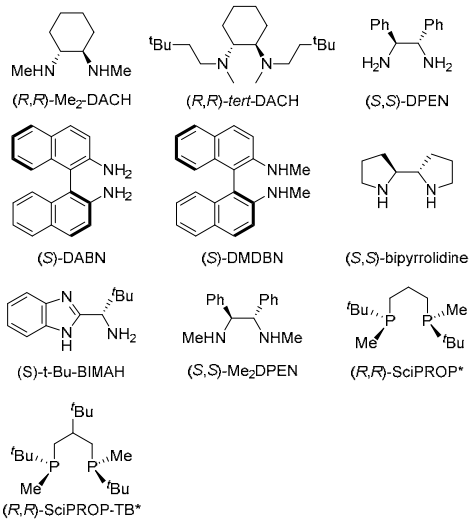

[a]Reactions were carried out on a 0.5 mmol scale using 3 mol% of $Fe(acac)_3$, 6 mol% of ligand, and 2.0 equivalents of the Grignard reagent unless otherwise noted. [b]Calibrated GC yield using undecane as an internal standard. [c]Er values were determined by HPLC analysis. [d]Mol% based on the substrate. [e]12 mol% of ligand was added.

Table 1 summarizes the result of chiral ligand screening for the asymmetric iron-catalyzed cross-coupling of *tert*-butyl 2-bromopropionate **1a** with the phenyl Grignard reagent **2a**. The axially chiral ligands such as BINAP and T-BINAP, which show high stereoselectivity in the iron-catalyzed carbometalation reactions,[8b] gave the racemic product in 33% and 39% yield, respectively (entries 1 and 2). While CHIRAPHOS, NORPHOS, or most of the other bisphosphine ligands gave low er (enantiomer ratio), notable chiral induction was observed when TangPhos, QuinoxP*, or BenzP*[10] was used: 79:21 to 85:15 er with 66–85% chemical yield (entries 20, 23, and 24). Although *t*-Bu-BisP* has a *tert*-butylmethylphosphine moiety, same chiral moiety as BenzP*, this alkane bisphosphine ligand resulted in low selectivity (entry 25), suggesting rigid backbone is essential for achieving high enantioselectivity as well as high chemical yield. Box ligands **A**, **C**, and **E** afforded the desired product in high yield of 78–80% with 76:24 to 77:23 er (entry 39, 41, and 43), but sterically demanding Box ligands **B** and **F** having *tert*-butyl groups on oxazoline rings resulted in low er (entries 40 and 44). Low er was observed when PyBox, PHOX, or monodentate phosphines were used as a ligand (entries 51–60). Among chiral diamines, only secondary diamines gave fair er of 65:35 and 72:28 with low chemical yields (entries 65 and 70). The author deduces that a small bite angle and a rigid backbone are the key factors for chiral bisphosphines to achieve good enantioselectivity because only TangPhos, QuinoxP* and BenzP* showed moderate to good er (entries 20, 23, and 24). Box ligands are the other promising chiral ligands for

this asymmetric reaction, but further tuning of ligand structure is required to obtain higher er.

Table 2. Effect of Ester-Protecting Groups on Iron-Catalyzed Enantioselective Cross-Coupling Reactions[a]

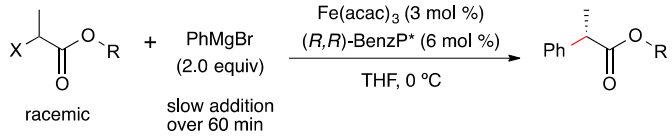

entry	α-bromopropionate	yield (%)[b]	er[c]	entry	α-chloropropionate	yield (%)[b]	er[c]
1	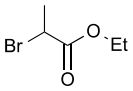	67	73:27	10	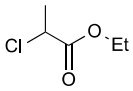	40	82:18
2	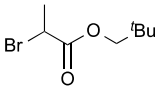	83	76:24	11	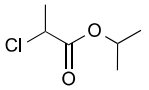	75	83:17
3	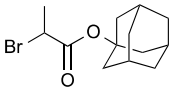	91	70:30	12	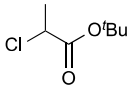	85	87:13
4	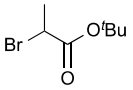	91	85:15	13	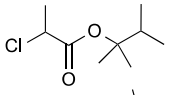	90	88:12
5	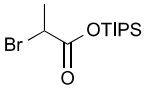	85	85:15	14	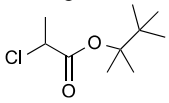	82	90:10
6	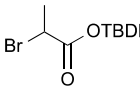	65	83:17	15	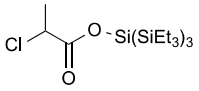	54	90:10
7	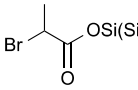	70	90:10	16	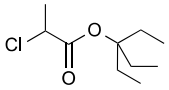	69	87:13
8	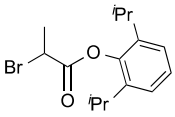	8	61:39	17	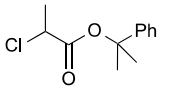	47	87:13
9	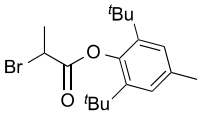	47	66:34	18	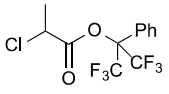	47	84:16

[a]Reactions were carried out on a 0.50 mmol scale using 3 mol% catalyst, 6 mol% (*R*,*R*)-BenzP*, and 2.0 equiv of PhMgBr at 0 °C. [b]NMR yields using 1,1,2,2-tetrachloroethane as an internal standard. [c]Er values were determined using chiral HPLC analysis.

Several α-halopropionates containing different ester-protecting groups were studied for the iron-catalyzed enantioselective cross-coupling reactions; the results are shown in Table 2. Entries 1–9 show the results of the cross-coupling reactions of α-bromopropionates containing various ester functionalities with PhMgBr in the presence of an Fe(acac)3/(*R*,*R*)-BenzP* catalyst. The yields and enantioselectivities of the cross-

coupling products improved with increasing steric hindrance of the ester-protecting group (Table 2, entries 1–4). Relatively bulky silyl esters (TIPS and TBDPS) provided comparable results to the *tert*-butyl ester (Table 2, entries 5 and 6) and a highly sterically hindered super silyl ester afforded the corresponding product with er of 90:10, albeit in a reduced yield of 70% (Table 2, entry 7). Sterically hindered aryl protecting groups (2,6-diisopropylphenyl and 2,6-di-*tert*-butyl-4-methylphenyl) resulted in significantly lower yields and enantioselectivities of the products (Table 2, entries 8 and 9). When α-chloropropionates were used under the same asymmetric cross-coupling conditions, slightly higher enantioselectivities were observed (Table 2, entries 10–18) because of the lack of the racemic background arylation (Table 2, entries 10 and 11). The steric effects of the ester-protecting groups affected both the yields and enantioselectivities of the cross-coupling products (Table 2, entries 10–15), and the optimal enantioselectivity with high yield was attained using 2,3,3-trimethylbutan-2-yl 2-chloropropionate (Table 2, entry 14). Some other bulky ester-protecting groups resulted in comparable enantioselectivities, but lower yields, of the cross-coupling products (Table 2, entries 16–18).

The reaction conditions are fully optimized as shown in Table 3. The coupling reaction proceeded in the temperature range of −40 to 40 °C, to give the desired product; the optimal selectivity (83:17 er) was observed both 0 and −40 °C (entries 2 and 3). The choice of solvent was critical in this reaction: ethereal solvents and toluene generally afforded the coupling products with good selectivities (74:26 to 84:16 er; entries 2 and 4–7); however, the use of *N*,*N*'-dimethylpropyleneurea (DMPU) and *N*-methylpyrrolidinone (NMP) as a solvent resulted in low yields with low er, suggesting that these strongly coordinating solvents displace the chiral ligands from iron centers, facilitating the formation of ferrate species[4d] (entries 8 and 9).

While racemic background reaction proceeded when bromopropionate **1a** was used as a substrate (entry 10),[9d] no background reaction was observed when chloropropionate **1b** was used (entry 11). 2,3,3-Trimethylbutan-2-yl 2-chloropropionate (Theptyl 2-chloropropionate; **1e**) was arylated with optimal enantioselectivity (90:10 er) in 82% yield (entry 15), but lower er and yields were observed in the coupling of sterically less demanding isopropyl ester **1c** or ethyl ester **1d** (entries 13 and 14). As shown in entry 15, slow addition of the Grignard reagent[4f,9a,h] was essential to achieve a high yield and enantioselectivity, and to avoid over-reduction of iron species or detachment of the formed aryl ferrate species from the chiral ligand (see the discussion regarding the time-course study described below). Again, the best er was obtained at 0 °C and no low-temperature conditions were required (entries 17 and 18).

Table 3. Screening of Reaction Conditions for Enantioselective Iron-Catalyzed Cross-Coupling of **1a–1e** with PhMgBr (**2a**)

entry[a]	1	ligand	solvent	temp (°C)	yield[b] (%)	er (*S*:*R*)[c]
1	**1a**	(*R*,*R*)-QuinoxP*	THF	40	39	78:22
2	**1a**	(*R*,*R*)-QuinoxP*	THF	0	66	83:17
3	**1a**	(*R*,*R*)-QuinoxP*	THF	−40	63	83:17
4	**1a**	(*R*,*R*)-QuinoxP*	toluene	0	33	74:26
5	**1a**	(*R*,*R*)-QuinoxP*	MTBE	0	50	81:19
6	**1a**	(*R*,*R*)-QuinoxP*	DME	0	42	84:16
7	**1a**	(*R*,*R*)-QuinoxP*	1,4-dioxane	0	61	80:20
8	**1a**	(*R*,*R*)-QuinoxP*	DMPU	0	2	60:40
9	**1a**	(*R*,*R*)-QuinoxP*	NMP	0	11	59:41
10	**1a**	none	THF	0	32	50:50
11	**1b**	none	THF	0	0	NA
12	**1b**	(*R*,*R*)-BenzP*	THF	0	91	87:13
13	**1c**	(*R*,*R*)-BenzP*	THF	0	75	83:17
14	**1d**	(*R*,*R*)-BenzP*	THF	0	40	82:18
15	**1e**	(*R*,*R*)-BenzP*	THF	0	82	90:10
16[d]	**1e**	(*R*,*R*)-BenzP*	THF	0	14	58:42
17	**1b**	(*R*,*R*)-BenzP*	THF	−20	62	87:13
18	**1b**	(*R*,*R*)-BenzP*	THF	−40	31	78:22

[a]Reactions were carried out on a 0.50 mmol scale using 3 mol% $Fe(acac)_3$, 6 mol% ligand, and 2.0 equiv of PhMgBr at 0 °C. PhMgBr was slowly added over 1.0 h using a syringe pump unless otherwise noted. [b]GC yields using undecane as an internal standard. Er values were determined by chiral HPLC analysis. The absolute configurations are shown in the parentheses. [d]PhMgBr was added in one portion.

Table 4 summarizes the results of the screening of the reaction conditions for asymmetric iron-catalyzed cross-coupling reactions of **1b** and **2a**. Slow addition of the Grignard reagent was a critical procedure for getting a high yield with good selectivity (entry 2). Trace metals have no impact on this cross-coupling reaction since other transition metal salts resulted in lower conversions or lower enantioselectivity (entries 3–6). $NiCl_2$·glyme and **BOX D** (the best combination for the enantioselective cross-coupling reactions of bromoketones with the aryl Grignard reagents)[3a] or **diamine A** (the best combination for the enantioselective cross-coupling reactions of bromoesters with the arylsilicon reagents)[3k] furnished desired product in low yield with unsatisfactory enantioselectivity (entries 7 and 8).

Table 4. Screening of Reaction Conditions for Enantioselective Iron-Catalyzed Cross-Coupling

entry[a]	catalyst	ligand	GC yield[b] /% (er, *S*:*R*)[c]		
			3	**1b**	**Ph-Ph**[d]
1	$Fe(acac)_3$	(*R*,*R*)-BenzP*	91(87:13)	0	14
2[e]	$Fe(acac)_3$	(*R*,*R*)-BenzP*	14 (58:42)	0	70
3	$Co(acac)_3$	(*R*,*R*)-BenzP*	49 (68:32)	9	46
4	$Ni(acac)_2$	(*R*,*R*)-BenzP*	0 (NA)	76	0
5	$Cu(acac)_2$	(*R*,*R*)-BenzP*	0 (NA)	79	17
6	$Pd(acac)_2$	(*R*,*R*)-BenzP*	0 (NA)	73	12
7[e]	$NiCl_2$·glyme	(*S*,*S*)-BOX D	18 (82:18)	75	14
8	$NiCl_2$·glyme	(*R*,*R*)-diamine A	13 (57:43)	78	11

[a]Reactions were carried out on a 0.50 mmol scale using 3 mol% catalyst, 6 mol% ligand, and 2.0 equiv of PhMgBr at 0 °C. [b]GC yields using undecane as an internal standard. [c]Er values were determined by chiral HPLC analysis. [d]Mol% based on the substrate. [e]Reactions were carried out using 7 mol% catalyst, 9 mol% ligand, 1.1 equiv of PhMgBr at –60 °C for 16 h. See ref 3a.

Table 5. Scope and Limitations of Enantioselective Iron-Catalyzed Cross-Coupling (R = theptyl)

entry[a]	product **3**	Isolated yield /%	er[b]	entry[a]	product **3**	Isolated yield /%	er[b]
1	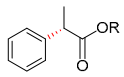	82	90:10	15	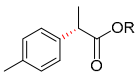	89	87:13
2	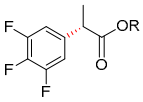	25	90:10	16	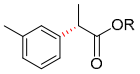	84	88:12
3	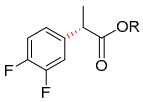	83	91:9	17	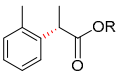	38	84:16
4	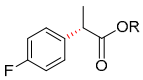	87	91:9	18	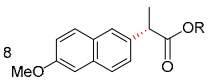	79	88:12
5	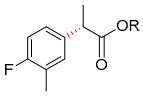	85	88:12	19	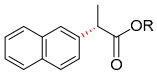	90	88:12
6	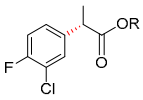	83	91:9	20	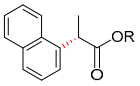	31	58:42
7	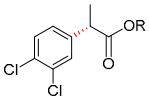	88	90:10	21	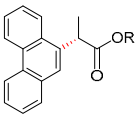	81	74:26
8	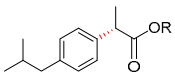	75	87:13	22	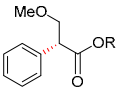	31	77:23
9	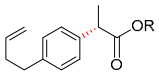	92	86:14	23	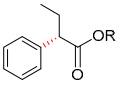	68	88:12
10	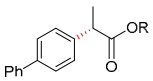	90	86:14	24	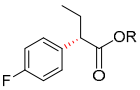	69	90:10
11	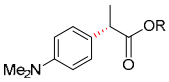	78	88:12	25	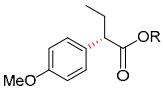	42	88:12
12	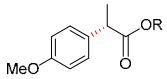	78	88:12	26	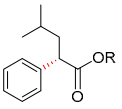	38	74:26
13	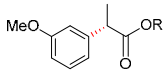	70	89:11	27	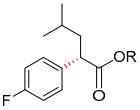	72	91:9
14	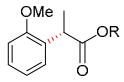	0	NA	28	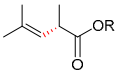	52	91:9

[a]Reactions were carried out on a 0.50–1.0 mmol scale. [b]Er values were determined by chiral HPLC analysis.

The data presented in Table 5 show the scope of the developed coupling reaction in the synthesis of a range of optically active α-arylalkanoic acid derivatives. The reactions of **1e** with various aryl Grignard reagents are shown in entries 1− 22. Electron-rich and -neutral aryl Grignard reagents reacted to give the desired products in high yields with adequate enantioselectivities (entries 1−7 and 9−14). A terminal olefin moiety, which often undergoes isomerization to an internal olefin under transition-metal catalysis,[12] remained intact under the present conditions (entry 13).

Ortho-substituted aryl Grignard reagents reacted slowly (entries 8, 11, and 15), while the use of a 9-phenanthryl Grignard reagent resulted in a good yield and reasonable selectivity (entry 16). As in entries 17−22, electron-deficient aryl Grignard reagents reacted to give coupling products in a relatively high er of ca. 9:1 and mostly in good yield with the exception of a 3,4,5-trifluorophenyl Grignard reagent (25% yield). Although chloroarenes are known to react with Grignard reagents via iron catalysis, a chlorinated aryl group was installed with the chloro group remaining intact (entries 21 and 22).[4c,13] Theptyl 2-chlorobutylate and theptyl 4-methyl-2-chloropentanoate (**1f** and **1g**) were cross-coupled to afford the products in good yields with adequate er, especially when 4-fluorophenyl Grignard reagent was employed (entries 23–27). Heteroaromatic Grignard reagents such as 2-thienyl- and 3-pyridyl- magnesium bromide did not result in the formation of cross-coupled products under the present conditions. The use of an alkenyl Grignard reagent furnished the corresponding α-chiral β,γ-unsaturated ester in 52% yield with 91:9 er (entry 28).

As shown in Table 6, the obtained cross-coupling products were readily deprotected under acidic conditions without any concomitant decrease in optical purity. Furthermore, the resulting 2-arylpropionic acids were enantioenriched by cocrystallization with octylamine; (*S*)-2-arylpropionic acids, including dexibuprofen and naproxen,[14] were obtained in optically pure or highly enriched forms (entries 1−4). 2-Arylbutyric acid and 2-aryl-4-methylpentanoic acid were also obtained in optically active forms using this method (entries 5 and 6).

Table 6. Enantioenrichment of Cross-Coupling Product after Deprotection

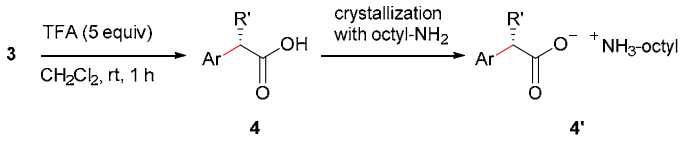

entry[a]	product **4** or **4'**	Isolated yield /%	er[b]
1	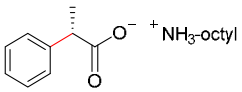	72	>99:1
2	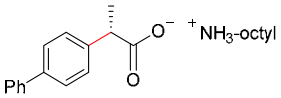	72	>99:1
3	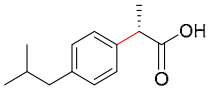	65	>99:1
4	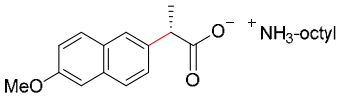	74	93:7
5	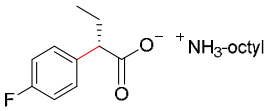	46	97:3
6	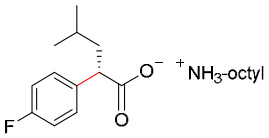	75	94:6

[a]Reactions were carried out on a 2 mmol scale. [b]Er values were determined by chiral HPLC analysis.

In order to gain insight into the nature of the present cross-coupling reaction, the author conducted a set of elementary mechanistic studies. Figure 1 shows the time course analysis for the coupling reaction of **1e** and PhMgBr (**2a**). No reaction of **1e** was observed during the addition of initial 0.12 equiv (i.e., 4 equiv to $Fe(acac)_3$) of PhMgBr and biphenyl was obtained in 1% yield as an exclusive product (i.e., 67% yield based on the partial reduction of Fe(III) to Fe(II)). This result suggests that trivalent $Fe(acac)_3$ was reduced to an iron(II) species[15] prior to the commencement of the cross-coupling reaction. After the addition of a supplemental amount of PhMgBr, the coupling reaction was initiated and the conversion of the substrate to the coupling product was observed, suggesting that diaryliron(II) species and chiral ligand were converted to the catalytically

active species in the presence of an excess amount of PhMgBr. The initial enantiomeric structure of substrate **1e** probably has no effect on the enantioselectivity of product **3** since no kinetic resolution of **1e** was observed during cross-coupling reaction.

(a) (b)

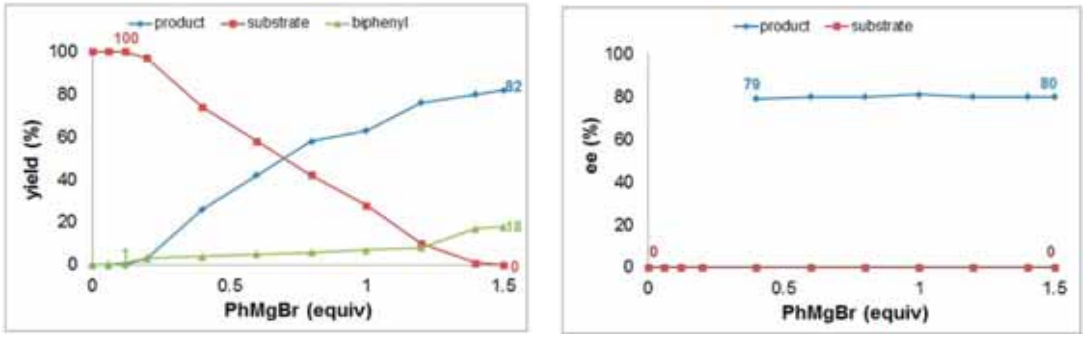

Figure 1. GC and HPLC trace of cross-coupling reaction of **1e** with PhMgBr: (a) Red, blue, and green lines show the recovery of substrate **1e**, the yield of product **3**, and the yield of biphenyl, respectively. (b) Red and blue lines show the enantiomeric excesses of **1e** and product **3**, respectively.

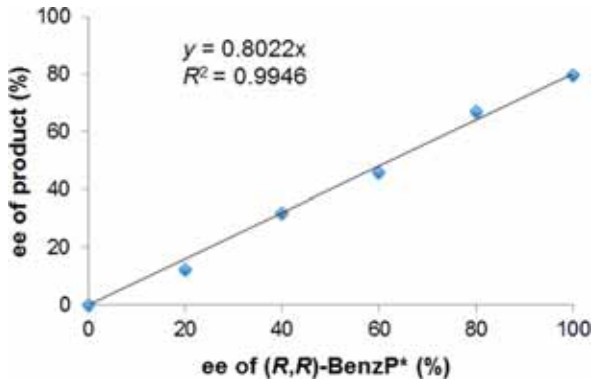

Figure 2. Dependence of enantiomeric excess of product **3** on that of (*R*,*R*)-BenzP*.

The enantioselectivity of product **3** was found to be directly proportional to the enantiomeric excess of the chiral ligand, and nonlinear effects (NLEs)[16] in the chiral induction were not observed (Figure 2). This result supports the conclusion that the enantioselectivity is determined under the influence of a chiral phosphine ligand that coordinates to an iron center.

Scheme 3. Cross-Coupling Reaction Using Radical Cyclization Substrate **1i** and **1j** (R = theptyl)

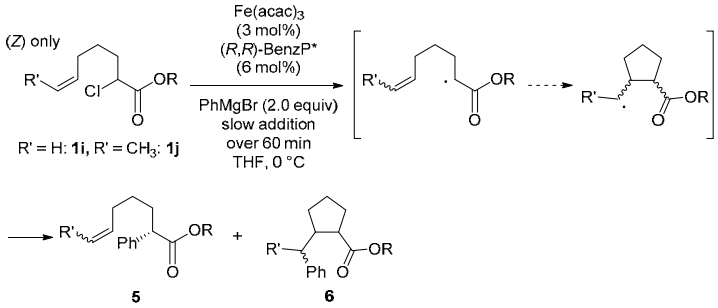

R'	**5**: yield (er)	**6**: yield (er)
H	12% (85:15)	40% (50:50) *anti*/*syn* = 58/42
CH_3	7% (87:13) (*Z*) only	35% (50:50)

To gain insights into the mechanism and determine whether this stereoconvergent cross-coupling reaction proceeds via a radical intermediate, the author studied the cross-coupling reaction using a radical probe substrate with a terminal alkenic moiety, **1i**, and PhMgBr reagent under the standard conditions (Scheme 3). This substrate provided the direct arylation (uncyclized) product **5** in 12% yield with 85:15 er, along with the cyclized cross-coupling product **6** in 40% yield, as racemic mixtures of diastereomers. The formation of cyclized products strongly suggests that the iron-catalyzed enantioselective cross-coupling reactions take place via alkyl radical intermediates, as proposed for previous achiral cross-coupling reactions catalyzed by iron and bisphosphine ligands.[9a–e]

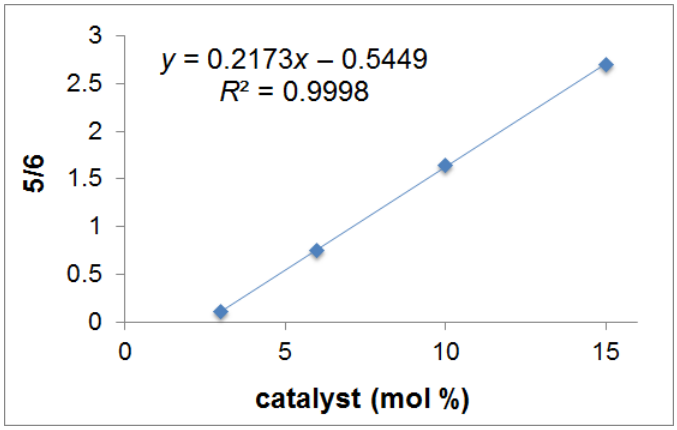

Figure 3. Dependence of ratio of uncyclized product **5** to cyclized product **6** on iron catalyst loading.

The cyclized products were obtained with almost no enantioselectivity, despite

the high enantioselectivity of uncyclized product **5**, suggesting that the cyclization reaction proceeds in the outer-sphere of the chiral environment created by (*R*,*R*)-BenzP*, supporting *out-of-cage* mechanism. The radical probe reaction with various catalyst loadings of $Fe(acac)_3$ and (*R*,*R*)-BenzP* (Figure 3) resulted in the observation of a first-order relationship between the ratio of **5**/**6** and the catalyst loading. This supports that the possibility that, once formed, the alkyl radical intermediate escapes from the solvent cage and undergoes sequential cyclization/arylation or direct arylation with an aryl iron species that is different from the one that reacts to generation the alkyl radical intermediate.[3h,17] We consider that enantioface selection occurred in the recombination of the alkyl radical with phenyliron species because only uncyclized product **5** was obtained as an optically active product.

The author also examined the reaction using the radical probe **1j** possessing geometrically defined (*Z*)-alkene. The direct arylation product **5** was isolated in 7% yield with 87:13 er and no isomerization of alkene along with the cyclized product **6**. Neither alkene-isomerized products nor substrate were found in the crude product, implying that the radical cyclization was irreversible.

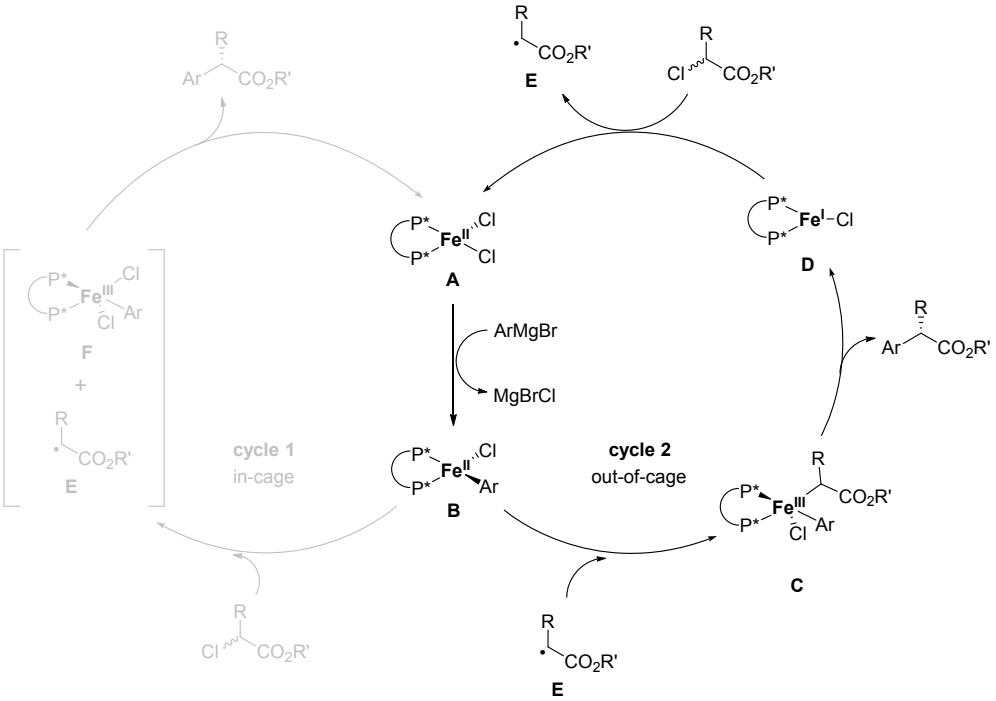

Figure 4. Possible catalytic cycle of enantioselective iron-catalyzed cross-coupling reaction.

Figure 4 illustrates a plausible reaction mechanism that is in good agreement

with the present and previous experimental observations and the computational study discussed in Chapter 7. The catalytic cycle starts from iron(II) species **A**, which is generated from the partial reduction of iron(III) salt in the presence of (*R*,*R*)-BenzP*, the limited concentration of the Grignard reagent, and an excess amount of the α-chloroester substrate. One of the chlorides of this iron(II) species **A** is replaced with the aryl group by the reaction with ArMgBr to give iron(II) species **B**, which abstracts the chloride from the substrate to generate alkyl radical intermediate **E** and iron(III) species **F**. The author proposed previously the mechanism depicted in Cycle 1, where arylation of alkyl radical **E** takes place with the aryl group of **F** in the solvent cage to give the arylation product and the iron(II) species **A**, which undergoes transmetalation with ArMgBr to regenerate **B** (in-cage mechanism).[9b,c,e] However, the observation of the first-order relationship between the ratio of **5**/**6** and the catalyst loading is not consistent with this cycle. In addition, the DFT and AFIR study discussed in Chapter 7 suggests that iron(I), iron(II), and iron (III) highly likely involves this cross-coupling reaction. The author, therefore, favors an alternative process based on a bimetallic mechanism.[17] Cycle 2 shows the favorable out-of-cage mechanism, in which alkyl radical intermediate **E** is generated by the reaction with iron(I) species **D**, and escapes from the solvent cage to react with another iron(II) species **B** to form the iron(III) species **C**. The coupling product is formed by the reductive elimination from species **C**, giving iron(I) species **D**. Abstraction of chloride from α-chloroester substrate by iron(I) species **D** gives radical intermediate **E** and regenerates the iron(II) species **A**.

Conclusion

In summary, the author has described the asymmetric iron-catalyzed cross-coupling reactions of racemic haloesters with the aryl Grignard reagents and demonstrated the scope with various Grignard reagents and chloroalkanoates. The rigid bisphosphine having a small bite angle, BenzP*, showed good reactivity as well as high selectivity. The mechanistic study using radical cyclization substrates **1i** and **1j** confirmed that this enantioselective iron-catalyzed cross-coupling proceeds via the radical mechanism.

Experimental Section

General Information

All the reactions were carried out in dry reaction vessels under a positive pressure of nitrogen. The following reagents and solvent were purchased and used as received: (*R*,*R*)-BenzP* from Nippon Chemical Industrial Co., Ltd.; $Fe(acac)_3$ (≥99.9%) from Sigma-Aldrich Co.; THF (deoxidized, stabilizer free) from Wako Pure Chemical Industries Ltd. Other commercial reagents and solvents were purchased from Wako Pure Chemical Industries Ltd., Sigma-Aldrich Co., and other commercial suppliers, and used without further purification. Column chromatography was performed on prepacked silica gel cartridges (SNAP Ultra; Biotage, Uppsala, Sweden). Gel permeation chromatography was performed on JAIGEL-1H and 2H (40 mm i.d.) with an LC-9104 (Japan Analytical Industry Co., Ltd.).

NMR spectra were recorded on a JEOL ECS-400 (392 MHz) and a JEOL ECS-500 spectrometer. GC analyses were performed on an Agilent 7890A instrument equipped with an FID detector and a capillary column, DB-1 (20 m length, 0.18 mm i.d., 0.18 μm film). IR spectra were recorded on a JASCO FT/IR-6100 Type A spectrometer. Enantiomer ratio (er) was determined by GC or HPLC analysis with a chiral stationary column.

Preparation of Materials

tert-Butyl 2-chloropropionate (**1b**)

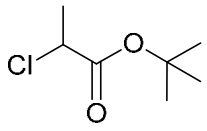

To a THF solution (170 mL) of *tert*-butanol (11.12 g, 150 mmol) and pyridine (13.3 mL, 1.1 equiv) was dropwise added 2-chloropropionyl chloride (16.0 mL, 1.1 equiv) at 0 °C, then stirred at same temperature for 1 h. After addition of MTBE (110 mL), the reaction mixture was successively washed with 1.0 M aqueous solution of hydrochloric acid (110 mL), 5% aqueous solution of sodium bicarbonate (110 mL), and brine (60 mL). The organic layer was dried over Na_2SO_4, evaporated in vacuo, and distilled under reduced pressure to give a colorless liquid (15.82 g, 64.1%). bp 80.2–81.7 °C / 50 mmHg.

FTIR (neat, cm^{-1}) ν 2981, 1738, 1369, 1294, 1151, 1072, 1065, 845; ^1H NMR (500 MHz, $CDCl_3$) δ 1.49 (s, 9H), 1.65 (d, J = 6.9 Hz, 3H), 4.29 (q, J = 6.9 Hz, 1H); ^{13}C NMR (125 MHz, $CDCl_3$) δ 21.5, 27.8, 53.7, 82.4, 169.2; HRMS (CI^+) *m/z* $[M+H]^+$ cacld for $C_7H_{14}ClO_2$: 165.0682; Found 165.0676. All analytical data are in good accordance with those reported in the literature.[18]

2,3,3-Trimethylbutan-2-ol

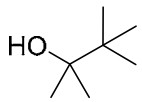

To an ether solution (200 mL) of 3,3-dimethyl-2-butanone (15.02 g, 150 mmol) was dropwise added MeMgBr (61.0 mL, 3.18 M in ether, 1.3 equiv) at 0 °C, then stirred at room temperature for 16 h. The reaction mixture was successively washed with saturated aqueous solution of ammonium chloride (80 mL) and brine (80 mL), dried over Na_2SO_4, evaporated in vacuo to give white crystals (16.13 g, 92.5%).

FTIR (neat, cm^{-1}) ν 3332, 2964, 1470, 1365, 1153, 1126, 945, 883, 619, 519, 482; ^1H NMR (500 MHz, $CDCl_3$) δ 0.96 (s, 9H), 1.20 (s, 6H), 1.69 (brs, 1H); ^{13}C NMR (125 MHz, $CDCl_3$) δ 25.3, 25.4, 37.4, 75.0; LRMS (CI^+) *m/z* 99 $[M–OH]^+$, All analytical data are in good accordance with those reported in the literature.[19]

2,3,3-Trimethylbut-2-yl 2-chloropropionate (1e)

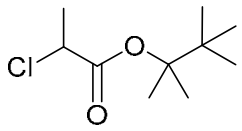

To a THF solution (40 mL) of 2,3,3-trimethylbutan-2-ol (5.81 g, 50 mmol) and DMAP (9.16 g, 1.5 equiv) was dropwise added 2-chloropropionyl chloride (5.82 mL, 1.2 equiv) at 0 °C, and resulting slurry mixture was stirred at 20 °C for 16 h. After addition of MTBE (60 mL), the reaction mixture was successively washed with 1.0 M aqueous solution of hydrochloric acid (30 mL), 5% aqueous solution of sodium bicarbonate (30 mL), and brine (30 mL). The organic layer was dried over Na_2SO_4, evaporated in vacuo, and resulted residue was purified by silica-gel column chromatography to furnish a colorless liquid (8.33 g, 81%).

bp 104.3–107.2 °C / 20 mmHg.

FTIR (neat, cm^{-1}) ν 2978, 1734, 1468, 1450, 1379, 1292, 1178, 1130, 1063, 847; ^1H NMR (500 MHz, $CDCl_3$) δ 0.97 (s, 9H), 1.52 (s, 3H), 1.53 (s, 3H), 1.66 (d, J = 6.9 Hz, 3H), 4.31 (q, J = 6.9 Hz, 1H); ^{13}C NMR (125 MHz, $CDCl_3$) δ 20.26, 20.29, 21.6, 25.1, 38.5, 54.2, 89.2, 169.0; LRMS (CI^+) *m/z* 207 $[M+H]^+$, 109 $[M+H–C_7H_{15}]^+$, 99 $[C_7H_{15}]^+$.

General Procedure A: Synthesis of 2-chloroesters from corresponding 2-chlorocarboxylic acids

To a THF solution (15 mL) of 2-chlorocarboxylic acid (1.2 equiv) and DMF (0.16 mL, 0.10 equiv), $(COCl)_2$ (2.03 mL, 1.2 equiv) was dropwise added at room temperature and stirred at same temperature for 1 h. After removing the solvent under reduced pressure (ca. 100 hPa), crude acyl chloride was obtained as a yellow oil and used without further purification.

To another flask was added 2,3,3-trimethylbutan-2-ol (2.32 g, 20 mmol), DMAP (3.67 g, 1.5 equiv), and THF (15 mL), and cooled to 0 °C. To this mixture was dropwise added pre-synthesized acyl chloride at 0 °C, and the resulting slurry mixture was stirred at 20 °C for 16 h. After addition of MTBE (30 mL), the reaction mixture was successively washed with 1.0 M aqueous solution of hydrochloric acid (15 mL), 5% aqueous solution of sodium bicarbonate (15 mL), and brine (15 mL). The organic layer was dried over Na_2SO_4, evaporated in vacuo, and resulted residue was purified by silica-gel column chromatography.

2,3,3-Trimethylbut-2-yl 2-chlorobutyrate (1f)

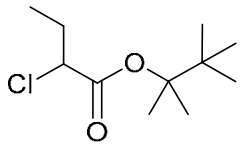

The title compound was synthesized according to General Procedure A: 2-Chlorobutyric acid (2.47 mL,1.2 equiv) was used. The product was obtained as a colorless liquid (1.91 g, 43%).

FTIR (neat, cm^{-1}) ν 2974, 1730, 1464, 1379, 1371, 1304, 1284, 1178, 1130, 939, 849; ^1H NMR (500 MHz, $CDCl_3$) δ 0.99 (s, 9H), 1.03 (t, J = 7.4 Hz, 3H), 1.525 (s, 3H), 1.528 (s, 3H), 1.92–2.06 (m, 2H), 4.14 (dd, J = 7.4, 6.0 Hz, 1H); ^{13}C NMR (125 MHz, $CDCl_3$) δ 10.4, 20.28, 20.32, 25.1, 28.5, 38.5, 60.5, 89.2, 168.5; LRMS (CI^+) *m/z* 123 $[M+H–C_7H_{15}]^+$, 99 $[C_7H_{15}]^+$.

2,3,3-Trimethylbut-2-yl 2-chloro-3-methoxypropionate (1g)

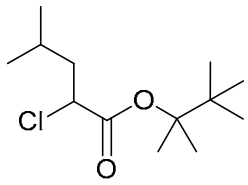

The title compound was synthesized according to General Procedure A: 2-Chloro-3-methoxypropionic acid (2.56 mL, 1.2 equiv) was used. The product was obtained as a colorless liquid (2.81 g, 59%).

FTIR (neat, cm^{-1}) ν 2973, 1734, 1466, 1379, 1371, 1286, 1176, 1122, 1028, 937, 847, 789; ^1H NMR (500 MHz, $CDCl_3$) δ1.00 (s, 9H), 1.54 (s, 6H), 3.41 (s, 3H), 3.71 (dd, J = 10.4, 6.2 Hz, 1H), 3.80 (dd, J = 10.4, 6.2 Hz, 1H), 4.32 (dd, J = 6.2, 6.2 Hz, 1H); ^{13}C NMR (125 MHz, $CDCl_3$) δ 20.4, 25.1, 38.5, 56.3, 59.3, 73.7, 89.8, 166.8; RMS (CI^+) *m/z* 237 $[M+H]^+$, 139 $[M+H–C_7H_{15}]^+$, 99 $[C_7H_{15}]^+$.

2-Chloro-4-methylpentanoic acid

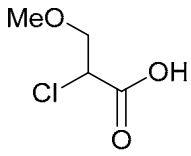

To a THF solution (100 mL) of diisopropylamine (18.2 mL, 2.6 equiv), BuLi (41.5 mL, 2.65 M in hexane, 2.2 equiv) was dropwise added at –20 °C and stirred at the same temperature for 0.5 h. After addition of DMPU (25 mL) and 4-methylpentanoic acid (5.81 g, 50 mmol), the resulting yellow solution was stirred at –20 °C for 2 h. The reaction mixture was cooled to –78 °C, and a THF solution (100 mL) of CCl_4 (24.1 mL, 5.0 equiv) was added in a single aliquot to give a black mixture. After stirring at –78 °C for 1 h, the mixture was heated to room temperature, added sodium chloride (20 g) and 2 M aqueous solution of hydrochloric acid (130 mL), extracted with MTBE (130 mL × 3), evaporated in vacuo, and resulted residue was purified by silica gel column chromatography (hexane/AcOEt/TFA = 90/10/0.1) to furnish a yellow liquid (6.75 g, 90%).

FTIR (neat, cm^{-1}) ν 3039, 2960, 1718, 1419, 1286, 1203, 1122, 922, 891, 683; ^1H NMR (500 MHz, $CDCl_3$) δ 0.95 (d, J = 5.5 Hz, 3H), 0.99 (d, J = 5.5 Hz, 3H), 1.84–1.93 (m, 3H), 4.36 (t, J = 6.8 Hz, 3H), 10.72 (brs, 1H); ^{13}C NMR (125 MHz, $CDCl_3$) δ 21.3, 22.5, 25.1, 43.3, 55.5, 175.9; HRMS (ES^-) *m/z* $[M–H]^-$ Cacld for $C_6H_{10}ClO_2$, 149.0369; Found 149.0388. All analytical data are in good accordance with those reported in the literature.[20]

2,3,3-Trimethylbut-2-yl 2-chloro-4-methylpentanoate (**1h**)

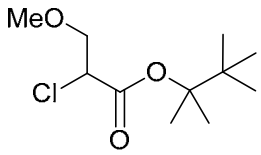

The title compound was synthesized according to General Procedure A: 2-Chloro-4-methylpentanoic acid (3.61 g, 1.2 equiv) was used. The product was obtained as a colorless liquid (2.57 g, 52%).

FTIR (neat, cm^{-1}) ν 2960, 1728, 1468, 1379, 1371, 1290, 1176, 1128, 937, 849, 789; ^1H NMR (500 MHz, $CDCl_3$) δ 0.92–0.98 (m, 6H), 1.00 (s, 9H), 1.52 (s, 3H), 1.53 (s, 3H), 1.77–1.84 (m, 3H), 4.18–4.22 (m, 1H); ^{13}C NMR (125 MHz, $CDCl_3$) δ 20.25, 20.30, 21.6, 22.5, 25.10, 25.27, 38.5, 43.8, 57.6, 89.1, 168.9; Anal. Calcd for $C_{13}H_{25}ClO_2$: C, 62.75; H, 10.13; Cl, 14.25. Found: C, 62.45; H, 9.87; Cl, 14.04. LRMS (CI^+) *m/z* 249 $[M+H]^+$, 151 $[M+H–C_7H_{15}]^+$, 99 $[C_7H_{15}]^+$.

2-Chloro-hept-6-enoic acid

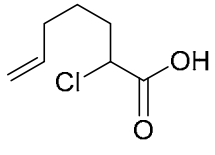

To a THF solution (100 mL) of diisopropylamine (18.2 mL, 2.6 equiv), BuLi (41.5 mL, 2.65 M in hexane, 2.2 equiv) was dropwise added at –20 °C and stirred at the same temperature for 0.5 h. After addition of DMPU (25 mL) and hept-6-enoic acid (6.36 g, 50 mmol), the resulting

yellow solution was stirred at –20 °C for 2 h. The reaction mixture was cooled to –78 °C, and a THF solution (100 mL) of CCl_4 (24.1 mL, 5.0 equiv) was added in a single aliquot to give a black mixture. After stirring at –78 °C for 1 h, the mixture was heated to room temperature, added sodium chloride (20 g) and 2 M aqueous solution of hydrochloric acid (130 mL), extracted with MTBE (130 mL × 3), evaporated in vacuo, and resulted residue was purified by silica gel column chromatography (hexane/AcOEt/TFA = 90/10/0.1) to furnish an orange liquid (7.04 g, 87%).

FTIR (neat, cm^{-1}) ν 3078, 2929, 1716, 1641, 1417, 1284, 1203, 991, 912, 866, 687, 635; ^1H NMR (500 MHz, $CDCl_3$) δ 1.52–1.70 (m, 2H), 1.93–2.01 (m, 2H), 2.04–2.16 (m, 2H), 4.34 (dd, *J* = 8.1, 5.8 Hz, 1H), 4.98–5.07 (m, 2H), 5.74–5.83 (m, 1H), 11.27 (brs, 1H); ^{13}C NMR (125 MHz, $CDCl_3$) δ 25.8, 32.8, 34.8, 56.1, 115.5, 137.6, 175.7; HRMS (ES^-) *m/z* $[M–H]^-$ Cacld for $C_7H_{10}ClO_2$: 161.0369; Found161.0372. All analytical data are in good accordance with those reported in the literature.[21]

2,3,3-Trimethylbut-2-yl 2-chloro-hept-6-enate (1i)

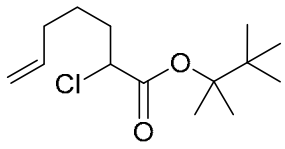

The title compound was synthesized according to General Procedure A: 2-Chloro-hept-6-enoic acid (3.92 g,1.2 equiv) was used. The product was obtained as a colorless liquid (2.48 g, 48%).

FTIR (neat, cm^{-1}) ν 2976, 1728, 1464, 1379, 1371, 1286, 1176, 1126, 991, 912, 847, 783; ^1H NMR (500 MHz, $CDCl_3$) δ 0.99 (s, 9H), 1.48–1.60 (m, 2H), 1.52 (s, 3H), 1.53 (s, 3H), 1.86–2.12 (m, 4H), 4.19 (dd, *J* = 6.2, 7.8 Hz, 1H) 4.96–5.05 (m, 2H), 5.73–5.82 (m, 1H); ^{13}C NMR (125 MHz, $CDCl_3$) δ 20.30, 20.31, 25.07, 25.09, 32.9, 34.4, 38.5, 58.9, 89.3, 115.3, 137.8, 168.6; LRMS (CI^+) *m/z* 163 $[M+H–C_7H_{15}]^+$, 99 $[C_7H_{15}]^+$.

(*Z*)-Oct-6-enoic acid

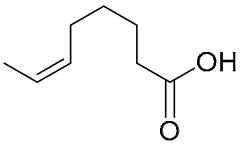

Lindlar catalyst (0.48 g) and quinoline (1.20 g) were added to an IPA solution (48 mL) of oct-6-ynoic acid[22] (2.40 g, 17.1 mmol) at 25 °C, and the mixture was stirred at that temperature for 6 h under the atmospheric pressure of hydrogen. After filtration to remove Lindlar catalyst, the solution was evaporated in vacuo, added AcOEt (48 mL), washed with a 1.0 M aqueous solution of hydrochloric acid (10 mL × 2), dried over Na_2SO_4, evaporated in vacuo, and the residue was purified by silica-gel column chromatography to furnish a colorless liquid (2.48 g, quant.)

FTIR (neat, cm^{-1}) ν 3013, 2930, 2860, 1705, 1412, 1288, 1231, 931, 700, 473; ^1H NMR (500 MHz, $CDCl_3$) δ 1.38–1.45 (m, 2H), 1.59–1.61 (m, 3H), 1.62–1.69 (m, 2H), 2.07 (q,

J = 7.1 Hz, 2H), 2.37 (t, J = 7.5 Hz, 2H), 5.33–5.39 (m, 1H), 5.43–5.41 (m, 1H); ^{13}C NMR (125 MHz, $CDCl_3$) δ 12.8, 24.2, 26.4, 28.9, 33.9, 124.3, 129.9, 179.8; HRMS (ES^-) *m/z* $[M–H]^-$ Cacld for $C_8H_{14}O_2$: 141.0916; Found 141.0920.

(*Z*)-2-Chlorooct-6-enoic acid

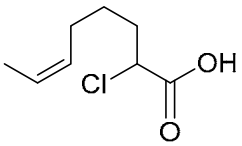

BuLi (11.7 mL, 2.65 M in hexane, 2.2 equiv) was added to a THF solution (30 mL) of diisopropylamine (5.14 mL, 2.6 equiv) at –20 °C, and the mixture was stirred at that temperature for 0.5 h. After addition of DMPU (7.5 mL) and (*Z*)-Oct-6-enoic acid (2.00 g, 14.1 mmol), the resulting yellow solution was stirred at –20 °C for 2 h. The reaction mixture was cooled to –78 °C, and a THF solution (30 mL) of CCl_4 (6.8 mL, 5.0 equiv) was added in a single aliquot, giving a black mixture. After stirring at –78 °C for 1 h, the mixture was heated to room temperature, and NaCl (8.0 g) and a 2 M aqueous solution of hydrochloric acid (40 mL) were added. The mixture was extracted with MTBE (40 mL × 3), the solvent was evaporated in vacuo, and the residue was purified by silica-gel column chromatography (hexane/AcOEt/TFA = 90/10/0.1) to furnish an orange liquid (2.61 g, quant.).

FTIR (neat, cm^{-1}) ν 3014, 2934, 2863, 1718, 1435, 1285, 1201, 917, 697; ^{1}H NMR (500 MHz, $CDCl_3$) δ 1.49–1.67 (m, 5H), 1.92–2.12 (m, 4H), 4.34 (dd, J = 8.1, 5.5 Hz, 1H), 5.33–5.39 (m, 1H), 5.47–5.53 (m, 1H); ^{13}C NMR (125 MHz, $CDCl_3$) δ 12.8, 25.7, 25.9, 34.2, 57.0, 125.0, 129.2, 175.3; HRMS (ES^-) *m/z* $[M–H]^-$ Cacld for $C_8H_{13}ClO_2$: 175.0526; Found 175.0520.

2,3,3-Trimethylbut-2-yl (*Z*)-2-chlorooct-6-enoate (1j)

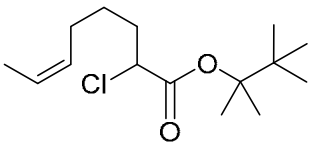

The title compound was synthesized according to general procedure A: (*Z*)-2-chlorooct-6-enoic acid (1.36 g, 1.2 equiv) was used. The product was obtained as a colorless liquid (1.69 g, 53%).

FTIR (neat, cm^{-1}) ν 2974, 1728, 1466, 1370, 1285, 1176, 1127, 938, 847, 784, 703, 506; ^{1}H NMR (500 MHz, $CDCl_3$): δ 0.99 (s, 9H), 1.43–1.58 (m, 2H), 1.52 (s, 3H), 1.52 (s, 3H), 1.59–1.61 (m, 3H), 1.86–2.04 (m, 2H), 2.08 (J = 7.4 Hz, 2H), 4.18 (dd, J = 7.4, 6.0 Hz, 1H), 5.32–5.38 (m, 1H), 5.44–5.51 (m, 1H); ^{13}C NMR (125 MHz, $CDCl_3$) δ 12.8, 20.28, 20.31, 25.1, 25.7, 26.0, 38.5, 59.0, 89.2, 124.8, 129.4, 168.6; Anal. Calcd for $C_{15}H_{27}ClO_2$: C, 65.55; H, 9.90; Cl, 12.90. Found: C, 65.23; H, 9.89; Cl, 13.02. LRMS (FAB^+, NaI) *m/z* 297 $[M+Na]^+$.

Enantioselective Cross-Coupling of Haloesters with Aryl Grignard Reagents

General Procedure B: Enantioselective cross-coupling

To a THF solution (1.0 mL) of $Fe(acac)_3$ (5.3 mg, 3 mol%), (*R*,*R*)-BenzP* (8.5 mg, 6 mol%), undecane (37.4 mg), and 2,3,3-trimethylbut-2-yl 2-chloroalkanoate (0.50 mmol), ArMgBr (0.50–1.0 M solution in THF, 2.0 equiv) was slowly added over 60 minutes using syringe pump at 0 °C. After stirring at the same temperature for 10 minutes, the resulting mixture was quenched with 1.0 M aqueous solution (1.0 mL) of hydrochloric acid and extracted with MTBE (1.0 mL × 3). The organic layer was dried over Na_2SO_4, evaporated in vacuo, and resulted residue was purified by silica gel column chromatography and gel permeation chromatography if necessary. The corresponding racemic sample could be synthesized by using 1,2-bis(3,5-di-*tert*-butylphenyl)phosphinobenzene instead of (*R*,*R*)-BenzP*.

***tert*-Butyl (*S*)-2-phenylpropionate** (Table 2, entry 4)

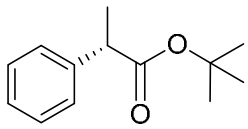

The reaction was carried out according to the General Procedure B using *tert*-butyl 2-chloropropionate (**1b**) (165 mg, 1.0 mmol) and PhMgBr (1.82 mL, 1.10 M in THF solution, 2.0 equiv). The title compound (187 mg, 91% yield, 87:13 er) was obtained as a colorless oil after silica gel column chromatography (hexane/AcOEt = 95/5).

The er was determined by HPLC on a CHIRALCEL OJ-3R (4.6 mm i.d., 150 mm length) with following conditions: 55% CH_3CN aq., 1.0 mL/min, 25 °C, retention times (t_r) = 10.9 min (minor) and 13.0 min (major).

Mp 33–35 °C; FTIR (neat, cm^{-1}) ν 2978, 2933, 1726, 1454, 1367, 1329, 1254, 1215, 1144, 1061, 849, 748, 698, 513; ^1H NMR (500 MHz, $CDCl_3$) δ 1.39 (s, 9H), 1.45 (d, J = 6.9 Hz, 3H), 3.61 (q, J = 6.9 Hz, 1H), 7.21–7.32 (m, 5H); ^{13}C NMR (125 MHz, $CDCl_3$) δ 18.5, 27.9, 46.5, 80.4, 126.8, 127.4, 128.4, 141.2, 173.8; Anal. Calcd for $C_{13}H_{18}O_2$: C, 75.69; H, 8.79. Found: C, 75.33; H, 8.81. HRMS (ES^+) *m/z* $[M]^+$ Calcd for $C_{13}H_{19}O_2$: 207.1385; Found 207.1363. $[\alpha]^{25}_D$ +41.8 (*c* 1.06, EtOH). *lit.* $[\alpha]^{20}_D$ +24.3 (*c* 3.3, $CHCl_3$, 95:5 er). All analytical data are in good accordance with those reported in the literature.[23]

2,3,3-Trimethylbut-2-yl (*S*)-2-phenylpropionate (Table 5, entry 1)

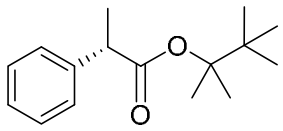

The reaction was carried out according to the General Procedure B using 2,3,3-trimethylbut-2-yl 2-chloropropionate (**1e**) (104 mg, 0.50 mmol) and PhMgBr (0.90 mL, 1.11 M in THF solution, 2.0 equiv). The title compound (102 mg, 82% yield, 90:10 er) was obtained as a colorless oil after silica gel column chromatography (hexane/toluene = 60/40).

The er was determined by HPLC on a CHIRALCEL OJ-3R (4.6 mm i.d., 150 mm length) with following conditions: 60% CH_3CN aq., 1.0 mL/min, 25 °C, retention times (t_r) = 13.3 min (minor) and 16.9 min (major).

FTIR (neat, cm^{-1}) ν 2975, 1725, 1454, 1378, 1369, 1204, 1172, 1128, 1064, 849; ^1H NMR (391.8 MHz, $CDCl_3$) δ 0.83 (s, 9H), 1.38 (s, 3H), 1.46 (s, 3H), 1.47 (d, J = 7.2 Hz, 3H), 3.62 (q, J = 7.2 Hz, 1H), 7.20–7.33 (m, 5H); ^{13}C NMR (98.5 MHz, $CDCl_3$) δ 18.2, 20.3, 20.6, 25.1 (3C), 38.5, 47.1, 87.2, 126.9, 127.6 (2C), 128.6 (2C), 141.4, 173.8; Anal. Calcd for $C_{16}H_{24}O_2$: C, 77.38; H, 9.74. Found: C, 77.33; H, 9.86. HRMS (EI^+) *m/z* $[M]^+$ Calcd for $C_{16}H_{24}O_2$: 248.1776; Found 248.1765. $[\alpha]^{25}_D$ +28.4 (*c* 0.76, EtOH).

2,3,3-Trimethylbut-2-yl (*S*)-2-(3,4,5-trifluorophenyl)propionate (Table 5, entry 2)

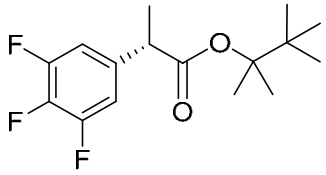

The reaction was carried out according to general procedure B, using 2,3,3-trimethylbut-2-yl 2-chloropropionate (**1e**; 104 mg, 0.5 mmol) and 3,4,5-trifluoro-C_6H_2MgBr (1.08 mL, 0.92 M in THF solution, 2.0 equiv). The title compound (38 mg, 25% yield, 90:10 er) was obtained as a colorless liquid after silica gel column chromatography (hexane/toluene = 90/10).

The er was determined by HPLC on a CHIRALCEL OD-3R column (4.6 mm i.d., 150 mm length) under the following conditions: 50% CH_3CN aq, 1.0 mL/min, 25 °C, retention times (t_r) = 23.4 min (minor) and 25.1 min (major).

FTIR (neat, cm^{-1}) ν 2978, 1727, 1623, 1595, 1461, 1379, 1371, 1178, 1120, 981; ^1H NMR (391.8 MHz, $CDCl_3$) δ 0.88 (s, 9H), 1.41 (s, 3H), 1.44 (d, J = 7.2 Hz, 3H), 1.47 (s, 3H), 3.56 (q, J = 7.2 Hz, 1H), 6.89–6.93 (m, 2H); ^{13}C NMR (98.5 MHz, $CDCl_3$) δ 18.1, 20.4, 20.6, 25.1 (3C), 38.5, 46.4, 88.2, 111.8 (dd, J = 16.0, 5.6 Hz, 2C), 137.4–137.7 (m, 1C), 140.1 (t, J = 15.5 Hz, 1C), 151.2 (ddd, J = 249.9, 9.4, 3.8 Hz, 2C), 172.4; HRMS (FAB^+) *m/z* $[M+Na]^+$ Calcd for $C_{16}H_{21}F_3O_2Na$: 325.1391, Found 325.1392. $[\alpha]^{25}_D$ +13.2 (*c* 1.04, EtOH).

2,3,3-Trimethylbut-2-yl (*S*)-2-(3,4-difluorophenyl)propionate (Table 5, entry 3)

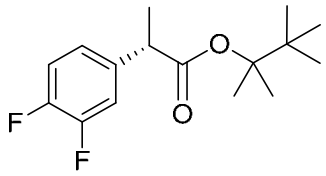

The reaction was carried out according to the general procedure B using 2,3,3-trimethylbut-2-yl 2-chloropropionate (**1e**) (104 mg, 0.50 mmol) and 3,4-difluoro-C_6H_3MgBr (1.01 mL, 0.99 M in THF solution, 2.0 equiv). The title compound (118 mg, 83% yield, 91:9 er) was obtained as a colorless liquid after silica gel column chromatography (hexane/toluene = 70/30).

The er was determined by HPLC on a CHIRALCEL OD-3R (4.6 mm i.d., 150 mm length) with following conditions: 50% CH_3CN aq., 1.0 mL/min, 25 °C, retention times (t_r) = 19.5 min (minor) and 21.3 min (major).

FTIR (neat, cm^{-1}) ν 2979, 1724, 1609, 1519, 1466, 1433, 1379, 1370, 1276, 1178, 1120, 1055, 934; ^1H NMR (391.8 MHz, $CDCl_3$) δ 0.86 (s, 9H), 1.39 (s, 3H), 1.44 (d, *J* = 7.2 Hz, 3H), 1.47 (s, 3H), 3.59 (q, *J* = 7.2 Hz, 1H), 6.97–7.01 (m, 1H), 7.07–7.13 (m, 2H); ^{13}C NMR (98.5 MHz, $CDCl_3$) δ 18.2, 20.3, 20.6, 25.1 (3C), 38.5, 46.3, 87.8, 116.4 (d, *J* = 16.9 Hz, 1C), 117.2 (d, *J* = 16.9 Hz, 1C), 123.6 (m, 1C), 138.3 (t, *J* = 4.7 Hz, 1C), 150.3 (dd, *J* = 249, 12.6 Hz, 1C), 149.4 (dd, *J* = 247, 12.2 Hz, 1C), 173.0; Anal. calcd for $C_{16}H_{22}F_2O_2$: C, 67.59; H, 7.80; F, 13.36. Found: C, 67.80; H, 7.79; F, 13.27. HRMS (EI^+) *m/z* $[M]^+$ Calcd for $C_{16}H_{22}F_2O_2$: 284.1588, Found 284.1577. $[\alpha]^{25}_D$ +24.9 (*c* 0.29, EtOH).

2,3,3-Trimethylbut-2-yl (*S*)-2-(4-fluorophenyl)propionate (Table 5, entry 4)

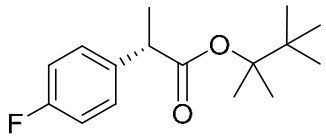

The reaction was carried out according to the General Procedure B using 2,3,3-trimethylbut-2-yl 2-chloropropionate (**1e**) (104 mg, 0.50 mmol) and 4-F-C_6H_4MgBr (0.84 mL, 1.197 M in THF solution, 2.0 equiv). The title compound (115 mg, 87% yield, 91:9 er) was obtained as a colorless liquid after silica gel column chromatography (hexane/toluene = 60/40).

The er was determined by HPLC on a CHIRALCEL OJ-3R (4.6 mm i.d., 150 mm length) with following conditions: 60% CH_3CN aq., 1.0 mL/min, 25 °C, retention times (t_r) = 8.9 min (minor) and 10.0 min (major).

FTIR (neat, cm^{-1}) ν 2977, 1724, 1509, 1466, 1379, 1370, 1224, 1175, 1128, 1054, 838; ^1H NMR (391.8 MHz, $CDCl_3$) δ 0.84 (s, 9H), 1.37 (s, 3H), 1.44 (d, *J* = 7.2 Hz, 3H), 1.46 (s, 3H), 3.61 (q, *J* = 7.2 Hz, 1H), 6.97–7.01 (m, 2H), 7.21–7.26 (m, 2H); ^{13}C NMR (98.5 MHz, $CDCl_3$) δ 18.3, 20.3, 20.6, 25.1 (3C), 38.5, 46.4, 87.4, 115.3 (d, *J* = 20.6 Hz, 2C), 129.1 (d, *J* = 7.5 Hz, 2C), 137.1 (d, *J* = 3.7 Hz, 1C), 161.9 (d, *J* = 245 Hz, 1C), 173.6; Anal. Calcd for $C_{16}H_{23}FO_2$: C, 72.15; H, 8.70; F, 7.13. Found: C, 72.28; H, 8.78; F, 6.87. HRMS (EI^+) *m/z* $[M]^+$ Calcd for $C_{16}H_{23}FO_2$: 266.1682, Found 266.1673. $[\alpha]^{25}_D$ +22.9 (*c* 0.39, EtOH).

2,3,3-Trimethylbut-2-yl (*S*)-2-(4-fluoro-3-methylphenyl)propionate (Table 5, entry 5)

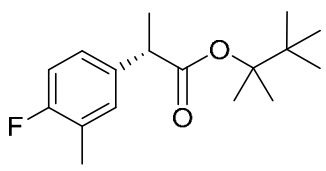

The reaction was carried out according to the General Procedure B using 2,3,3-trimethylbut-2-yl 2-chloropropionate (**1e**) (104 mg, 0.50 mmol) and 4-F-3-Me-C_6H_3MgBr (1.33 mL, 0.75 M in THF solution, 2.0 equiv). The title compound (120

mg, 85% yield, 88:12 er) was obtained as a colorless liquid after silica gel column chromatography (hexane/toluene = 60/40).

The er was determined by HPLC on a CHIRALCEL OJ-3R (4.6 mm i.d., 150 mm length) with following conditions: 60% CH_3CN aq., 1.0 mL/min, 25 °C, retention times (t_r) = 8.9 min (minor) and 10.0 min (major).

FTIR (neat, cm^{-1}) ν 2976, 1724, 1504, 1465, 1465, 1378, 1369, 1245, 1176, 1120, 1057; ^1H NMR (391.8 MHz, $CDCl_3$) δ 0.86 (s, 9H), 1.38 (s, 3H), 1.43 (d, *J* = 7.2 Hz, 3H), 1.46 (s, 3H), 2.25 (s, 3H), 3.57 (q, *J* = 7.2 Hz, 1H), 6.92 (t, *J* = 8.9 Hz, 1H), 7.03–7.06 (m, 1H), 7.08 (d, *J* = 7.2 Hz, 1H); ^{13}C NMR (98.5 MHz, $CDCl_3$) δ 14.6 (d, *J* = 2.8 Hz, 1C), 18.3, 20.3, 20.6, 25.1 (3C), 38.5, 46.3, 87.3, 114.9 (d, *J* = 22.5 Hz, 1C), 124.8 (d, *J* = 17.8 Hz, 1C), 126.3 (d, *J* = 7.5 Hz, 1C), 130.6 (d, *J* = 5.6 Hz, 1C), 136.7 (d, *J* = 3.8 Hz, 1C), 160.4 (d, *J* = 243 Hz, 1C), 173.7; Anal. calcd for $C_{17}H_{25}FO_2$: C, 72.82; H, 8.99; F, 6.78. Found: C, 72.68; H, 9.11; F, 6.70. HRMS (EI^+) *m/z* $[M]^+$ Calcd for $C_{17}H_{25}FO_2$: 280.1839, Found 280.1837. $[\alpha]^{25}_D$ +24.7 (*c* 0.46, EtOH).

2,3,3-Trimethylbut-2-yl (*S*)-2-(3-chloro-4-fluorophenyl)propionate (Table 5, entry 6)

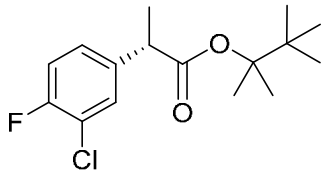

The reaction was carried out according to the General Procedure B using 2,3,3-trimethylbut-2-yl 2-chloropropionate (**1e**) (104 mg, 0.50 mmol) and 3-Cl-4-F-C_6H_3MgBr (2.0 mL, 0.50 M in THF solution, 2.0 equiv). The title compound (125 mg, 83% yield, 91:9 er) was obtained as a colorless liquid after silica gel column chromatography (hexane/toluene = 60/40).

The er was determined by HPLC on a CHIRALCEL OJ-3R (4.6 mm i.d., 150 mm length) with following conditions: 60% CH_3CN aq., 1.0 mL/min, 25 °C, retention times (t_r) = 29.4 min (minor) and 32.6 min (major).

FTIR (neat, cm^{-1}) ν 2977, 1724, 1500, 1465, 1379, 1370, 1247, 1204, 1176, 1126, 1061; ^1H NMR (391.8 MHz, $CDCl_3$) δ 0.86 (s, 9H), 1.39 (s, 3H), 1.44 (d, *J* = 7.2 Hz, 3H), 1.47 (s, 3H), 3.59 (q, *J* = 7.2 Hz, 1H), 7.07 (t, *J* = 8.8 Hz, 1H), 7.12–7.16 (m, 1H), 7.32 (dd, *J* = 7.2, 2.3 Hz, 1H); ^{13}C NMR (98.5 MHz, $CDCl_3$) δ 18.2, 20.3, 20.6, 25.1 (3C), 38.5, 46.2, 87.9, 116.5 (d, *J* = 21.6 Hz, 1C), 120.9 (d, *J* = 17.8 Hz, 1C), 127.3 (d, *J* = 6.6 Hz, 1C), 129.8, 138.3 (d, *J* = 3.8 Hz, 1C), 157.2 (d, *J* = 248 Hz, 1C), 173.0; Anal. Calcd for $C_{16}H_{22}ClFO_2$: C, 63.89; H, 7.37; F, 6.32; Cl, 11.79. Found: C, 63.99; H, 7.35; F, 6.37; Cl, 11.89. HRMS (EI^+) *m/z* $[M]^+$ Calcd for $C_{16}H_{22}ClFO_2Na$: 323.1190, Found 323.1203. $[\alpha]^{25}_D$ +18.3 (*c* 0.34, EtOH).

2,3,3-Trimethylbut-2-yl (*S*)-2-(3,4-dichlorophenyl)propionate (Table 5, entry 7)

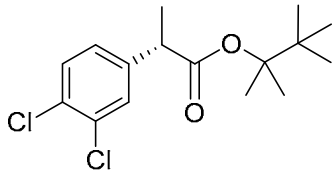

The reaction was carried out according to the General Procedure B using 2,3,3-trimethylbut-2-yl 2-chloropropionate (**1e**) (104 mg, 0.50 mmol) and 3,4-dichloro-C_6H_3MgBr (2.0 mL, 0.50 M in THF solution, 2.0 equiv). The title compound (140 mg, 88% yield, 90:10 er) was obtained as a colorless liquid after silica gel column chromatography (hexane/toluene = 60/40).

The er was determined by HPLC on a CHIRALCEL OD-3R (4.6 mm i.d., 150 mm length) with following conditions: 55% CH_3CN aq., 1.0 mL/min, 25 °C, retention times (t_r) = 22.3 min (minor) and 25.0 min (major).

FTIR (neat, cm^{-1}) ν 2976, 1724, 1467, 1378, 1370, 1206, 1176, 1127, 1031, 846; ^1H NMR (391.8 MHz, $CDCl_3$) δ 0.86 (s, 9H), 1.39 (s, 3H), 1.44 (d, *J* = 7.2 Hz, 3H), 1.47 (s, 3H), 3.59 (q, *J* = 7.2 Hz, 1H), 7.11 (dd, *J* = 8.3, 2.0 Hz, 1H), 7.37–7.39 (m, 2H); ^{13}C NMR (98.5 MHz, $CDCl_3$) δ 18.1, 20.4, 20.6, 25.2 (3C), 38.5, 46.3, 88.0, 127.1, 129.7, 130.5, 131.0, 132.6, 141.4, 172.7; Anal. Calcd for $C_{16}H_{22}Cl_2O_2$: C, 60.58; H, 6.99; Cl, 22.35. found C, 60.63; H, 7.01; Cl, 22.10. HRMS (FAB^+) *m/z* $[M]^+$ Calcd for $C_{16}H_{22}Cl_2O_2$: 316.0997, 318.0970, Found 316.0982, 318.0967. $[\alpha]^{25}_D$ +18.9 (*c* 0.27, EtOH).

2,3,3-Trimethylbut-2-yl (*S*)-2-[4-(2-methylpropyl)phenyl]propionate (Table 5, entry 8)

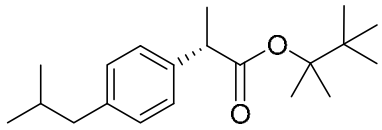

The reaction was carried out according to the General Procedure B using 2,3,3-trimethylbut-2-yl 2-chloropropionate (**1e**) (620 mg, 3.0 mmol) and [4-(2-methylpropyl)phenyl]magnesium bromide (7.07 mL, 0.846 M in THF solution, 2.0 equiv). The title compound was obtained as a colorless liquid (690 mg, 75% yield, 87:13 er).

The er was determined by HPLC on a CHIRALCEL OJ-3R (4.6 mm i.d., 150 mm length) with following conditions: 60% CH_3CN aq., 1.0 mL/min, 25 °C, retention times (t_r) = 18.3 min (minor) and 19.4 min (major).

FTIR (neat, cm^{-1}) ν 2956, 1726, 1464, 1377, 1369, 1205, 1173, 1128, 939, 849, 787, 557, 517; ^1H NMR (500 MHz, $CDCl_3$) δ 0.81 (s, 9H), 0.87 (s, 3H), 0.88 (s, 3H), 1.37 (s, 3H), 1.45 (s, 3H), 1.45 (d, *J* = 6.9 Hz, 3H), 1.78–1.87 (m, 1H), 2.44 (d, *J* = 6.9 Hz, 2H), 3.60 (q, *J* = 6.9 Hz, 1H), 7.05–7.09 (m, 2H), 7.14–7.18 (m, 2H); ^{13}C NMR (125 MHz, $CDCl_3$) δ 18.0, 20.2, 20.4, 22.27, 22.28, 24.9, 30.2, 38.3, 45.0, 46.6, 86.9, 127.2, 129.1, 138.6, 140.1, 173.9; Anal. Calcd for $C_{20}H_{32}O_2$: C, 78.89; H, 10.59. Found: C, 78.77; H, 10.59. HRMS (ES^+) *m/z* $[M+H]^+$ Calcd for $C_{20}H_{33}O_2$: 305.2481, Found 305.2475. $[\alpha]^{25}_D$ +21.6 (*c* 0.22, EtOH).

2,3,3-Trimethylbut-2-yl (*S*)-2-(4-(but-3-en-1-yl)phenyl)propionate (Table 5, entry 9)

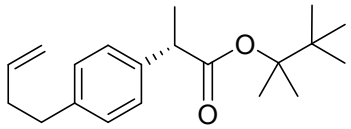

The reaction was carried out according to the General Procedure B using 2,3,3-trimethylbut-2-yl 2-chloropropionate (**1e**) (104 mg, 0.50 mmol) and 4-(but-3-en-1-yl)-C_6H_4MgBr (1.1 mL, 0.91 M in THF solution, 2.0 equiv). The title compound (140 mg, 92% yield, 86:14 er) was obtained as a colorless liquid after silica gel column chromatography (hexane/toluene = 60/40).

The er was determined by HPLC on a CHIRALCEL OJ-3R (4.6 mm i.d., 150 mm length) with following conditions: 60% CH_3CN aq., 1.0 mL/min, 25 °C, retention times (t_r) = 13.0 min (minor) and 26.2 min (major).

FTIR (neat, cm^{-1}) ν 2978, 2933, 2877, 1725, 1514, 1455, 1378, 1369, 1208, 1172, 1129, 1054, 910; ^1H NMR (391.8 MHz, $CDCl_3$) δ 0.84 (s, 9H), 1.38 (s, 3H), 1.44 (d, *J* = 7.2 Hz, 3H), 1.46 (s, 3H), 2.31–2.37 (m, 2H), 2.67 (t, *J* = 7.6 Hz, 2H), 3.59 (q, *J* = 7.2 Hz, 1H), 4.94–5.04 (m, 2H), 5.78–5.87 (m, 1H), 7.11 (d, *J* = 8.1Hz, 2H), 7.18 (d, *J* = 8.1 Hz, 2H); ^{13}C NMR (98.5 MHz, $CDCl_3$) δ 18.2, 20.3, 20.6, 25.1 (3C), 35.1, 35.6, 38.5, 46.7, 87.1, 115.0, 127.5 (2C), 128.6 (2C), 138.2, 138.9, 140.4, 174.0; Anal. Calcd for $C_{20}H_{30}O_2$: C, 79.42; H, 10.00. Found: C, 79.35; H, 10.01. HRMS (FAB^+) *m/z* $[M+H]^+$ Calcd for $C_{20}H_{31}O_2$: 303.2324, found 303.2332. $[\alpha]^{25}_D$ +24.1 (*c* 0.53, EtOH).

2,3,3-Trimethylbut-2-yl (*S*)-2-[(1,1'-biphenyl)-4-yl]propionate (Table 5, entry 10)

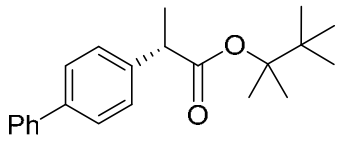

The reaction was carried out according to the general procedure using 2,3,3-trimethylbut-2-yl 2-chloropropionate (**1e**) (104 mg, 0.50 mmol) and 4-Ph-C_6H_4MgBr (0.94 mL, 1.06 M in THF solution, 2.0 equiv). The title compound (146 mg, 90% yield, 86:14 er) was obtained as a white solid after silica gel column chromatography (hexane/toluene = 50/50).

The er was determined by HPLC on a CHIRALCEL OJ-3R (4.6 mm i.d., 150 mm length) with following conditions: 70% CH_3CN aq., 1.0 mL/min, 25 °C, retention times (t_r) = 10.0 min (minor) and 15.9 min (major).

Mp 38–39 °C; FTIR (neat, cm^{-1}) ν 2974, 1721, 1485, 1375, 1368, 1207, 1175, 1128, 1036, 848; ^1H NMR (391.8 MHz, $CDCl_3$) δ 0.86 (s, 9H), 1.40 (s, 3H), 1.48 (s, 3H), 1.50 (d, *J* = 7.2 Hz, 3H), 3.67 (q, *J* = 7.2 Hz, 1H), 7.31–7.35 (m, 3H), 7.41 (t, *J* = 7.6 Hz, 2H), 7.53–7.59 (m, 4H); ^{13}C NMR (98.5 MHz, $CDCl_3$) δ 18.2, 20.4, 20.6, 25.2 (3C), 38.5, 46.8, 87.3, 127.1 (2C), 127.3 (3C), 128.0 (2C), 128.8 (2C), 139.8, 140.5, 141.0, 173.8; Anal. Calcd for $C_{22}H_{28}O_2$: C, 81.44; H, 8.70. Found: C, 81.45; H, 8.78. HRMS (FAB^+) *m/z* $[M]^+$ Calcd

for $C_{22}H_{28}O_2$: 324.2089, Found 324.2087. $[\alpha]^{25}_D$ +15.0 (*c* 1.01, EtOH).

2,3,3-Trimethylbut-2-yl (*S*)-2-(4-(dimethylamino)phenyl)propionate (Table 5, entry 11)

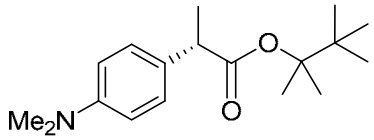

The reaction was carried out according to the General Procedure B using 2,3,3-trimethylbut-2-yl 2-chloropropionate (**1e**) (104 mg, 0.50 mmol) and 4-Me_2N-C_6H_4MgBr (1.08 mL, 0.923 M in THF solution, 2.0 equiv). The title compound (114 mg, 78% yield, 88:12 er) was obtained as a colorless liquid after silica gel column chromatography (hexane/EtOAc = 90/10).

The er was determined by HPLC on a CHIRALCEL OJ-3R (4.6 mm i.d., 150 mm length) with following conditions: 60% CH_3CN aq., 1.0 mL/min, 25 °C, retention times (t_r) = 15.4 min (minor) and 17.9 min (major).

FTIR (neat, cm^{-1}) ν 2973, 2877, 1722, 1520, 1465, 1464, 1377, 1368, 1346, 1229, 1170, 1127, 1055, 946; ^1H NMR (391.8 MHz, $CDCl_3$) δ 0.88 (s, 9H), 1.38 (s, 3H), 1.42 (d, *J* = 7.2 Hz, 3H), 1.46 (s, 3H), 2.91 (s, 6H), 3.53 (q, *J* = 7.2 Hz, 1H), 6.70 (d, *J* = 8.9 Hz, 2H), 7.15 (d, *J* = 8.9 Hz, 2H); ^{13}C NMR (98.5 MHz, $CDCl_3$) δ 18.3, 20.4, 20.6, 25.2 (3C), 38.5, 40.8 (2C), 46.1, 86.8, 112.9 (2C), 128.2 (2C), 129.4, 149.7, 174.5; Anal. Calcd for $C_{18}H_{29}NO_2$: C, 74.18; H, 10.03; N, 4.81. Found: C, 74.05; H, 10.31; N, 4.52. HRMS (FAB^+) *m/z* $[M]^+$ Calcd for $C_{18}H_{29}NO_2$: 291.2198, Found 291.2194. $[\alpha]^{25}_D$ +21.5 (*c* 0.35, EtOH).

2,3,3-Trimethylbut-2-yl (*S*)-2-(4-methoxyphenyl)propionate (Table 5, entry 12)

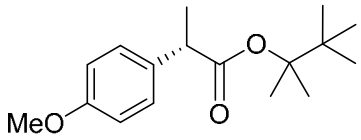

The reaction was carried out according to the General Procedure B using 2,3,3-trimethylbut-2-yl 2-chloropropionate (**1e**) (104 mg, 0.50 mmol) and 4-MeO-C_6H_4MgBr (0.95 mL, 1.05 M in THF solution, 2.0 equiv). The title compound (110 mg, 78% yield, 88:12 er) was obtained as a colorless oil after silica gel column chromatography (hexane/toluene = 50/50).

The er was determined by HPLC on a CHIRALCEL OJ-3R (4.6 mm i.d., 150 mm length) with following conditions: 60% CH_3CN aq., 1.0 mL/min, 25 °C, retention times (t_r) = 10.0 min (minor) and 12.2 min (major).

FTIR (neat, cm^{-1}) ν 2974, 1722, 1512, 1465, 1378, 1369, 1245, 1176, 1127, 1036, 833; ^1H NMR (391.8 MHz, $CDCl_3$) δ 0.86 (s, 9H), 1.38 (s, 3H), 1.43 (d, *J* = 7.2 Hz, 3H), 1.46 (s, 3H), 3.58 (q, *J* = 7.2 Hz, 1H), 3.79 (s, 3H), 6.84 (d, *J* = 6.7 Hz, 2H), 7.19 (d, *J* = 6.7 Hz, 2H); ^{13}C NMR (98.5 MHz, $CDCl_3$) δ 18.3, 20.3, 20.6, 25.2 (3C), 38.5, 46.2, 55.4,

87.1, 113.9 (2C), 128.6 (2C), 133.6, 158.6, 174.1; Anal. Calcd for $C_{17}H_{26}O_3$: C, 73.35; H, 9.41. Found: C, 73.31; H, 9.60. HRMS (FAB$^+$) *m/z* $[M]^+$ Calcd for $C_{17}H_{26}O_3$: 278.1882, Found: 278.1886. $[\alpha]^{25}_D$ +21.8 (*c* 0.99, EtOH).

2,3,3-Trimethylbut-2-yl (*S*)-2-(3-methoxyphenyl)propionate (Table 5, entry 13)

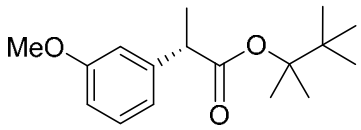

The reaction was carried out according to the General Procedure B using 2,3,3-trimethylbut-2-yl 2-chloropropionate (**1e**) (104 mg, 0.50 mmol) and 3-MeO-C_6H_4MgBr (0.98 mL, 1.02 M in THF solution, 2.0 equiv). The title compound (98 mg, 70% yield, 89:11 er) was obtained as a colorless liquid after silica gel column chromatography (hexane/toluene = 50/50).

The er was determined by HPLC on a CHIRALCEL OJ-3R (4.6 mm i.d., 150 mm length) with following conditions: 50% CH_3CN aq., 1.0 mL/min, 25 °C, retention times (t_r) = 13.7 min (minor) and 17.4 min (major).

FTIR (neat, cm^{-1}) ν 2974, 1723, 1600, 1585, 1465, 1455, 1378, 1370, 1259, 1178, 1128, 1045, 848; ^1H NMR (391.8 MHz, $CDCl_3$) δ 0.85 (s, 9H), 1.39 (s, 3H), 1.45 (d, *J* = 7.2 Hz, 3H), 1.47 (s, 3H), 3.60 (q, *J* = 7.2 Hz, 1H), 3.79 (s, 3H), 6.78 (dd, *J* = 7.8, 0.8 Hz, 1H), 6.82 (t, *J* = 2.1 Hz, 1H), 6.86 (d, *J* = 7.8 Hz, 1H), 7.21 (t, *J* = 7.8 Hz, 1H); ^{13}C NMR (98.5 MHz, $CDCl_3$) δ 18.2, 20.3, 20.6, 25.1 (3C), 38.5, 47.1, 55.3, 87.2, 112.4, 113.2, 120.0, 129.5, 142.9, 159.8, 173.7; Anal. Calcd for $C_{17}H_{26}O_3$: C, 73.35; H, 9.41. Found: C, 73.19; H, 9.55. HRMS (FAB$^+$) *m/z* $[M]^+$ Calcd for $C_{17}H_{26}O_3$: 278.1882, Found 278.1883. $[\alpha]^{25}_D$ +22.5 (*c* 0.39, EtOH).

2,3,3-Trimethylbut-2-yl (*S*)-2-(4-tolyl)propionate (Table 5, entry 15)

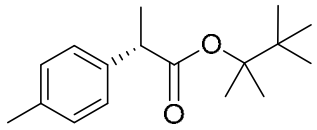

The reaction was carried out according to the General Procedure B using 2,3,3-trimethylbut-2-yl 2-chloropropionate (**1e**) (104 mg, 0.50 mmol) and 4-Me-C_6H_4MgBr (0.97 mL, 1.03 M in THF solution, 2.0 equiv). The title compound (120 mg, 89% yield, 87:13 er) was obtained as a colorless liquid after silica gel column chromatography (hexane/toluene = 60/40).

The er was determined by HPLC on a CHIRALCEL OJ-3R (4.6 mm i.d., 150 mm length) with following conditions: 60% CH_3CN aq., 1.0 mL/min, 25 °C, retention times (t_r) = 12.5 min (minor) and 19.3 min (major).

FTIR (neat, cm^{-1}) ν 2973, 1725, 1514, 1465, 1378, 1369, 1203, 1172, 1128, 1054, 936; ^1H NMR (391.8 MHz, $CDCl_3$) δ 0.85 (s, 9H), 1.38 (s, 3H), 1.44 (d, *J* = 7.2 Hz, 3H), 1.46 (s, 3H), 2.31 (s, 3H), 3.59 (q, *J* = 7.2 Hz, 1H), 7.10 (d, *J* = 8.1Hz, 2H), 7.16 (d, *J* = 8.1

Hz, 2H); ^{13}C NMR (98.5 MHz, $CDCl_3$) δ 18.3, 20.3, 20.6, 21.2, 25.2 (3C), 38.5, 46.7, 87.1, 127.5 (2C), 129.2 (2C), 136.4, 138.4, 174.0; Anal. Calcd for $C_{17}H_{26}O_2$: C, 77.82; H, 9.99. Found: C, 77.47; H, 10.09. HRMS (EI$^+$) *m/z* $[M]^+$ Calcd for $C_{17}H_{26}O_2$: 262.1933, Found 262.1922. $[\alpha]^{25}_D$ +24.9 (*c* 0.47, EtOH).

2,3,3-Trimethylbut-2-yl (*S*)-2-(3-tolyl)propionate (Table 5, entry 16)

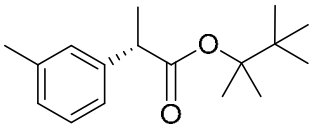

The reaction was carried out according to the General Procedure B using 2,3,3-trimethylbut-2-yl 2-chloropropionate (**1e**) (104 mg, 0.50 mmol) and 3-Me-C_6H_4MgBr (1.28 mL, 0.78 M in THF solution, 2.0 equiv). The title compound (111 mg, 84% yield, 88:12 er) was obtained as a colorless liquid after silica gel column chromatography (hexane/toluene = 60/40).

The er was determined by HPLC on a CHIRALCEL OD-3R (4.6 mm i.d., 150 mm length) with following conditions: 55% CH_3CN aq., 1.0 mL/min, 25 °C, retention times (t_r) = 45.9 min (minor) and 48.6 min (major).

FTIR (neat, cm^{-1}) ν 2973, 1725, 1514, 1465, 1378, 1369, 1240, 1178, 1128, 1056, 939; ^{1}H NMR (391.8 MHz, $CDCl_3$) δ 0.85 (s, 9H), 1.38 (s, 3H), 1.44 (d, *J* = 7.2 Hz, 3H), 1.46 (s, 3H), 2.33 (s, 3H), 3.59 (q, *J* = 7.2 Hz, 1H), 7.02–7.08 (m, 3H), 7.18 (t, *J* = 7.6 Hz, 1H); ^{13}C NMR (98.5 MHz, $CDCl_3$) δ 18.2, 20.3, 20.6, 21.5, 25.1 (3C), 38.5, 47.0, 87.1, 124.6, 127.6, 128.4 (2C), 138.0, 141.3, 173.9; HRMS (EI$^+$) *m/z* $[M]^+$ Calcd for $C_{17}H_{26}O_2$: 262.1933, found 262.1925. $[\alpha]^{25}_D$ +26.9 (*c* 0.38, EtOH).

2,3,3-Trimethylbut-2-yl (*S*)-2-(2-tolyl)propionate (Table 5, entry 17)

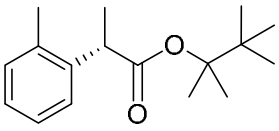

The reaction was carried out according to the General Procedure B using 2,3,3-trimethylbut-2-yl 2-chloropropionate (**1e**) (104 mg, 0.5 mmol) and 2-Me-C_6H_4MgBr (1.1 mL, 0.905 M in THF solution, 2.0 equiv). The title compound (70 mg, 38% yield, 84:16 er) was obtained as a colorless liquid after silica gel column chromatography (hexane/toluene = 60/40).

The er was determined by HPLC on a CHIRALCEL OD-3R (4.6 mm i.d., 150 mm length) with following conditions: 55% CH_3CN aq., 1.0 mL/min, 25 °C, retention times (t_r) = 16.0 min (minor) and 17.1 min (major).

FTIR (neat, cm^{-1}) ν 2974, 1724, 1465, 1378, 1369, 1240, 1178, 1128, 1056, 939; ^{1}H NMR (391.8 MHz, $CDCl_3$) δ 0.78 (s, 9H), 1.39 (s, 3H), 1.44 (d, *J* = 7.2 Hz, 3H), 1.47 (s, 3H), 2.35 (s, 3H), 3.85 (q, *J* = 7.2 Hz, 1H), 7.09–7.19 (m, 3H), 7.23 (t, *J* = 7.6 Hz, 1H); ^{13}C NMR (98.5 MHz, $CDCl_3$) δ 17.7, 19.8, 20.2, 20.6, 25.0 (3C), 38.4, 42.9, 87.1, 126.3, 126.5, 126.7, 130.4, 135.6, 140.0, 174.1; Anal. calcd for $C_{17}H_{26}O_2$ C, 77.82; H, 9.99.

Found: C, 77.52; H, 9.94. HRMS (FAB$^+$) *m/z* [M+Na]$^+$ Calcd for $C_{17}H_{26}O_2Na$: 285.1830, found 285.1833. $[\alpha]^{25}_D$ +37.7 (*c* 1.01, EtOH).

2,3,3-Trimethylbutan-2-yl (*S*)-2-(6-methoxynaphth-2-yl)propionate (Table 5, entry 18)

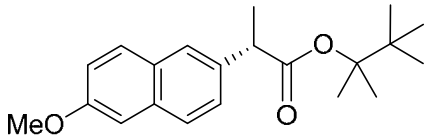

The reaction was carried out according to general procedure B: 6-methoxy-2-naphthylmagnesium bromide (13.0 mL, 0.46 M in THF solution, 2.0 equiv) was slowly added over 90 min using a syringe pump, to a THF solution (4.0 mL) of$Fe(acac)_3$ (31.8 mg, 3 mol%), (*R*,*R*)-BenzP* (51 mg, 6 mol%), and 3,3-trimethylbut-2-yl-2-chloropropionate (**1e**; 620 mg, 3.0 mmol) at 0 °C. The title compound (852 mg, 79% yield, 87:13 er) was obtained as a colorless liquid after silica gel column chromatography (hexane/toluene = 50/50).

The er was determined by HPLC on a CHIRALCEL OD-3R column (4.6 mm i.d., 150 mm length) under the following conditions: 50% CH_3CN aq, 1.0 mL/min, 25 °C, retention times (t_r) = 42.2 min (minor) and 46.5 min (major).

FTIR (neat, cm^{-1}) ν 2975, 2877, 1720, 1606, 1483, 1463, 1378, 1369, 1263, 1194, 1174, 1127, 1032, 927; ^{1}H NMR (391.8 MHz, $CDCl_3$) δ 0.83 (s, 9H), 1.38 (s, 3H), 1.47 (s, 3H), 1.53 (d, *J* = 7.2 Hz, 3H), 3.76 (q, *J* = 7.2 Hz, 1H), 3.88 (s, 3H), 7.09–7.13 (m, 2H), 7.38 (dd, *J* = 8.5, 1.8 Hz, 1H), 7.67 (t, *J* = 10.0 Hz, 3H); ^{13}C NMR (98.5 MHz, $CDCl_3$) δ 18.3, 20.3, 20.6, 25.1 (3C), 38.5, 47.0, 55.3, 87.3, 105.7, 118.9, 125.9, 126.5, 127.0, 129.1, 129.3, 133.6, 136.5, 157.6, 173.9; HRMS (FAB$^+$) *m/z* [M]$^+$ Calcd for $C_{21}H_{28}O_3$: 328.2038, Found 328.2031. $[\alpha]^{25}_D$ +19.4 (*c* 1.00, EtOH).

2,3,3-Trimethylbut-2-yl (*S*)-2-(naphth-2-yl)propionate (Table 5, entry 19)

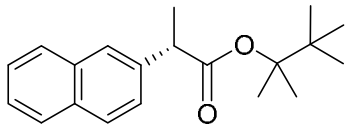

The reaction was carried out according to the General Procedure B using 2,3,3-trimethylbut-2-yl 2-chloropropionate (**1e**) (104 mg, 0.5 mmol) and 2-naphthyl magnesium bromide (1.16 mL, 0.862 M in THF solution, 2.0 equiv). The title compound (145 mg, 90% yield, 88:12 er) was obtained as a colorless liquid after silica gel column chromatography (hexane/toluene = 60/40).

The er was determined by HPLC on a CHIRALCEL OD-3R (4.6 mm i.d., 150 mm length) with following conditions: 65% CH_3CN aq., 1.0 mL/min, 25 °C, retention times (t_r) = 10.1 min (minor) and 11.6 min (major)

FTIR (neat, cm^{-1}) ν 2975, 2877, 1725, 1465, 1454, 1378, 1369, 1173, 1128, 1064, 939, 848; ^{1}H NMR (391.8 MHz, $CDCl_3$) δ 0.83 (s, 9H), 1.38 (s, 3H), 1.47 (s, 3H), 1.55 (d, *J* =

7.2 Hz, 3H), 3.80 (q, *J* = 7.2 Hz, 1H), 7.40–7.45 (m, 3H), 7.72 (s, 1H), 7.78–7.81 (m, 3H); ^{13}C NMR (98.5 MHz, $CDCl_3$) δ 18.3, 20.3, 20.6, 25.1 (3C), 38.5, 47.2, 87.4, 125.7, 126.0, 126.1, 126.2, 127.7, 127.9, 128.2, 132.6, 133.6, 138.8, 173.8; Anal. Calcd for $C_{20}H_{26}O_2$: C, 80.50; H, 8.78. Found: C, 80.21; H, 8.67. HRMS (FAB$^+$) *m/z* $[M]^+$ Calcd for $C_{20}H_{26}O_2$: 298.1933, Found 298.1944. $[\alpha]^{25}_D$ +23.2 (*c* 1.02, EtOH).

2,3,3-Trimethylbut-2-yl (*S*)-2-(naphth-1-yl)propionate (Table 5, entry 20)

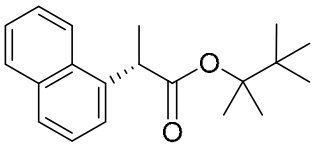

The reaction was carried out according to the General Procedure B using 2,3,3-trimethylbut-2-yl 2-chloropropionate (**1e**) (207 mg, 1.0 mmol) and 1-naphthylmagnesium bromide (5.4 mL, 0.37 M in THF solution, 2.0 equiv). The title compound was obtained as a colorless liquid (91 mg, 31% yield, 58:42 er).

The er was determined by HPLC on a CHIRALCEL OD-3R (4.6 mm i.d., 150 mm length) with following conditions: 60% CH_3CN aq., 1.0 mL/min, 25 °C, retention times (t_r) = 42.2 min (minor) and 46.5 min (major)

FTIR (neat, cm^{-1}) ν 2976, 1718, 1464, 1377, 1321, 1238, 1176, 1126, 1093, 1049, 939, 849, 777, 548, 438; ^{1}H NMR (500 MHz, $CDCl_3$) δ 0.63 (s, 9H), 1.37 (s, 3H), 1.42 (s, 3H), 1.65 (d, *J* = 7.4 Hz, 3H), 4.37 (q, *J* = 7.4 Hz, 1H), 7.41–7.52 (m, 4H), 7.72–7.76 (m, 1H), 7.82–7.86 (m, 1H), 8.08 (d, *J* = 8.9 Hz, 1H); ^{13}C NMR (125 MHz, $CDCl_3$) δ 17.6, 20.1, 20.3, 24.7, 38.1, 43.2, 87.2, 123.4, 124.4, 125.4, 126.0, 127.4, 128.8, 131.5, 133.9, 137.5, 174.2; HRMS (ES$^+$) *m/z* $[M+H]^+$ Calcd for $C_{20}H_{27}O_2$: 299.2011, Found 299.2000. $[\alpha]^{25}_D$ +14.7 (*c* 0.13, EtOH).

2,3,3-Trimethylbut-2-yl (*S*)-3-methoxy-2-phenylpropionate (Table 5, entry 22)

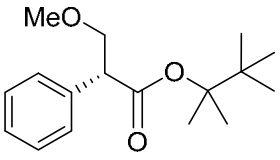

The title compound was synthesized according to General Procedure B using 2,2,3-trimethylbut-2-yl 2-chloro-3-methoxypropionate (237 mg, 1.00 mmol) and PhMgBr (1.82 mL, 1.10 M solution in THF, 2.0 equiv). The product was obtained as a colorless liquid (118 mg, 42%, 77:23 er).

The er was determined by HPLC on a CHIRALCEL OD-3R (4.6 mm i.d., 150 mm length) with following conditions: 40% CH_3CN aq., 1.0 mL/min, 25 °C, retention times (t_r) = 42.0 min (minor), 44.6 min (major).

FTIR (neat, cm^{-1}) ν 2978, 2922, 2879, 1724, 1454, 1379, 1369, 1275, 1255, 1173, 1120, 1024, 970, 937, 847, 735, 698, 515; ^{1}H NMR (500 MHz, $CDCl_3$) δ 0.87 (s, 9H), 1.39 (s, 3H), 1.49 (s, 3H), 3.36 (s, 3H), 3.60 (dd, *J* = 8.9, 6.0 Hz, 1H), 3.80 (dd, *J* = 8.9, 6.0 Hz, 1H), 3.96 (dd, *J* = 8.9, 8.9 Hz, 1H), 7.23–7.33 (m, 5H); ^{13}C NMR (125 MHz, $CDCl_3$) δ

20.2, 20.6, 25.1, 38.3, 53.3, 59.0, 87.7, 127.3, 128.0, 128.6, 136.8, 171.3; HRMS (ES) *m/z* $[M+H]^+$ Cacld for $C_{17}H_{27}O_3$: 279.1960; Found 279.1966. $[\alpha]^{25}_D$ +12.1 (*c* 0.54, EtOH).

2,3,3-Trimethylbut-2-yl (*S*)-2-phenylbutyrate (Table 5, entry 23)

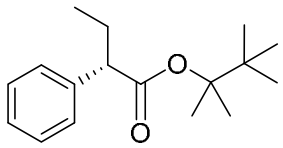

The title compound was synthesized according to General Procedure B using 2,2,3-trimethylbut-2-yl 2-chlorobutyrate (221 mg, 1.00 mmol) and PhMgBr (1.82 mL, 1.10 M solution in THF, 2.0 equiv). The product was obtained as a colorless liquid (177 mg, 67%, 88:12 er).

The er was determined by HPLC on a CHIRALCEL OD-3R (4.6 mm i.d., 150 mm length) with following conditions: 50% CH_3CN aq., 1.0 mL/min, 25 °C, retention times (t_r) = 22.1 min (minor), 24.0 min (major).

FTIR (neat, cm^{-1}) ν 2964, 2877, 1724, 1454, 1379, 1369, 1273, 1200, 1173, 1128, 1076, 939, 845, 735, 698, 515; ^1H NMR (500 MHz, $CDCl_3$) δ 0.87 (s, 9H), 0.90 (t, *J* = 7.4 Hz, 3H), 1.38 (s, 3H), 1.46 (s, 3H), 1.72–1.81 (m, 1H), 2.04–2.13 (m, 1H), 3.36 (t, *J* = 7.4 Hz, 1H), 7.20–7.32 (m, 5H); ^{13}C NMR (125 MHz, $CDCl_3$) δ 12.2, 20.2, 20.5, 25.0, 26.1, 38.3, 55.0, 87.1, 126.8, 127.9, 128.4, 139.8, 173.2; HRMS (ES^+) *m/z* $[M+H]^+$ Cacld for $C_{17}H_{27}O_2$: 263.2011; Found 263.2021. $[\alpha]^{25}_D$ +22.7 (*c* 0.29, EtOH).

2,3,3-Trimethylbut-2-yl (*S*)-2-(4-fluorophenyl)butyrate (Table 5, entry 24)

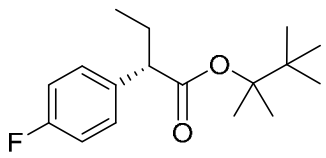

The title compound was synthesized according to General Procedure B using 2,2,3-trimethylbut-2-yl 2-chlorobutyrate (221 mg, 1.00 mmol) and (4-F-C_6H_4)MgBr (1.82 mL, 1.10 M solution in THF, 2.0 equiv). The product was obtained as a colorless liquid (197 mg, 69%, 90:10 er).

The er was determined by HPLC on a CHIRALCEL OD-3R (4.6 mm i.d., 150 mm length) with following conditions: 50% CH_3CN aq., 1.0 mL/min, 25 °C, retention times (t_r) = 23.3 min (minor), 25.7 min (major).

FTIR (neat, cm^{-1}) ν 2966, 1724, 1508, 1464, 1379, 1369, 1273, 1225, 1174, 1126, 1078, 839, 812, 781, 525; ^1H NMR (500 MHz, $CDCl_3$) δ 0.88 (s, 9H), 0.89 (t, *J* = 7.4 Hz, 3H), 1.38 (s, 3H), 1.46 (s, 3H), 1.68–1.77 (m, 1H), 2.01–2.11 (m, 1H), 3.34 (t, *J* = 7.4 Hz, 1H), 6.96–7.02 (m, 2H), 7.21–7.27 (m, 2H); ^{13}C NMR (125 MHz, $CDCl_3$) δ 12.1, 20.2, 20.5, 25.0, 26.1, 38.3, 42.0, 54.2, 87.3, 115.2 (d, *J* = 21.4 Hz), 129.4 (d, *J* = 8.1 Hz), 135.5 (d, *J* = 3.5 Hz), 161.8 (d, *J* = 245 Hz), 173.0; HRMS (FAB^+) *m/z* $[M+H]^+$ Cacld for $C_{17}H_{26}FO_2$: 281.1917; Found 281.1919. $[\alpha]^{25}_D$ +20.2 (*c* 1.00, EtOH).

2,3,3-Trimethylbut-2-yl (*S*)-2-(4-methoxyphenyl)butyrate (Table 5, entry 25)

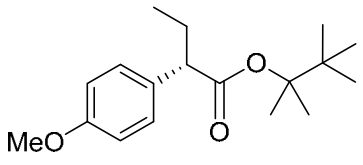

The title compound was synthesized according to General Procedure B using 2,2,3-trimethylbut-2-yl 2-chlorobutyrate (221 mg, 1.00 mmol) and (4-MeO-C_6H_4)MgBr (2.16 mL, 0.927 M solution in THF, 2.0 equiv). The product was obtained as a colorless liquid (116 mg, 42%, 88:12 er).

The er was determined by HPLC on a CHIRALCEL OD-3R (4.6 mm i.d., 150 mm length) with following conditions: 50% CH_3CN aq., 1.0 mL/min, 25 °C, retention times (t_r) = 21.8 min (minor), 23.4 min (major).

FTIR (neat, cm^{-1}) ν 2964, 2877, 1722, 1610, 1511, 1461, 1376, 1369, 1247, 1174, 1126, 1036, 939, 831, 808, 781, 532; ^1H NMR (500 MHz, $CDCl_3$) δ 0.86–0.92 (m, 12H), 1.39 (s, 3H), 1.45 (s, 3H), 1.68–1.77 (m, 1H), 2.00–2.10 (m, 1H), 3.30 (t, *J* = 7.4 Hz, 1H), 3.79 (s, 3H), 6.82–6.86 (m, 2H), 7.19–7.22 (m, 2H); ^{13}C NMR (125 MHz, $CDCl_3$) δ 12.2, 20.2, 20.5, 25.1, 26.2, 38.3, 54.2, 55.2, 87.0, 113.8, 128.8, 131.9, 158.5, 173.5; HRMS (ES^+) *m/z* $[M+H]^+$ Cacld for $C_{18}H_{29}O_2$: 293.2117; Found 293.2137. $[\alpha]^{25}_D$ +19.4 (*c* 0.20, EtOH).

2,3,3-Trimethylbut-2-yl (*S*)-4-methyl-2-phenylpentanoate (Table 5, entry 26)

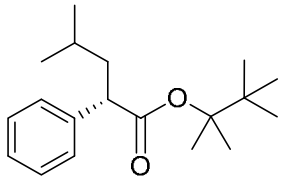

The title compound was synthesized according to General Procedure B using 2,2,3-trimethylbut-2-yl 2-chloro-4-methylpentanoate (249 mg, 1.00 mmol) and PhMgBr (1.82 mL, 1.10 M solution in THF, 2.0 equiv). The product was obtained as a colorless liquid (109 mg, 38%, 74:26 er).

The er was determined by HPLC on two columns of CHIRALCEL OD-3R (4.6 mm i.d., 150 mm length) with following conditions: 50% CH_3CN aq., 1.0 mL/min, 25 °C, retention times (t_r) = 76.5 min (minor), 80.0 min (major).

FTIR (neat, cm^{-1}) ν 2956, 2872, 1724, 1466, 1454, 1377, 1369, 1273, 1171, 1128, 937, 847, 733, 698, 517; ^1H NMR (500 MHz, $CDCl_3$) δ 0.87 (s, 9H), 0.91 (d, *J* = 6.9 Hz, 6H), 1.37 (s, 3H), 1.45 (s, 3H), 1.46–1.53 (m, 1H), 1.59–1.65 (m, 1H), 1.92–1.99 (m, 1H), 3.56 (t, *J* = 7.4 Hz, 1H), 7.20–7.32 (m, 5H); ^{13}C NMR (125 MHz, $CDCl_3$) δ 20.2, 20.4, 22.4, 22.6, 25.0, 25.8, 38.3, 41.9, 51.1, 87.1, 126.8, 127.9, 128.4, 140.0, 173.4; HRMS (ES^+) *m/z* $[M+H]^+$ Cacld for $C_{19}H_{31}O_2$: 291.2324; Found 291.2373. $[\alpha]^{25}_D$ +12.5 (*c* 0.19, EtOH).

2,3,3-Trimethylbut-2-yl (*S*)-4-methyl-2-(4-fluorophenyl)pentanoate (Table 5, entry 27)

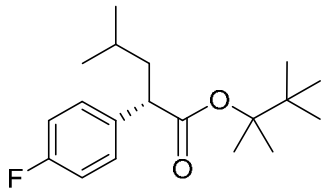

The title compound was synthesized according to General Procedure B using 2,2,3-trimethylbut-2-yl 2-chloro-4-methylpentanoate (249 mg, 1.00 mmol) and (4-F-C_6H_4)MgBr (1.82 mL, 1.10 M solution in THF, 2.0 equiv). The product was obtained as a colorless oil (221 mg, 72%, 91:9 er).

The er was determined by HPLC on two columns of CHIRALCEL OD-3R (4.6 mm i.d., 150 mm length) with following conditions: 50% CH_3CN aq., 1.0 mL/min, 25 °C, retention times (t_r) = 80.4 min (minor), 85.8 min (major).

FTIR (neat, cm^{-1}) ν 2958, 2873, 1724, 1508, 1466, 1379, 1369, 1273, 1225, 1173, 1126, 937, 839, 802, 787, 525; ^1H NMR (500 MHz, $CDCl_3$) δ 0.88 (s, 9H), 0.90 (d, *J* = 6.9 Hz, 3H), 0.91 (d, *J* = 6.9 Hz, 3H), 1.37 (s, 3H), 1.43 (s, 3H), 1.45–1.53 (m, 1H), 1.56–1.62 (m, 1H), 1.90–1.96 (m, 1H), 3.54 (t, *J* = 7.4 Hz, 1H), 6.96–7.01 (m, 2H) , 7.23–7.27 (m, 2H); ^{13}C NMR (125 MHz, $CDCl_3$) δ 20.2, 20.4, 22.3, 22.6, 25.1, 25.8, 38.3, 42.0, 50.2, 87.3, 115.2 (d, *J* = 20.8 Hz), 129.3 (d, *J* = 8.1 Hz), 135.7 (d, *J* = 2.9 Hz), 161.8 (d, *J* = 245 Hz), 173.2; HRMS (CI^+) *m/z* $[M+H]^+$ Cacld for $C_{19}H_{30}FO_2$: 309.2230; Found 309.2119. $[\alpha]^{25}_D$ +17.2 (*c* 0.48, EtOH).

2,3,3-Trimethylbut-2-yl (*S*)-2,4-dimethylpent-3-enoate (Table 5, entry 28)

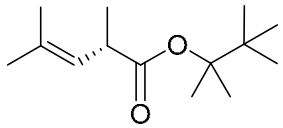

The reaction was carried out according to the General Procedure B using 2,3,3-trimethylbut-2-yl 2-chloropropionate (**1e**) (104 mg, 0.50 mmol) and (2-methylprop-1-en-1-yl) magnesium bromide (1.62 mL, 0.62 M in THF solution, 2.0 equiv). The title compound (61 mg, 52% yield, 91:9 er) was obtained as a colorless liquid after silica gel column chromatography (hexane/toluene = 60/40).

The er was determined by HPLC on a CHIRALDEX B-DA 90 °C, He 1.5 mL/min, retention times (t_r) = 60.0 min (minor) and 61.0 min (major)

FTIR (neat, cm^{-1}) ν 2972, 2932, 1726, 1455, 1378, 1369, 1259, 1172, 1128, 1062, 847; ^1H NMR (391.8 MHz, $CDCl_3$) δ 0.96 (s, 9H), 1.16 (d, *J* = 7.2 Hz, 3H), 1.46 (s, 3H), 1.47 (s, 3H), 1.66 (d, *J* = 1.3 Hz, 3H), 1.70 (d, *J* = 0.9 Hz, 3H), 3.18–3.26 (m, 1H), 5.13 (dt, *J* = 9.4, 1.3 Hz, 1H); ^{13}C NMR (98.5 MHz, $CDCl_3$) δ 18.2 (2C), 20.6 (2C), 25.2 (3C), 25.8, 38.5, 40.6, 86.7, 124.7, 133.3, 174.9; HRMS (FAB^+) *m/z* $[M+Na]^+$ Calcd for $C_{14}H_{26}O_2Na$: 249.1830, found 249.1825. $[\alpha]^{25}_D$ +53.4 (*c* 0.56, EtOH).

Octylammonium (*S*)-2-phenylpropionate (Table 6, entry 1)

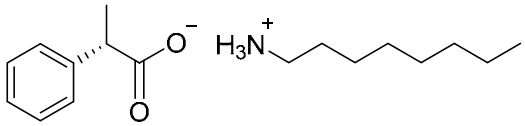

TFA (0.72 mL, 5 equiv) was added dropwise to a CH_2Cl_2 solution (5.7 mL) of 2,3,3-trimethylbut-2-yl (*S*)-2-phenylpropionate (470 mg, 1.9 mmol) at room temperature and stirred at that temperature for 1 h. A crude liquid, (*S*)-2-phenylpropionic acid (284 mg, quantitative), was obtained after removing the volatile solvents under reduced pressure. Octylamine (248 μL, 1.5 mmol) was added to a CH_3CN (20 mL) solution of (*S*)-2-phenylpropionic acid (225 mg, 1.5 mmol), following which it was heated at 60 °C to dissolve the entire solid. The mixture was allowed to cool to room temperature, with stirring, and a white solid product formed. After stirring for 1 h, the white solid was collected by filtration, washed with CH_3CN (3.0 mL), and dried under reduced pressure to provide the title compound (341 mg, 1.22 mmol, 81%). The same recrystallization procedure from CH_3CN (15 mL) furnished the optically pure title compound (303 mg, 1.08 mmol, 72%, >99:1 er) as a white solid.

The er was determined by HPLC on a CHIRALCEL OJ-3R column (4.6 mm i.d., 150 mm length) under the following conditions: 10 mM H_3PO_4 aq/CH_3CN = 75/25, 1.0 mL/min, 25 °C, retention times (t_r) = 17.4 min (major) and 19.1 min (minor).
Mp 95–96 °C; FTIR (neat, cm^{-1}) ν 2953, 2924, 2855, 2682, 1639, 1552, 1450, 1384, 1360, 1282, 1187, 1062; ^1H NMR (391.8 MHz, $CDCl_3$) δ 0.90 (t, *J* = 6.9 Hz, 3H), 1.01–1.31 (m, 12H), 1.37 (d, *J* = 7.1 Hz, 3H), 2.26 (t, *J* = 8.1 Hz, 2H), 3.46 (q, *J* = 7.2 Hz, 1H), 7.15–7.18 (m, 1H), 7.21–7.26 (m, 4H), 7.67 (brs); ^{13}C NMR (98.5 MHz, $CDCl_3$) δ 14.2, 19.6, 22.8, 26.7, 28.1, 29.2, 29.3, 31.9, 39.3, 49.0, 126.2, 127.5 (2C), 128.4 (2C), 144.2, 181.6; Anal. Calcd for $C_{17}H_{29}NO_2$: C, 73.07; H, 10.46. Found: C, 73.09; H, 10.61. HRMS (FAB+) *m/z* $[M+H]^+$ Calcd for $C_{17}H_{30}NO_2$: 280.2277, Found 280.2276. $[\alpha]^{25}_D$ +4.9 (*c* 1.01, EtOH).

Octylammonium (*S*)-2-[(1,1'-biphenyl)-4-yl]propionate (Table 6, entry 2)

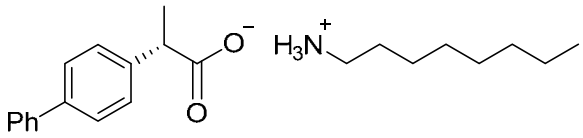

TFA (0.84 mL, 5 equiv) was added dropwise to a CH_2Cl_2 solution (6.6 mL) of 2,3,3-trimethylbut-2-yl (*S*)-2-[(1,1'-biphenyl)-4-yl]propionate (714 mg, 2.2 mmol) at room temperature, and the mixture was stirred at that temperature for 1 h. A crude white solid, (*S*)-2[(1,1'-biphenyl)-4-yl]propionic acid (500 mg, quantitative), was obtained after removing volatile solvents under reduced pressure. Octylamine (248 μL, 1.5 mmol) was added to a CH_3CN (23 mL) solution of (*S*)-2-([1,1'-biphenyl]-4-yl)propanoic acid (340 mg, 1.5 mmol), and the mixture was heated to 80 °C to dissolve all the solid. The mixture was allowed to cool to room temperature, with stirring, and a white solid product formed. After stirring for 1 h, the white solid was collected by filtration, washed with CH_3CN (3.0 mL), and dried under reduced pressure to provide the title compound (496 mg, 93%, 86:14 er).

Recrystallization from the MTBE solvent was then performed as follows. The title compound (178 mg, 0.50 mmol) in MTBE (20 mL) was dissolved at 75 °C. The mixture was stirred at room temperature for 1 h, and a white solid appeared, which was collected by filtration and washed with MTBE (3 mL) to afford the title compound. The same procedure was used for the second recrystallization from MTBE (20 mL), furnishing the optically pure title compound (138 mg, 0.39 mmol, 77%, >99:1 er) as a white solid.

The er was determined by HPLC on a CHIRALCEL OJ-3R column (4.6 mm i.d., 150 mm length) under the following conditions: 10 mM H_3PO_4 aq/CH_3CN = 60/40, 1.0 mL/min, 25 °C, retention times (t_r) = 12.4 min (minor) and 14.4 min (major).
Mp 129–130 °C; FTIR (neat, cm^{-1}) ν 2954, 2926, 2854, 2689, 1638, 1542, 1486, 1382, 1361, 1282, 1187, 1065; ^1H NMR (391.8 MHz, $CDCl_3$) δ 0.84 (t, *J* = 7.2 Hz, 3H), 1.02–1.16 (m, 8H), 1.19–1.24 (m, 2H), 1.27–1.35 (m, 2H), 1.42 (d, *J* = 7.2 Hz, 3H), 2.34 (t, *J* = 7.8 Hz, 2H), 3.53 (q, *J* = 7.2 Hz, 1H), 7.22 (br), 7.28–7.34 (m, 3H), 7.36–7.40 (m, 2H), 7.46–7.52 (m, 4H); ^{13}C NMR (98.5 MHz, $CDCl_3$) δ 14.2, 19.6, 22.8, 26.8, 28.4, 29.3 (2C), 31.9, 39.5, 48.6, 126.9 (2C), 127.0 (2C), 127.2, 128.0 (2C), 128.9 (2C), 139.1, 140.8, 143.2, 181.5; Anal. Calcd for $C_{23}H_{33}NO_2$: C, 77.70; H, 9.36; N, 3.94. Found: C, 77.38; H, 9.51; N, 3.90. HRMS (FAB^+) *m/z* $[M+H]^+$ Calcd for $C_{23}H_{34}NO_2$: 356.2590, Found 356.2588. $[\alpha]^{25}_D$ –11.0 (*c* 1.01, EtOH).

Octylammonium (*S*)-2-[4-(2-methylpropyl)phenyl]propionate (Table 6, entry 3)

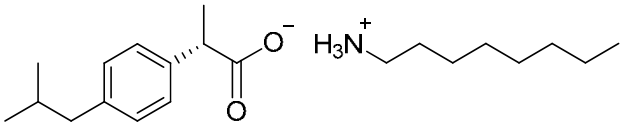

TFA (0.69 mL, 5.0 equiv) was added dropwise to a CH_2Cl_2 solution (5.5 mL) of 2,3,3-trimethylbut-2-yl (*S*)-2-[4-(2-methylpropyl)phenyl]propionate (550 mg, 1.8 mmol) at room temperature, and the mixture was stirred at that temperature for 1 h. A crude white solid (398 mg, quantitative) was obtained after removing the volatile solvents under reduced pressure. CH_3CN (27.5 mL) and octylamine (299 μL, 1.0 equiv) were added to the crude solid, and the mixture was heated to 60 °C to dissolve the solid entirely. The mixture was allowed to cool to room temperature, with stirring, and white crystals formed. After stirring for 1 h, the white crystals were collected by filtration, washed with CH_3CN (1.7 mL), and dried under reduced pressure (454 mg, 75%, 92:8 er). Recrystallization from CH_3CN (27.5 mL) furnished optically pure crystals (394 mg, 65%, >99:1 er).

The er was determined by HPLC on a CHIRALCEL OJ-3R column (4.6 mm i.d., 150 mm length) under the following conditions: CH_3CN/10 mM H_3PO_4 aq = 35/65, 1.0 mL/min, 25 °C, retention times (t_r) = 25.8 min (minor) and 27.8 min (major).
Mp 105–106 °C; FTIR (neat, cm^{-1}) ν 2953, 2926, 2857, 2798, 2685, 1640, 1556, 1382, 1362, 1282, 1187, 1063, 881, 846, 792, 593; ^1H NMR (500 MHz, $CDCl_3$) δ 0.88 (d, *J* = 6.5 Hz, 6H), 0.89 (t, *J* = 7.1 Hz, 3H), 1.13–1.36 (m, 12H), 1.38 (d, *J* = 7.1 Hz, 3H), 1.78–1.86 (m, 1H), 2.33–2.39 (m, 2H), 2.41 (d, *J* = 7.1 Hz, 2H), 3.49 (q, *J* = 7.1 Hz, 1H), 5.93 (brs, 3H), 7.02–7.06 (m, 2H), 7.15–7.18 (m, 2H); ^{13}C NMR (125 MHz, CDCl3) δ 14.1, 19.6, 22.40, 22.41, 22.6, 26.6, 28.0, 29.1, 29.2, 30.2, 31.8, 39.2, 45.1, 48.4, 127.0 (2C), 128.9 (2C), 139.2, 141.3, 181.7; Anal. Calcd for $C_{21}H_{37}NO_2$: C, 75.17; H, 11.11; N, 4.17. Found: C, 75.00; H, 10.89; N, 4.26. HRMS (ES^-) *m/z* $[M–H]^-$ Calcd for $C_{13}H_{17}O_2$: 205.1229, Found 205.1229. $[\alpha]^{25}_D$ +0.36 (*c* 1.00, EtOH).

(*S*)-2-[4-(2-methylpropyl)phenyl]propionic acid (dexibuprofen)

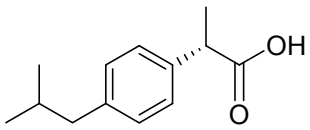

An AcOEt solution (30 mL) of octylammonium (*S*)-2-[4-(2-methylpropyl)phenyl]propionate (300 mg, 0.89 mmol) was washed with a 1.0 M aqueous solution of hydrochloric acid (10 mL), dried over Na_2SO_4, and the solvent was evaporated in vacuo to furnish colorless crystals (184 mg, quantitative, >99:1 er).

The er was determined by HPLC on a CHIRALCEL OJ-3R column (4.6 mm i.d., 150 mm length) under the following conditions: CH_3CN/10 mM H_3PO_4 aq = 35/65, 1.0 mL/min, 25 °C, retention times (t_r) = 25.8 min (minor) and 27.8 min (major).

Mp 50–51 °C; FTIR (neat, cm^{-1}) ν 2953, 2923, 2870, 1708, 1509, 1467, 1418, 1282, 1229, 1184, 1054, 950, 865, 779, 658, 591; ^1H NMR (500 MHz, $CDCl_3$) δ 0.89 (d, *J* = 6.5 Hz, 6H), 1.50 (d, *J* = 7.1 Hz, 3H), 1.78–1.89 (m, 1H), 2.44 (d, *J* = 7.1 Hz, 2H), 3.71 (q, *J* = 7.1 Hz, 1H), 5.93 (brs, 3H), 7.08–7.11 (m, 2H), 7.20–7.23 (m, 2H); ^{13}C NMR (125 MHz, $CDCl_3$) δ 18.1, 22.4, 30.2, 44.8, 45.0, 127.3 (2C), 129.4 (2C), 137.0, 140.9, 180.2; Anal. Calcd for $C_{13}H_{18}O_2$: C, 75.69; H, 8.80. Found: C, 75.76; H, 8.85. HRMS (ES^-) *m/z* [M–H]$^-$ Calcd for $C_{13}H_{17}O_2$: 205.1229, Found 205.1224. $[\alpha]^{25}_D$ +59.0 (*c* 1.00, EtOH). *lit.* $[\alpha]^{25}_D$ +59.5 (*c* 1.0, EtOH). All analytical data are in good accordance with those reported in the literature.[24]

Octylammonium (*S*)-2-(6-methoxynaphth-2-yl)propionate (Table 6, entry 4)

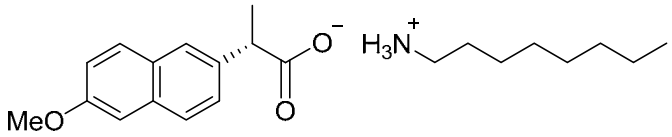

TFA (0.84 mL, 5 equiv) was added dropwise to a CH_2Cl_2 solution (6.6 mL) of 2,3,3-trimethylbut-2-yl (*S*)-2-(6-methoxynaphth-2-yl)propionate (723 mg, 2.2 mmol) at room temperature, and the mixture was stirred at that temperature for 1 h. A crude white solid, (*S*)-2-(6-methoxynaphthal-2-yl)propionic acid (508 mg, quantitative), was obtained after removing the volatile solvents under reduced pressure. Octylamine (248 μL, 1.5 mmol) was added to a CH_3CN (23 mL) solution of (*S*)-2-(6-methoxynaphthal-2-yl)propionic acid (346 mg, 1.5 mmol), and the mixture was heated to 75 °C to dissolve all the solid. The mixture was allowed to cool to room temperature, with stirring, and a white solid product formed. After stirring for 1 h, the white solid was collected by filtration, washed with CH_3CN (3.0 mL), and dried under reduced pressure to provide the title compound (496 mg, 92%, 89:11 er). Recrystallization from MTBE was then performed as follows. The title compound (286 mg, 0.79 mmol) was dissolved in MTBE (32 mL) at 60 °C. Then the mixture was stirred at room temperature for 1 h. A white solid formed, and it was collected by filtration and washed with MTBE (5 mL) to afford the title compound. The same procedure was used to perform the second recrystallization from MTBE (25 mL), furnishing the title compound (226 mg, 0.63 mmol, 80%, 93:7 er) as a white solid.

The er value was determined by HPLC on a CHIRALCEL AD-3R column (4.6 mm i.d., 150 mm length) under the following conditions: 30% CH_3CN aq, 1.0 mL/min, 25 °C, retention times (t_r) = 21.3 min (minor) and 24.4 min (major).

Mp 127–128 °C; FTIR (neat, cm^{-1}) ν 2957, 2923, 2851, 1630, 1604, 1531, 1505, 1485, 1458, 1387, 1362, 1254, 1210, 1162, 1032, 924; ^1H NMR (391.8 MHz, $CDCl_3$) δ 0.74–

0.80 (m, 2H), 0.87–0.95 (m, 5H), 1.04–1.19 (m, 6H), 1.21–1.29 (m, 2H), 1.42 (d, J = 7.2 Hz, 3H), 2.09 (t, J = 8.1 Hz, 2H), 3.57 (q, J = 7.2 Hz, 1H), 3.88 (s, 3H), 7.01 (d, J = 2.2 Hz, 1H), 7.08 (dd, J = 8.9, 2.6 Hz, 1H), 7.35 (dd, J = 8.3, 2.0 Hz, 1H), 7.44 (br), 7.54–7.57 (m, 2H), 7.61 (d, J = 8.9 Hz, 1H); ^{13}C NMR (98.5 MHz, $CDCl_3$) δ 14.2, 19.6, 22.8, 26.6, 28.1, 29.1, 29.3, 31.9, 39.4, 48.8, 55.3, 105.6, 118.8, 125.5, 126.8, 126.9, 129.1, 129.2, 133.3, 139.3, 157.4, 181.7; Anal. Calcd for $C_{22}H_{33}NO_3$: C, 73.49; H, 9.25; N, 3.90. Found: C, 73.44; H, 9.47; N, 3.84. HRMS (FAB$^+$) m/z $[M+H]^+$ Calcd for $C_{22}H_{34}NO_3$: 360.2539, Found 360.2543. $[\alpha]^{25}_D$ –5.6 (*c* 1.02, EtOH).

Octylammonium (*S*)-2-(4-fluorophenyl)butanoate (Table 6, entry 5)

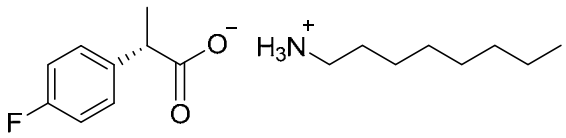

TFA (0.11 mL, 5.0 equiv) was added dropwise to a CH_2Cl_2 solution (0.81 mL) of 2,3,3-trimethylbut-2-yl (*S*)-2-(4-fluorophenyl)butyrate (81 mg, 0.29 mmol) at room temperature, and the mixture was stirred at that temperature for 1 h. A crude white solid (53 mg, quantitative) was obtained after removing the volatile solvents under reduced pressure. CH_3CN (4.1 mL) and octylamine (48 μL, 1.0 equiv) were added to this crude white solid, and the mixture was heated to 50 °C to dissolve the solid completely. The mixture was allowed to cool to room temperature with stirring, resulting in the formation of white crystals. After stirring for 1 h, the white crystals were collected by filtration, washed with CH_3CN (0.3 mL), and dried under reduced pressure (62 mg, 69%, 95:5 er). Recrystallization from CH_3CN (4.1 mL) furnished optically enriched crystals (41 mg, 46%, 97:3 er).

The er values were determined by HPLC on a CHIRALCEL OJ-3R column (4.6 mm i.d., 150 mm length) under the following conditions: CH_3CN/10 mM H_3PO_4 aq = 35/65, 1.0 mL/min, 25 °C, retention times (t_r) = 9.7 min (minor) and 11.0 min (major). Mp 85–86 °C; FTIR (neat, cm^{-1}) ν 2958, 2930, 2857, 2230, 1633, 1556, 1508, 1381, 1332, 1240, 1215, 1159, 841, 754, 563, 531; ^{1}H NMR (500 MHz, $CDCl_3$) δ 0.82 (t, J = 7.5 Hz, 3H), 0.90 (t, J = 6.8 Hz, 3H), 1.10–1.35 (m, 12H), 1.58–1.68 (m, 1H), 1.88–1.97 (m, 1H), 2.37 (t, J = 7.8 Hz, 2H), 3.18 (t, J = 7.8 Hz, 1H), 6.88–6.95 (m, 2H), 7.10 (brs, 3H), 7.19–7.25 (m, 2H); ^{13}C NMR (125 MHz, $CDCl_3$) δ 12.5, 14.1, 22.6, 26.6, 27.3, 28.4, 29.12, 29.15, 31.8, 39.5, 56.2, 114.9 (d, J = 20.8 Hz, 2C), 129.2 (d, J = 6.9 Hz, 2C), 137.9 (d, J = 3.5 Hz), 161.5 (d, J = 245 Hz), 180.6; Anal. Calcd for $C_{18}H_{30}FNO_2$: C, 69.41; H, 9.71; F, 6.10; N, 4.50. Found: C, 69.06; H, 9.48; F, 6.04; N, 4.51. HRMS (ES$^-$) *m/z* $[M–H]^-$ Calcd for $C_{10}H_{10}FO_2$: 181.0670, Found 181.0665. $[\alpha]^{25}_D$ +0.65 (*c* 1.00, EtOH).

Octylammonium (*S*)-4-methyl-2-(4-fluorophenyl)pentanoate (Table 6, entry 6)

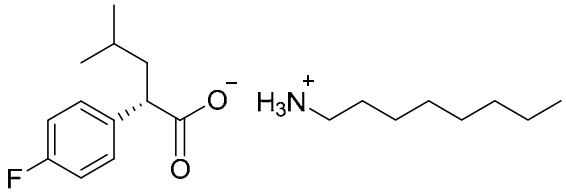

TFA (0.23 mL, 5.0 equiv) was added dropwise to a CH_2Cl_2 solution (1.9 mL) of 2,3,3-trimethylbut-2-yl (*S*)-4-methyl-2-(4-fluorophenyl)pentanoate (188 mg, 0.61 mmol) at room temperature, and the mixture was stirred at that temperature for 1 h. A crude white solid (137 mg, quantitative) was obtained after removing the volatile solvents under reduced pressure. CH_3CN (9.4 mL) and octylamine (101 μL, 1.0 equiv) were added to this crude white product, and the mixture was heated to 60 °C to dissolve the solid completely. The mixture was allowed to cool to room temperature, with stirring, and white crystals formed. After stirring for 1 h, the white crystals were collected by filtration, washed with CH_3CN (0.6 mL), and dried under reduced pressure (179 mg, 86%, 93:7 er). Recrystallization from CH_3CN (9.4 mL) furnished optically enriched crystals (155 mg, 75%, 94:6 er).

The er values were determined by HPLC on a CHIRALCEL OJ-3R column (4.6 mm i.d., 150 mm length) under the following conditions: CH_3CN/10 mM H_3PO_4 aq = 35/65, 1.0 mL/min, 25 °C, retention times (t_r) = 9.1 min (major) and 11.5 min (minor). Mp 134–135 °C; FTIR (neat, cm^{-1}) ν 2958, 2928, 2855, 2224, 1628, 1532, 1509, 1381, 1278, 1223, 1159, 1088, 851, 840, 811, 739, 687, 566, 524; ^1H NMR (500 MHz, $CDCl_3$) δ 0.860 (d, *J* = 6.5 Hz, 3H), 0.862 (d, *J* = 6.5 Hz, 3H), 0.90 (t, *J* = 7.1 Hz, 3H), 1.10–1.39 (m, 13H), 1.55–1.62 (m, 1H), 1.73–1.80 (m, 1H), 2.35 (t, *J* = 7.8 Hz, 2H), 3.49 (t, *J* = 7.8 Hz, 1H), 6.87–6.94 (m, 2H) , 7.13 (brs, 3H), 7.20–7.25 (m, 2H); ^{13}C NMR (125 MHz, $CDCl_3$) δ 14.1, 22.1, 22.6, 23.0, 25.8, 26.7, 28.1, 29.2 (2C), 31.8, 39.4, 43.4, 52.4, 114.9 (d, *J* = 22.0 Hz, 2C), 129.2 (d, *J* = 8.1 Hz, 2C), 138.2 (d, *J* = 3.5 Hz), 161.4 (d, *J* = 244 Hz), 181.0; Anal. Calcd for $C_{20}H_{34}FNO_2$: C, 70.75; H, 10.09; F, 5.60; N, 4.13. Found: C, 70.57; H, 9.85; F, 5.58; N, 4.17. HRMS (ES^-) *m/z* $[M–H]^-$ Calcd for $C_{13}H_{17}O_2$: 205.1229, Found 205.1229.$[\alpha]^{25}_D$ +0.36 (*c* 1.00, EtOH).

Radical Cyclization Reaction

The radical cyclization reaction was carried out according to General Procedure B using 2,2,3-trimethylbut-2-yl 2-chlorohept-6-enoate (130 mg, 0.50 mmol) and PhMgBr (0.91 mL, 1.10 M solution in THF, 2.0 equiv). The crude product were purified by preparative HPLC (Wakopak Wakosil-II 5C18 HG Prep, 50 mm i.d., 250 mm length, 80% CH_3CN aq.) to give acyclic product (18 mg, 12% yield, 85:15 er) and cyclic products (60 mg, 40% yield, *trans*/*cis* = 58/42). The diastereomers of cyclic products could be separated on a Chiralpak AZ-3R (4.6 mm i.d., 150 mm length, 55% CH_3CN aq.).

2,3,3-Trimethylbut-2-yl (*S*)-2-phenylhept-6-enoate (3g)

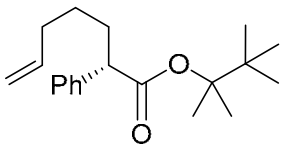

The er was determined by HPLC on two columns of CHIRALCEL OJ-3R (4.6 mm i.d., 150 mm length) with following conditions: 60% CH_3CN aq., 1.0 mL/min, 25 °C. t_r = 10.5 min, t_s = 11.5 min.

FTIR (neat, cm^{-1}) ν 2976, 2926, 1726, 1456, 1379, 1369, 1275, 1173, 1130, 993, 910, 847, 733, 698, 548; ^1H NMR (500 MHz, $CDCl_3$) δ 0.86 (s, 9H), 1.31–1.78 (m, 2H), 1.37 (s, 3H), 1.46 (s, 3H), 2.03–2.19 (m, 4H), 3.44 (t, *J* = 7.8 Hz, 1H) 4.91–5.01 (m, 2H), 5.72–5.81 (m, 1H), 7.20–7.32 (m, 5H); ^{13}C NMR (125 MHz, $CDCl_3$) δ 20.2, 20.5, 25.0, 26.8, 32.4, 33.5, 38.3, 53.1, 87.2, 114.7, 126.9, 127.8, 128.4, 138.4, 139.8, 173.2; HRMS (FAB^+) *m/z* $[M+H]^+$ Cacld for $C_{20}H_{31}O_2$: 303.2324; Found 303.2328.

2,3,3-Trimethylbut-2-yl (1*S, 2*R**)-2-benzylcyclopentanecarboxylate (5)**

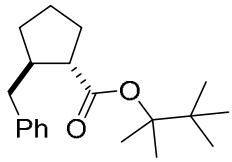

The er was determined by HPLC on two columns of CHIRALCEL OJ-3R (4.6 mm i.d., 150 mm length) with following conditions: 50% CH_3CN aq., 1.0 mL/min, 25 °C. t_a = 37.0 min, t_b = 39.6 min.

^1H NMR (500 MHz, $CDCl_3$) δ1.00 (s, 9H), 1.47–1.59 (m, 3H), 1.535 (s, 3H), 1.537 (s, 3H), 1.70–1.86 (m, 2H), 1.94–2.01 (m, 1H), 2.36–2.42 (m, 2H), 2.81–2.89 (m, 2H), 7.15–7.19 (m, 3H), 7.25–7.28 (m, 2H); ^{13}C NMR (125 MHz, $CDCl_3$) δ 20.5, 20.6, 23.3, 25.2, 27.7, 30.3, 36.8, 38.3, 45.1, 49.2, 86.9, 125.8, 128.2, 128.9, 141.6, 174.6; HRMS (FAB^+) *m/z* $[M+H]^+$ Cacld for $C_{20}H_{31}O_2$: 303.2324; Found 303.2320.

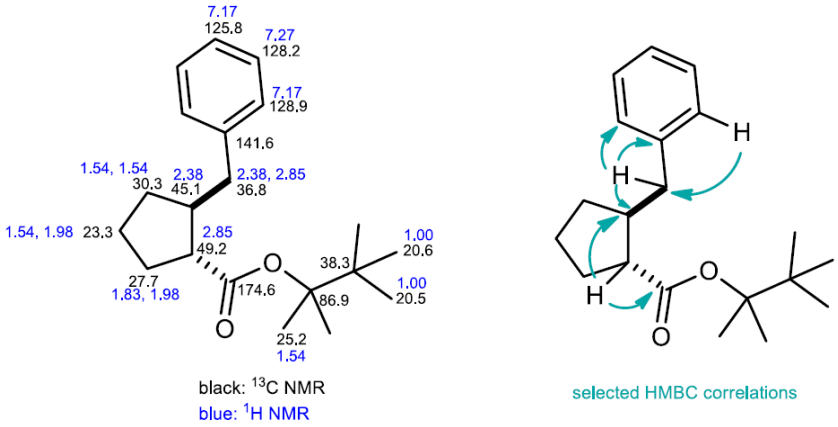

Figure 5. NMR signal assignments for *trans*-**6** based on HMQC and selected correlations in HMBC.

2,3,3-Trimethylbut-2-yl (1*S, 2*S**)-2-benzylcyclopentanecarboxylate (6)**

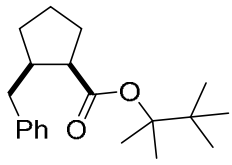

The er was determined by HPLC on two columns of CHIRALCEL OJ-3R (4.6 mm i.d., 150 mm length) with following conditions: 50% CH_3CN aq., 1.0 mL/min, 25 °C. t_a = 39.3 min, t_b = 44.1 min.

^{1}H NMR (500 MHz, $CDCl_3$) δ 0.98 (s, 9H), 1.22–1.29 (m, 1H), 1.441 (s, 3H), 1.446 (s, 3H), 1.68–1.66 (m, 2H), 1.71–1.85 (m, 2H),1.89–1.97 (m, 1H), 2.32–2.43 (m, 2H), 2.53 (dd, *J* = 13.3, 8.8 Hz, 1H), 2.87 (dd, *J* = 13.3, 5.2 Hz, 1H), 7.15–7.19 (m, 3H), 7.24–7.27 (m, 2H); ^{13}C NMR (125 MHz, $CDCl_3$) δ 20.41, 20.44, 24.4, 25.2, 30.2, 32.1, 38.4, 41.1, 45.7, 51.5, 86.5, 125.8, 128.2, 129.0, 141.0, 175.5; HRMS (FAB$^+$) *m/z* $[M+H]^+$ Cacld for $C_{20}H_{31}O_2$: 303.2324; Found 303.2319.

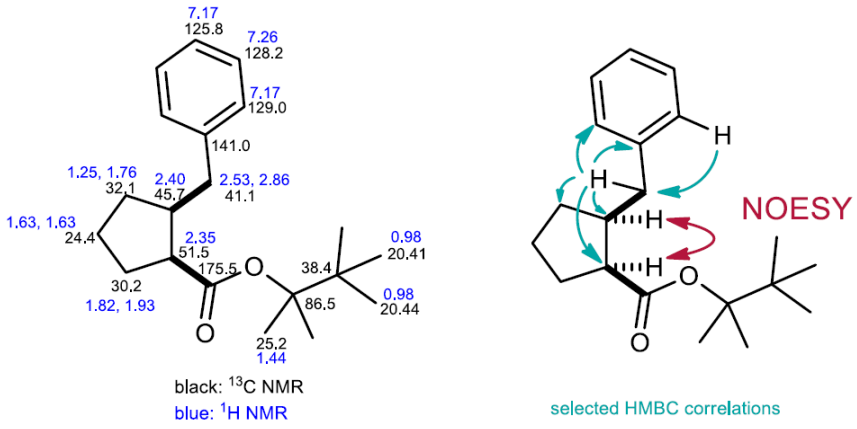

Figure 6. NMR signal assignments for *trans*-**6** based on HMQC and selected correlations in HMBC.

Experimental procedure using substrate 1j

The radical cyclization reaction was carried out according to general procedure B, using 2,3,3-Trimethylbut-2-yl (*Z*)-2-chlorooct-6-enoate (**1j**; 412 mg, 1.50 mmol) and PhMgBr (2.73 mL, 1.10 M solution in THF, 2.0 equiv). The crude product was purified by preparative HPLC (Wakopak Wakosil-II 5C18 HG Prep, 50 mm i.d., 250 mm length, 80% CH_3CN aq) to give an acyclic product (33 mg, 7% yield, 87:13 er) and a cyclic product as a single diastereomer (174 mg, 37%, 50:50 er). Other cyclic diastereomers were obtained as a mixture.

2,3,3-Trimethylbut-2-yl (*S*)-(*Z*)-2-phenyloct-6-enoate

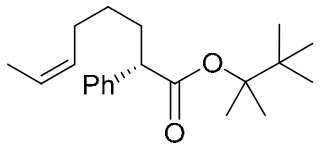

The er was determined by HPLC on two CHIRALCEL OJ-3R columns (4.6 mm i.d., 150 mm length) under the following conditions: 60% CH_3CN aq, 1.0 mL/min, 25 °C, retention times (t_r) = 11.5 min (minor) and 12.6 min (major).

FTIR (neat, cm^{-1}) ν 2959, 1724, 1454, 1378, 1368, 1276, 1173, 1127, 1031, 939, 848, 732, 697, 518; ^1H NMR (500 MHz, $CDCl_3$) δ 0.87 (s, 9H), 1.21–1.41 (m, 2H), 1.38 (s, 3H), 1.45(s, 3H), 1.57–1.59 (m, 3H), 1.71-1.78 (m, 1H), 2.01–2.11 (m, 3H), 3.45 (t, *J* = 7.9 Hz, 1H) 5.30–5.36 (m, 1H), 5.40–5.46 (m, 1H), 7.20–7.31 (m, 5H); ^{13}C NMR (125 MHz, $CDCl_3$) δ 12.7, 20.2, 20.5, 25.0, 26.6, 27.4, 32.5, 38.3, 53.1, 87.2, 124.1, 126.9, 127.9, 128.41, 128.42, 130.1, 139.9, 173.2 Anal. Calcd for $C_{21}H_{32}O_2$: C, 79.70; H, 10.19. Found: C, 79.44; H, 10.24. HRMS (FAB^+) *m/z* $[M+H]^+$ Cacld for $C_{21}H_{32}O_2$: 317.2480; Found 317.2550.

2,3,3-Trimethylbut-2-yl 2-(1-phenylethyl)cyclopentanecarboxylate

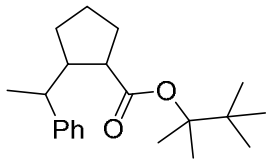

The er was determined by HPLC on two CHIRALCEL OJ-3R columns (4.6 mm i.d., 150 mm length) under the following conditions: 65% CH_3CN aq, 1.0 mL/min, 25 °C, retention times (t_r) = 11.5 min and 15.6 min.

FTIR (neat, cm^{-1}) ν 2960, 2873, 1719, 1453, 1377, 1368, 1176, 1125, 846, 760, 699, 536; ^1H NMR (500 MHz, $CDCl_3$) δ 0.80 (s, 9H), 1.24 (d, *J* = 6.9 Hz, 3H), 1.42 (s, 3H), 1.43 (s, 3H), 1.64–1.75 (m, 2H), 1.78–1.97 (m, 4H), 2.07–2.15 (m, 1H), 2.36–2.48 (m, 1H), 2.95–3.01 (m, 1H), 7.12–7.26 (m, 5H); ^{13}C NMR (125 MHz, $CDCl_3$) δ 20.25, 20.33, 22.6, 23.6, 25.0, 29.5, 30.7, 38.1, 41.1, 47.4, 51.1, 86.0, 125.8, 127.2, 128.2, 147.5, 175.1; Anal. Calcd for $C_{21}H_{32}O_2$: C, 79.70; H, 10.19. Found: C, 79.35; H, 10.26. HRMS (FAB^+) *m/z* $[M+H]^+$ Cacld for $C_{21}H_{32}O_2$: 317.2480; Found 317.2512.

References and Notes

[1] (a) Uozumi, Y. In *Comprehensive Chirality*; Shibasaki, M., Ed.; Carreira, E. M., Yamamoto, H., Eds.-in-Chief; Elsevier: Oxford, 2012; Vol. 4, p 18. (b) Sarli, V. In *Stereoselective Synthesis of Drug and Natural Products*; Andrushko, V., Andrushko, N., Eds.; John Wiley and Sons, Inc.: Hoboken, NJ, 2013; Vol. 1, p 369. Enantioconvergent asymmetric couplings of achiral secondary alkyl Grignard and zinc reagents are described in ref 1a. (c) Taylor, B. L. H.; Jarvo, E. R. *Synlett* **2011**, 2761–2765. (d) Swift, E. C.; Jarvo, E. R. *Tetrahedron* **2013**, *69*, 5799–5817. Stereospecific asymmetric cross couplings are reviewed in refs 1c and 1d.

[2] (a) Netherton, M. R.; Fu, G. C. *Adv. Synth. Catal.* **2004**, *346*, 1525–1532. (b) Terao, J.; Kambe, N. *Acc. Chem. Res.* **2008**, *41*, 1545–1554. (c) Rudolph, A.; Lautens, M. *Angew. Chem., Int. Ed.* **2009**, *48*, 2656–2670.

[3] Leading references: with Grignard reagents: (a) Lou, S.; Fu, G. C. *J. Am. Chem. Soc.* **2010**, *132*, 1264–1266. With organozinc reagents: (b) Fischer, C.; Fu, G. C. J. Am. Chem. Soc. 2005, 127, 4594–4595. (c) Lundin, P. M.; Esquivias, J.; Fu, G. C. *Angew. Chem., Int. Ed.* **2009**, *48*, 154–156. (d) Oelke, A. J.; Sun, J.; Fu, G. C. *J. Am. Chem. Soc.* **2012**, *134*, 2966–2969. (e) Choi, J.; Fu, G. C. *J. Am. Chem. Soc.* **2012**, *134*, 9102–9105. (f) Binder, J. T.; Cordier, C. J.; Fu, G. C. *J. Am. Chem. Soc.* **2012**, *134*, 17003–17006. (g) Liang, Y.; Fu, G. C. *J. Am. Chem. Soc.* **2014**, *136*, 5520–5524. (h) Choi, J.; Martín-Gago, P.; Fu, G. C. *J. Am. Chem. Soc.* **2014**, *136*, 12161–12165. With organoboron reagents: (i) Lundin, P. M.; Fu, G. C. *J. Am. Chem. Soc.* **2010**, *132*, 11027–11029. (j) Wilsily, A.; Tramutola, F.; Owston, N. A.; Fu, G. C. *J. Am. Chem. Soc.* **2012**, *134*, 5794–5797. With organosilicon reagents: (k) Dai, X.; Strotman, N. A.; Fu, G. C. *J. Am. Chem. Soc.* **2008**, *130*, 3302–3303.

[4] Selected reviews: (a) Nakamura, E.; Hatakeyama, T.; Ito, S.; Ishizuka, K.; Ilies, L.; Nakamura, M. *Org. React.* **2014**, *83*, 1–209. (b) Czaplik, W. M.; Mayer, M.; Cvengroš, J.; von Wangelin, A. J. *ChemSusChem* **2009**, *2*, 396–417. (c) Sherry, B. D.; Fürstner, A. *Acc. Chem. Res.* **2008**, *41*, 1500–1511. Selected papers: (d) Fürstner, A.; Leitner, A.; Méndez, M.; Krause, H. *J. Am. Chem. Soc.* **2002**, *124*, 13856–13863. (e) Cahiez, G.; Habiak, V.; Duplais, C.; Moyeux, A. *Angew. Chem., Int. Ed.* **2007**, *46*, 4364–4366. (f) Noda, D.; Sunada, Y.; Hatakeyama, T.; Nakamura, M.; Nagashima, H. *J. Am. Chem. Soc.* **2009**, *131*, 6078–6079. (g) Bedford, R. B.; Carter, E.; Cogswell, P. M.; Gower, N. J.; Haddow, M. F.; Harvey, J. N.; Murphy, D. M.; Neeve, E. C.; Nunn, J. *Angew. Chem., Int. Ed.* **2013**, *52*, 1285–1288. (h) Bedford, R. B.; Brenner, P. B.; Carter, E.; Carvell, T. W.; Cogswell, P. M.; Gallagher, T.; Harvey, J. N.; Murphy, D. M.; Neeve, E. C.; Nunn, J.; Pye, D. R. *Chem. Eur. J.* **2014**, *20*, 7935–7938.

[5] Reviews: (a) Gosmini, C.; Bégouin, J.-M.; Moncomble, A. *Chem. Commun.* **2008**, 3221–3233. (b) Cahiez, G.; Moyeux, A. *Chem. Rev.* **2010**, *110*, 1435–1462. (c) Iwasaki, T.; Takagawa, H.; Okamoto, K.; Singh, S. P.; Kuniyasu, H.; Kambe, N. *Synthesis* **2014**, *46*, 1583–1592. Selected papers: (d) Ohmiya, H.; Yorimitsu, H.; Oshima, K. *J. Am. Chem. Soc.* **2006**, *128*, 1886–1889. (e) Iwasaki, T.; Takagawa, H.; Singh, S. P.; Kuniyasu, H.; Kambe, N. *J. Am. Chem. Soc.* **2013**, *135*, 9604–9607.

[6] Selected papers: (a) Terao, J.; Todo, H.; Begum, S. A.; Kuniyasu, H.; Kambe, N. *Angew. Chem., Int. Ed.* **2007**, *46*, 2086–2089. (b) Shen, R.; Iwasaki, T.; Terao, J.; Kambe, N. *Chem. Commun.* **2012**, *48*, 9313–9315. (c) Yang, C.-T.; Zhang, Z.-Q.; Liang, J.; Liu, J.-H.; Lu, X.-Y.; Chen, H.- H.; Liu, L. *J. Am. Chem. Soc.* **2012**, *134*, 11124–11127. For enantioselective allylic cross couplings, see: (d) Hornillos, V.; Pérez, M.; Fañanás-Mastral, M.; Feringa, B. L. *J. Am. Chem. Soc.* **2013**, *135*, 2140–2143. (e) Hojoh, K.; Shido, Y.; Ohmiya, H.; Sawamura, M. *Angew. Chem., Int. Ed.* **2014**, *53*, 4954–4948.

[7] (a) Tsuji, T.; Yorimitsu, H.; Oshima, K. *Angew. Chem., Int. Ed.* **2002**, *41*, 4137–4139. (b) Mao, J.; Liu, F.; Wang, M.; Wu, L.; Zheng, B.; Liu, S.; Zhong, J.; Bian, Q.; Walsh, P. J. *J. Am. Chem. Soc.* **2014**, *136*, 17662–17668. For the use of chiral bisoxazoline ligands in Ni-catalyzed asymmetric cross coupling, see ref 3a.

[8] (a) Gopalaiah, K. *Chem. Rev.* **2013**, *113*, 3248–3296. (b) Nakamura, M.; Hirai, A.; Nakamura, E. *J. Am. Chem. Soc.* **2000**, *122*, 978–979. (c) Egami, H.; Matsumoto, K.; Oguma, T.; Kunisu, T.; Katsuki, T. *J. Am. Chem. Soc.* **2010**, *132*, 13633–13635. One enantioselective C−C bond formation via organometallic addition has been reported in ref 8b. The enantioselective oxidative cross- and homocoupling of 2-naphthols was reported in 8c and the references cited therein.

[9] (a) Nakamura, M.; Matsuo, K.; Ito, S.; Nakamura, E. *J. Am. Chem. Soc.* **2004**, *126*, 3686–3687. (b) Hatakeyama, T.; Kondo, Y.; Fujiwara, Y.; Takaya, H.; Ito, S.; Nakamura, E.; Nakamura, M. *Chem. Commun.*

2009, 1216–1218. (c) Hatakeyama, T.; Hashimoto, T.; Kondo, Y.; Fujiwara, Y.; Seike, H.; Takaya, H.; Tamada, Y.; Ono, T.; Nakamura, M. *J. Am. Chem. Soc.* **2010**, *132*, 10674–10676. (d) Jin, M.; Nakamura, M. *Chem. Lett.* **2011**, *40*, 1012–1014. (e) Hatakeyama, T.; Fujiwara, Y.; Okada, Y.; Itoh, T.; Hashimoto, T.; Kawamura, S.; Ogata, K.; Takaya, H.; Nakamura, M. *Chem. Lett.* **2011**, *40*, 1030–1032. (f) Hatakeyama, T.; Okada, Y.; Yoshimoto, Y.; Nakamura, M. *Angew. Chem., Int. Ed.* **2011**, *50*, 10973–10976. (g) Hatakeyama, T.; Hashimoto, T.; Kathriarachchi, K. K. A. D. S.; Zenmyo, T.; Seike, H.; Nakamura, M. *Angew. Chem., Int. Ed.* **2012**, *51*, 8834–8837. (h) Ghorai, S. K.; Jin, M.; Hatakeyama, T.; Nakamura, M. *Org. Lett.* **2012**, *14*, 1066–1069. (i) Kawamura, S.; Kawabata, T.; Ishizuka, K.; Nakamura, M. *Chem. Commun.* **2012**, *48*, 9376–9378.

[10] Imamoto, T.; Tamura, K.; Zhang, Z.; Horiuchi, Y.; Sugiya, M.; Yoshida, K.; Yanagisawa, A.; Gridnev, I. D. *J. Am. Chem. Soc.* **2012**, *134*, 1754–1769.

[11] (a) Landoni, M. F.; Soraci, A. *Curr. Drug Metab.* **2001**, *2*, 37–51. (b) Duggan, K. C.; Hermanson, D. J.; Musee, J.; Prusakiewicz, J. J.; Scheib, J. L.; Carter, B. D.; Banerjee, S.; Oates, J. A.; Marnett, L. J. *Nat. Chem. Biol.* **2011**, *7*, 803–809.

[12] (a) Jennerjahn, R.; Jackstell, R.; Piras, I.; Franke, R.; Jiao, H.; Bauer, M.; Beller, M. *ChemSusChem* **2012**, *5*, 734–739. (b) Mayer, M.; Welther, A.; von Wangelin, A. J. *ChemCatChem.* **2011**, *3*, 1567–1571. (c) Chen, C.; Dugan, T. R.; Brennessel, W. W.; Weix, D. J.; Holland, P. L. *J. Am. Chem. Soc.* **2014**, *136*, 945–955. (d) Bai, X.-F.; Song, T.; Deng, W.-H.; Wei, Y.-L.; Li, L.; Xia, C.-G.; Xu, L.-W. *Synlett* **2014**, *25*, 417–422. (e) Lim, H. J.; Smith, C. R.; RajanBabu, T. V. *J. Org. Chem.* **2009**, *74*, 4565–4572. (f) Arisawa, M.; Terada, Y.; Nakagawa, M.; Nishida, A. *Angew. Chem., Int. Ed.* **2002**, *41*, 4732–4734. (g) Shirakawa, E.; Ikeda, D.; Masui, S.; Yoshida, M.; Hayashi, T. *J. Am. Chem. Soc.* **2012**, *134*, 272–279.

[13] Hatakeyama, T.; Hashimoto, S.; Ishizuka, K.; Nakamura, M. *J. Am. Chem. Soc.* **2009**, *131*, 11949–11963.

[14] Dexibuprofen and naproxen are optically active nonsteroidal anti-inflammatory drugs and are commonly used for clinical purposes.

[15] (a) Takaya, H.; Nakajima, S.; Nakagawa, N.; Isozaki, K.; Iwamoto, T.; Imayoshi, R.; Gower, N. J.; Adak, L.; Hatakeyama, T.; Honma, T.; Takagaki, M.; Sunada, Y.; Nagashima, H.; Hashizume, D.; Takahashi, O.; Nakamura, M. *Bull. Chem. Soc. Jpn.* **2015**, *88*, 410–418. (b) Daifuku, S. L.; Al-Afyouni, M. H.; Snyder, B. E. R.; Kneebone, J. L.; Neidig, M. L. *J. Am. Chem. Soc.* **2014**, *136*, 9132–9143. (c) Daifuku, S. L.; Al-Afyouni, M. H.; Snyder, B. E. R.; Kneebone, J. L.; Neidig, M. L. *J. Am. Chem. Soc.* **2014**, *136*, 11847–11853. Although stepwise reduction of Fe(III)$(acac)_3$ by PhMgBr has been reported to produce Fe(II) and Fe(I) species possessing one acetylacetonato group, the lack of the counteranion effect of the iron precatalysts on either yield or er indicates displacement of the original counteranion in the present enantioselective coupling reaction: (d) Lefèvre, G.; Jutand, A. *Chem. Eur. J.* **2014**, *20*, 4796–4805.

[16] Review for nonlinear effect: Satyanarayana, T.; Abraham, S.; Kagan, H. B. *Angew. Chem., Int. Ed.* **2009**, *48*, 456–494 and references cited therein.

[17] Similar bimetallic mechanisms are reported for a nickel catalyst; see: (a) Breitenfeld, J.; Wodrich, M. D.; Hu, X. *Organometallics* **2014**, *33*, 5708–5715. (b) Biswas, S.; Weix, D. J. *J. Am. Chem. Soc.* **2013**, *135*, 16192–16197. (c) Schley, N. D.; Fu, G. C. *J. Am. Chem. Soc.* **2014**, *136*, 16588–16593.

[18] Lawrence, N. J.; Davies, C. A.; Gray, M. *Org. Lett.* **2004**, *6*, 4957–4960.

[19] Zhang, J.; Yang, N.; Yang, L. *Molecules* **2012**, *17*, 6415–6423.

[20] Tanasova, M.; Yang, Q.; Olmsted, C. C.; Yasileiou, C.; Li, X.; Anyika, M.; Borhan, B. *Eur. J. Org. Chem.* **2009**, 4242–4253.

[21] Snider, B. B.; Kulkarni, Y. S. *J. Org. Chem.* **1987**, *52*, 307–310.

[22] Song, D.; Blond, G.; Fürstner, A. *Tetrahedron* **2003**, *59*, 6899–6904.

[23] Huang, Z.; Liu, Z.; Zhou, J. *J. Am. Chem. Soc.* **2011**, *133*, 15882–15885.

[24] Chavez-Flores, D.; Salvador, J. M. *Tetrahedron: Asymmetry* **2012**, *23*, 237–239.

CHAPTER 6

Iron-Catalyzed Enantioselective Suzuki-Miyaura Coupling of Racemic Alkyl Bromides

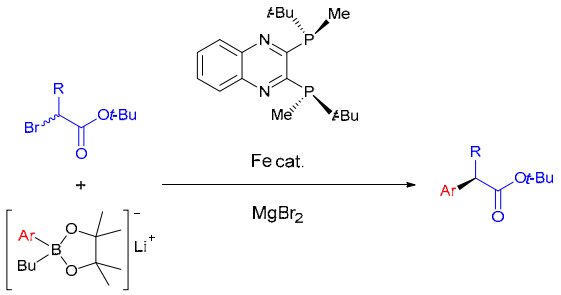

Abstract

The first iron-catalyzed enantioselective Suzuki–Miyaura coupling reaction has been developed. In the presence of catalytic amounts of $FeCl_2$ and (*R*,*R*)-QuinoxP*, lithium arylborates are cross-coupled with *tert*-butyl α-bromopropionate in an enantioconvergent manner, enabling facile access to various optically active α-arylpropionic acids including several nonsteroidal anti-inflammatory drugs (NSAIDs) of commercial importance. (*R*,*R*)-QuinoxP* is specifically able to induce chirality when compared to analogous *P*-chiral ligands that give racemic products, highlighting the critical importance of transmetalation in the present asymmetric cross-coupling system.

Reproduced from *Chem. Commun.* **2019**, *55*, 1128–1131. with permission from the Royal Society of Chemistry.

Introduction

Transition-metal-catalyzed coupling reactions with organoboron reagents, namely Suzuki–Miyaura coupling reactions, are among the most powerful methods for the construction of carbon-carbon bonds in both academic and industrial chemical syntheses.[1] Intensive studies involving catalysts and ligands have firmly established this synthetic method; however enantioselective versions remain challenging, particularly for the construction of sp^3 carbon centers. Owing to the appreciable significance of such stereogenic centers in current pharmaceutical design,[2] considerable effort has been devoted to developing enantioselective cross couplings involving alkyl reagents.[3]

Enantioconvergent coupling reactions of alkyl halides with boron nucleophiles represent the most sophisticated approaches because they directly synthesize optically active molecules from readily available racemic halides. Fu and co-workers have made significant progress in such transformations through the use of nickel catalysts (Figure 1a).[4] At present, the scope of this type of enantioconvergent reaction has been expanded to various combinations of alkyl halides and nucleophiles,[3a,3e,5] and to other transition-metal catalysts;[6] however, the use of organoboron reagents is still severely limited to nickel catalysis.

Iron has gained considerable attention due to its cost-effectiveness and safe properties, which advantages this metal catalyst in pharmaceutical and agrochemical syntheses.[7] Over the past decade, Nakamura group and others have developed iron-catalyzed coupling reactions involving organoboron reagents,[8] including those with alkyl halides.[9] However, the application of an organoboron reagent to an enantioselective iron-catalyzed coupling reaction has not been achieved so far. Here the author reports the first examples of iron-catalyzed enantioselective couplings of organoboron reagents to produce optically active α-aryl esters from racemic α-haloesters and arylboron reagents (Figure 1b).

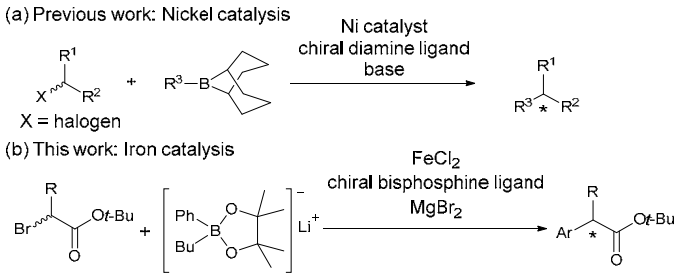

Figure 1. Enantioconvergent couplings of alkyl halides with organoboron reagents

Results and Discussion

The studies began by screening ligands in the coupling of *tert*-butyl α-bromopropionate (**1**) with the lithium phenylborate **2a**, which was easily prepared from the

boronic ester and BuLi (Table 1).[9b] In the previously reported enantioselective iron-catalyzed coupling of aryl Grignard reagents, *P*-chiral bisphosphine ligand of (*R,R*)-BenzP* was the most effective among a variety of ligands.[6c] Based on these results, the author initially examined several *P*-chiral bisphosphines[10] and found that the ligand backbone has a remarkable effect on enantioselectivity. As shown in Table 1, to surprise, the present reaction with (*R,R*)-BenzP* **L1** did not exhibit chiral induction at all.

Table 1. Chiral Ligand Screening

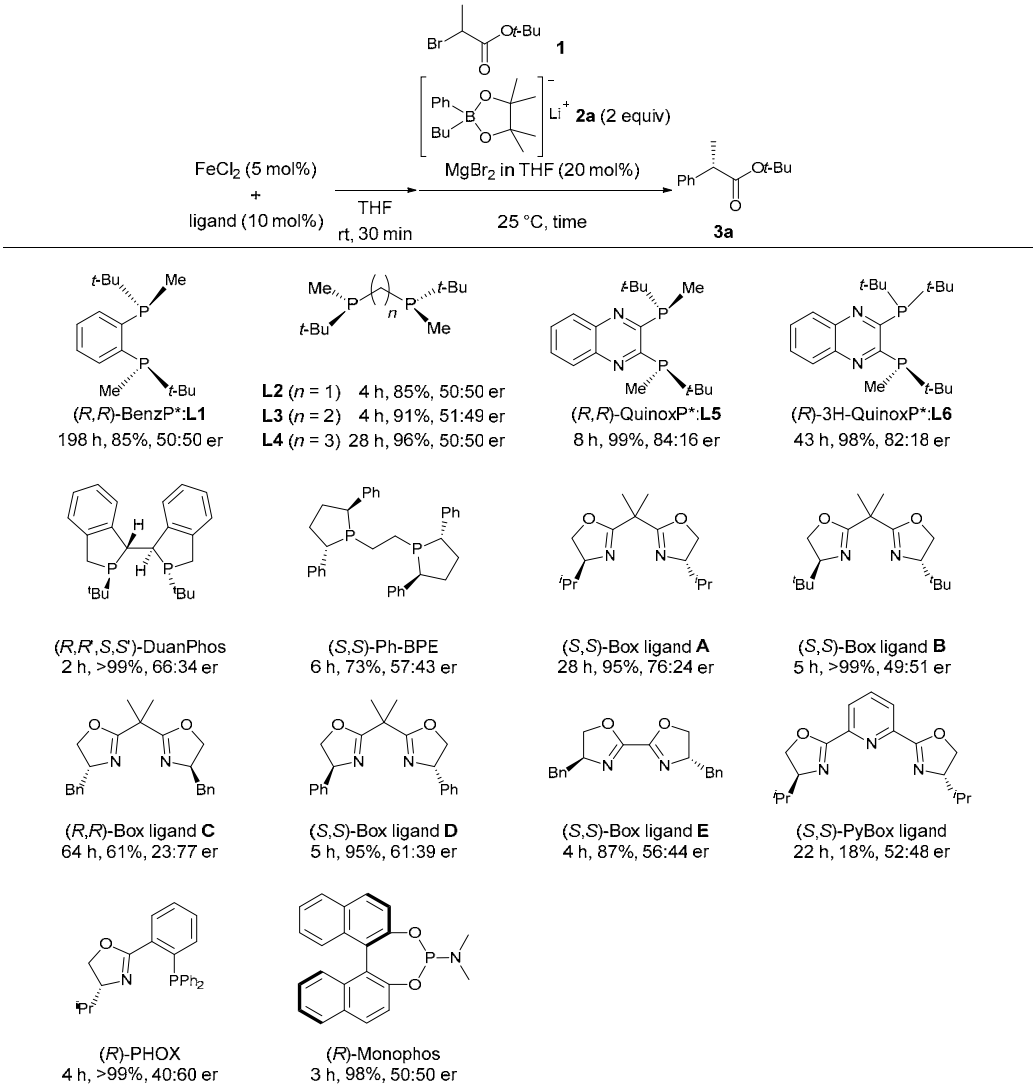

[a] Yields and er values were determined by GC and HPLC, respectively.

The use of *P*-chiral ligands **L2**–**L4**, which have aliphatic backbones, were also totally ineffective, providing the racemic coupling product. In sharp contrast, chiral ligands bearing quinoxaline backbones were specifically able to induce chirality; (*R,R*)-QuinoxP* **L5** was

found to be optimal and gave product **3a** in 94% yield with 84:16 er. C_1-Symmetric (*R*)-3H-QuinoxP* **L6** also provided **3a** with comparable enantioselectivity. Other types of chiral ligand, including nitrogen-based ones and monodentate one, were less effective in this reaction. It is noteworthy that the yield is affected by the synthetic procedure; the arylborate, α-haloester, and $MgBr_2$ need to be added in this order to the mixture of $FeCl_2$ and the chiral ligand as depicted in Table 1.

Table 2. Optimization of Alkyl Bromides for Iron-Catalyzed Enantioselective Coupling with Phenyl Boron Reagent

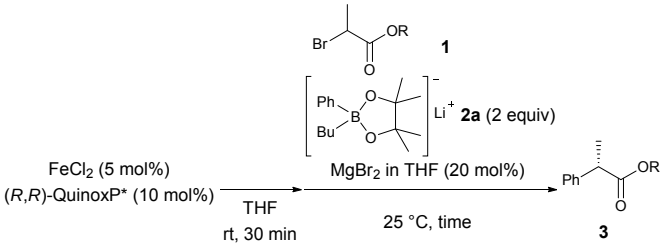

entry	R	time (h)	yield [%] (er)[a]
1	Me	4	95 (56:44)
2	*i*-Pr	5	82 (73:27)
3	*t*-Bu	5	99 (84:16)
4		6	92 (85:15)

[a] Yields and er values were determined by GC and HPLC, respectively.

The effect of ester groups of α-bromopropionate was studied and the results are provided in Table 2. The steric hindrance clearly impacted on the enantioselectivity: methyl ester gave the lowest er of 56:44 and 2,3,3-trimethylbut-2yl ester, which shows the highest selectivity in the enantioselective iron-catalyzed cross-coupling reactions with aryl Grignard reagents as discussed in Chapter 5, gave the highest er of 85:15 (entries 1 and 4). *tert*-Butyl ester also showed good enantioselectivity (84:16 er) and the highest yield of 99%, and therefore the author chose *tert*-butyl ester as a substrate (entry 3).

Optically active α-aryl esters are useful intermediates for the synthesis of several bioactive molecules, such as α-arylpropionic acids, which are well known to be nonsteroidal anti-inflammatory drugs (NSAIDs). [11] Indeed, the coupling product was smoothly transformed into α-phenylpropionic acid without any loss of optical purity upon hydrolysis with TFA (Scheme 1). Notably, this sequential method involving coupling and hydrolysis did not require any chromatographic purification, and simple liquid-liquid extraction provided pure α-phenylpropionic acid in high yield.

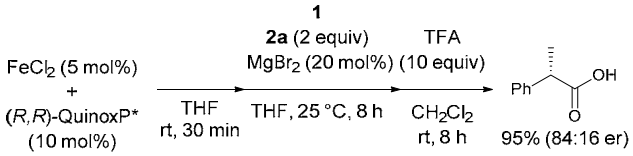

Scheme 1. Synthesis of Chiral α-Phenylpropionic Acid by Iron-Catalyzed Enantioconvergent Coupling and Hydrolysis.

With the optimal procedure in hand, the author examined the scope of the arylboron reagent (Table 3). Both electron-rich (entries 1–3) and deficient (entry 4) arylborates provided the coupling products in high yields and with reasonable enantioselectivities. The chloro substituent, which is potentially useful for further synthetic elaborations including cross-couplings, was untouched under the present reaction conditions; the product was obtained in 83% yield with 84:16 er (entry 5). *Ortho*-substituted phenyl- and 2-naphthylborates were also amenable to the reaction (entries 6 and 7). Coupling with the indolylborate also proceeded smoothly and enantioselectively (entry 8); however, hydrolysis of the coupling product failed due to the decomposition of the indolyl unit under acidic conditions. Furthermore, the developed synthetic method was applied to the synthesis of a variety of bioactive α-phenylpropionic acids with enantioselectivities in excess of 80:20 (entries 9–13).

Table 3. Arylboron Reagent Scope

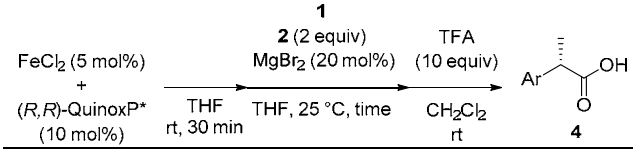

entry	product		time (h)	yield [%] (er)[a]
1	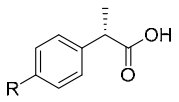	**4b:** R = Me	6	90 (81:19)
2[b]		**4c:** R = OMe	35	85 (82:18)
3		**4d:** R = NMe_2	3	89 (82:18)
4		**4e:** R = CF_3	23	81 (76:24)
5		**4f:** R = Cl	12	83 (84:16)
6	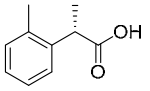	**4g**	20	65 (88:12)
7	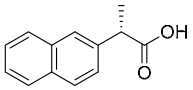	**4h**	19	91 (77:23)
8[c]	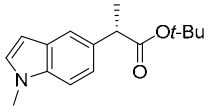	**3i**	15	80 (81:19)
9	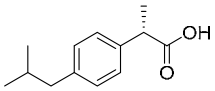	(*S*)-Ibuprofen **4j**	5	95 (82:18)
10	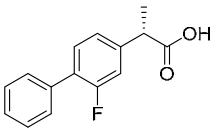	(*S*)-Flurbiprofen **4k**	16	51 (84:16)
11	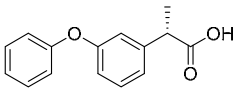	(*S*)-Fenoprofen **4l**	22	52 (82:18)
12	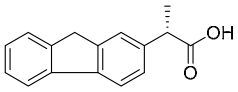	(*S*)-Cicloprofen **4m**	13	49 (81:19)
13[b]	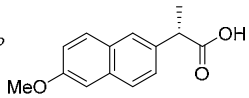	(*S*)-Naproxen **4n**	22	80 (80:20)

[a] Isolated yields; er values determined by HPLC. [b] $FeCl_2$ (1 mol %) and (*R,R*)-QuinoxP* (2 mol %) were used. [c] Hydrolysis failed due to the decomposition of the indolyl group. Yield was determined by ^1H NMR .

The author next turned to the specific chiral-inducing ability of (*R,R*)-QuinoxP* compared to other *P*-chiral bisphosphine ligands. Nakamura group previously reported that both (*R,R*)-QuinoxP* and (*R,R*)-BenzP* induced comparable enantioselectivities in iron-catalyzed couplings involving aryl Grignard reagents, which is in stark contrast to the present system.[6c,12] Therefore, the observed difference between (*R,R*)-QuinoxP* and (*R,R*)-BenzP* in the present system cannot be attributed to their chiral induction abilities in the enantiodetermining step. To examine the difference between the two ligands, the author performed stoichiometric reactions of pre-formed complexes, namely $FeCl_2$/(*R,R*)-QuinoxP*

$\mathbf{A_1}$ and $FeCl_2$/(*R*,*R*)-BenzP* $\mathbf{A_2}$, with phenyl borate **2a** in the presence of $MgBr_2$ (Figure 2). The reaction of $\mathbf{A_2}$ proceeded quite slowly, and more than 60% of the starting iron complex remained even after 62 h. On the other hand, iron complex $\mathbf{A_1}$ was completely consumed within 2 h under the same conditions. These results indicate that (*R*,*R*)-QuinoxP* is crucial to facilitate transmetalation, which is most likely the key step for the generation of the active iron species in the enantioselective catalytic cycle (*vide infra*). The electron-withdrawing nature of the quinoxaline backbone renders the iron center more electrophilic, thereby accelerating transmetalation.[13]

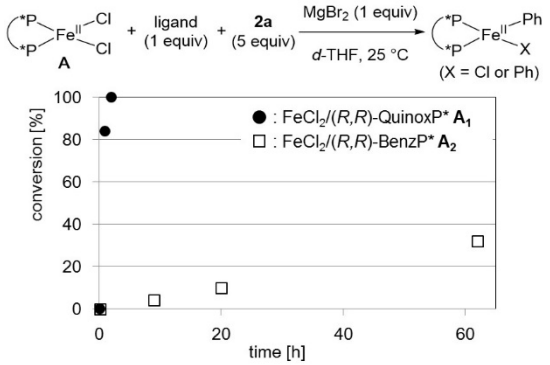

Figure 2. Stoichiometric reactions of $FeCl_2$/bisphosphine with borate **2a** in the presence of $MgBr_2$. Conversions of $FeCl_2$/(*R*,*R*)-QuinoxP* $\mathbf{A_1}$ (circles) and $FeCl_2$/(*R*,*R*)-BenzP* $\mathbf{A_2}$ (squares) were determined by ^1H NMR spectroscopy. The produced iron complex was unable to be characterized by NMR techniques.

Based on the experimental and theoretical studies on the iron-catalyzed couplings of alkyl halides, the author presents a plausible mechanism in Figure 3.[6c,9b,13a,14] Transmetalation of $FeCl_2$/bisphosphine **A** with the boron reagent[15] and subsequent reductive elimination provides $Fe^{I}X$/bisphosphine **B**, which is the active species during the first C–Br bond-activation step. Complex **B** then abstracts the bromine atom from the alkyl bromide to generate the corresponding alkyl radical; this radical recombines with complex **C**, which is generated by the transmetalation of **A** with the boron reagent,[16] to produce Fe^{III}BrArAlkyl/bisphosphine **D**. Reductive elimination of complex **D** provides the coupling product. In the case of (*R*,*R*)-BenzP*, transmetalation with the arylborate is quite slow. As a consequence, the racemic background reaction triggered by ligand dissociation from complex **A** dominates (Figure 3, left).[17]

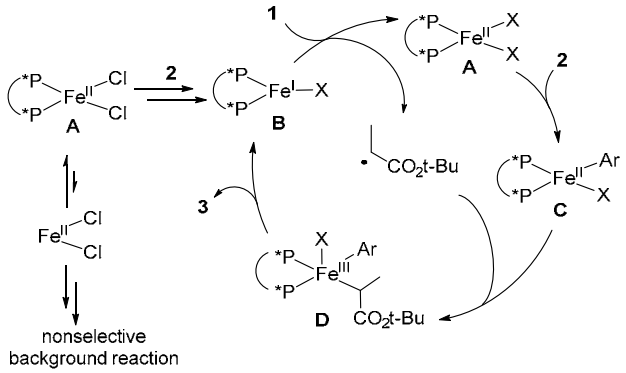

Figure 3. Plausible mechanism for the enantioselective coupling reaction of an arylboron reagent.

DFT calculations reveal that the recombination and the final reductive elimination are exergonic, with ΔG values of 14.1 and 22.6 kcal/mol, respectively (Figure 4). In addition, the energy barrier for reductive elimination is predicted to be 11.8 kcal/mol. Although the transition state for the recombination step was unable to be optimized due to the flatness of the potential energy surface, the calculated energy profile suggests that each step proceeds irreversibly under the reaction conditions; hence, the author concludes that recombination is most likely to be the enantiodetermining step.

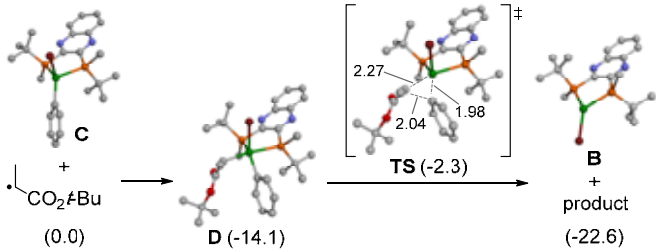

Figure 4. Recombination and reductive elimination steps calculated at the B3LYP/6-311G* level of theory with GD3BJ empirical dispersion. Relative energies (kcal/mol) are shown in parentheses. Bond lengths are given in Å. H atoms are omitted for clarity. Color code: grey, C; green, Fe; red, Br; orange, P; purple, N. For full details, see the Experimental Section.

Conclusion

In summary, the author developed the first iron-catalyzed enantioselective coupling reactions involving organoboranes, in which the use of a *P*-chiral ligand containing an electron-deficient quinoxaline backbone is the key to attaining high enantioselectivities. This reaction enables facile access to a variety of optically active α-arylpropionic esters from racemic α-bromoesters, which are readily deprotected to the corresponding α-arylpropionic acids, including several pharmaceutical compounds. Although the enantioselectivity can still be improved, the combination of an iron catalyst with a boron reagent clearly endows this method with practical advantages over other coupling reactions. Efforts to further develop more-selective iron catalysts are underway.

Experimental Section

General Information

All reactions dealing with air- or moisture-sensitive compounds were carried out in well-dried reaction vessels under a positive pressure of dry argon. Air- and moisture-sensitive liquids and solutions were transferred via a syringe or a PTFE cannula. Flash column chromatography was performed on Wakogel 60N, 38–100 μm or on a Biotage SP1 Flash Purification System with prepacked silica cartridges. Preparative recycling gel permeation chromatography (GPC) was performed with a Japan Analytical Industry LC-9204 instrument equipped with JAIGEL-1H/JAIGEL-2H columns using chloroform as eluent.

^{1}H and ^{13}C NMR spectra were recorded on a JEOL ECS-400NR NMR spectrometer (391.8 and 98.5 MHz, respectively). The ^{1}H chemical shift values are reported in parts per million (ppm, δ scale) and referenced to the 1H resonance of tetramethylsilane (δ 0.00). The ^{13}C chemical shift values are reported in parts per million and referenced to the ^{13}C resonance of $CDCl_3$ (δ 77.16). Data are presented as chemical shift, multiplicity, coupling constant in Hertz (Hz) and signal area integration in natural numbers. NMR yield was determined for a crude product by 1H NMR analysis by using 1,1,2,2-tetrachloroethane as an internal standard.

GC analysis was conducted with Shimadzu GC-2010 and GC-2010 Plus instruments equipped with an FID detector and a capillary column, ZB-1MS (Phenomenex Inc., 10 m × 0.10 mm i.d., 0.10 μm film thickness). GC yield was determined for a crude product using undecane as an internal standard.

The er values were determined by GC or HPLC analysis using a chiral stationary column. IR spectra were recorded on PerkinElmer Spectrum One FT-IR spectrometers and reported in cm^{-1}. High resolution mass spectra (HRMS) were obtained using electron ionization (EI) on a JEOL JMS-700 mass spectrometer.

Unless otherwise noted, commercially available materials were used without purification. Tetrahydrofuran (THF), purchased from Wako Pure Chemical Industries, Ltd. (Wako), was distilled over benzophenone ketyl. The water content of the solvents was determined with a Karl Fischer Moisture Titrator (MKC-610, Kyoto Electronics Company) to be less than 15 ppm. Metal salts were purchased, and purities, commercial suppliers and production numbers are as follows: $FeCl_2$ (99.998%, Aldrich Inc., 429368), $MgBr_2$ (≥99.99%, Aldrich Inc., 495093).

Preparation of Starting Materials

Methyl 2-bromopropionate

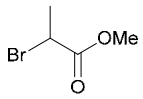

To a solution of 2-bromopropionic acid (0.9 mL, 10 mmol) in MeOH (5 mL) was added thionyl chloride (0.9 mL, 12 mmol) at 0 °C, and then the mixture was stirred at room temperature for 12 h. The reaction mixture was quenched with sat. $NaHCO_3$ aq. (30 mL) and the aqueous layer was extracted with CH_2Cl_2 (10 mL × 3). The organic layers were combined, dried with $MgSO_4$, and filtered. The solvent was removed under reduced pressure to afford the crude product. The crude product was purified by distillation to give the title product as a colorless liquid (800 mg, 48%).

^1H NMR ($CDCl_3$) δ 1.83 (d, J = 6.9 Hz, 3H), 3.79 (s, 3H), 4.39 (q, J = 6.8 Hz, 1H); ^{13}C NMR ($CDCl_3$) δ 21.8, 39.9, 53.1, 170.8; Anal. calcd for $C_4H_7BrO_2$, C, 28.77; H, 4.23. found C, 28.91; H, 4.24. All analytical data are in good accordance with those reported in the literature.[18]

Isopropyl 2-bromopropionate

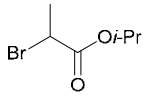

To a solution of 2-bromopropionic acid (0.9 mL, 10 mmol) in *i*-PrOH (5 mL) was added thionyl chloride (0.9 mL, 12 mmol) at 0 °C, and then the mixture was stirred at room temperature for 12 h. The reaction mixture was quenched with sat. $NaHCO_3$ aq. (30 mL) and the aqueous layer was extracted with CH_2Cl_2 (10 mL × 3). The organic layers were combined, dried with $MgSO_4$, and filtered. The solvent was removed under reduced pressure to afford the crude product. The crude product was purified by distillation to give the title product as a colorless liquid (1.24 g, 64%).

^1H NMR ($CDCl_3$) δ 1.28 (d, J = 6.3 Hz, 6H), 1.81 (d, J = 7.0 Hz, 3H), 4.32 (q, J = 7.0 Hz, 1H), 5.06 (hept, J = 6.3 Hz, 1H); ^{13}C NMR ($CDCl_3$) δ 21.5, 21.67, 21.70, 40.8, 69.7, 169.9; Anal. calcd for $C_6H_{11}BrO_2$, C, 36.95; H, 5.68. found C, 36.93; H, 5.64. All analytical data are in good accordance with those reported in the literature.[18]

2,3,3-Trimethylbut-2-yl 2-bromopropionate

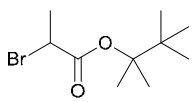

To a solution of 2-bromopropionic acid (3.6 mL, 40 mmol) in Et_2O (40 mL) was added trifluoroacetic anhydride (7.4 mL, 52 mmol) at room temperature, and the mixture was stirred for 18 h. After addition of 2,3,3-trimethylbutan-2-ol (15.59 g, 134 mmol), the resulting solution was stirred at 40 °C for 5 days. The reaction mixture was added to a solution of $NaHCO_3$ (10.2 g, 120 mmol) in water (100 mL), and the aqueous layer was extracted with EtOAc (20 mL × 3). The organic layers were combined, dried with $MgSO_4$, and filtered. The solvent was removed

under reduced pressure to afford the crude product. The crude product was purified by distillation to give the title product as a colorless liquid (1.10 g, 11%).
^{1}H NMR ($CDCl_3$) δ 1.00 (s, 9H), 1.52 (s, 6H), 1.79 (d, *J* = 7.0 Hz, 3H), 4.30 (q, *J* = 7.0 Hz, 1H); ^{13}C NMR (CDCl3) δ 20.2, 20.4, 21.9, 25.3 (3C), 38.7, 42.6, 89.2, 169.2; Anal. calcd for $C_{10}H_{19}BrO_2$, C, 47.82; H, 7.63. found C, 48.08; H, 7.64. All analytical data are in good accordance with those reported in the literature.[19]

Synthesis of 4,4,5,5,-Tetramethyl-2-aryl-1,3,2-dioxaborolanes

General Procedure A: Arylboronic acid and pinacol (1.2 equiv) were dissolved in THF with molecular sieves 4 Å at room temperature, and the mixture was stirred at the temperature for 12 h. Then the solvent was evaporated in vacuo, and excess pinacol was removed by silica gel column chromatography (toluene = 100%).

2-Phenyl-4,4,5,5-tetramethyl-1,3,2-dioxaborolane

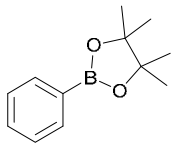

The title product was synthesized according to the general procedure A using phenylboronic acid (7.87 g, 65 mmol) and pinacol (9.18 g, 78 mmol). The product was obtained as a colorless solid (12.5 g, 94%) after distillation.

^{1}H NMR ($CDCl_3$) δ 1.34 (s, 12H), 7.36 (tt, *J* = 7.0, 1.1 Hz, 2H), 7.45 (tt, *J* = 7.4, 1.6 Hz, 1H), 7.81 (d, *J* = 6.6 Hz, 2H); ^{13}C NMR ($CDCl_3$) δ25.0 (4C), 83.9 (2C), 127.8 (2C), 131.4, 134.9 (2C); Anal. calcd for $C_{12}H_{17}BO_2$, C, 70.63; H, 8.40. found C, 70.44; H, 8.39. All analytical data are in good accordance with those reported in the literature.[20]

4,4,5,5-Tetramethyl-2-(*p*-tolyl)-1,3,2-dioxaborolane

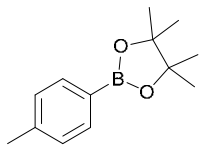

The title product was synthesized according to the general procedure A using *p*-tolylboronic acid (1.35 g, 10 mmol) and pinacol (1.39 g, 12 mmol). The product was obtained as a white solid (1.45 g, 66%) after distillation.

^{1}H NMR ($CDCl_3$) δ 1.33 (s, 12H), 2.36 (s, 3H), 7.18 (dd, *J* = 8.1, 0.5 Hz, 2H), 7.70 (d, *J* = 8.0 Hz, 2H); ^{13}C NMR ($CDCl_3$) δ 21.9, 25.0 (4C), 83.7 (2C), 128.7 (2C), 134.9 (2C), 141.5; Anal. calcd for $C_{13}H_{19}BO_2$, C, 71.59; H, 8.78. found C, 71.46; H, 8.79. All analytical data are in good accordance with those reported in the literature.[21]

4,4,5,5-Tetramethyl-2-(*o*-tolyl)-1,3,2-dioxaborolane

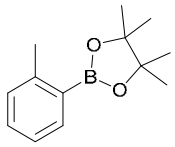

The title product was synthesized according to the general procedure A using *o*-tolylboronic acid (1.35 g, 10 mmol) and pinacol (1.39 g, 12 mmol). The product was obtained as a colorless liquid (1.81 g, 83%) after distillation.

^{1}H NMR ($CDCl_3$) δ 1.34 (s, 12H), 2.54 (s, 3H), 7.13–7.17 (m, 2H), 7.31 (td, *J* = 7.5, 1.6 Hz,1H), 7.76 (dd, *J* = 7.6, 1.7 Hz, 1H); ^{13}C NMR ($CDCl_3$) δ 22.4, 25.0 (4C), 83.5 (2C), 124.8, 129.9, 130.9, 136.0, 145.0; Anal. calcd for $C_{13}H_{19}BO_2$, C, 71.59; H, 8.78. found C, 71.64; H, 8.79. All analytical data are in good accordance with those reported in the literature.[21]

4,4,5,5-Tetramethyl-2-(4-trifluoromethylphenyl)-1,3,2-dioxaborolane

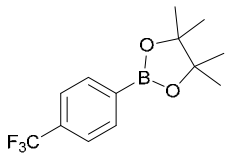

The title product was synthesized according to the general procedure A using 4-trifluoromethylphenylboronic acid (1.04 g, 5 mmol) and pinacol (0.83 g, 7 mmol). The product was obtained as a white solid (0.68 g, 47%) after recrystallization (MeOH / hexane).

^{1}H NMR ($CDCl_3$) δ 1.35 (s, 12H), 7.61 (d, *J* = 8.3 Hz, 2H), 7.91 (d, *J* = 7.6 Hz, 2H); ^{13}C NMR ($CDCl_3$) δ 25.0 (4C), 84.4 (2C), 124.3 (q, *J* = 272.4 Hz), 124.5 (d, *J* = 3.8 Hz, 2C), 133.0 (q, *J* = 32.9 Hz), 135.2 (2C); Anal. calcd for $C_{13}H_{16}BF_3O_2$, C, 57.39; H, 5.93. found C, 57.18; H, 6.02. All analytical data are in good accordance with those reported in the literature.[21]

4,4,5,5-Tetramethyl-2-(naphthalen-2-yl)-1,3,2-dioxaborolane

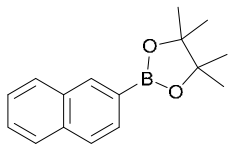

The title product was synthesized according to the general procedure A using 2-naphthylboronic acid (1.72 g, 10 mmol) and pinacol (1.17 g, 10 mmol). The product was obtained as a colorless solid (2.04 g, 80%).

^{1}H NMR ($CDCl_3$) δ 1.39 (s, 12 H), 7.48 (m, 2 H), 7.81–7.84 (m, 3H), 7.85–7.89 (m, 1H), 8.37 (s, 1H); ^{13}C NMR ($CDCl_3$) δ 24.9 (4C), 83.9 (2C), 125.8, 127.0 (2C), 127.7, 128.7, 130.4, 132.8, 135.0, 136.2; Anal. calcd for $C_{16}H_{19}BO_2$, C, 75.62; H, 7.54. found C, 75.51; H, 7.57. All analytical data are in good accordance with those reported in the literature.[22]

4,4,5,5-Tetramethyl-2-[4-(2-methylpropyl)phenyl]-1,3,2-dioxaborolane

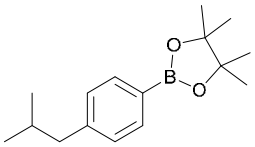

The title product was synthesized according to the general procedure A using 4-(2-methylpropyl)phenylboronic acid (0.99 g, 6 mmol) and pinacol (0.83 g, 7 mmol). The product was obtained as a colorless liquid (0.84 g, 57%) after distillation.

IR (neat, cm^{-1}) 2955, 1612, 1466, 1398, 1358, 1318, 1272, 1215, 1143, 1089, 1022, 963, 860, 735, 658; ^1H NMR ($CDCl_3$) δ 0.89 (d, J = 6.6 Hz, 6H), 1.34 (s, 12H), 1.87 (hept, J = 6.9 Hz, 1H), 2.48 (d, J = 7.2 Hz, 2H), 7.16 (d, J = 8.0 Hz, 2H), 7.72 (d, J = 8.0 Hz, 2H); ^{13}C NMR ($CDCl_3$) δ 22.5 (2C), 25.0 (4C), 30.3, 45.8, 83.8 (2C), 128.7 (2C), 134.8 (2C), 145.3; HRMS (EI^+): *m*/*z* $[M]^+$ calcd for $C_{16}H_{25}BO_2$ 260.1951, found 260.1950. Anal. calcd for $C_{16}H_{25}BO_2$, C, 73.86; H, 9.69. found C, 73.83; H, 9.73.

4,4,5,5-Tetramethyl-2-(2-fluoro-4-biphenylyl)-1,3,2-dioxaborolane

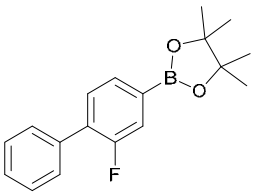

The title product was synthesized according to the general procedure A using 2-fluoro-4-biphenylboronic acid (1.24 g, 6 mmol) and pinacol (1.08 g, 9 mmol). The product was obtained as a white solid (1.31 g, 77%) after recrystallization (hexane / toluene).

IR (neat, cm^{-1}) 2977, 1517, 1404, 1355, 1327, 1202, 1140, 1089, 965, 913, 851, 770, 727, 702, 681; ^1H NMR ($CDCl_3$) δ 1.36 (s, 12H), 7.37 (m, 1H), 7.42–7.47 (m, 3H), 7.56–7.59 (m, 3H), 7.63 (dd, J = 7.6, 1.0 Hz, 1H); ^{13}C NMR ($CDCl_3$) δ 24.9, 84.2 (2C), 122.0 (J = 20.7 Hz), 127.9, 128.5 (2C), 129.1 (2C), 130.3, 130.7, 131.8 (J = 13.1 Hz), 135.8, 159.5 (J = 248.9 Hz); HRMS (EI^+): *m*/*z* $[M]^+$ calcd for $C_{18}H_{20}BFO_2$ 298.1544, found 298.1543. Anal. calcd for $C_{18}H_{20}BFO_2$, C, 72.51; H, 6.76. found C, 72.36; H, 6.75.

4,4,5,5-Tetramethyl-2-(3-phenoxyphenyl)-1,3,2-dioxaborolane

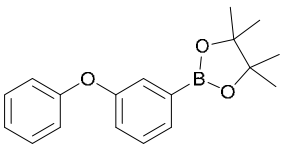

The title product was synthesized according to general procedure A using 3-phenoxybenzeneboronic acid (1.0 g, 5 mmol) and pinacol (0.67 g, 6 mmol). The product was obtained as a white solid (1.14 g, 82%) after recrystallization (hexane).

IR (neat, cm^{-1}) 2981, 1594, 1576, 1487, 1423, 1353, 1325, 1307, 1237, 1140, 1069, 966, 921, 856, 789, 706, 695, 672; ^1H NMR ($CDCl_3$) δ 1.33 (s, 12H), 6.98 (d, J = 7.6 Hz, 2H), 7.05–7.12 (m, 2H), 7.29–7.36 (m, 3H), 7.48 (d, J = 2,5 Hz, 1H), 7.56 (dt, J = 7.3, 1.0 Hz, 1H); ^{13}C NMR ($CDCl_3$) δ 24.9 (4C), 83.9 (2C), 118.5 (2C), 122.3, 122.9, 125.3, 129.2, 129.7(2C), 129.8, 156.5, 157.7; HRMS (EI^+): *m*/*z* $[M]^+$ calcd for $C_{18}H_{21}BO_3$ 296.1587, found 296.1589. Anal. calcd for $C_{18}H_{21}BO_3$, C, 73.00; H, 7.15. found C, 73.06; H, 7.17.

4,4,5,5-Tetramethyl-2-(2-fluorenyl)-1,3,2-dioxaborolane

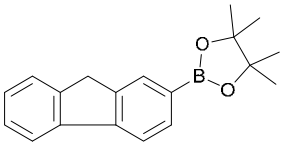

Bis(pinacolato)diboron (1.54 g, 6 mmol), 2-bromofluorene (1.22 g, 5 mmol), potassium acetate (0.32 g, 3 mmol) and [1,1'-bis(diphenylphosphino)ferrocene]-palladium(II) dichloride (28 mg, 0.1 mmol) were dissolved in 1,4-dioxane (5 mL), and the mixture was stirred at 90 °C for 45 h. Then water (3 mL) was added to the reaction mixture and the aqueous layer was extracted with EtOAc (20 mL ×3). The organic layers were combined, dried with $MgSO_4$, and filtered. The solvent was removed under reduced pressure to afford the crude product. The title product was obtained as a white solid (0.83 g, 57%) after recycling GPC.

IR (neat, cm^{-1}) 2975, 1613, 1418, 1353, 1313, 1266, 1143, 1079, 963, 856, 771, 736, 664; ^1H NMR ($CDCl_3$) δ 1.37 (s, 12H), 3.60 (s, 2H), 7.30–7.41 (m, 2H), 7.55 (d, J = 7.4 Hz, 1H), 7.78–7.50 (m, 3H), 8.00 (s, 1H); ^{13}C NMR ($CDCl_3$) δ 24.0 (4C), 36.7, 83.9 (2C), 119.3, 120.4, 125.1, 126.7, 127.2, 131.3, 133.4, 141.5, 142.5, 143.9, 144.6; HRMS (EI^+): m/z $[M]^+$ calcd for $C_{19}H_{21}BO_2$ 292.1638, found 292.1637. Anal. calcd for $C_{19}H_{21}BO_2$, C, 78.10; H, 7.24. found C, 78.23; H, 7.25.

4,4,5,5-Tetramethyl-2-(6-methoxynaphthalen-2-yl)-1,3,2-dioxaborolane

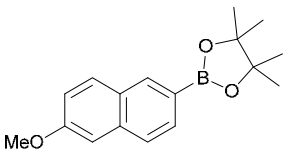

To a solution of 2-bromo-4-methoxynaphthalene (4.71 g, 20 mmol) in toluene-THF (4:1 v/v, 80 mL), BuLi (14.5 mL, 1.66 M in hexane, 24 mmol) was added dropwise over 7 min at −78 °C, and the mixture was stirred at that temperature for 30 min. Then 2-isopropoxy-4,4,5,5-tetramethyl-1,3,2-dioxaborolane (6.12 mL, 30 mmol) was added dropwise over 5 min. The reaction mixture was stirred for 1 h and warmed up to room temperature. After stirring for 30 h, the reaction mixture was quenched by a solution of NH_4Cl (1.78 g, 33 mmol) in water (30 mL). The aqueous layer was extracted with EtOAc (20 mL × 3). The organic layers were combined, dried with $MgSO_4$, and filtered. The solvent was removed under reduced pressure to afford the crude product. The title product was obtained as a white solid (5.40 g, 95%) after filtration using MeOH.

^1H NMR ($CDCl_3$) δ 1.38 (s, 12H), 3.92 (s, 3H), 7.12–7.14 (m, 2H), 7.71 (d, J = 8.2 Hz, 1H), 7.79 (t, J = 10.9 Hz, 2H), 8.29 (s, 1H); ^{13}C NMR ($CDCl_3$) δ 24.9 (4C), 55.3, 83.8 (2C), 105.6, 118.7, 125.9, 128.4, 130.2, 131.1, 136.0, 136.4, 158.5; Anal. calcd for $C_{17}H_{21}BO_3$, C, 71.86; H, 7.45. found C, 71.95; H, 7.40. All analytical data are in good accordance with those reported in the literature.[23]

Iron-Catalyzed Enantioselective Coupling

General Procedure B: To a solution of arylboronic acid pinacol ester (1.1 mmol) in THF (2 mL), BuLi (0.65 mL, 1.60 M in hexane, 1.05 mmol) was added at −40 °C. The mixture was stirred at that temperature for 30 min, and then at 0 °C for 30 min. The solvent was removed under reduced pressure at room temperature. To the residual borate, THF (1.1 mL) was added. This borate (1.0 M, in THF) was used for the following cross coupling.

To a flame–dried Schlenk flask filled up with argon gas, FeCl2 (3.6 mg, 5 mol%), (*R,R*)-QuinoxP* (16.4 mg, 10 mol%), and THF (0.5 mL) were added. This mixture was stirred at 25 °C for 30 minutes. Then undecane (36.44 mg, 0.2331 mmol), lithium borate (1.0 M THF solution, 1.0 mL, 1.00 mmol), *tert*-butyl 2-bromopropionate (104.36 mg, 0.4991 mmol) and $MgBr_2$ (0.2 M THF solution, 0.50 mL, 0.10 mmol) were added. This mixture was stirred at 25 °C for 5 hours, and quenched with sat. NH_4Cl aq. (2 mL) and the aqueous layer was extracted with EtOAc (2 mL × 4). The organic layers were combined, dried with $MgSO_4$, and filtered. The solvent was removed under reduced pressure to afford the crude product.

***tert*-Butyl (*S*)-2-phenylpropionate**

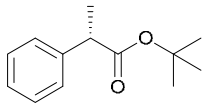

The reaction was performed according to the general procedure B: the corresponding lithium borate (0.40 mL, 1.0 M in THF, 0.40 mmol) and *tert*-butyl 2-bromopropionate (39.8 mg, 0.19 mmol) were used. The product was obtained in 99% yield with 84:16 er.

The er was determined by HPLC on a CHIRALCEL OJ-3R column (4.6 mm i.d., 150 mm length) under the following conditions: 50 % CH_3CN aq, 1.0 mL/min, 25 °C, retention times (t_r) = 14.8 min (major) and 18.21 min (minor).

^{1}H NMR ($CDCl_3$) δ 1.39 (s, 9H), 1.45 (d, J = 7.2 Hz, 3H), 3.61 (q, J = 7.1 Hz, 1H), 7.21–7.31 (m, 5H). The NMR spectrum is in good accordance with previous literature data.[6c]

2,3,3-Trimethylbut-2-yl (*S*)-2-phenylpropionate

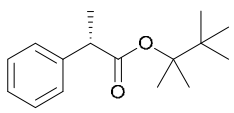

The reaction was performed according to the general procedure B: the corresponding lithium borate (0.60 mL, 1.0 M in THF, 0.60 mmol) and 2,3,3-trimethylbut-2-yl 2-bromopropionate (76.5 mg, 0.30 mmol) were used. The product was obtained in 92% yield with 85:15 er.

The er was determined by HPLC on a CHIRALCEL OJ-3R column (4.6 mm i.d., 150 mm length) under the following conditions: 60 % CH_3CN aq, 1.0 mL/min, 25 °C, retention times (t_r) = 13.3 min (major) and 16.8 min (minor).

^{1}H NMR ($CDCl_3$) δ 0.83 (s, 9H), 1.38 (s, 3H), 1.46 (s, 3H), 1.47 (d, J = 6.5 Hz, 3H), 3.63

(q, J = 7.2 Hz, 1H), 7.21–7.34 (m, 5H). The NMR spectrum is in good accordance with previous literature data.[6c]

Methyl (*S*)-2-phenylpropionate

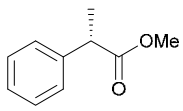

The reaction was performed according to the general procedure B: the corresponding lithium borate (1.0 mL, 1.0 M in THF, 1.0 mmol) and methyl 2-bromopropionate (81.3 mg, 0.49 mmol) were used. The product was obtained in 88% yield with 56:44 er.

The er was determined by HPLC on a CHIRALCEL OJ-3R column (4.6 mm i.d., 150 mm length) under the following conditions: 50 % CH_3CN aq, 1.0 mL/min, 25 °C, retention times (t_r) = 6.5 min (major) and 7.1 min (minor).

^{1}H NMR ($CDCl_3$) δ 1.50 (d, J = 7.2 Hz, 3H), 3.66 (s, 3H), 3.72 (q, J = 7.2 Hz, 1H), 7.23–7.34 (m, 5H); ^{13}C NMR ($CDCl_3$) δ 18.6, 45.4, 52.0, 127.1, 127.5 (2C), 128.6 (2C), 140.6, 175.0; The NMR spectrum is in good accordance with previous literature data.[24]

Isopropyl (*S*)-2-phenylpropionate

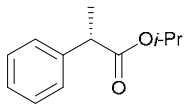

The reaction was performed according to the general procedure B: the corresponding lithium borate (0.60 mL, 1.0 M in THF, 0.60 mmol) and isopropyl 2-bromopropionate (58.4 mg, 0.30 mmol) were used. The product was obtained in 82% yield with 75:25 er.

The er was determined by HPLC on a CHIRALCEL OD-3 column (4.6 mm i.d., 150 mm length) under the following conditions: hexane, 1.0 mL/min, 3 °C, retention times (t_r) = 23.1 min (major) and 27.4 min (minor).

^{1}H NMR ($CDCl_3$) δ 1.13 (d, J = 6.2 Hz, 3H) 1.22 (d, J = 6.3 Hz, 3H), 1.48 (d, J = 7.2 Hz, 3H), 3.67(q, J = 7.2 Hz, 1H), 4.99 (sept, J = 6.3 Hz, 1H), 7.22–7.35 (m, 5H). The NMR spectrum is in good accordance with previous literature data.[25]

Synthesis of α-arylpropionic acid

General procedure C: The coupling reaction was performed according to the general procedure B. Then, to a solution of the crude product in CH_2Cl_2 (1.5 mL) was added trifluoroacetic acid (0.38 mL, 5 mmol) at room temperature, and the mixture was stirred for 6 h. Then the reaction mixture was quenched by sat. $NaHCO_3$ aq. (5 mL). The aqueous layer was extracted with CH_2Cl_2 (2 mL × 5). The organic layers were combined and extracted with 2 M NaOH aq. (2 mL × 5) to separate the desired carboxylic acid from other byproducts. Then the aqueous layers were combined and washed with hexane (2 mL × 10). To the aqueous layer, 2 M HCl aq was added to adjust the pH 3. Finally, the

acidic aqueous layer was extracted by CH_2Cl_2 (2 mL × 5). The organic layers were combined, dried with $MgSO_4$, and filtered. The solvent was removed under reduced pressure to afford the semi-purified product.

(*S*)-2-Phenylpropionic acid

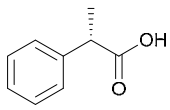

The reaction was performed according to the general procedure C: the corresponding lithium borate (0.40 mL, 1.0 M in THF, 0.40 mmol) and *tert*-butyl 2-bromopropionate (39.8 mg, 0.19 mmol) were used. The semi-purified product was further purified by silica gel column chromatography (hexane/EtOAc = 95/5 to 40/60) to give the title product in 95% yield (27.2 mg) with 84:16 er as a yellow liquid.

The er was determined by HPLC on a CHIRALCEL OJ-3R column (4.6 mm i.d., 150 mm length) under the following conditions: 10 mM H_3PO_4 aq/CH_3CN = 75/25, 1.0 mL/min, 25 °C, retention times (t_r) = 15.3 min (major) and 16.9 min (minor).
^{1}H NMR ($CDCl_3$) δ 1.51 (d, *J* = 7.2 Hz, 3H), 3.74 (q, *J* = 7.2 Hz, 1H), 7.25–7.36 (m, 5H); ^{13}C NMR ($CDCl_3$) δ 18.1, 45.3, 127.4, 127.6 (2C), 128.8 (2C), 139.7, 180.5; Anal. calcd for $C_9H_{10}O_2$, C, 71.98; H, 6.71. found C, 71.75; H, 6.82. $[\alpha]^{20}_D$ +51.0 (c 0.47, EtOH). Analytical data are in good accordance with those reported in the literature.[26]

(*S*)-2-(4-Methylphenyl)propionic acid

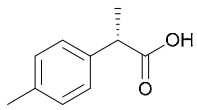

The reaction was performed according to the general procedure C: the corresponding lithium borate (0.40 mL, 1.0 M in THF, 0.40 mmol) and *tert*-butyl 2-bromopropionate (35.8 mg, 0.17 mmol) were used. The semi-purified product was further purified by silica gel column chromatography (hexane/EtOAc = 95/5 to 40/60) to give the title product in 90% yield (25.4 mg) with 81:19 er as a yellow liquid.

The er was determined by HPLC on a CHIRALCEL OD-3 column (4.6 mm i.d., 150 mm length) under the following conditions: hexane/*i*-PrOH/TFA = 99/1/0.1, 1.0 mL/min, 20 °C, retention times (t_r) = 11.6 min (minor) and 13.3 min (major).
^{1}H NMR ($CDCl_3$) δ 1.50 (d, *J* = 7.2 Hz, 3H), 2.33 (s, 3 H), 3.70 (q, *J* = 7.2 Hz, 1H), 7.14 (d, *J* = 8.2 Hz, 2H), 7.21 (d, *J* = 8.2 Hz, 2H); ^{13}C NMR ($CDCl_3$) δ 18.3, 21.2, 45.0, 127.6 (2C), 129.5 (2C), 137.0, 137.2, 180.4; Anal. calcd for $C_{10}H_{12}O_2$, C, 73.15; H, 7.37. found C, 72.57; H, 7.59. $[\alpha]^{20}_D$ + 49.0 (c 0.34, EtOH). All analytical data are in good accordance with those reported in the literature.[26]

(*S*)-2-(4-Methoxyphenyl)propionic acid

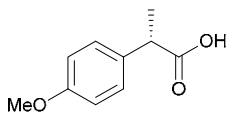

The reaction was performed according to general procedure C: the corresponding lithium borate (0.40 mL, 1.0 M in THF, 0.40 mmol) and *tert*-butyl 2-bromopropionate (48.2 mg, 0.23 mmol) were used. The semi-purified product was further purified by silica gel column chromatography (hexane/EtOAc = 95/5 to 40/60) to give the title product in 85% yield (35.2 mg) with 82:18 er as a white solid.

The er was determined by HPLC on a CHIRALCEL OD-3 column (4.6 mm i.d., 150 mm length) under the following conditions: hexane/*i*-PrOH/TFA = 99/1/0.1, 1.0 mL/min, 25 °C, retention times (t_r) = 27.6 min (minor) and 30.3 min (major).
^{1}H NMR ($CDCl_3$) δ 1.49 (d, *J* = 7.2 Hz, 3H), 3.69 (q, *J* = 7.2 Hz, 1 H), 3.79 (s, 3H), 6.86 (d, *J* = 8.6 Hz, 2H), 7.24 (d, *J* = 8.7 Hz, 2H); ^{13}C NMR ($CDCl_3$) δ 18.2, 44.5, 55.4, 114.2 (2C), 128.7 (2C), 132.0, 159.0, 180.8; Anal. calcd for $C_{10}H_{12}O_3$, C, 66.65; H, 6.71. found C, 66.54; H, 6.79. $[\alpha]^{20}_D$ + 36.6 (c 0.51, EtOH). All analytical data are in good accordance with those reported in the literature.[27]

(*S*)-2-[4-(Dimethylamino)phenyl]propionic acid

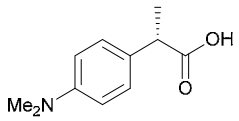

The reaction was performed according to general procedure C: the corresponding lithium borate (1.00 mL, 1.0 M in THF, 1.00 mmol) and *tert*-butyl 2-bromopropionate (104.9 mg, 0.50 mmol) were used. The semi-purified product was further purified by silica gel column chromatography (hexane/EtOAc = 95/5 to 40/60) to give the title product in 89% yield (86.0 mg) with 82:18 er as a white solid.

The er was determined by HPLC on a CHIRALCEL OD-3 column (4.6 mm i.d., 150 mm length) under the following conditions: hexane/*i*-PrOH/TFA = 95/5/0.1, 1.0 mL/min, 25 °C, retention times (t_r) = 9.8 min (minor) and 10.9 min (major).
^{1}H NMR ($CDCl_3$) δ 1.47 (d, *J* = 7.2 Hz, 3H), 2.92 (s, 6 H), 3.64 (q, 7.2 Hz, 1H), 6.70 (d, *J* = 8.8 Hz, 2H), 7.18 (d, *J* = 8.7 Hz, 2H); ^{13}C NMR ($CDCl_3$) δ 18.2, 40.9 (2C), 44.4, 113.1 (2C), 128.0, 128.4 (2C), 150.0, 180.8; Anal. calcd for $C_{11}H_{15}NO_2$, C, 68.37; H, 7.82; N, 7.25. found C, 68.38; H, 7.92; N, 6.92. $[\alpha]^{20}_D$ + 37.5 (c 0.53, EtOH). All analytical data are in good accordance with those reported in the literature.[28]

(*S*)-2-[4-(Trifluoromethyl)phenyl]propionic acid

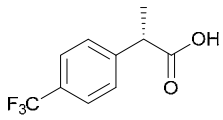

The reaction was performed according to general procedure C: the corresponding lithium borate (0.40 mL, 1.0 M in THF, 0.40 mmol) and *tert*-butyl 2-bromopropionate (43.45 mg, 0.21 mmol) were used.

The semi-purified product was further purified by silica gel column chromatography (hexane/EtOAc = 95/5 to 40/60) to give the title product in 81% yield (36.9 mg) with 76:24 er as a yellow solid.

The er was determined by HPLC on a CHIRALCEL OJ-3R column (4.6 mm i.d., 150 mm length) under the following conditions: 10 mM H_3PO_4 aq/CH_3CN = 75/25, 1.0 mL/min, 25 °C, retention times (t_r) = 24.6 min (minor) and 28.3 min (major).
^{1}H NMR ($CDCl_3$) δ 1.54 (d, *J* = 7.2 Hz, 3H), 3.81 (q, *J* = 7.2 Hz, 1H), 7.44 (d, *J* = 8.1 Hz, 2H), 7.59 (d, *J* = 8.1 Hz, 2H); ^{13}C NMR ($CDCl_3$) δ18.2, 45.4, 124.2 (q, *J* = 172.4), 125.8 (d, *J* = 3.8 Hz, 2C), 128.2 (2C), 129.9 (q, *J* = 31.9 Hz), 143.7, 180.2; Anal. calcd for $C_{10}H_9F_3O_2$: C, 55.05; H, 4.16. found C, 55.55; H, 4.38. $[\alpha]^{20}_D$ + 23.2 (c 0.54, EtOH). All analytical data are in good accordance with those reported in the literature.[29]

(*S*)-2-(4-Chlorophenyl)propionic acid

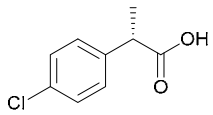

The reaction was performed according to general procedure C: the corresponding lithium borate (1.00 mL, 1.0 M in THF, 1.00 mmol) and *tert*-butyl 2-bromopropionate (100.3 mg, 0.48 mmol) were used. The semi-purified product was further purified by silica gel column chromatography (hexane/EtOAc = 95/5 to 40/60) to give the title product in 83% yield (72.9 mg) with 84:16 er as a yellow solid.

The er was determined by HPLC on a CHIRALCEL OD-3R column (4.6 mm i.d., 150 mm length) under the following conditions: 10 mM H_3PO_4 aq/CH_3CN = 80/20, 1.0 mL/min, 25 °C, retention times (t_r) = 43.9 min (major) and 46.5 min (minor).
^{1}H NMR ($CDCl_3$) δ 1.49 (d, *J* = 7.2 Hz, 3H), 3.71 (q, *J* = 7.2 Hz, 1H), 7.44 (d, *J* = 8.1 Hz, 2H), 7.23–7.31 (m, 4H); ^{13}C NMR ($CDCl_3$) δ 18.2, 44.9, 129.0 (2C), 129.1 (2C), 133.5, 138.3, 189.6; Anal. calcd for $C_9H_9ClO_2$, C, 58.55; H, 4.91. found C, 58.62; H, 5.16. $[\alpha]^{20}_D$ + 33.6 (c 0.48, EtOH). All analytical data are in good accordance with those reported in the literature.[27]

(*S*)-2-(2-Methylphenyl)propionic acid

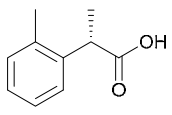

The reaction was performed according to general procedure C: the corresponding lithium borate (0.40 mL, 1.0 M in THF, 0.40 mmol) and *tert*-butyl 2-bromopropionate (42.2 mg, 0.20 mmol) were used. The semi-purified product was further purified by silica gel column chromatography (hexane/EtOAc = 95/5 to 40/60) to give the title product in 65% yield (21.4 mg) with 88:12 er as a yellow solid.

The er was determined by HPLC on a CHIRALCEL OD-3R column (4.6 mm

i.d., 150 mm length) under the following conditions: 10 mM H_3PO_4 aq/CH_3CN = 75/25, 1.0 mL/min, 25 °C, retention times (t_r) = 17.1 min (major) and 20.1 min (minor).
^{1}H NMR ($CDCl_3$) δ 1.49 (d, *J* = 7.2 Hz, 3H), 2.38 (s, 3 H), 3.98 (q, *J* = 7.1 Hz, 1H), 7.16–7.21 (m, 3H), 7.28–7.30 (m, 1H); ^{13}C NMR ($CDCl_3$) δ 17.7, 19.8, 41.2, 126.6, 126.7, 127.3, 130.7, 136.1, 138.5, 180.7; Anal. calcd for $C_{10}H_{12}O_2$, C, 73.15; H, 7.37. found C, 72.69; H, 7.55 $[\alpha]^{20}_D$ + 55.4 (c 0.43, EtOH). All analytical data are in good accordance with those reported in the literature.[29,30]

(*S*)-2-(Naphthalen-2-yl)propionic acid

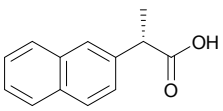

The reaction was performed according to general procedure C: the corresponding lithium borate (0.60 mL, 1.0 M in THF, 0.60 mmol) and *tert*-butyl 2-bromopropionate (62,4 mg, 0.30 mmol) were used. The semi-purified product was further purified by silica gel column chromatography (hexane/EtOAc = 95/5 to 40/60) to give the title product in 91% yield (54.2 mg) with 77:23 er as a white solid.

The er was determined by HPLC on a CHIRALCEL OJ-3R column (4.6 mm i.d., 150 mm length) under the following conditions: 10 mM H_3PO_4 aq/CH_3CN = 70/30, 1.0 mL/min, 25 °C, retention times (t_r) = 33.5 min (major) and 37.0 min (minor).
^{1}H NMR ($CDCl_3$) δ 1.60 (d, *J* = 7.2 Hz, 3H), 3.90 (q, *J* = 7.1 Hz, 1H), 7.42–7.49 (m, 3H), 7.75 (s, 1H), 7.79–7.81 (m, 3H); ^{13}C NMR ($CDCl_3$) δ 18.1, 45.4, 125.7, 125.9, 126.2, 126.3, 127.6, 127.8, 128.4, 132.7, 133.4, 137.1, 180.2; Anal. calcd for $C_{13}H_{12}O_2$, C, 77.98; H, 6.04. found C, 77.37; H, 6.05. $[\alpha]^{20}_D$ + 35.5 (c 0.36, EtOH). Analytical data are in good accordance with those reported in the literature.[27]

***tert*-Butyl (*S*)-2-(1-Methyl-1H-indol-5-yl) propionate**

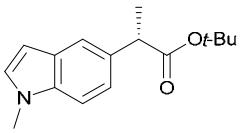

The reaction was performed according to general procedure B: the corresponding lithium borate (1.00 mL, 1.0 M in THF, 1.00 mmol) and *tert*-butyl 2-bromopropionate (100.7 mg, 0.48 mmol) were used. The semi-purified product was further purified by GPC to give the title product in 61% yield (75.6 mg) with 81:19 er as a white solid.

The er was determined by HPLC on a CHIRALCEL OJ-3R column (4.6 mm i.d., 150 mm length) under the following conditions: 55% CH_3CN aq, 1.0 mL/min, 25 °C, retention times (t_r) = 13.0 min (major) and 17.0 min (minor).
IR (neat, cm^{-1}) 2972, 2936, 1710, 1513, 1492, 1447, 1424, 1365, 1339, 1311, 1248, 1152, 1139, 1086, 1052, 1014, 875, 847, 803, 784, 762, 736, 682; ^{1}H NMR ($CDCl_3$) δ 1.38 (s, 9H), 1.49 (d, *J* = 7.2 Hz, 3H), 3.70 (q, *J* = 7.2 Hz, 1H), 3.75 (s, 3H), 6.43 (dd, *J* = 3.1, 0.8

Hz, 1H), 7.01 (d, J = 3.1 Hz, 1H), 7.17 (dd, J = 8.4, 1.7 Hz, 1H), 7.25 (d, J = 8.5 Hz, 1H), 7.53 (s, 1H); ^{13}C NMR ($CDCl_3$) δ19.3, 28.1 (3C), 33.0, 46.6, 80.2, 101.0, 109.2, 119.5, 121.4, 128.7, 129.2, 132.4, 135.0, 174.8; HRMS (EI^+): m/z $[M]^+$ calcd for $C_{16}H_{21}NO_2$ 259.1572, found 259.1575. Anal. calcd for $C_{16}H_{21}NO_2$, C, 74.10; H, 8.16; N, 5.40. found C, 74.03; H, 8.25; N, 5.31. $[\alpha]^{20}_D$ + 26.3 (c 0.50, EtOH).

(*S*)-2-[(2-Methylpropyl)phenyl]propionic acid [(*S*)-ibuprofen]

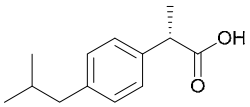

The reaction was performed according to general procedure C: the corresponding lithium borate (1.00 mL, 1.0 M in THF, 1.00 mmol) and *tert*-butyl 2-bromopropionate (100.4 mg, 0.48 mmol) were used. The semi-purified product was further purified by silica gel column chromatography (hexane/EtOAc = 95/5 to 40/60) to give the title product in 95% yield (93.6 mg) with 82:18 er as a yellow liquid.

The er was determined by HPLC on a CHIRALCEL OJ-3R column (4.6 mm i.d., 150 mm length) under the following conditions: 10 mM H_3PO_4 aq/CH_3CN = 70/30, 1.0 mL/min, 25 °C, retention times (t_r) = 45.4 min (minor) and 49.3 min (major).
^{1}H NMR ($CDCl_3$) δ 0.89 (d, J = 6.6 Hz, 6H), 1.49 (d, J = 7.1 Hz, 3H), 1.84 (hept, J = 6.8 Hz, 1H), 2.44 (d, J = 7.2 Hz, 2H), 3.70 (q, J = 7.2 Hz, 1H), 7.09 (d, J = 8.0 Hz, 2H), 7.21 (d, J = 8.1 Hz, 2H); ^{13}C NMR ($CDCl_3$) δ 18.2, 22.5 (2C), 30.3, 45.1, 45.2, 127.4(2C), 129.5 (2C), 137.1, 141.0, 181.0; Anal. calcd for $C_{13}H_{18}O_2$, C, 75.69; H, 8.80. found C, 75.57; H, 8.94. $[\alpha]^{20}_D$ +28.9 (c 0.51, EtOH). Analytical data are in good accordance with those reported in the literature.[6c]

(*S*)-2-(2-Fluoro-4-biphenylyl)propionic acid [(*S*)-flurbiprofen]

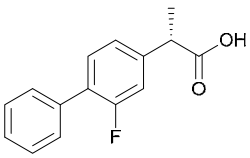

The reaction was performed according to general procedure C: the corresponding lithium borate (1.00 mL, 1.0 M in THF, 1.00 mmol) and *tert*-butyl 2-bromopropionate (100.7 mg, 0.48 mmol) were used. The semi-purified product was further purified by silica gel column chromatography (hexane/EtOAc = 95/5 to 40/60) to give the title product in 56% yield (61.1 mg) with 81:19 er as a yellow solid.

The er was determined by HPLC on a CHIRALCEL OJ-3R column (4.6 mm i.d., 150 mm length) under the following conditions: 10 mM H_3PO_4 aq/CH_3CN = 70/30, 1.0 mL/min, 25 °C, retention times (t_r) = 58.5 min (minor) and 62.3 min (major).
^{1}H NMR ($CDCl_3$) δ 1.55 (d, J = 7.2 Hz, 3H), 3.78 (q, J = 7.2 Hz, 1H), 7.12–7.18 (m, 2H), 7.48–7.35 (m, 4H), 7.52 (d, J = 8.4 Hz, 2H); ^{13}C NMR ($CDCl_3$) δ 18.1, 45.0, 115.5 (J = 23.5 Hz), 123.8, 127.9, 128.3 (J = 13.1 Hz), 128.6 (2C), 129.1 (2C), 131.0, 135.5, 141.0,

159.8 (J = 249.0 Hz), 180.4; Anal. calcd for $C_{15}H_{13}FO_2$, C, 73.76; H, 5.36. found C, 73.37; H, 5.46. $[\alpha]^{20}_D$ + 23.8 (c 0.49, EtOH). All analytical data are in good accordance with those reported in the literature.[31]

(*S*)-2-(3-Phenoxyphenyl)propionic acid [(*S*)-phenoprofen]

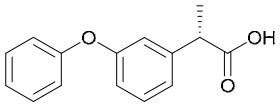

The reaction was performed according to general procedure C: the corresponding lithium borate (1.00 mL, 1.0 M in THF, 1.00 mmol) and *tert*-butyl 2-bromopropionate (107.8 mg, 0.52 mmol) were used. The semi-purified product was further purified by silica gel column chromatography (hexane/EtOAc = 95/5 to 40/60) to give the title product in 52% yield (64.9 mg) with 82:18 er as a yellow liquid.

The er was determined by HPLC on a CHIRALCEL OJ-3R column (4.6 mm i.d., 150 mm length) under the following conditions: 10 mM H_3PO_4 aq/CH_3CN = 70/30, 1.0 mL/min, 25 °C, retention times (t_r) = 61.2 min (major) and 68.3 min (minor).
^{1}H NMR ($CDCl_3$) δ 1.50 (d, J = 7.2 Hz, 3H), 3.71 (q, J = 7.2 Hz, 1H), 6.88 (ddd, J = 8.2, 2.5, 0.86 Hz, 1H), 7.00–7.02 (m, 3H), 7.06 (d, J = 7.8 Hz, 1H), 7.10 (tt, J = 7.3, 1.1 Hz, 1H), 7.28–7.35 (m, 3H); ^{13}C NMR ($CDCl_3$) δ 18.0, 45.1, 117.5, 118.2, 119.0 (2C), 122.4, 123.4, 129.8 (2C), 129.9, 141.7, 156.9, 157.5, 179.8; Anal. calcd for $C_{15}H_{14}O_3$, C, 74.36; H, 5.82. found C, 74.27; H, 5.86. $[\alpha]^{20}_D$ +26.6 (c 0.52, EtOH). Analytical data are in good accordance with those reported in the literature.[31]

(*S*)-2-(2-Fluorenyl)propionic acid [(*S*)-cicloprofen]

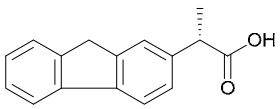

The reaction was performed according to general procedure C: the corresponding lithium borate (1.00 mL, 1.0 M in THF, 1.00 mmol) and *tert*-butyl 2-bromopropionate (103.9 mg, 0.50 mmol) were used. The semi-purified product was further purified by silica gel column chromatography (hexane/EtOAc = 95/5 to 40/60) to give the title product in 49% yield (58.0mg) with 81:19 er as a white solid.

The er was determined by HPLC on a CHIRALCEL OJ-3R column (4.6 mm i.d., 150 mm length) under the following conditions: 10 mM H_3PO_4 aq/CH_3CN = 70/30, 1.0 mL/min, 25 °C, retention times (t_r) = 73.7 min (minor) and 80.2 min (major).
^{1}H NMR ($CDCl_3$) δ 1.57 (d, J = 7.2 Hz, 3H), 3.82 (q, J = 7.1 Hz, 1H), 3.88 (s, 2H), 7.27–7.38 (m, 3H), 7.51–7.53 (m, 2H), 7.72–7.76 (m, 2H); ^{13}C NMR ($CDCl_3$) δ 18.5, 37.0, 45.6, 120.0, 120.1, 124.4, 125.1, 126.5, 126.8, 126.9, 138.5, 141.2, 141.4, 143.4, 143.9, 180.8; Anal. calcd for $C_{16}H_{14}O_2$, C, 80.65; H, 5.92; Found: C, 80.32; H, 5.97. $[\alpha]^{20}_D$ + 36.7 (c 0.49, EtOH). All analytical data are in good accordance with those reported in the

literature.[32]

(*S*)-2-(6-Methoxynaphth-2-yl)propionic acid [(*S*)-naproxen]

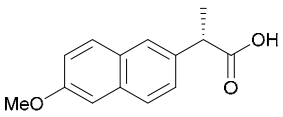

The reaction was performed according to general procedure C: the corresponding lithium borate (151 mg, 0.53 mmol) and *tert*-butyl 2-bromopropionate (48.0 mg, 0.23 mmol) were used. The semi-purified product was further purified by silica gel column chromatography (hexane/EtOAc = 95/5 to 40/60) to give the title product in 83% yield (42.3 mg) with 80:20 er as a yellow liquid.

The er was determined by HPLC on a CHIRALPAK AD-3R column (4.6 mm i.d., 150 mm length) under the following conditions: 10 mM H_3PO_4 aq/CH_3CN = 70/30, 1.0 mL/min, 25 °C, retention times (t_r) = 18.1 min (minor) and 21.1 min (major).
^{1}H NMR ($CDCl_3$) δ 1.57 (d, *J* = 7.2 Hz, 3H), 3.86 (q, *J* = 7.2 Hz, 1H), 3.90 (s, 3H), 7.09–7.14 (m, 2H), 7.40 (dd, *J* = 8.4, 1.5 Hz, 1H), 7.68 (d, *J* = 8.9 Hz, 3H); ^{13}C NMR ($CDCl_3$) δ 18.1, 45.3, 55.3, 105.6, 119.0, 126.1, 126.2, 127.2, 128.9, 129.3, 133.8, 134.9, 157.7, 180.5; Anal. calcd for $C_{16}H_{14}O_2$, C, 80.65; H, 5.92; Found: C, 80.32; H, 5.97. $[\alpha]^{20}_D$ + 29.8 (c 0.44, EtOH). All analytical data are in good accordance with those reported in the literature.[27]

Synthesis and stoichiometric reaction of $FeCl_2$/(*R*,*R*)-QuinoxP* and $FeCl_2$/(*R*,*R*)-BenzP*

Synthesis of $FeCl_2$/(*R*,*R*)-BenzP*: $FeCl_2$/(*R*,*R*)-BenzP* was synthesized according to the previously reported method.[13a]

Synthesis of $FeCl_2$/(*R*,*R*)-QuinoxP*: To a mixture of $FeCl_2$ (16.6 mg, 0.13 mmol) and (*R*,*R*)-QuinoxP* (32.7 mg, 0.12 mmol) was added EtOH (1.0 ml), and the mixture was stirred at 50 ºC for 3h. After filtration, the filtrate was condensed and recrystallized from Et2O and hexane to afford the iron complex (32.2 mg, 66% yield).
^{1}H NMR (*d*-THF) δ 7.67, 8.80, 9.0, 91.73; Anal. calcd for $C_{18}H_{28}Cl_2FeN_2P_2$ C, 46.88; H, 6.12, N, 6.08 found C, 46.83; H, 6.06; N, 6.00. HRMS (FAB$^+$): *m*/*z* $[M]^+$ calcd for $C_{18}H_{28}Cl_2FeN_2P_2$ 460.0455, found 460.0455.

Stoichiometric reaction of iron complex with phenyl borate: To a mixture of $FeCl_2$/(*R*,*R*)-QuinoxP* (9.2 mg, 0.02 mmol) and (*R*,*R*)-QuinoxP* (6.7 mg, 0.02 mmol) in *d*-THF (0.5 ml) was added lithium phenylborate (0.84 M *d*-THF solution, 0.12 mL, 0.1 mmol), which was generated according to the general procedure B, and $MgBr_2$ (0.2 M *d*-

THF solution, 0.1 mL, 0.02 mmol). The mixture was stirred at 25 °C, and conversion of the iron complex was monitored by the change of the signal at 91.73 ppm in ^{1}H NMR. The same reaction was performed by using $FeCl_2$/(*R*,*R*)-BenzP* (8.2 mg, 0.02 mmol) and (*R*,*R*)-BenzP* (5.6 mg, 0.02 mmol).

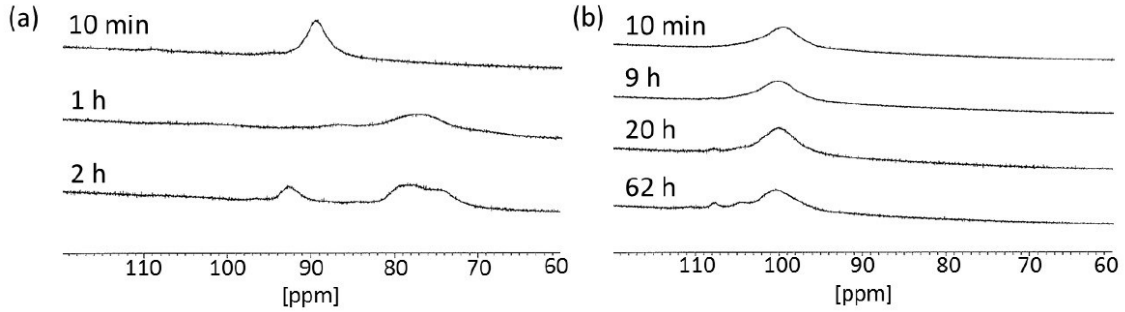

Figure 5. Stoichiometric reaction of (a) $FeCl_2$/(*R*,*R*)-QuinoxP* and (b) $FeCl_2$/(*R*,*R*)-BenzP* with phenyl boron reagent **2a** in the presence of $MgBr_2$

DFT Calculation

All calculations were carried out by using the Gaussian 09 program packages.[33] Geometry optimizations were performed at B3LYP/6-311G** with GD3BJ empirical dispersion.[34] Vibrational frequencies were calculated at the same level to characterize each stationary points (no imaginary frequencies for minima and one imaginary frequency for transition states).

Energies and optimized structures at recombination and reductive elimination step are shown in Figures 6 and 7. The reaction of iron complex **C** (S=2) with alkyl radical produce complex **D** (S=3/2). Optimization of the transition state at this recombination failed because this process would be almost barrierless as is the case with the previous report of iron-catalyzed enantioselective coupling with Grignard reagents. The resulting complex **D** undergo reductive elimination with an activation barrier of 11.8 kcal/mol to afford the complex **B** (S=3/2) and the product.

Iron complex **D** has a distorted trigonal bipyramidal structure, where the distance of Fe–C*ipso* (Ph) and Fe–C*ipso* (alkyl) is 1.98 and 2.05 Å, respectively. In **TS**, distance of Fe–C*ipso* (alkyl) is obviously elongated (2.27 Å), and on the other hand that of Fe–C*ipso* (Ph) hardly changes compared with complex **D**. However, C*ipso* (Ph) is significantly distorted in **TS** as shown by the dihedral angle of ∠C1C2C3Fe (Figures 7b and 7c). The previous report about the theoretical calculation of iron-catalyzed enantioselective coupling of Grignard reagents also suggested such structural changes at reductive elimination (elongation of Fe–C*ipso* (alkyl) and deformation of C*ipso* (Ph)).[13a]

Table 4. Gibbs Free Energy (G) at 298.150 K and 1.0000 atm.

	G (hartree)	G (kcal/mol)
FePhBr/(*R*,*R*)-QuinoxP* **C**	−5564.62479	−3491857.70197
Alkyl radical generated from **1a**	−424.999265	−266691.288780
FePhBr(alkyl)/(*R*,*R*)-QuinoxP* **D**	−5989.646488	−3758563.067684
FeBr/(*R*,*R*)-QuinoxP* **B**	−5332.962659	−3346487.398149
Transition state at reductive elimination **TS**	−5989.627694	−3758551.274261
Product **3a**	−656.697378	−412084.171668

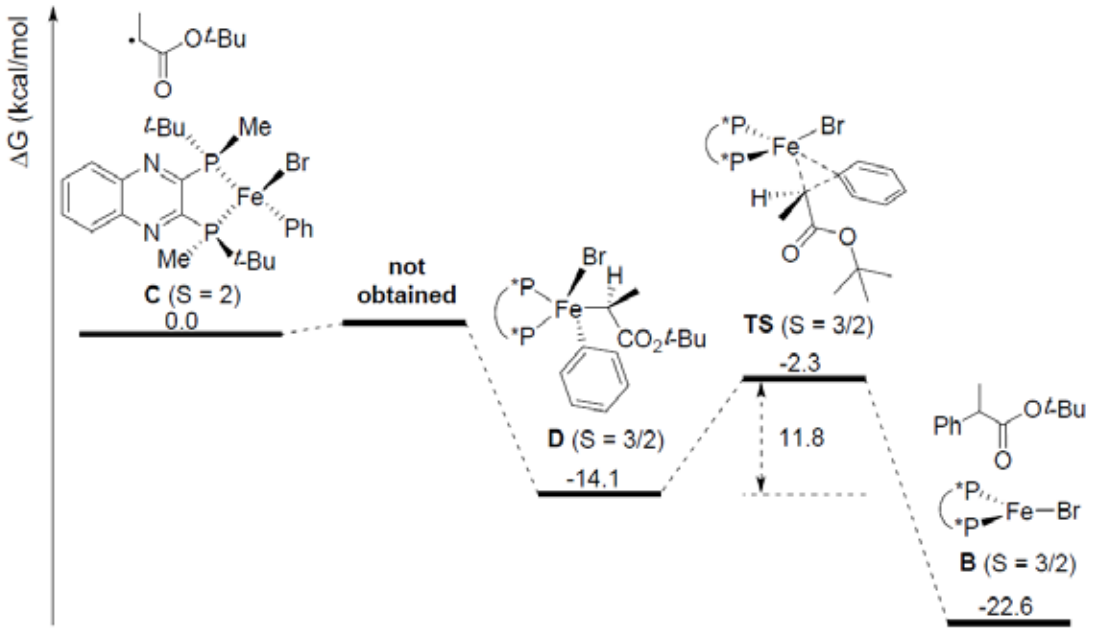

Figure 6. Energy profile for recombination and reductive elimination step.

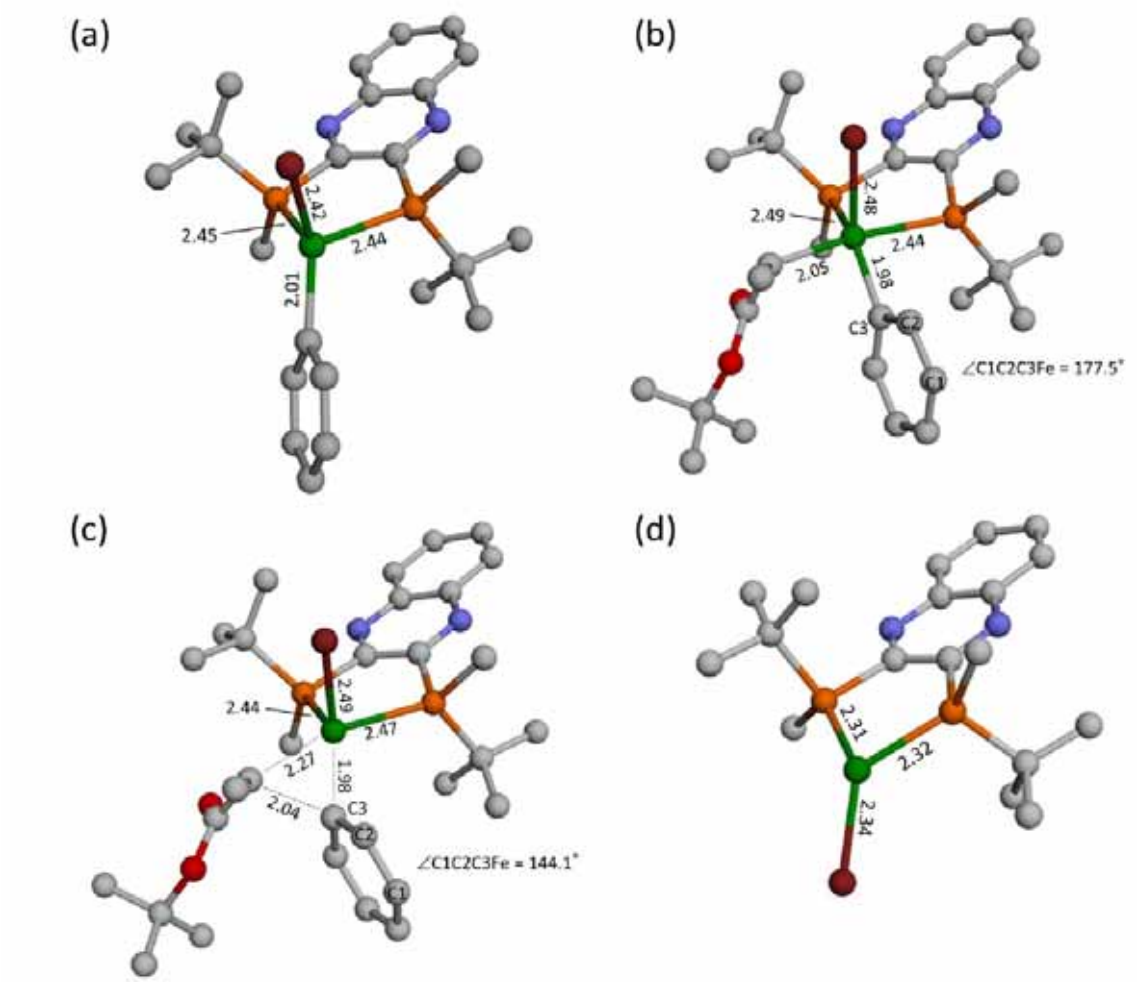

Figure 7. Optimized structure of (a) **C**, (b) **D**, (c) **TS**, and (d) **B**. The bond lengths are given in Å. H atoms are omitted for clarity: grey; C: green; Fe: red; Br: orange; P: purple; N.

Cartesian coordinates for optimized compounds.

FePhBr/(*R*,*R*)-QuinoxP* **C**
C 1.701439 0.329487 -0.52425
C 1.580576 -0.81132 0.341616
C 3.856407 -1.09096 0.278651
C 3.966986 -0.00905 -0.64471
P -0.10394 -1.39858 0.853634
P 0.201637 1.357693 -0.91273
C 0.189188 -1.95931 2.571813
H -0.6444 -2.58754 2.887674
H 1.130851 -2.50108 2.653632
H 0.20546 -1.07318 3.20724
C 0.139145 1.177454 -2.74254
H -0.59367 1.8737 -3.15214
H 1.119728 1.368876 -3.1785
H -0.17256 0.163065 -2.98853
C 0.732988 3.139682 -0.59798
C -0.33057 -2.95685 -0.18257
C 0.710187 -4.03501 0.136405
H 0.542926 -4.89869 -0.51569
H 1.729172 -3.67973 -0.01808
H 0.626583 -4.37962 1.169062
C -1.7477 -3.47649 0.114294
H -1.93644 -4.37 -0.48907
H -1.86264 -3.75935 1.163834
H -2.50884 -2.7338 -0.12911
C -0.23624 -2.53469 -1.65636
H -0.99156 -1.78497 -1.89815
H 0.752058 -2.13966 -1.90395
H -0.41763 -3.40362 -2.29579
C -0.57241 3.955744 -0.59852
H -0.33345 5.01512 -0.46339
H -1.11425 3.857646 -1.54397

H -1.23455 3.649992 0.213291
C 1.695554 3.679586 -1.66274
H 1.988783 4.698408 -1.38921
H 2.594032 3.067441 -1.73416
H 1.225772 3.728853 -2.64769
C 1.383466 3.198875 0.792876
H 0.738569 2.762528 1.557891
H 2.347223 2.686545 0.803912
H 1.558203 4.245633 1.059833
Fe -1.6551 0.433162 0.396345
C -3.29475 -0.16458 -0.6101
C -3.36576 -0.25948 -2.01081
C -4.43793 -0.57321 0.102523
C -4.49466 -0.74891 -2.66796
H -2.52139 0.055675 -2.61855
C -5.57303 -1.06499 -0.53954
H -4.44433 -0.5084 1.187525
C -5.60273 -1.15796 -1.93021
H -4.51242 -0.80893 -3.7517
H -6.43608 -1.3735 0.041815
H -6.48371 -1.54069 -2.43379
Br -1.62769 1.539227 2.543947
N 2.865094 0.690851 -1.02192
N 2.64045 -1.48176 0.741784
C 5.239199 0.348573 -1.15096
C 5.022977 -1.77694 0.692343
C 6.353427 -0.33907 -0.73817
H 7.329846 -0.06666 -1.12047
C 6.245281 -1.40431 0.190604
H 7.140901 -1.92783 0.502901
H 5.296762 1.170429 -1.85357
H 4.91202 -2.58995 1.398817

Alkyl radical generated from **1a**
C 2.183305 0.755292 -0.0006
H 2.048097 1.829976 -0.00064
C 3.537429 0.156787 0.000357
H 4.115093 0.4846 -0.87355
H 4.110021 0.476467 0.880745
H 3.473856 -0.93116 -0.00432
C 0.99549 -0.07696 -0.00054
O 1.015014 -1.29691 -0.0002
O -0.12631 0.683382 -0.00097
C -1.46341 0.070749 0.000098
C -2.38714 1.286032 0.0002
C -1.65917 -0.75985 -1.26912
H -1.00022 -1.62573 -1.27613
H -2.69561 -1.10292 -1.32262
H -1.45532 -0.14957 -2.1523
C -1.65787 -0.75898 1.270081
H -1.45308 -0.14819 2.152701
H -2.69434 -1.10178 1.324816
H -0.99912 -1.62501 1.277042
H -3.43106 0.964533 0.00074
H -2.20947 1.899466 0.8858
H -2.21031 1.8991 -0.88582

FePhBr(alkyl)/(*R*,*R*)-QuinoxP* **D**
C -2.34115 -0.66614 -0.55885
C -2.52479 0.669778 -0.06353
C -4.79332 0.440867 -0.28012
C -4.60542 -0.83222 -0.89448
P -1.0431 1.738588 0.228284
P -0.66304 -1.46572 -0.45452
C -1.59228 2.860796 1.563722
H -0.83607 3.632333 1.708657
H -2.55592 3.306183 1.321519
H -1.67274 2.269817 2.474548
C -0.25134 -1.71968 -2.22834
H 0.610262 -2.38177 -2.27994
H -1.103 -2.13203 -2.76873
H 0.032806 -0.765 -2.66652
C -1.05462 -3.20237 0.216411
C -1.05021 2.816954 -1.33537
C -2.43004 3.423035 -1.62863
H -2.33843 4.081793 -2.49856
H -3.17862 2.666198 -1.85807
H -2.80172 4.023049 -0.79698
C -0.04027 3.959753 -1.14019
H 0.011017 4.54175 -2.06585
H -0.35479 4.638425 -0.34492
H 0.959043 3.600516 -0.9137
C -0.62715 1.924605 -2.50802
H 0.361796 1.49674 -2.34564
H -1.3419 1.11455 -2.67011
H -0.58859 2.519482 -3.42563
C 0.260248 -3.78652 0.759505
H 0.099534 -4.84126 1.004079
H 1.076373 -3.71618 0.039394
H 0.560199 -3.27763 1.676349
C -1.60816 -4.11921 -0.88422
H -1.86895 -5.08212 -0.43284
H -2.50395 -3.69936 -1.34029
H -0.86748 -4.31315 -1.66253
C -2.06716 -3.09196 1.367461
H -1.75484 -2.35723 2.110718
H -3.0619 -2.83109 1.007253
H -2.13555 -4.06602 1.862183
Fe 0.745597 0.175101 0.783539
C 2.042884 1.580138 0.264651
C 2.659607 1.628003 -0.98656
C 2.332245 2.589887 1.189663
C 3.52316 2.670553 -1.32183
H 2.478368 0.842708 -1.71214
C 3.19749 3.632052 0.861541
H 1.881298 2.565397 2.176914
C 3.791747 3.678771 -0.39906
H 3.987884 2.693655 -2.30198

H 3.407527 4.408201 1.589691
H 4.462761 4.490089 -0.65655
C 2.428038 -0.92569 1.189995
H 1.822486 -1.75804 1.550102
C 3.327687 -0.3902 2.288376
H 3.904844 0.469761 1.951867
H 2.727709 -0.09328 3.150358
H 4.037705 -1.1564 2.620489
C 3.082135 -1.37598 -0.06018
O 2.525396 -2.02401 -0.93806
O 4.366708 -0.98684 -0.13691
C 5.253479 -1.39548 -1.23601
C 6.570793 -0.72231 -0.85931
C 5.395958 -2.91773 -1.23647
H 4.456243 -3.39665 -1.50537
H 6.163537 -3.21342 -1.95631
H 5.701846 -3.26568 -0.247
C 4.748215 -0.86785 -2.5792
H 4.648401 0.21766 -2.54355
H 5.474377 -1.11832 -3.35719
H 3.788533 -1.31053 -2.83671
N -3.36099 -1.36807 -1.00423
N -3.72233 1.187657 0.097014
C -5.73035 -1.55775 -1.35317
C -6.10356 0.94532 -0.10599
C -6.99035 -1.0395 -1.18168
H -7.855 -1.59436 -1.52576
C -7.17827 0.214975 -0.54986
H -8.1834 0.598463 -0.42142
H -5.56186 -2.51986 -1.82059
H -6.218 1.910524 0.371149
H 6.43622 0.359453 -0.80072
H 7.335392 -0.9438 -1.60769
H 6.916308 -1.07937 0.112704
Br -0.3331 -0.15371 2.99273

FeBr/(*R*,*R*)-QuinoxP* **B**
Fe -2.08533 0.304327 0.193639
P -0.52336 -1.26149 0.886093
C -0.73175 -2.93272 0.025154
C -0.64787 -2.66504 -1.48568
C 1.135416 -0.65159 0.305188
C 1.204144 0.635552 -0.32704
C 3.441469 0.326949 -0.71282
C 3.390507 -0.91638 -0.01575
P -0.3117 1.702414 -0.31525
C 0.126813 3.007371 0.98161
C 0.454884 2.261485 2.283584
C -0.16941 2.56547 -1.93057
C -0.13883 -1.67824 2.638449
C -2.1454 -3.42068 0.384533
C 0.30992 -3.97511 0.446359
C 1.306772 3.892171 0.566514
C -1.13533 3.863237 1.178618
H -0.85248 3.415654 -1.94402
H 0.853537 2.887852 -2.12229
H -0.48414 1.865789 -2.70601
H -0.95237 -2.27086 3.058496
H 0.798311 -2.23065 2.710765
H -0.05373 -0.75386 3.210483
H 1.542858 4.588394 1.378431
H 2.197092 3.301944 0.3479
H 1.070092 4.48596 -0.31851
H -0.9447 4.636797 1.929375
H -1.43399 4.364264 0.254699
H -1.98148 3.261629 1.520948
H -0.36943 1.613345 2.592469
H 1.350423 1.644976 2.182614
H 0.632405 2.983069 3.086628
H -2.33933 -4.37027 -0.12403
H -2.25101 -3.59614 1.458978
H -2.9095 -2.70533 0.074697
H 0.136613 -4.89918 -0.11537
H 1.325633 -3.63342 0.252489
H 0.228862 -4.21826 1.508308
H -1.40167 -1.94088 -1.80366
H 0.33773 -2.29115 -1.77426
H -0.82751 -3.59635 -2.03115
N 2.211705 -1.38831 0.477754
N 2.324586 1.096683 -0.83946
C 4.574198 -1.67274 0.144897
C 4.670019 0.77375 -1.25107
C 5.803864 0.014441 -1.08797
H 6.746892 0.354884 -1.49868
C 5.7564 -1.21251 -0.38365
H 6.663957 -1.79242 -0.26556
H 4.510421 -2.61046 0.682747
H 4.680206 1.718494 -1.78028
Br -4.1291 -0.05689 -0.89696

Transition state at reductive elimination **TS**
C -1.5945 4.02589 2.818531
C -2.49157 3.754013 1.786947
C -2.22828 2.724939 0.884444
C -1.07039 1.935849 0.978156
C -0.1867 2.236141 2.029436
C -0.4343 3.263359 2.938986
Fe -0.654 0.464938 -0.33437
C -2.92227 -0.47021 2.110497
C -4.11848 -0.25456 1.3178
O -4.22534 -1.18466 0.341001
C -5.39499 -1.22338 -0.55258
C -5.51857 0.082389 -1.33904
P 0.629946 -1.30525 0.773577
C 0.485847 -3.05543 0.084799
C 0.906461 -3.00352 -1.3906
C 2.424371 -0.87827 0.520889
C 2.809578 0.068625 -0.4921

C 5.018037 -0.31117 0.006947
C 4.6336 -1.20763 1.047628
P 1.493831 0.987339 -1.42845
C 2.083656 2.773247 -1.55184
C 2.485387 3.257652 -0.15208
C 0.577971 -1.49974 2.599093
C 1.717287 0.292216 -3.11483
C 0.850862 3.560284 -2.03498
C 3.249764 2.953035 -2.53183
C 1.350035 -4.06115 0.852533
C -1.00179 -3.43483 0.188557
Br -1.80933 -0.34428 -2.29288
C -2.69987 0.295247 3.357491
O -4.9231 0.637534 1.529226
C -5.06523 -2.38728 -1.48326
C -6.64868 -1.51999 0.272175
H -0.31114 -2.06209 2.882969
H 1.474954 -2.00889 2.949055
H 0.516852 -0.51076 3.052238
H 1.115875 0.872152 -3.81518
H 2.767309 0.309325 -3.40747
H 1.339521 -0.72776 -3.12787
H 1.244431 -5.04719 0.388581
H 2.405171 -3.78677 0.839038
H 1.03704 -4.15225 1.89454
H -1.14977 -4.42532 -0.25279
H -1.33378 -3.49111 1.22857
H -1.64267 -2.72945 -0.34302
H 0.272139 -2.31902 -1.95578
H 1.951499 -2.70364 -1.50284
H 0.797816 -3.99904 -1.83109
H 1.123922 4.612175 -2.16425
H 0.481772 3.192209 -2.99624
H 0.034791 3.504048 -1.31203
H 3.553824 4.00502 -2.5313
H 4.10558 2.343476 -2.24348
H 2.964326 2.696367 -3.55395
H 1.672946 3.131417 0.563794
H 3.370666 2.735319 0.214895
H 2.722275 4.325109 -0.19918
H -2.95682 2.521858 0.105638
H 0.727838 1.657457 2.15066
H -3.40315 4.33472 1.694239
H 0.270473 3.467723 3.738905
H -1.79981 4.822384 3.52519
H -2.30191 -1.31638 1.850294
H -3.0966 -0.25829 4.222487
H -1.64028 0.472976 3.540849
H -3.21789 1.252574 3.312282
H -6.87325 -0.69779 0.949573
H -7.49926 -1.66655 -0.3986
H -6.50996 -2.43496 0.853937
H -4.57795 0.303058 -1.84484
H -6.30041 -0.03052 -2.09532
H -5.77869 0.910518 -0.68309
N 3.322062 -1.47938 1.273052
N 4.077704 0.31894 -0.74398
C 5.629647 -1.82851 1.838256
C 6.391702 -0.06632 -0.22988
C 6.954597 -1.57018 1.588702
H 7.721135 -2.04479 2.189452
C 7.337301 -0.68695 0.548148
H 8.389962 -0.50168 0.371147
H 5.310707 -2.5013 2.624448
H 6.658599 0.616043 -1.02705
H -4.14532 -2.18059 -2.03108
H -4.93408 -3.30718 -0.90848
H -5.8786 -2.53525 -2.19765

Product **3a**
C 0.542854 1.542798 0.252853
H 0.81808 2.409988 -0.34935
C 0.32158 1.98373 1.707384
H 1.245322 2.404966 2.109509
H -0.46036 2.745053 1.767282
H 0.023087 1.142633 2.332393
C -0.72953 1.012393 -0.40366
O -1.09634 1.335884 -1.50659
O -1.35396 0.131523 0.397512
C -2.54026 -0.62224 -0.05576
C -2.85055 -1.50739 1.147692
C -3.69126 0.34283 -0.33575
H -3.46741 0.980899 -1.18809
H -4.59934 -0.22726 -0.54805
H -3.87865 0.969625 0.539483
C -2.17571 -1.46757 -1.27533
H -1.30247 -2.08648 -1.05649
H -3.01145 -2.12733 -1.52169
H -1.95707 -0.83992 -2.13692
C 1.649887 0.508284 0.111757
C 1.602598 -0.70857 0.800616
C 2.737412 0.762267 -0.72576
C 2.624062 -1.64211 0.658437
H 0.756092 -0.92712 1.438641
C 3.761826 -0.17082 -0.86866
H 2.779956 1.698343 -1.27167
C 3.708387 -1.37648 -0.1759
H 2.573303 -2.58044 1.199154
H 4.599276 0.045027 -1.52217
H 4.503543 -2.10471 -0.28544
H -3.732 -2.11967 0.944886
H -2.00928 -2.16954 1.362562
H -3.04605 -0.89616 2.031073

References and Notes

[1] For selected reviews, see: (a) N. Miyaura and A. Suzuki, *Chem. Rev.*, **1995**, *95*, 2457–2483; (b) S. Kotha, K. Lahiri and D. Kashinath, *Tetrahedron*, **2002**, *58*, 9633–9695; (c) J. S. Carey, D. Laffan, C. Thomson and M. T. Williams, *Org. Biomol. Chem.*, **2006**, *4*, 2337–2347; (d) J. Magano and J. R. Dunetz, *Chem. Rev.*, **2011**, *111*, 2177–2250; (e) A. Suzuki, *Angew. Chem. Int. Ed.*, **2011**, *50*, 6722–6737; (f) D. G. Brown and J. Boström, *J. Med. Chem.*, **2016**, *59*, 4443–4458.

[2] F. Lovering, J. Bikker and C. Humblet, *J. Med. Chem.*, **2009**, *52*, 6752–6756.

[3] For a review, see: (a) A. H. Cherney, N. T. Kadunce and S. E. Reisman, *Chem. Rev.*, **2015**, *115*, 9587–9652; For reviews related to stereospecific Suzuki–Miyaura-type couplings using chiral substrates, see: (b) D. Leonori and V. K. Aggarwal, *Angew. Chem. Int. Ed.*, **2015**, *54*, 1082–1096; (c) X.-P. Zeng, Z.-Y. Cao, Y.-H. Wang, F. Zhou and J. Zhou, *Chem. Rev.*, **2016**, *116*, 7330–7396; (d) J. P. G. Rygus and C. M. Crudden, *J. Am. Chem. Soc*, **2017**, *139*, 18124–18137; For a review relating to enantioconvergent couplings, see: (e) V. Bhat, E. R. Welin, X. Guo and B. M. Stoltz, *Chem. Rev.*, **2017**, *117*, 4528–4561.

[4] (a) B. Saito and G. C. Fu, *J. Am. Chem. Soc*, **2008**, *130*, 6694–6695; (b) P. M. Lundin and G. C. Fu, *J. Am. Chem. Soc*, **2010**, *132*, 11027–11029; (c) N. A. Owston and G. C. Fu, *J. Am. Chem. Soc.*, **2010**, *132*, 11908–11909; (d) Z. Lu, A. Wilsily and G. C. Fu, *J. Am. Chem. Soc.*, **2011**, *133*, 8154–8157; (e) S. L. Zultanski and G. C. Fu, *J. Am. Chem. Soc.*, **2011**, *133*, 15362–15364; (f) A. Wilsily, F. Tramutola, N. A. Owston and G. C. Fu, *J. Am. Chem. Soc*, **2012**, *134*, 5794–5797.

[5] G. C. Fu, *ACS Cent. Sci.*, **2017**, *3*, 692–700.

[6] (a) J. Mao, F. Liu, M. Wang, B. Zheng, S. Liu, J. Zhong, Q. Bian and P. J. Walsh, *J. Am. Chem. Soc*, **2014**, *136*, 17662–17668; (b) F. Liu, Q. Bian, J. Mao, Z. Gao, D. Liu, S. Liu, X. Wang, Y. Wang, M. Wang and J. Zhong, *Tetrahedron: Asymmetry*, **2016**, *27*, 663–669; (c) M. Jin, L. Adak and M. Nakamura, *J. Am. Chem. Soc.*, **2015**, *137*, 7128–7134.

[7] For selected reviews, see: (a) C. Bolm, J. Legros, J. L. Paih and L. Zani, *Chem. Rev.*, **2004**, *104*, 6217–6254; (b) W. M. Czaplik, M. Mayer, J. Cvengroš and A. J. von Wangelin, *ChemSusChem*, **2009**, *2*, 396–417; (c) I. Bauer and H.-J. Knölker, *Chem. Rev.*, **2015**, *115*, 3170–3387; (d) J. Legros and B. Figadère, *Nat. Prod. Rep.*, **2015**, *32*, 1541–1555; (e) O. M. Kuzmina, A. K. Steib, A. Moyeux, G. Cahiez and P. Knochel, *Synthesis*, **2015**, *47*, 1696–1705; (f) R. B. Bedford and P. B. Brenner, *Top. Organomet. Chem.*, **2015**, *50*, 19–46; (g) A. Fürstner, *ACS Cent. Sci.*, **2016**, *2*, 778–789; (h) K. S. Egorova and V. P. Ananikov, *Angew. Chem. Int. Ed.*, **2016**, *55*, 12150–12162; (i) A. Guérinot and J. Cossy, *Top. Curr. Chem.*, **2016**, *374*, 49–74; (j) A. Piontek, E. Bisz and M. Szostak, *Angew. Chem. Int. Ed.*, **2018**, *57*, 11116–11128.

[8] For examples of iron-catalyzed couplings of organoboron reagents: (a) Y. Guo, D. J. Young and T. S. A. Hor, *Tetrahedron Lett.*, **2008**, *49*, 5620–5621; (b) A. Deb, S. Manna, A. Maji, U. Dutta and D. Maiti, *Eur. J. Org. Chem.*, **2013**, 5251–5256; (c) Y. Zhong and W. Han, *Chem. Commun.*, **2014**, *50*, 3874–3877; (d) A. Deb, S. Agasti, T. Saboo and D. Maitia, *Adv. Synth. Catal.*, **2014**, *356*, 705–710; (e) R. Shang, L. Ilies, S. Asako and E. Nakamura, *J. Am. Chem. Soc.*, **2014**, *136*, 14349–14352; (f) L. Ilies, Y. Itabashi, R. Shang and E. Nakamura, *ACS Catal.*, **2017**, *7*, 89–92.

[9] (a) R. B. Bedford, M. A. Hall, G. R. Hodges, M. Huwe and M. C. Wilkinson, *Chem. Commun.*, **2009**, 6430–6432; (b) T. Hatakeyama, T. Hashimoto, Y. Kondo, Y. Fujiwara, H. Seike, H. Takaya, Y. Tamada, T. Ono and M. Nakamura, *J. Am. Chem. Soc.*, **2010**, *132*, 10674–10676; (c) T. Hashimoto, T. Hatakeyama and M. Nakamura, *J. Org. Chem.*, **2012**, *77*, 1168–1173; (d) T. Hatakeyama, T. Hashimoto, K. K. A. D. S. Kathriarachchi, T. Zenmyo, H. Seike and M. Nakamura, *Angew. Chem. Int. Ed.*, **2012**, *51*, 8834–8837; (e) R. B. Bedford, P. B. Brenner, E. Carter, J. Clifton, P. M. Cogswell, N. J. Gower, M. F. Haddow, J. N. Harvey, J. A. Kehl, D. M. Murphy, E. C. Neeve, M. L. Neidig, J. Nunn, B. E. R. Snyder and J. Taylor, *Organometallics*, **2014**, *33*, 5767–5780; (f) R. B. Bedford, P. B. Brenner, E. Carter, T. W. Carvell, P. M. Cogswell, T. Gallagher, J. N. Harvey, D. M. Murphy, E. C. Neeve, J. Nunn and D. R. Pye, *Chem. Eur. J.*, **2014**, *20*, 7935–7938; (g) N. Nakagawa, T. Hatakeyama and M. Nakamura, *Chem. Lett.*, **2015**, *44*, 486–488; (h) R. B. Bedford, T. Gallagher, D. R. Pye and W. Savage, *Synthesis*, **2015**, *47*, 1761–1765; (i) S. Nakajima, H. Takaya and M. Nakamura, *Chem. Lett.*, **2017**, *46*, 711–714.

[10] T. Imamoto, *Chem. Rec.*, **2016**, *16*, 2659–2673.

[11] (a) P. J. Harrington and E. Lodewijk, *Org. Process Res. Dev.*, **1997**, *1*, 72–76; (b) M. F. Landoni and A. Soraci, *Curr. Drug Metab.*, **2001**, *2*, 37–51.

[12] On the basis of the DFT calculations, coupling reactions with either boron- or Grignard reagents proceed

through similar mechanisms, in which the nucleophile is not directly involved in the enantiodetermining step; see ref 13a.

[13] (a) A. K. Sharma, W. M. C. Sameera, M. Jin, L. Adak, O. Chiemi, T. Iwamoto, M. Kato, M. Nakamura and K. Morokuma, *J. Am. Chem. Soc*, **2017**, *139*, 16117–16125; (b) T. Imamoto, K. Sugita and K. Yoshida, *J. Am. Chem. Soc.*, **2005**, *127*, 11934–11935.

[14] (a) T. Hatakeyama, Y. Fujiwara, Y. Okada, T. Itoh, S. Hashimoto, K. Kawamura, K. Ogata, H. Takaya and M. Nakamura, *Chem. Lett.*, **2011**, *40*, 1030–1032; (b) H. Takaya, S. Nakajima, N. Nakagawa, K. Isozaki, T. Iwamoto, R. Imayoshi, N. Gower, L. Adak, T. Hatakeyama, T. Honma, M. Takagaki, Y. Sunada, H. Nagashima, D. Hashizume, O. Takahashi and M. Nakamura, *Bull. Chem. Soc. Jpn.*, **2015**, *88*, 410–418.

[15] When the coupling reaction was performed using $FeCl_2$/(*R,R*)-QuinoxP* (5 mol%) instead of a mixture of $FeCl_2$ (5 mol%) and (*R,R*)-QuinoxP* (10 mol%), the reaction proceeded quantitatively to provide the product with 79:21 er, which is almost identical to that obtained under optimal conditions. Therefore, the author concluded that (*R*,*R*)-QuinoxP* is coordinated to iron in 1:1 ratio.

[16] Based on the previous mechanistic study, complex **C** is the predominant iron species in the reaction mixture.

[17] In the absence of chiral ligands, the background coupling reaction proceeded rapidly, with the racemic product obtained in 98% yield after 1 h.

[18] J. Mao, F. Liu, M. Wang, L. Wu, B. Zheng, S. Liu, J. Zhong, Q. Bian, P. J. Walsh, *J. Am. Chem. Soc.* **2014**, *136*, 17662–17668.

[19] L. Luo, H. Yamamoto, *Eur. J. Org. Chem.* **2014**, 7803–7805.

[20] J. Hu, H. Sun, W. Cai, X. Pu, Y. Zhang, Z. Shi, *J. Org. Chem.* **2016***, 81*, 14–24.

[21] F. Mo, Y. Jiang, D. Qiu, Y. Zhang,; J. Qang, *Angew. Chem. Int. Ed.* **2010**, *49*, 1846–1849.

[22] M.Jiang, H. Yang, H. Fu, *Org. Lett.* **2016**, *18*, 5248–5251.

[23] L. Guo, M. Rueping, *Chem. Eur. J.* **2016**, *22*, 16787–16790.

[24] C. Kuhakarn, W. Panchan, S. Chiampanichayakul, N. Samakkanad, M. Pohmakotr, V.;Reutrakul, T. Jaipetch, *Synthesis* **2009**, 929–934.

[25] P. H. Gehrtz, V. Hirschbeck, I. Fleischer, *Chem. Commun.* **2015**, *51*, 12574–12577.

[26] H. Jang, B. Jung, A. H. Hoveyda, *Org. Lett.* **2014**, *16*, 4658–4661.

[27] Z.-L. Wu, Z.-Y. Li, *Tetrahedron: Asymmetry* **2001**, *12*, 3305–3312.

[28] S. Ghosh, S. N. Pardo, R. G. Salomon, *J. Org. Chem.* **1982**, *47*, 4692–4702.

[29] M. Greenhalgh, S. Thomas, *J. Am. Chem. Soc.* **2012**, *134*, 11900–11903.

[30] C. H. Senanayake, T. J. Bill, R. D. Larsen, J. Leazer, P. J. Reider, *Tetrahedron Lett.* **1992**, *33*, 5901–5904.

[31] C. E. Stivala, A. Zakarian, *J. Am. Chem. Soc.* **2011**, *133*, 11936–11939.

[32] M. García, C. D. Campo, E. F. Llama, E. F. J. V. Sinisterra, *J. Chem. Soc. Perkin Trans. 1* **1995**, 1771–1773.

[33] Gaussian 09 (Revision E.01), M. J. Frisch, G. W. Trucks, H. B. Schlegel, G. E. Scuseria, M. A. Robb, J. R. Cheeseman, G. Scalmani, V. Barone, B. Mennucci, G. A. Petersson, H. Nakatsuji, M. Caricato, X. Li, H. P. Hratchian, A. F. Izmaylov, J. Bloino, G. Zheng, J. L. Sonnenberg, M. Hada, M. Ehara, K. Toyota, R. Fukuda, J. Hasegawa, M. Ishida, T. Nakajima, Y. Honda, O. Kitao, H. Nakai, T. Vreven, J. A. Montgomery, Jr., J. E. Peralta, F. Ogliaro, M. Bearpark, J. J. Heyd, E. Brothers, K. N. Kudin, V. N. Staroverov, T. Keith, R. Kobayashi, J. Normand, K. Raghavachari, A. Rendell, J. C. Burant, S. S. Iyengar, J. Tomasi, M. Cossi, N. Rega, J. M. Millam, M. Klene, J. E. Knox, J. B. Cross, V. Bakken, C. Adamo, J. Jaramillo, R. Gomperts, R. E. Stratmann, O. Yazyev, A. J. Austin, R. Cammi, C. Pomelli, J. W. Ochterski, R. L. Martin, K. Morokuma, V. G. Zakrzewski, G. A. Voth, P. Salvador, J. J. Dannenberg, S. Dapprich, A. D. Daniels, O. Farkas, J. B. Foresman, J. V. Ortiz, J. Cioslowski, and D. J. Fox, Gaussian, Inc., Wallingford CT, 2013.

[34] (a) Grimme, S.; *J. Comp. Chem.*, **2006**, *27*, 1787–1799. (b) S. Grimme, S. Ehrlich, L. Goerigk, *J. Comp. Chem*. **2011**, *32*, 1456–1465.

CHAPTER 7

DFT and AFIR Study on the Mechanism and the Origin of the Enantioselectivity in Iron-Catalyzed Cross-Coupling Reactions

Abstract

Mechanism of the full catalytic cycle for Fe-chiral-bisphosphine catalyzed cross-coupling reaction between alkyl halides and the Grignard reagents was rationalized by using density functional theory (DFT) and multi-component artificial force induced reaction (MC-AFIR) methods. The computed mechanism consists of (a) C–Cl activation, (b) transmetalation, (c) C–Fe bond formation, and (d) C–C bond formation through reductive elimination. The survey on the pre-reactant complexes suggested that formation of Fe^{II}(BenzP*)Ph_2 and Fe^{I}(BenzP*)Ph complexes are thermodynamically feasible. Fe^{I}(BenzP*)Cl complex is the active intermediate for the C–Cl activation. Fe^{II}(BenzP*)Ph_2 complex can be formed if the concentration of the Grignard reagent is high. However, it leads to biphenyl (byproduct) instead of the cross-coupling product. This explains why the slow addition of the Grignard reagent is critical for the cross-coupling reaction. The MC-AFIR method was used for systematic determination of transition states for the C–Fe bond formation and C–C bond formation starting from the key intermediate Fe^{II}(BenzP*)PhCl. According to the detailed analysis, the C–C bond

formation is the selectivity-determining step. The computed enantiomeric ratio of 95:5 is in good agreement with the experimental ratio (90:10). Energy decomposition analysis suggested that the origin of the enantioselectivity is the deformation of Ph-ligand in Fe-complex, which is induced by the bulky *tert*-butyl group of BenzP* ligand. The study provides important mechanistic insights for the cross-coupling reaction between alkyl halides and the Grignard reagents, and guides the design of efficient Fe-based catalysts for cross-coupling reactions.

Introduction

Cross-coupling reactions are important to synthesize a variety of organic compounds.[1] Transition metal complexes have been used as catalysts to perform cross-coupling reactions in chemo- and stereoselective fashion.[2] In 2010, the Nobel Prize in Chemistry was awarded to Heck, Negishi, and Suzuki for the development of palladium-catalyzed cross-coupling reactions.[3] Development of new methods involving non-toxic and readily available metals such as iron has been very active in cross-coupling chemistry.[4] Iron is known to catalyze many enzymatic reactions and industrially relevant chemical transformations. However, the development of iron-based catalysts for cross-coupling reactions is far behind than the palladium-based methodologies, because of challenges in controlling their coordination geometry, oxidation states, and spin states. For example, there is only one example in the literature to date for successful asymmetric cross-coupling with iron catalysts and is in stark contrast to those with palladium and nickel catalysts.[2,5]

The first iron-catalyzed coupling reaction was reported in 1941 by Kharasch and co-workers.[6] Recently, the development of an iron-based catalyst for cross-coupling reactions has been very active.[7] The $FeCl_3$, $FeCl_2$, and $Fe(acac)_3$ (acac = acetylacetonate) are used extensively to catalyze coupling reactions of the Grignard reagent with alkyl or aryl halides. Although some of these reactions can be achieved by the simple iron salts (i.e. without the addition of ligands), selective carbon-carbon bond formations have been achieved by the combination of an iron salt with bidentate amine, bidentate phosphine, and NHC ligands.[8] In the majority of these reactions, there is no consensus on the oxidation state of iron species involved in the reaction mechanism.[9] Thus, Fe^{II}/Fe^{0}, Fe^{0}/Fe^{II}, Fe^{I}/Fe^{III}, and Fe^{II}/Fe^{III} mechanisms were proposed for the iron-catalyzed cross-coupling reactions without ligands.[10] In the absence of strong reducing agents, Norrby and coworkers proposed Fe^{I}/Fe^{III} mechanism, where Fe^{I} is proposed as an active species under the ligand-free condition.[9,11] In the presence of the bidentate phosphine and amine ligands, recent studies suggested that the reactions may occur through a Fe^{II}/Fe^{III} catalytic cycle.[12] Further, Nakamura and others argue that Fe^{II} species is the active intermediate for the reaction,[12] while Bedford suggested that Fe^{I} species is the active species.[13] Another important aspect in iron-catalyzed reactions is the spin state, which can be changed by modifying the ligands[14a] or can change during the reaction spontaneously to avoid high activation barrier.[14b-e]

Development of chiral catalysts for enantioselective cross-coupling reactions of racemic alkyl halides is a significant synthetic approach in the pharmaceutical industry, as they produce asymmetric carbon centers. Recently, the author has reported the first

iron-catalyzed enantioselective cross-coupling reaction between aryl Grignard reagents (ArMgBr) and organic halides (R–Cl) with high enantiomeric ratio (Scheme 1).[5] The enantioselectivity of this reaction is induced by the *P*-chiral bisphosphine ligand, (*R*,*R*)-BenzP*,[15] where a high enantiomeric ratio (90:10) was observed.

Scheme 1. Fe-catalyzed C–C Coupling Reaction by M. Nakamura and Co-workers.[5]

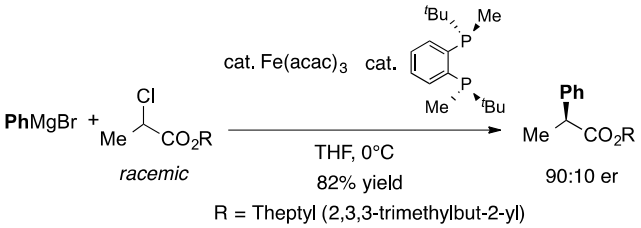

The iron-catalyzed asymmetric coupling reactions involve two important steps (Scheme 2); (a) iron-mediated C–Cl activation leading to an alkyl radical, and (b) its recombination for the C–C bond formation. The author has previously proposed that organoiron(II) intermediate as the active species for both steps (*out-of-cage*, $Fe^{II}/Fe^{III}/Fe^{I}$ mechanism).[5] A minor reaction path may be also possible through an *in-cage* Fe^{II}/Fe^{III} mechanism, in which the C–C bond formation occurs between the organoiron(III) intermediate and the radical species. Both reaction mechanisms are illustrated in Scheme 2. Despite the synthetic advancements, the detailed mechanism of the reaction and the origin of enantioselectivity are not established. For further development of Fe-catalysis, mechanistic studies through computational methods become critical.[16]

Scheme 2. The Proposed *in-cage* and *out-of-cage* Mechanisms with Fe^{II} as Active Species (P⁀P, X, and R denote (*R*,*R*)-BenzP*, Ph or Cl, and theptyl group, respectively).[5]

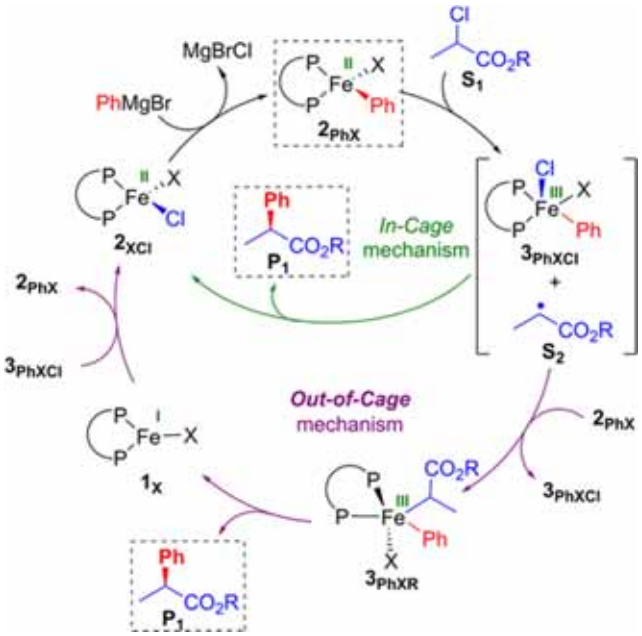

In this study, the author has used density functional theory (DFT) and the multi-component artificial force induced reaction method (MC-AFIR) to rationalize the mechanisms and enantioselectivity of the iron-catalyzed cross-coupling reaction between ArMgBr and α-chloropropiontates. Nakamura group has previously used MC-AFIR method for the mechanistic studies of complex catalytic reactions. [17,18]

Computational methods

DFT, as implemented in Gaussian09 program, was used to optimize all structures.[19] The B3LYP functional, including the empirical dispersion corrections, with Becke-Johnson damping (D3BJ), was employed.[20] Optimization of closed shell singlet spin states was performed with the restricted-B3LYP (RB3LYP) and the high spin states were calculated by unrestricted-B3LYP (UB3LYP) method. The 6-31G(d) basis sets were used for C and H, the 6-31+G(d,p) basis sets were applied for O, P, Cl, and Mg and the SDD basis sets and the associated effective core potentials were used for Fe and Br (BS1).[21] The integral equation formalism-Polarizable Continuum Model (IEF-PCM) was used as the implicit solvation model for geometry optimizations, where THF (tetrahydrofuran) was used as the solvent (ε = 7.4257).[22] Nature of the stationary points, minima or transition states (TS), were confirmed by performing vibrational frequency

calculations at 298.15 K and 1 atm. TSs were confirmed by performing intrinsic reaction coordinate (IRC) calculations for 15 steps for both forward and backward directions (i.e. pseudo-IRC), and the final structures were further optimized to locate minima.[23] Potential energies of stationary points were further improved by using SDD (Fe, Br) and cc-PVTZ (H, C, O, Mg, P, Cl) basis sets (BS2). The results reported in the paper are at B3LYP-D3BJ/BS2//B3LYP-D3BJ/BS1 level of theory.

The selectivity determining steps of the mechanism was studied by the MC-AFIR method in the GRRM (Global Reaction Route Mapping) strategy.[17, 24] The ONIOM(B3LYP-D3:PM6-D3) method in Gaussian09 program was used.[25] The SDD basis sets and associated effective core potentials were used for Fe and Br, and 3-21G basis sets were employed for other atoms (BS3) in the ONIOM high-level. The artificial force parameter of 300 kJ/mol was used for the C–Cl activation step by Fe^{II}, while 200 kJ/mol was used for other steps (*vide infra*). The approximate TSs were fully optimized using B3LYP-D3BJ/BS1 method. In the results and discussion section, Gibbs free energies of the stationary points were reported. The author has used Cylview program to generate ball and stick geometries of optimized structures.[26]

Nomenclature: $\mathbf{S_1}$, $\mathbf{P_1}$, and $\mathbf{S_2}$ denote the α-chloropropionate (substrate), coupling product, and ester radical species, respectively. **1**, **2**, and **3** represent Fe^{I}(BenzP*), Fe^{II}(BenzP*), Fe^{III}(BenzP*) complexes, respectively. **4** is Fe^{III} species without the BenzP* ligand. Other ligands are given in subscript and defined as Cl (chloride), Br (bromide), Ph (phenyl), R (ester radical), and A (acetylacetonate). The spin state of iron-complexes is given as superscript. For example, Fe^{II}PhCl(BenzP*) in quintet state (S=2) can be written as $^{5}\mathbf{2}_{\mathbf{PhCl}}$.

Results and discussion

In the iron-catalyzed asymmetric cross-coupling reaction (Scheme 1), iron(III) salts viz., $FeCl_3$, $Fe(acac)_3$ are used as the pre-catalysts. However, the active species for the reaction, in the presence of phosphine ligands, is not established.[27] Therefore, the first step is to study the possible pre-reactant iron complexes in the solution.

Pre-reactant Iron Complexes in Solution. The author has studied the possible iron species generated through the transmetalation process. A summary of the analysis is shown in Figure 1, where the author reports only the ground state energies of the intermediates.

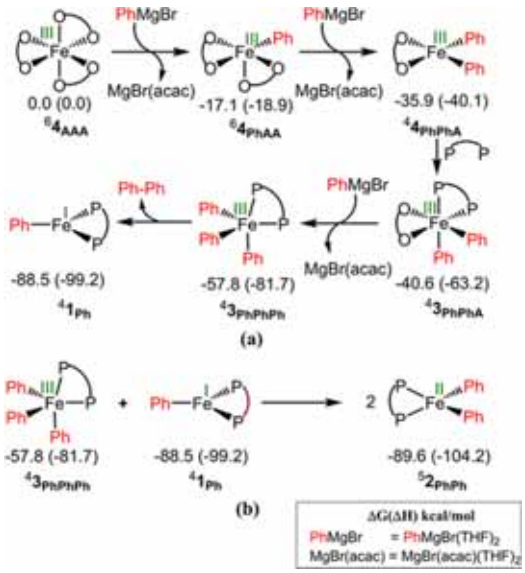

Figure 1. Possible pre-reactant complexes in solution (ΔG values are in kcal/mol, and ΔH values are given in parenthesis); (a) formation of the iron(I) active intermediate through consecutive transmetalation and reductive elimination processes. The energy required for the ligand exchange would be few kcal/mol, and would easily occur under the experimental conditions. (b) Formation of the iron(II) active intermediate from comproportionation of phenyliron(I) and triphenyliron(III) species. According to the calculations, two THF (solvent) molecules can be coordinated to PhMgBr and MgBr(acac) complexes (see Figure 2).

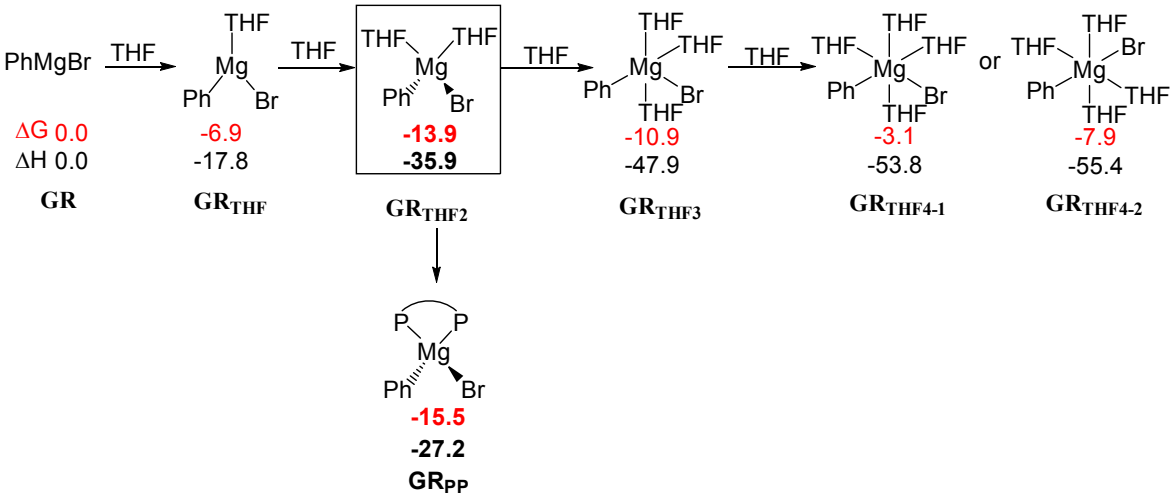

Figure 2. Grignard reagent in THF solution. ΔG values are in kcal/mol, and ΔH values are in parenthesis.

Starting from $\mathbf{4}_{\mathbf{AAA}}$, an Fe^{I} species $\mathbf{1}_{\mathbf{Ph}}$ complex can be formed through the $\mathbf{4}_{\mathbf{AAA}}$

→ **4**$_{PhAA}$ → **4**$_{PhPhA}$ → **3**$_{PhPhA}$ → **3**$_{PhPhPh}$ → **1**$_{Ph}$ path (Figure 3). This is the most likely path, as it generates the thermodynamically most stable Fe^{I} complex. Another relatively high energy Fe^{I} complex **5**$_{PhTHF}$ may be also formed through the **4**$_{AAA}$ → **4**$_{PhAA}$ → **4**$_{PhPhA}$ → **4**$_{PhPhPh}$ → **4**$_{PhPhPhTHF}$ → **5**$_{PhTHF}$ path. The ground state of two Fe^{III}-complexes (**4**$_{AAA}$ and **4**$_{PhAA}$) is the sextet state. For other Fe^{III}-complexes, the ground state is the quartet. For Fe^{I}-complexes, the quartet spin state becomes the ground state, except for **1'**$_{Ph}$, where two molecules of BenzP* coordinate to Fe^{I} and the doublet state is the ground state.

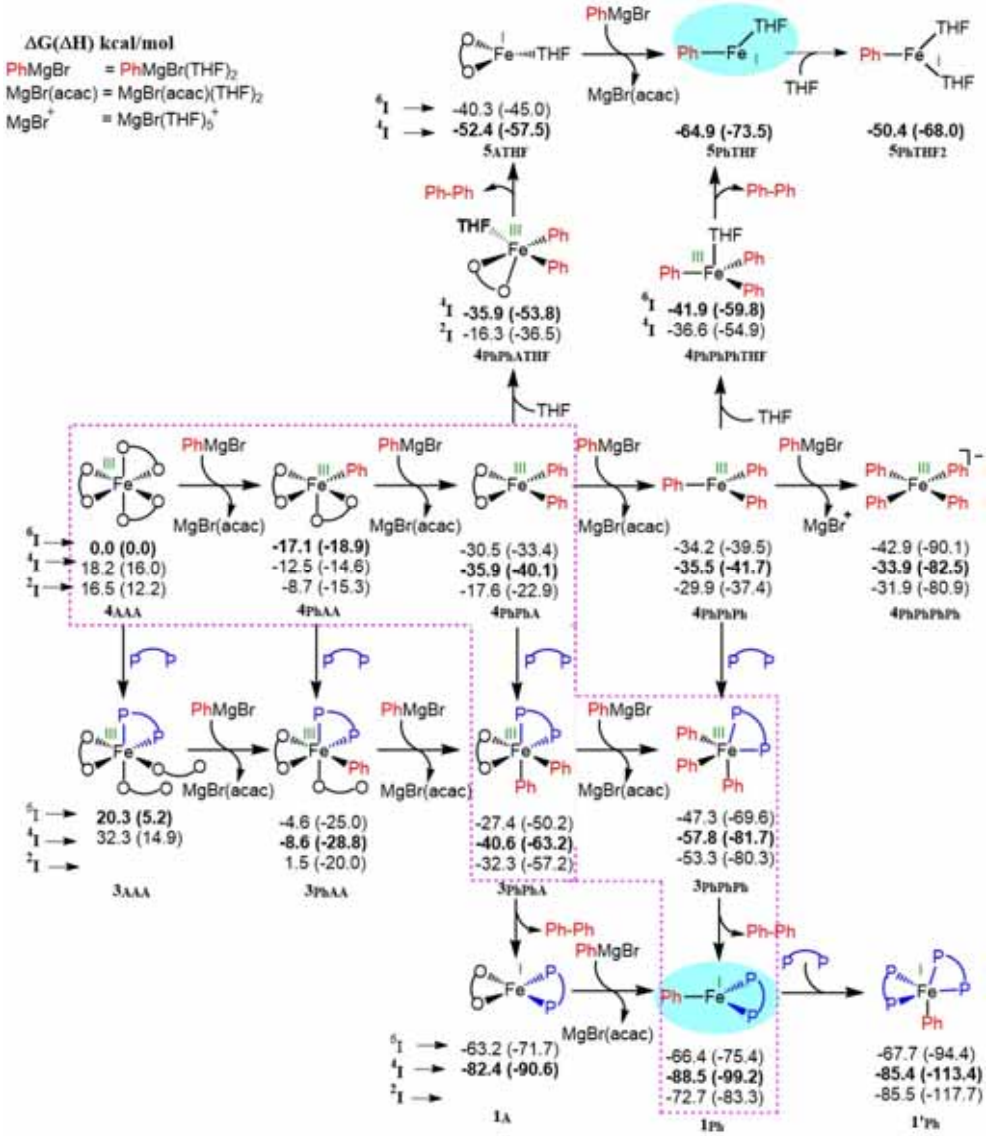

Figure 3. Relative energies [ΔG(ΔH) in kcal/mol] of the possible pre-reactant complexes in solution, and their spin states. In this analysis, PhMgBr and MgBr(acac) are coordinated to two THF (solvent) molecules, as shown at top left of figure.

After Fe^{I} species is formed, Fe^{II} complexes can be generated by

comproportionation between Fe^{I} and Fe^{III} species (Figure 4). Based on the relative energies of Fe^{I} and Fe^{II}, both species may be formed. The lowest energy species in purple boxes in Figure 4 would be the possible Fe^{I} and Fe^{II} active species in solution. Comproportionation between two Fe^{I} ($^{4}\mathbf{1_{Ph}}$) species leading to formation of Fe^{0} [Fe(BenzP*)(THF)$_2$] and Fe^{II} ($\mathbf{2_{PhPh}}$) is less likely [ΔG(ΔH) = 9.2 (-2.6) kcal/mol].

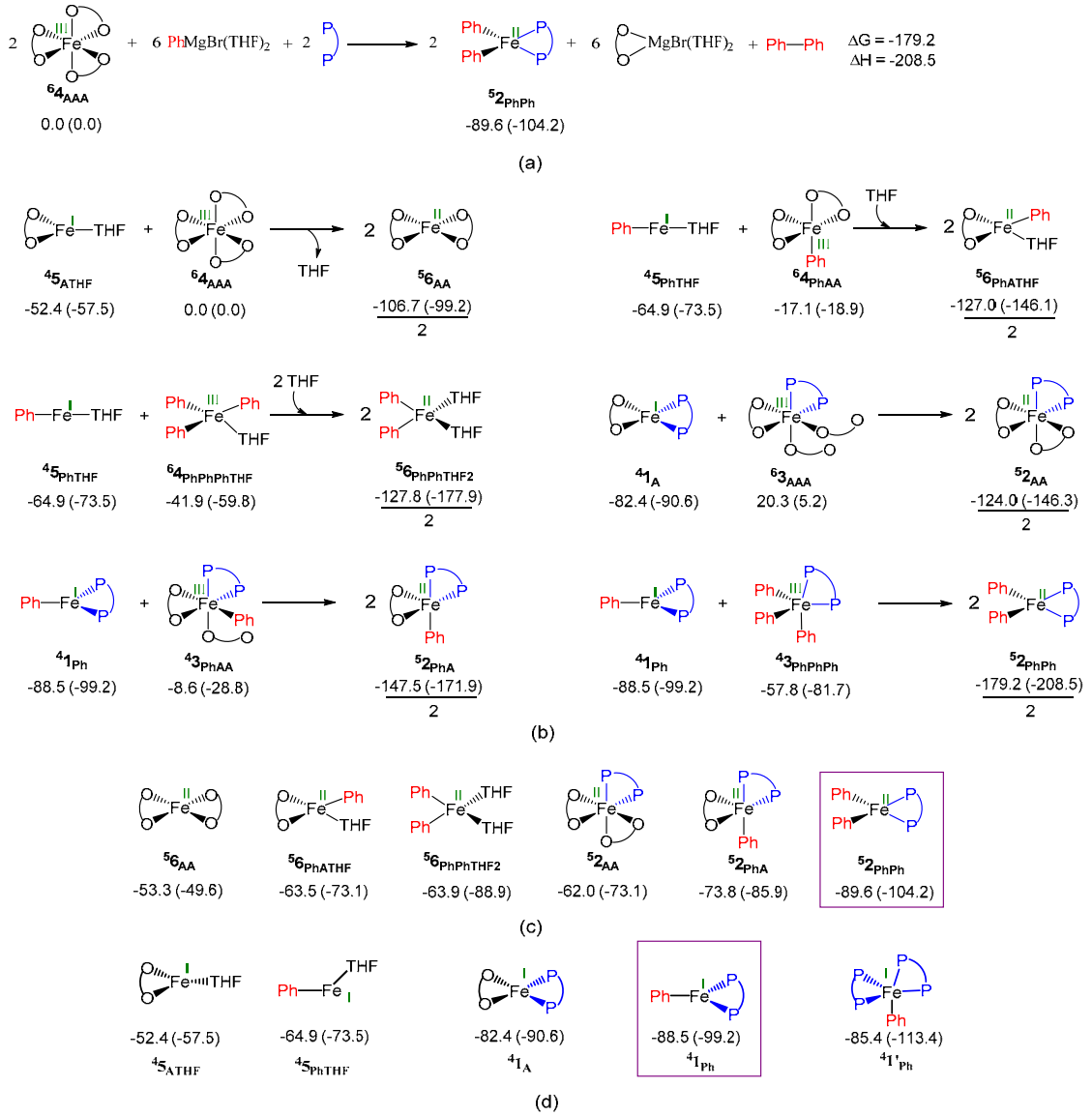

Figure 4. (a) Method for calculation of energy for $\mathbf{2_{PhPh}}$ complex (note: similar procedure was used to calculate relative energies of the other possible Fe^{II} species). All energies [ΔG(ΔH) in kcal/mol] are reported relative to Fe(acac)$_3$ ($^{6}\mathbf{4_{AAA}}$) complex. (b) Formation of Fe^{II}-species through the comproportionation of Fe^{I} and Fe^{III} complexes (c) Relative energies of various Fe^{II} complexes. (d) Relative energies of the possible Fe(I) species.

The activation barrier for biphenyl formation was calculated from various Fe(III)

species to check its feasibility (Figure 5). The biphenyl formation from five possible Fe^{III} species is studied because it can occur at any step. The lower activation barrier for ^{4}**TS3**$_{PhPh}$ suggested that the biphenyl can occur from **4**$_{PhPhA}$, which will be followed by BenzP* coordination, leading to the formation of **1**$_{A}$ and then **1**$_{Ph}$. Similarly, the activation barrier for biphenyl formation through other TSs is also feasible and hence, also depend on the activation barrier of transmetalation.

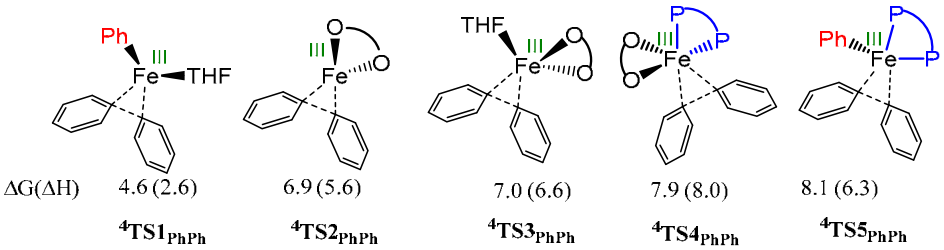

Figure 5. The activation barrier [ΔG(ΔH, in kcal/mol)] for biphenyl formation starting from various Fe^{III} species (**4**$_{PhPhPhTHF}$, **4**$_{PhPhA}$, **4**$_{PhPhATHF}$, **3**$_{PhPhA}$ and **3**$_{PhPhPh}$) in the quartet spin state.

The author concludes from Figure 1 that the formation of ^{4}**1**$_{Ph}$ and ^{5}**2**$_{PhPh}$ are thermodynamically favorable, and are the possible active intermediates in the solution. A marginal energy difference between ^{4}**1**$_{Ph}$ and ^{5}**2**$_{PhPh}$ means that both complexes can be formed in solution under the reaction conditions.

Other possible Fe^{II}/Fe^{I} complexes in solution. Although Fe^{II} species (^{5}**2**$_{PhPh}$) is the thermodynamically most stable species, coordination or exchange of other ligands in solution, in particular, Br^{-}, Cl^{-}, *acac*, and THF, may be possible. Among the complexes formed by ligand coordination or exchange, ^{5}**2**$_{PhPh}$ is still the thermodynamically most stable complex (Figure 6). Based on the analysis, the author argues that ^{5}**2**$_{PhPh}$ is the thermodynamically most stable complex, while ^{5}**2**$_{PhCl}$ (7.6 kcal/mol) and ^{5}**2**$_{ClCl}$ (16.5 kcal/mol) complexes may exist when the concentration of the Grignard reagent is low. Similarly, among iron(I) species ^{4}**1**$_{Ph}$ is lower in energy than ^{4}**1**$_{Cl}$ by 3.4 kcal/mol (see Figure 7 for other iron(I) species). The reaction mechanism for the formation of chlorinated iron(I) and iron(II), at the beginning of the reaction, is shown in Schemes 2 and 3, respectively.

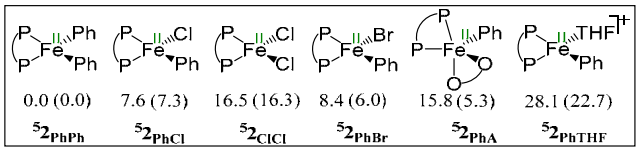

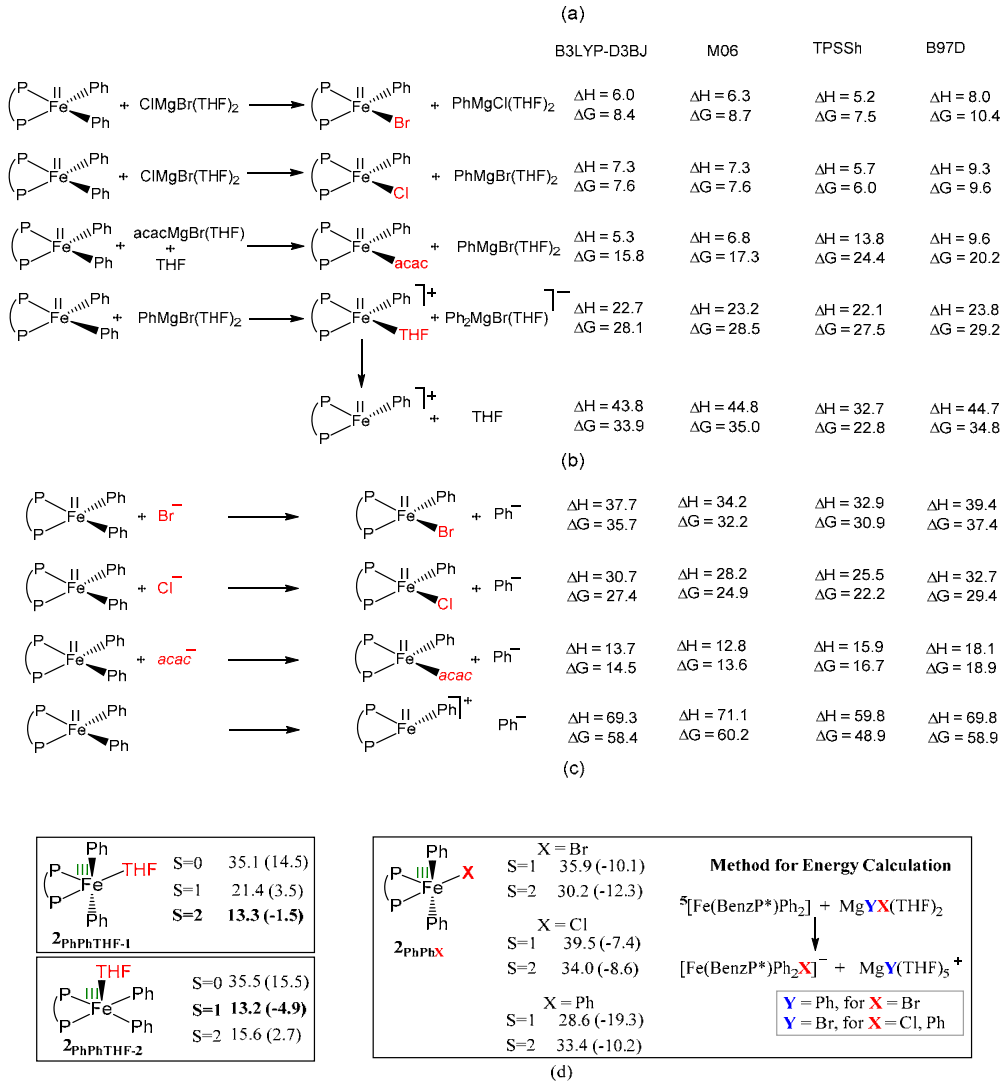

Figure 6. (a) Relative Gibbs free energies (ΔG, in kcal/mol) of Fe^{II} complexes with different ligand combinations in the quintet spin state. ΔH values are given in parenthesis. (b-c) Two methods of energy calculations from **2$_{PhPh}$** complex; (b) by the ligands exchange from the Grignard reagent, and (c) using anionic ligands. The reaction paths in (b) are thermodynamically feasible than that of (c). Therefore, the author uses reactions in (b) for the discussion. The PCM$_{THF}$/B3LYP-D3BJ/BS1 optimized geometry is used for calculation with BS2 basis set [SDD (Fe,Br) and cc-PVTZ(others)] for energy calculations. (d) Energies [ΔG(ΔH), in kcal/mol] of THF and anionic ligand coordination to **2$_{PhPh}$** in different spin states. The energies of complexes show that THF or anionic ligand coordination to **2$_{PhPh}$** is less likely.

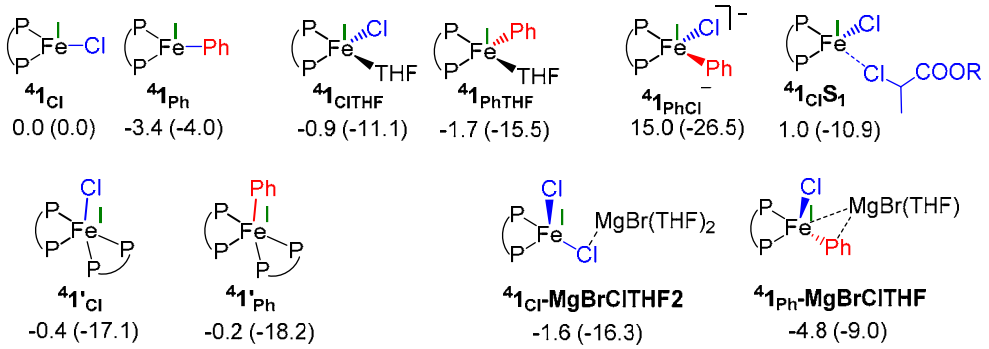

Figure 7. Relative energies [ΔG(ΔH), in kcal/mol] of Fe^{I} complexes with different ligand combinations. Energies are with respect to $^{4}\mathbf{1}_{Cl}$.

Among different Fe^{I}-species $^{4}\mathbf{1}_{Ph}$ is lower in energy. The Fe^{I}-species coordinated to MgBrCl ($^{4}\mathbf{1}_{Ph}$**-MgBrClTHF**) is slightly lower in energy than $^{4}\mathbf{1}_{Ph}$ (1.4 kcal/mol) (Figure 7). The formation of chlorinated Fe^{I} species from $^{4}\mathbf{1}_{Ph}$ at start of reaction involves the reaction of $^{4}\mathbf{1}_{Ph}$ with substrate leading to Fe^{I}(BenzP)Cl ($^{4}\mathbf{1}_{Cl}$) and product (Scheme 3). Afterward, $^{4}\mathbf{1}_{Cl}$ will be the active-species for the reaction, as the concentration of the Grignard reagent is low which will reduce the probability of transmetalation. The $\mathbf{2}_{PhCl}$ and $\mathbf{2}_{ClCl}$ (shown in Figure 6) can be generated at the start of reaction from $\mathbf{2}_{PhPh}$, by following Scheme 3.

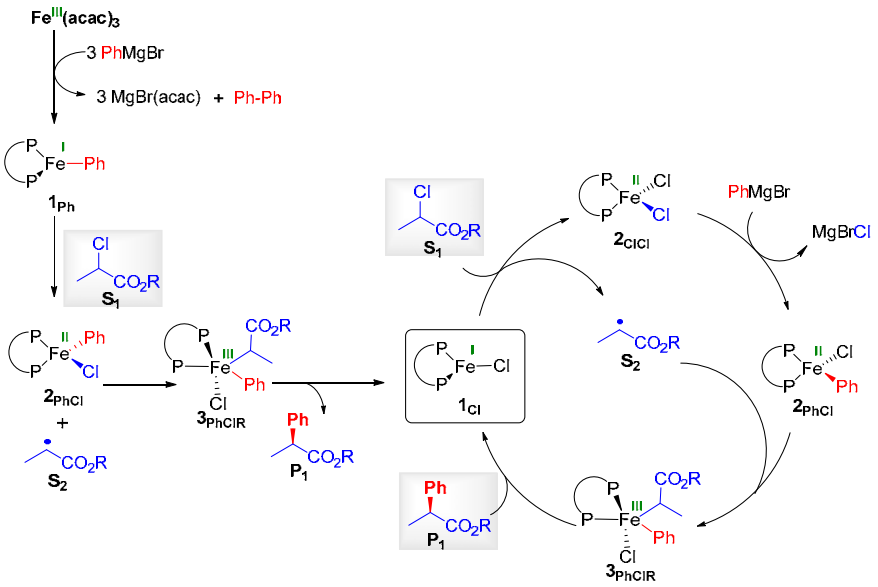

Scheme 3. $\mathbf{1}_{Cl}$ formation at beginning of the reaction from $\mathbf{1}_{Ph}$.

According to B3LYP-D3BJ results, quintet state, with distorted tetrahedral geometry, is the ground state for $\mathbf{2}_{\mathbf{PhPh}}$, $\mathbf{2}_{\mathbf{PhCl}}$, and $\mathbf{2}_{\mathbf{ClCl}}$ complexes (Figure 8). A similar conclusion can be made with ONIOM[CCSD(T): B3LYP-D3BJ]. The author has crystallized the $\mathbf{2}_{\mathbf{ClCl}}$ complex (Figure 20 and Table 13 in Experimental sections). The geometry provided by B3LYP-D3BJ/BS1 (and other levels of theory) for the quintet ground state agrees well with the experimental structure. Further details are provided in Table 1.

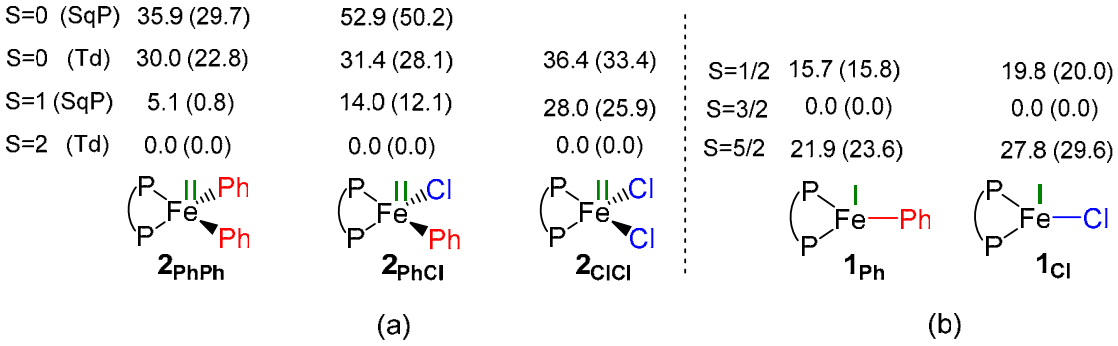

Figure 8. (a) Relative energies of the possible spin states for $\mathbf{2}_{\mathbf{PhPh}}$, $\mathbf{2}_{\mathbf{PhCl}}$ and $\mathbf{2}_{\mathbf{ClCl}}$ complexes from B3LYP-D3BJ/BS1. SqP and Td correspond to square planar and tetrahedral geometry of Fe^{II} species, respectively. (b) Relative energies of the possible spin states for $\mathbf{1}_{\mathbf{Ph}}$ and $\mathbf{1}_{\mathbf{Cl}}$ complexes ΔG values are in kcal/mol, and ΔH values are given in parenthesis.

Table 1. Structural Parameters of Optimized[a] $^{5}2_{ClCl}$ in Comparison to Crystal Structure at Different Level of Theory

	Crystal 1	**Crystal 2**	L1[b]	L2[b]	L3[b]	L4[b]	L5[b]
d Fe-P1	2.421	2.405	2.453	2.447	2.488	2.463	2.456
d Fe-P2	2.405	2.400	2.445	2.435	2.472	2.461	2.456
d Fe-Cl1	2.232	2.228	2.252	2.279	2.285	2.291	2.269
d Fe-Cl2	2.224	2.219	2.248	2.274	2.282	2.295	2.269
∠P1-Fe-P2	83.57	84.45	83.48	84.27	83.60	83.57	83.47
∠Cl1-Fe-Cl2	119.24	123.48	133.04	113.59	121.90	126.53	123.44
d C1-C2	5.337	5.357	5.310	5.095	5.161	4.855	4.686
d C3-C4	4.098	4.130	4.183	4.497	4.453	4.580	4.688

[a]Basis sets (BS1): SDD(Fe,Br); 6-31G*(C,H); 6-31+G** (P,Cl). [b] L1=BLYP-D3BJ; L2=PCM_{THF}/OPBE; L3=PCM_{THF}/TPSSh; L4=PCM_{THF}/B3LYP-D3BJ; L5= M06. All structures are in quintet spin state.

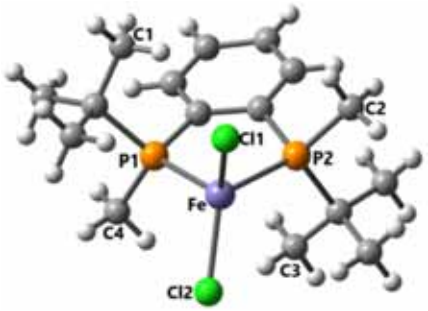

All level of theories gives structural parameters close to the crystal structure in quintet spin state. At PCM_{THF}/B3LYP-D3BJ level of theory Fe–P and Fe–Cl bond distances vary by 0.06 and 0.07 respectively. The conformation of phosphine is slightly different in the solvent phase, which is clear from '*d* C1-C2' and '*d* C3-C4'. Gas phase structure has phosphine conformation close to crystal structure but have larger ∠ Cl1-Fe-Cl2. Further quintet spin state is the ground state (Figure 8). The triplet state has a square planar structure and is different from the crystal structure. In singlet state tetrahedral geometry have larger ∠ Cl1-Fe-Cl2 (146°) and very short Fe-P distance (*d* Fe-P1=2.22 and *d* Fe-P1=2.23) (parameters not given in Table 1).

Reaction mechanism. After establishing the thermodynamically stable complexes in solution, now the author is in the position to discuss the reaction mechanism of the catalytic cycle, specifically the carbon-chlorine (C–Cl) activation, transmetalation, and carbon-carbon (C–C) bond formation steps are discussed.

The Carbon–Chlorine bond activation. The first step of the mechanism is the C–Cl bond cleavage, and occurs through an atom-transfer mechanism, leading to an alkyl radical (Figure 10a). The author has explored the approximate reaction paths for the C–

Cl activation starting from the thermodynamically most stable intermediate $^{5}\mathbf{2}_{\mathbf{PhPh}}$. For this purpose, an MC-AFIR search was performed, where the artificial force of 300 kJ/mol was applied between Fe-atom and Cl-atom. Also, a negative force was added between the Cl-atom and the C-atom of the substrate to break the C–Cl bond (Figure 10a). A restricted MC-AFIR search was performed for 25 paths. Depending on the substrate approach directions, reaction paths can be categorized into four groups, namely D_1, D_2 D_3 and D_4 (Figure 10b). In D_1 and D_2, Cl-transfer occurs parallel to P–Fe–P plane, while in D_3 and D_4 the Cl-transfer occurs from the direction perpendicular to the plane of P–Fe–P.

After refining the approximate TSs and calculating the TSs in the possible spin states, the author has found that the Cl-transfer occurs through the triplet state. The lowest energy TS, $^{3}\mathbf{TS1\text{-}2}_{\mathbf{PhPh}}\mathbf{\text{-}3}_{\mathbf{PhPhCl}}$, has an activation barrier of 19.8 kcal/mol (all calculated TSs are summarized in Table 2). In $^{3}\mathbf{TS1\text{-}2}_{\mathbf{PhPh}}\mathbf{\text{-}3}_{\mathbf{PhPhCl}}$, Cl-transfer occurs through the D_3, where the Cl-atom approaches Fe from the axial position. In the quintet state, Cl-transfer through D_2 ($^{5}\mathbf{TS8\text{-}2}_{\mathbf{PhPh}}\mathbf{\text{-}3}_{\mathbf{PhPhCl}}$, 24.0 kcal/mol**)** is the lowest energy TS, which is however 4.2 kcal/mol above $^{3}\mathbf{TS1\text{-}2}_{\mathbf{PhPh}}\mathbf{\text{-}3}_{\mathbf{PhPhCl}}$**.** The author has not located the TSs for the singlet state, as the energy of $^{1}\mathbf{2}_{\mathbf{PhPh}}$ is higher than the triplet and quintet lowest energy TSs. It is important to note that the ground state of $\mathbf{2}_{\mathbf{PhPh}}$ is a quintet, while the lowest energy TS for the C–Cl activation is a triplet. Therefore, the C–Cl activation undergoes a spin crossover (Figure 9).

Table 2. TSs Obtained for Cl-atom Transfer Reaction Catalyzed by Fe^{II}-Species $\mathbf{2_{PhPh}}$ in Quintet and Triplet Spin States (energies are in kcal/mol and torsion angles are in degrees)

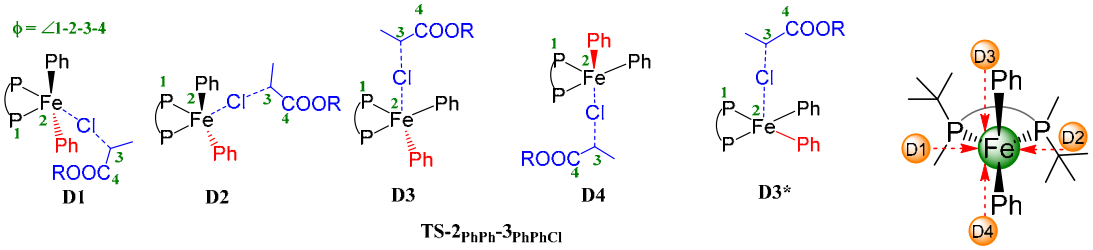

	Type	*Stereochemistry*[c]	ϕ	Spin on Fe	ΔH[a]	ΔG[a]	ΔΔH	ΔΔG
^{3}**TS1** = ^{3}**TS-2$_{PhPh}$-3$_{PhPhCl}$**	D3*	*R*	-112	2.68	2.0	19.8	0.0	0.0
^{3}**TS2**	D3*	*R*	1	2.69	1.6	19.8	-0.4	0.0
^{3}**TS3**	D3*	*S*	65	2.65	1.1	19.9	-0.9	0.2
^{3}**TS4**	D3*[b]	*S*	-103	2.69	2.1	20.1	0.1	0.3
^{3}**TS5**	D3*	*S*	-149	2.69	1.5	21.5	-0.5	1.8
^{3}**TS6**	D3*	*R*	-152	2.69	1.8	21.8	-0.2	2.1
^{3}**TS7**	D3	*R*	-108	2.61	8.3	26.6	6.3	6.8
^{5}**TS8** = ^{5}**TS-2$_{PhPh}$-3$_{PhPhCl}$**	D2	*R*	65	3.64	7.9	24.0	5.9	4.3
^{5}**TS9**	D3	*R*	-1	3.68	11.4	26.5	9.4	6.7
^{5}**TS10**	D3	*S*	-58	3.68	10.3	26.5	8.4	6.8
^{5}**TS11**	D3	*R*	-140	3.65	10.5	26.8	8.5	7.0
^{5}**TS12**	D3	*R*	-114	3.67	10.8	27.3	8.8	7.6
^{5}**TS13**	D4	*S*	-160	3.70	10.8	27.5	8.8	7.7
^{5}**TS14**	D3	*R*	-79	3.69	8.5	27.6	6.5	7.9
^{5}**TS15**	D3	*R*	-2	3.71	11.7	27.6	9.8	7.9
^{5}**TS16**	D3	*S*	-141	3.65	11.4	28.2	9.5	8.4
^{5}**TS17**	D3	*R*	136	3.66	12.7	28.6	10.7	8.9
^{5}**TS18**	D2	*S*	-81	3.66	13.1	28.7	11.1	8.9
^{5}**TS19**	D2	*S*	-27	3.62	9.7	28.7	7.7	9.0
^{5}**TS20**	D3	*R*	-14	3.71	10.6	29.2	8.6	9.5
^{5}**TS21**	D1	*R*	134	3.66	15.5	31.5	13.5	11.8
^{5}**TS22**	D2	*R*	-42	3.65	14.7	33.2	12.7	13.4

[a] Energies are reported relative to $^5\mathbf{2_{PhPh}}$ + $\mathbf{S_1}$. [b] **D3*** and **D3** have different geometry. [c] *R* and *S* denote the stereochemistry of chiral center in substrate, $\mathbf{S_1}$.

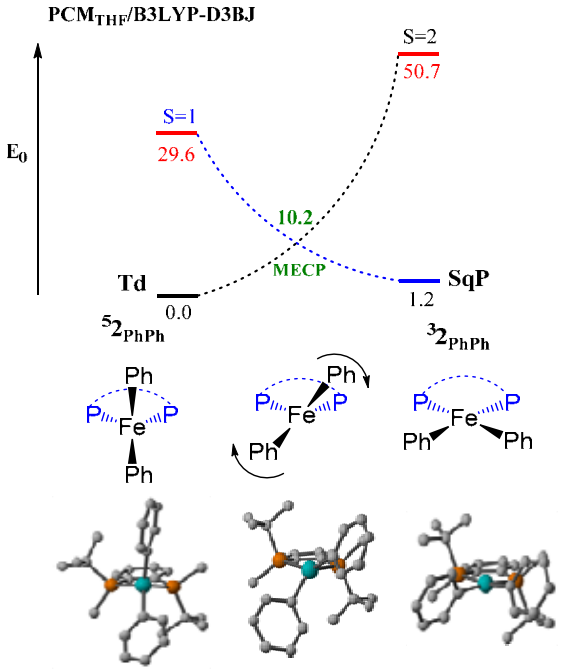

Figure 9. Minimum energy crossing point (MECP) for **2$_{PhPh}$** complex. The MECP is energetically lower than the activation barrier of the C-Cl activation by $^3Fe^{II}$-complex (^{3}**2$_{PhPh}$**). Therefore, spin-crossing is possible before the C-Cl activation, suggesting Td and SqP geometries may be in an equilibrium. The total electronic energy without zero point energy correction is reported here. The energies for Td geometry in triplet spin and SqP geometry in quintet spin state (energies in red color) are obtained by using Td geometry of quintet spin and SqP geometry of triplet spin state, respectively. The MECP calculation is performed using the GRRM program. The energies are at PCM$_{THF}$ /B3LYP-D3BJ/BS1 level of theory.

The author's attention then turned into the C–Cl bond activation by relatively high-energy active intermediates, specifically **2$_{PhCl}$** and **2$_{ClCl}$.** In the case of **2$_{PhCl}$**, the C–Cl activation occurs through the quintet state (25.8 kcal/mol), while the triplet TS is relatively higher in energy (34.6 kcal/mol). The activation barrier for the C–Cl activation through **2$_{ClCl}$** in the quintet state is 38.3 kcal/mol, and for triplet state is 47.5 kcal/mol (see Tables 3 and 4). Therefore, both **2$_{PhCl}$** and **2$_{PhCl}$** would not contribute to the C–Cl activation.

Table 3. Energies (kcal/mol) of Different TSs Obtained for Cl-Atom Transfer Reaction Catalyzed by Fe^{II} $\mathbf{2_{PhCl}}$ Species in Quintet and Triplet States

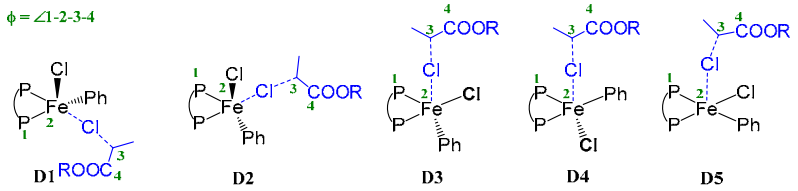

	Type	*Stereochemistry* [b]	ϕ	Spin on Fe	ΔH [a]	ΔG [a]
^{5}**TS1** = ^{5}**TS-2$_{PhCl}$-3$_{PhClCl}$**	D2	*R*	57	3.54	11.2	25.8
^{5}**TS2**	D1	*R*	56	3.52	12.0	27.0
^{5}**TS3**	D2	*R*	60	3.57	11.3	27.1
^{5}**TS4**	D4	*S*	-59	3.61	14.8	28.9
^{5}**TS5**	D3	*S*	-43	3.57	21.3	35.4
^{3}**TS6** = ^{3}**TS-2$_{PhCl}$-3$_{PhClCl}$**	D5	*S*	-65	2.73	17.5	34.6
^{3}**TS7**	D5	*S*	-66	2.72	17.7	34.7
^{3}**TS8**	D4	*S*	-57	2.65	20.3	37.8
^{3}**TS9**	D2	*R*	66	2.65	20.2	37.4

[a] Energies are with respect to ^{5}**2$_{PhCl}$** and **S1**. [b] *R* and *S* denote the stereochemistry of chiral center in substrate, **S1**. Note. As the TSs are relatively higher in energy, they would not contribute for the reaction.

Table 4. Energies[a] (kcal/mol) of TSs Obtained for Cl-Atom Transfer Reaction Catalyzed by Fe^{II} $\mathbf{2_{ClCl}}$ Species

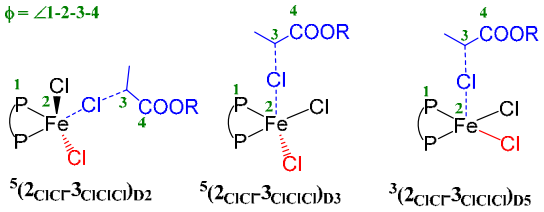

	Type	*Stereochemistry* [b]	ϕ	Spin Density (Fe)	ΔH [a]	ΔG [a]
^{5}**TS1-2$_{ClCl}$-3$_{ClClCl}$**	D2	*R*	58.5	3.37	23.7	38.3
^{5}**TS2-2$_{ClCl}$-3$_{ClClCl}$**	D3	*S*	-58.1	3.49	28.3	43.2
^{3}**TS3-2$_{ClCl}$-3$_{ClClCl}$**	D5	*R*	-60.0	2.75	30.3	47.5

[a] Energies are with respect to ^{5}**2$_{ClCl}$** and **S1**. [b] *R* and *S* denote the stereochemistry of chiral center in substrate, **S1**. Note: As the TSs are relatively higher in energy, they would not contribute for the reaction.

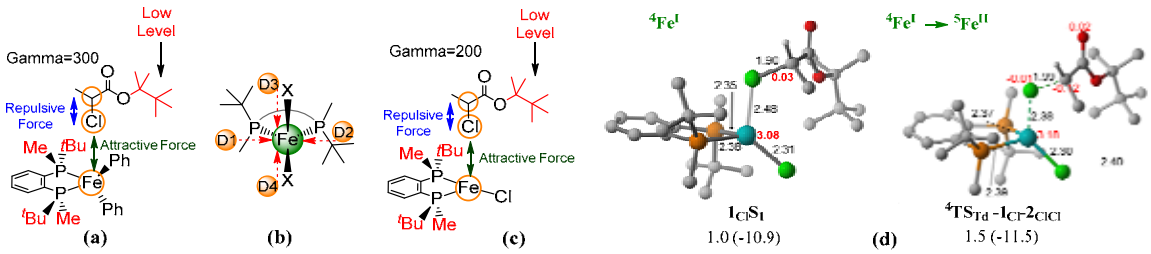

Figure 10. Cl-atom transfer step by Fe^{II} and Fe^{I}. (a) Details of AFIR calculation for the reaction between $^5\mathbf{2}_{PhPh}$ and substrate. (b) Four possible approach directions for the substrate. (c) Details of AFIR calculation for the reaction between $^4\mathbf{1}_{Cl}$ and substrate. (d) Optimized pre-reacting complex and transition state for C-Cl activation by Fe^{I} ($^4\mathbf{1}_{Cl}$). The energies [ΔG (ΔH)] are reported relative to $^4\mathbf{1}_{Cl}$. H-atoms are omitted for clarity. Distances are given in Å. Mulliken spin densities on atoms involved in reaction coordinate is shown in red.

Then, the author has explored the C–Cl activation through the Fe^{I} complex, $\mathbf{1}_{Cl}$. For this purpose, an MC-AFIR was performed (in a quartet spin state), where the artificial force of 200 kJ/mol was applied between Cl and Fe, with a negative force between C and Cl (Figure 10). 50 approximate TSs were determined from the MC-AFIR search. After refining them, $^4\mathbf{TS}_{Td}$-$\mathbf{1}_{Cl}$-$\mathbf{2}_{ClCl}$ becomes the lowest energy TS (relative energies of all refined TSs are summarized in Table 5), where the barrier for the C–Cl activation is only 1.5 kcal/mol and is almost a barrierless process. The author has also checked the square-planar geometry for the TS and is however 15.3 kcal/mol higher than $^4\mathbf{TS}_{Td}$-$\mathbf{1}_{Cl}$-$\mathbf{2}_{ClCl}$. The C–Cl activation in the doublet spin state is relatively higher in energy (24.8 kcal/mol).

Table 5. Energies[a] (kcal/mol) of TSs Obtained for Cl-Atom Transfer Reaction Catalyzed by Fe^{I} $\mathbf{1}_{Cl}$ Species in Quartet Spin State, Leading to Quintet $^{5}\mathbf{2}_{PhPh}$

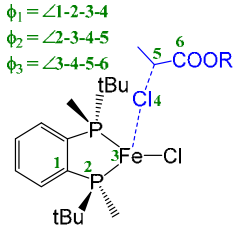

^{4}**TS$_{Td}$-1$_{Cl}$-2$_{PhPh}$** [b]	ΔH [a]	ΔG [a]	ϕ_1	ϕ_2	ϕ_3	Spin Density (Fe)
	S-substrate (**S$_1$**) with formation of ^{2}**S$_2$** radical and ^{5}**2$_{ClCl}$**					
^{4}**TS1** = ^{4}**TS$_{Td}$-1$_{Cl}$-2$_{ClCl}$**	-11.5	1.5	85	131	105	3.18
^{4}**TS2**	-11.4	2.3	86	129	104	3.18
^{4}**TS3**	-11.6	2.4	85	130	103	3.18
^{4}**TS4**	-11.4	2.7	85	131	102	3.18
^{4}**TS5**	-11.5	2.8	86	133	100	3.17
^{4}**TS6**	-9.6	3.8	90	130	-110	3.25
^{4}**TS7**	-8.3	4.6	121	-130	-48	3.15
^{4}**TS8**	-8.1	4.8	121	-133	-45	3.14
^{4}**TS9**	-8.5	6.0	123	-41	-81	3.18
^{4}**TS10**	-8.7	6.2	124	-130	-49	3.16
^{4}**TS11**	-8.6	6.5	116	-34	-86	3.18
^{4}**TS12**	-7.8	6.8	113	64	57	3.13
^{4}**TS13**	-6.7	6.9	85	-66	49	3.17
^{4}**TS14**	-8.6	7.0	81	130	24	3.17
^{4}**TS15**	-8.7	7.0	121	-128	-48	3.15
^{4}**TS16**	-6.8	7.1	86	-63	45	3.16
	S-substrate (**S$_1$**) with formation of ^{2}**S$_{2\text{-}C1}$** radical and ^{5}**2$_{ClCl}$**					
^{4}**TS17**	-9.8	2.4	133	-156	91	3.14
^{4}**TS18**	-10.6	2.5	98	132	72	3.19
^{4}**TS19**	-9.7	2.7	136	-155	90	3.14
^{4}**TS20**	-9.5	3.4	137	-155	87	3.14
^{4}**TS21**	-9.6	3.5	135	-155	89	3.14
^{4}**TS22**	-9.6	3.9	135	-154	90	3.14
^{4}**TS23**	-9.6	3.9	136	-155	89	3.14
^{4}**TS24**	-8.5	4.0	79	55	-149	3.13
^{4}**TS25**	-10.4	4.2	94	134	-169	3.23
^{4}**TS26**	-9.6	4.2	137	-155	88	3.14
^{4}**TS27**	-10.9	4.7	90	131	41	3.17
^{4}**TS28**	-8.3	4.7	79	53	-148	3.12
^{4}**TS29**	-8.2	5.1	79	54	-149	3.13
^{4}**TS30**	-10.5	5.4	85	130	26	3.17
^{4}**TS31**	-9.4	5.9	97	-1	-106	3.18
^{4}**TS32**	-9.1	6.0	115	-61	-131	3.19
^{4}**TS33**	-8.6	6.3	111	-83	-123	3.20
^{4}**TS34**	-8.9	6.8	115	-61	-132	3.19
^{4}**TS35**	-8.1	8.2	121	67	-9	3.10
	R-substrate (**S$_1$**) with formation of ^{2}**S$_2$** radical and ^{5}**2$_{ClCl}$**					
^{4}**TS36**	-10.1	4.1	89	136	30	3.18

^{4}TS37	-7.7	4.4	134	-153	91	3.17
^{4}TS38	-9.4	4.6	88	136	28	3.19
^{4}TS39	-7.7	4.6	136	-153	88	3.17
^{4}TS40	-10.2	4.9	95	129	-168	3.21
^{4}TS41	-7.5	5.0	110	-78	-122	3.17
^{4}TS42	-10.0	5.3	88	135	34	3.18
^{4}TS43	-8.4	5.4	134	-155	91	3.18
^{4}TS44	-9.7	5.7	85	132	24	3.20
^{4}TS45	-7.0	6.3	96	-7	-86	3.17
	R-substrate (**S_1**) with formation of ^{2}**$S_{2\text{-}Cl}$** radical and ^{5}**2_{ClCl}**					
^{4}TS46	-11.1	2.2	90	130	113	3.23
^{4}TS47	-11.2	2.6	88	134	-108	3.18
^{4}TS48	-7.8	3.2	136	-155	89	3.17
^{4}TS49	-8.3	3.2	120	-128	-50	3.16
^{4}TS50	-10.3	5.1	87	135	34	3.18
^{4}TS51	-8.7	5.6	113	-34	-84	3.18
^{4}TS52	-7.3	6.3	111	-82	-118	3.18
^{4}TS53	-7.0	6.3	111	-146	-80	3.11
^{4}TS54	-7.7	8.9	120	79	-22	3.10

[a] Energies are with respect to separated ^{4}**1_{Cl}** and **S_1**. [b] In all TSs the Fe-center have tetrahedral geometry.

Free energy profile for the C–Cl activation step is shown in Figure 11 (left), where the author has used ^{4}**1_{Cl}** as the reference energy point. After C–Cl activation by ^{3}**1_{Cl}**, $^5Fe^{II}$ species (^{5}**2_{ClCl}**, −28.8 kcal/mol) and an alkyl radical (**S_2**) can be formed. The author has also checked the C–Cl activation from **1_{Ph}**, which is 5.0 kcal/mol (not shown in Figure 11). On the other hand, barrier for the C–Cl activation is substantially higher with Fe^{II} complexes; ^{3}**2_{PhPh}** (19.8 kcal/mol) (Figure 11, right), ^{5}**2_{PhCl}** (25.8 kcal/mol), and ^{5}**2_{ClCl}** (38.3 kcal/mol). The author has also checked the possibilities for the C–Cl activation by Fe^{III} complex (^{4}**3_{PhClCl}**), but the calculated barrier is too high (50.3 kcal/mol).

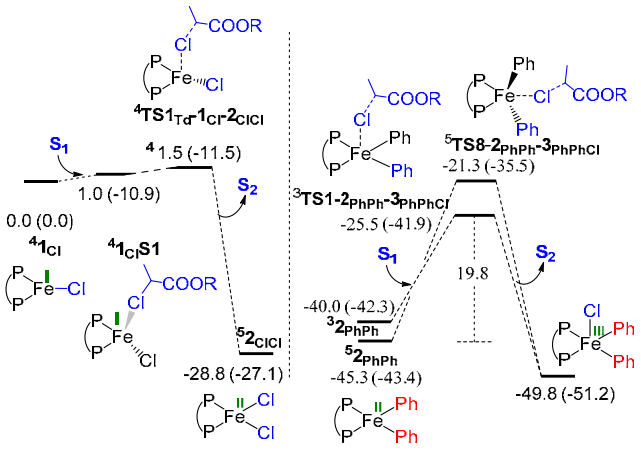

Figure 11. C–Cl activation through the Fe^{I} ($^{4}\mathbf{1_{Cl}}$) and Fe^{II} ($^{4}\mathbf{2_{PhPh}}$) species. The energies [ΔG(ΔH)] of stationary points are with respect to $^{4}\mathbf{1_{Cl}}$.

The author concluded that the active species for C–Cl activation is Fe^{I}, $^{4}\mathbf{1_{Cl}}$. Involvement of other Fe^{I} species, $^{4}\mathbf{1_{Ph}}$, is less likely due to its low concentration of the Grignard reagent.[5] If the starting species in the reaction is $Fe^{II}Ph_2$(BenzP*), initially the C–Cl activation will occur through Fe^{II} ($\mathbf{2_{PhPh}}$) and then Fe^{I} ($\mathbf{1_{Cl}}$) would be formed through the reductive elimination from Fe^{III} species ($\mathbf{3_{PhPhCl}}$) and then $^{4}\mathbf{1_{Cl}}$ will be the active species.

Transmetalation. Next step of the mechanism is the transmetalation, which involves the transfer of ligand (Ph) from Mg to the iron(II) complexes (Figure 12, Top). Starting from $^{5}\mathbf{2_{ClCl}}$ complex, the transmetalation proceeds via the formation of a pre-reacting-complex (PRC) between $^{5}\mathbf{2_{ClCl}}$ and $PhMgBr(THF)_2$, and is endergonic by 8.1 kcal/mol. The activation free energy barrier for the transmetalation process is 9.9 kcal/mol, and involves the transfer of the Ph group from Mg to Fe-center, giving rise to $^{5}\mathbf{2_{PhCl}}$ complex. Transmetalation of $^{5}\mathbf{2_{PhCl}}$ occurs through a barrier of 9.7 kcal/mol, leading to $^{5}\mathbf{2_{PhPh}}$. The author thus concludes that the above transmetalation process is possible under the reaction conditions, where the concentration of PhMgBr is high enough for the sequential Ph transfers. Therefore, the remaining steps of the mechanism were studied from both $^{5}\mathbf{2_{PhPh}}$ and $^{5}\mathbf{2_{PhCl}}$ species as the starting species (*vide infra*).

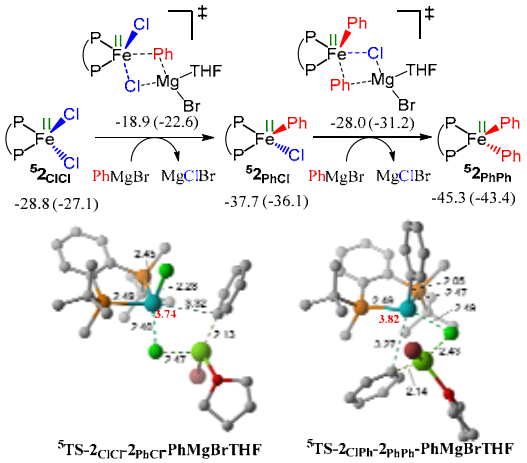

Figure 12. Transmetalation from intermediate $^{5}\mathbf{2}_{\mathbf{ClCl}}$ and $^{5}\mathbf{2}_{\mathbf{PhCl}}$. The energies [ΔG(ΔH)] of stationary points are with respect to $^{4}\mathbf{1}_{\mathbf{Cl}}$. H-atoms are omitted for clarity. Bond distances are given in Å. Mulliken spin density on Fe is shown in red.

The Carbon-Carbon bond formation. In this section, the author discusses the C–C bond formation through two mechanisms, namely the *outer-sphere* or *inner-sphere* mechanisms (Scheme 4). The *outer-sphere* mechanism involves the direct C–C coupling between a radical intermediate S_2 and an aryl group. In the case of the *inner-sphere* mechanism, the first step is coordination of the radical species ($\mathbf{S_2}$) to the Fe-center (i.e. Fe–C bond formation), followed by the reductive elimination (i.e. C–C bond formation).

Scheme 4. Schematic Representation of the C–C Bond Formation.

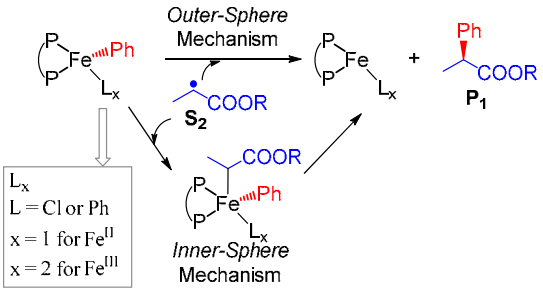

The author has systematically determined the TSs for C–C coupling from $^{5}\mathbf{2}_{\mathbf{PhCl}}$ in the quartet spin state. For this purpose, four separate MC-AFIR searches (four for the Fe–C and four for C–C bond formations) were performed with the artificial force of 200 kJ/mol (Scheme 5), because there are two low-energy conformations of Fe-Complex

(^{5}**2**$_{\mathbf{PhCl}}$ and ^{5}**2**$_{\mathbf{PhCl\text{-}C1}}$) and two low energy conformations of ^{2}**S**$_{\mathbf{2}}$ (^{2}**S**$_{\mathbf{2}}$ and ^{2}**S**$_{\mathbf{2\text{-}C1}}$). After refining the TSs for Fe–C bond formation and CC bond formation, more than 50 distinct TSs were determined. The discussion is based on the lowest energy TSs, and all calculated TSs are summarized in Tables 6–8.

Scheme 5. (a) Conformations of 2_{PhCl} and S_2. Relative Free Energies (in kcal/mol) are Given in Parenthesis. (b) Artificial Force and ONIOM Partitioning for MC-AFIR Calculations for Fe–C and C–C Bond Formation

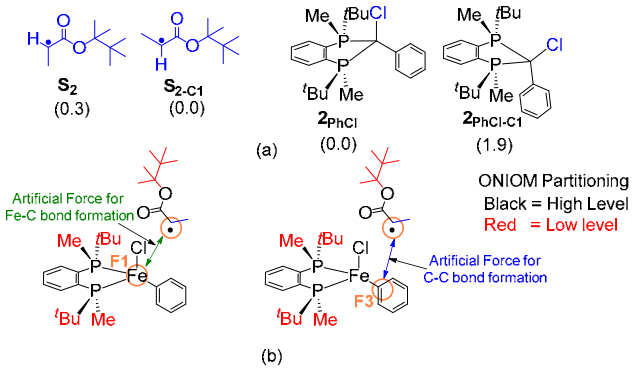

Table 6. Energies[a] (kcal/mol) of TSs Optimized for C-Fe Bond Formation from Fe^{II} Species, $\mathbf{2_{PhCl}}$ Leading to Formation of $\mathbf{3_{PhClR}}$

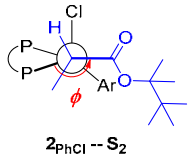

$\mathbf{2_{PhCl}}$ -- $\mathbf{S_2}$

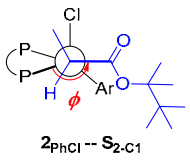

$\mathbf{2_{PhCl}}$ -- $\mathbf{S_{2\text{-}C1}}$

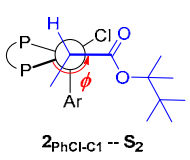

$\mathbf{2_{PhCl\text{-}C1}}$ -- $\mathbf{S_2}$

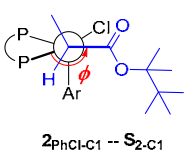

$\mathbf{2_{PhCl\text{-}C1}}$ -- $\mathbf{S_{2\text{-}C1}}$

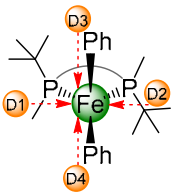

^{4}**TS-2$_{PhCl}$-3$_{PhClR}$**	ϕ	Addition Direction	Chiral Face [b]	C-Fe Distance	Spin density (Fe)	ΔH	ΔG	ΔΔH	ΔΔG
TS for Fe-C bond formation between $\mathbf{2_{PhCl}}$ and $\mathbf{S_2}$ lowest energy conformation									
^{4}**TS1**	111	D2	*re*	3.41	3.77	-5.7	8.2	0.0	0.0
^{4}**TS2**	23	D1	*si*	2.99	3.74	-4.7	12.2	1.1	4.0
^{4}**TS3**	85	D1	*si*	3.02	3.73	-3.6	13.1	2.2	4.9
^{4}**TS4**	82	D1	*si*	3.02	3.73	-3.6	13.3	2.1	5.1
^{4}**TS5**	-33	D1	*si*	2.92	3.74	-5.1	13.3	0.7	5.1
^{4}**TS6**	77	D1	*si*	3.06	3.74	-3.6	13.8	2.1	5.6
^{4}**TS7**	-106	D1	*re*	3	3.74	-4.3	14.7	1.4	6.5
^{4}**TS8**	-39	D3	*si*	2.78	3.67	4.8	22.3	10.5	14.1
^{4}**TS9**	68	D4	*si*	3.05	2.43	8.0	25.4	13.7	17.2
^{4}**TS10**	50	D2	*re*	2.97	2.96	8.9	29.0	14.6	20.9
TS for Fe-C bond formation between lowest energy conformation of $\mathbf{2_{PhCl}}$ and $\mathbf{S_{2\text{-}C1}}$									
^{4}**TS11**	160	D1	*si*	3.11	3.75	-8.1	8.8	-2.4	0.6
^{4}**TS12**	138	D2	*si*	3.21	3.79	-7.1	9.0	-1.3	0.8
^{4}**TS13**	-157	D2	*re*	3.07	3.77	-8.1	9.1	-2.3	0.9
^{4}**TS14**	120	D2	*re*	3.35	3.77	-5.5	9.2	0.3	1.0
^{4}**TS15**	159	D1	*si*	3.04	3.75	-7.8	9.3	-2.1	1.1
^{4}**TS16**	71	D1	*re*	3.04	3.75	-7.9	9.8	-2.1	1.6
^{4}**TS17**	136	D2	*si*	3.18	3.79	-7.1	10.0	-1.3	1.8
^{4}**TS18**	-142	D1	*re*	2.98	3.75	-6.1	10.7	-0.4	2.5
^{4}**TS19**	165	D1	*si*	3.1	3.77	-8.2	11.1	-2.4	2.9
^{4}**TS20**	85	D1	*re*	3.07	3.75	-8.0	11.3	-2.3	3.1
^{4}**TS21**	-141	D1	*re*	2.97	3.75	-6.3	11.4	-0.6	3.2
^{4}**TS22**	15	D1	*si*	3.01	3.73	-5.7	13.6	0.0	5.4
^{4}**TS23**	-10	D1	*si*	2.89	3.72	-4.8	14.6	1.0	6.4
^{4}**TS24**	92	D1	*re*	2.88	2.99	15.2	34.1	21.0	25.9
^{4}**TS25**	121	D2	*si*	2.94	2.30	12.3	29.9	18.1	21.7
TS for Fe-C bond formation between $\mathbf{2_{PhCl\text{-}C1}}$ and $\mathbf{S_2}$									
^{4}**TS26**	-54	D1	*si*	3.1	3.75	-7.2	8.6	-1.4	0.4
^{4}**TS27**	-138	D1	*si*	3.13	3.75	-6.1	9.2	-0.3	1.0
^{4}**TS28**	-47	D1	*si*	3.06	3.75	-6.8	9.7	-1.0	1.5
^{4}**TS29**	-134	D1	*si*	3.07	3.75	-5.7	9.7	0.0	1.5
^{4}**TS30**	-42	D1	*si*	2.99	3.74	-7.6	10.7	-1.9	2.5
^{4}**TS31**	157	D1	*re*	3.21	3.76	-4.6	11.1	1.2	2.9
^{4}**TS32**	-39	D1	*si*	3.01	3.75	-7.4	11.4	-1.6	3.2
^{4}**TS33**	-130	D1	*si*	3.29	3.76	-5.6	11.5	0.2	3.3
^{4}**TS34**	-128	D1	*re*	3.16	3.78	-4.9	11.7	0.8	3.5
^{4}**TS35**	-119	D1	*re*	3.11	3.78	-4.9	12.0	0.9	3.8
^{4}**TS36**	-122	D1	*re*	3.1	3.78	-4.8	12.1	0.9	3.9
^{4}**TS37**	155	D1	*re*	3.21	3.76	-4.3	12.4	1.5	4.2
^{4}**TS38**	-69	D1	*re*	2.91	3.71	-4.0	12.6	1.7	4.4
^{4}**TS39**	-123	D1	*re*	3.06	3.77	-5.5	13.1	0.3	4.9

^{4}TS40	-69	D1	*re*	2.92	3.72	-4.1	13.2	1.7	5.0
^{4}TS41	4	D1	*si*	2.97	3.74	-5.3	13.4	0.5	5.2
^{4}TS42	-28	D2	*si*	3	3.80	-2.8	15.6	3.0	7.4
^{4}TS43	144	D4	*re*	3.12	3.80	-0.1	17.1	5.6	8.9
^{4}TS44	45	D1	*re*	2.95	2.25	10.4	27.5	16.1	19.3
TS for Fe-C bond formation between **$2_{PhCl-C1}$** and **S_{2-C1}**									
^{4}TS45	157	D1	*si*	3.25	3.78	-7.7	8.2	-1.9	0.0
^{4}TS46	160	D1	*si*	3.31	3.78	-7.6	8.2	-1.9	0.0
^{4}TS47	-135	D1	*re*	3.3	3.80	-6.5	8.4	-0.8	0.2
^{4}TS48	-133	D1	*re*	3.21	3.79	-6.6	8.7	-0.8	0.5
^{4}TS49	74	D1	*re*	3.08	3.75	-8.0	8.9	-2.3	0.7
^{4}TS50	-142	D1	*si*	3.18	3.76	-6.3	9.4	-0.5	1.2
^{4}TS51	-143	D1	*si*	3.13	3.76	-6.1	9.5	-0.4	1.3
^{4}TS52	158	D1	*si*	3.17	3.77	-7.5	9.7	-1.8	1.5
^{4}TS53	-130	D1	*re*	3.28	3.79	-6.6	9.7	-0.9	1.5
^{4}TS54	39	D1	*si*	3.06	3.75	-6.5	9.8	-0.8	1.6
^{4}TS55	23	D1	*si*	3.02	3.74	-6.1	10.2	-0.4	2.0
^{4}TS56	-136	D1	*re*	3.28	3.80	-7.1	10.6	-1.4	2.4
^{4}TS57	23	D1	*si*	3	3.74	-6.0	10.9	-0.3	2.8
^{4}TS58	-142	D1	*si*	3.17	3.76	-6.0	11.3	-0.2	3.1
^{4}TS59	-50	D1	*re*	2.98	3.72	-5.2	11.4	0.5	3.2
^{4}TS60	-51	D1	*re*	2.99	3.72	-5.1	11.6	0.6	3.4
^{4}TS61	-65	D1	*re*	3.09	3.74	-5.4	11.7	0.3	3.5
^{4}TS62	25	D1	*si*	2.99	3.74	-5.8	12.2	0.0	4.0
^{4}TS63	-60	D1	*re*	3.09	3.74	-5.5	12.3	0.2	4.1
^{4}TS64	-14	D1	*si*	2.98	3.74	-5.5	13.1	0.3	4.9
^{4}TS65	46	D1	*si*	3.06	3.74	-3.1	14.5	2.7	6.3
^{4}TS66	159	D1	*si*	2.85	2.27	11.2	30.1	16.9	21.9
^{4}TS67	-137	D1	*re*	2.96	2.72	13.1	31.3	18.9	23.2

[a] Energies are with respect to **2_{PhCl}** and **S_2**. The TS leading to two lowest energy **3_{PhClR}** intermediate could not be optimized and their potential energy surface (PES) is explored by relaxed PES-scan and are low energy processes. The barrier for this step is mainly due to loss of entropy. The TSs in blue involve reaction from triplet **$^3 2_{PhCl}$** and **$^2 S_2$**, whereas other TSs are for reaction of quintet **$^5 2_{PhCl}$** and **$^2 S_2$**. [b] *re*-face addition will lead to formation of *S*-product (major) and *si*-face addition will lead to formation of minor *S*-product.

Table 7a. Energies[a] of Fe^{III} Intermediates $^{4}\mathbf{3}_{\mathbf{PhClR}}$ Generated by C-Fe Bond Formation in Quintet State

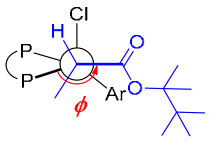

$\mathbf{2}_{\mathbf{PhCl}}$ -- $\mathbf{S}_{\mathbf{2}}$

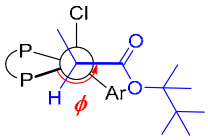

$\mathbf{2}_{\mathbf{PhCl}}$ -- $\mathbf{S}_{\mathbf{2\text{-}C1}}$

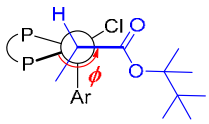

$\mathbf{2}_{\mathbf{PhCl\text{-}C1}}$ -- $\mathbf{S}_{\mathbf{2}}$

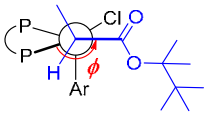

$\mathbf{2}_{\mathbf{PhCl\text{-}C1}}$ -- $\mathbf{S}_{\mathbf{2\text{-}C1}}$

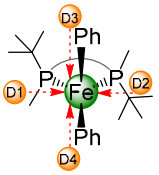

^{4}**I-3**$_{\mathbf{PhClR}}$	Pro-Chiral face of $\mathbf{S}_{\mathbf{2}}$-Addition direction	ϕ	Spin density on Fe	ΔH	ΔG
Intermediates formed by $\mathbf{2}_{\mathbf{PhCl}}$ and $\mathbf{S}_{\mathbf{2}}$					
I1 = $^{4}\mathbf{3}_{\mathbf{PhClR}}$	*re*-D1	65	3.26	-20.5	-2.3
I2	*si*-D2	301	3.28	-19.7	-1.0
I3	*re*-D2	182	3.29	-17.5	1.0
I4	*re*-D2	43	3.29	-17.2	1.9
I5	*re*-D2	42	3.29	-17.1	2.5
I6	*re*-D2	43	3.29	-17.1	2.8
I7	*si*-D1	189	3.28	-16.3	3.6
I8	*si*-D2	148	3.30	-14.7	4.0
I9	*re*-D2	117	3.28	-15.2	4.1
I10	*si*-D1	31	3.33	-12.7	6.3
I11	*si*-D1	89	3.30	-9.9	9.4
I12	*si*-D1	79	3.29	-8.9	10.7
I13	*si*-D1	221	3.30	-9.6	10.8
I14	*re*-D1	263	3.32	-7.7	13.5
Intermediates formed by $\mathbf{2}_{\mathbf{PhCl}}$ and $\mathbf{S}_{\mathbf{2\text{-}C1}}$					
I15	*si*-D1	183	3.27	-17.4	0.5
I16	*re*-D1	352	3.29	-18.3	1.4
I17	*si*-D1	185	3.28	-17.6	1.5
I18	*re*-D2	188	3.28	-18.1	1.8
I19	re-D2	129	3.29	-15.6	3.2
I20	*re*-D1	98	3.31	-16.3	3.4
I21	*si*-D2	127	3.30	-14.6	4.2
I22	*si*-D2	135	3.30	-14.5	5.2
I23	*re*-D1	258	3.32	-13.0	5.3
I24	*re*-D1	83	3.29	-14.6	5.4
I25	*re*-D1	262	3.31	-12.7	6.9
I26	*re*-D1	214	3.29	-11.0	6.9
I27	*si*-D1	63	3.29	-11.4	7.3
I28	*si*-D1	63	3.28	-11.4	7.5
I29	*si*-D1	345	3.35	-7.6	10.9
Intermediates formed by $\mathbf{2}_{\mathbf{PhCl\text{-}C1}}$ and $\mathbf{S}_{\mathbf{2}}$					
I30	*re*-D2	46	3.28	-17.3	1.3
I31	*re*-D1	49	3.31	-15.5	4.1
I32	*re*-D1	207	3.31	-13.5	4.5
I33	*re*-D1	207	3.31	-13.3	5.6
I34	*re*-D1	223	3.30	-13.0	5.9
I35	*si*-D1	300	3.29	-13.4	6.0
I36	*si*-D1	314	3.30	-13.7	6.6
I37	*si*-D1	295	3.26	-14.9	6.6
I38	*si*-D1	165	3.31	-15.0	6.7
I39	*re*-D1	274	3.29	-13.3	9.0

I40	*re*-D1	202	3.30	-10.1	9.4
I41	*re*-D1	302	3.26	-7.5	12.8
Intermediates formed by $\mathbf{2_{PhCl\text{-}C1}}$ and $\mathbf{S_{2\text{-}C1}}$					
I42	*si*-D1	165	3.31	-16.2	3.4
I43	*si*-D1	166	3.31	-16.3	3.6
I44	*si*-D1	74	3.28	-14.4	3.9
I45	*si*-D1	163	3.31	-16.1	4.1
I46	*re*-D1	91	3.32	-17.0	5.0
I47	*re*-D1	229	3.32	-13.7	5.5
I48	*re*-D1	119	3.31	-12.4	6.1
I49	*si*-D1	204	3.27	-14.5	6.3
I50	*si*-D1	22	3.31	-12.5	6.7
I51	*si*-D1	214	3.31	-11.1	7.3
I52	*si*-D1	24	3.31	-12.5	7.5
I53	*re*-D1	296	3.27	-10.3	8.9
I54	*re*-D1	298	3.27	-10.4	9.4
$\mathbf{3_{PhClR}}$ conformers by addition from D_3 and D_4 direction					
	Conformation of $\mathbf{2_{PhCl}}$ and $\mathbf{S_2}$	Pro-Chiral face of S_2-Addition direction	ϕ	Spin density on Fe	ΔΔ H	ΔΔ G
I55	$\mathbf{2_{PhCl\text{-}C1}\text{-}S_{2\text{-}C1}}$	*re*-D4	-127	3.28	-13.1	5.7
I56	$\mathbf{2_{PhCl\text{-}C1}\text{-}S_{2\text{-}C1}}$	*re*-D4	-129	3.29	-13.2	6.3
I57	$\mathbf{2_{PhCl\text{-}C1}\text{-}S_2}$	*re*-D3	32	3.20	-3.1	15.5
I58	$\mathbf{2_{PhCl\text{-}C1}\text{-}S_{2\text{-}C1}}$	*re*-D4	-91	3.29	-2.2	16.9
I59	$\mathbf{2_{PhCl}\text{-}S_{2\text{-}C1}}$	*re*-D3	155	3.21	-1.5	18.0
I60	$\mathbf{2_{PhCl}\text{-}S_{2\text{-}C1}}$	*re*-D3	152	3.22	-2.4	19.8
I61	$\mathbf{2_{PhCl}\text{-}S_2}$	*si*-D3	-44	3.19	3.0	21.8

[a] Energies are with respect to $\mathbf{2_{PhCl}}$ and $\mathbf{S_2}$.

Table 7b. Energies[a] of Fe^{III} Intermediates $\mathbf{3_{PhClR}}$ Generated by C-Fe Bond Formation in Sextet and Doublet Spin State

$\mathbf{^4I\text{-}3_{PhClR}}$ [b]	Pro-Chiral face of $\mathbf{S_2}$-Addition direction	ϕ	Spin density on Fe	ΔH	ΔG
		$\mathbf{^6 3_{PhClR}}$			
I62 (I60)	*re*-D3	155	4.20	-3.6	14.3
I63 (I20)	*re*-D2	127	4.16	-0.9	16.1
I64 (I55)	*re*-D4	162	4.19	-3.3	16.8
I65 (I1)	*re*-D1	52	4.18	-0.9	16.6
		$\mathbf{^2 3_{PhClR}}$			
I66 (I1)	*re*-D1	59	1.24	-2.3	19.1
I67 (I55)	*re*-D4	143	1.36	-0.1	22.8
I68 (I60)	*re*-D3	154	1.32	6.3	28.5
I69 (I20)	*re*-D2	125	1.16	7.9	29.1

[a] Energies are with respect to $\mathbf{2_{PhCl}}$ and $\mathbf{S_2}$.

Table 7c. Energies[a] of Stationary Points for Coordination of O-Atom of $^{2}\mathbf{S_2}$ to Fe-Atom of Fe^{II} Species, $^{5}\mathbf{2_{PhCl}}$ Leading to Formation of $^{4}\mathbf{3_{PhClRo}}$

	ΔH	ΔG	Spin density on Fe
$^{4}\mathbf{TS\text{-}2_{PhCl}\text{-}3_{PhClRo}}$	-7.0	7.9	3.80
$^{4}\mathbf{3_{PhClRo}}$	-5.2	8.5	3.79

[a] Energies are with respect to $^{5}\mathbf{2_{PhCl}}$ and $^{2}\mathbf{S_2}$.

Table 8a. Energies of TSs[a] for C-C Bond Formation (from $^{4}\mathbf{3}_{\mathbf{PhClR}}$ or $^{5}\mathbf{2}_{\mathbf{PhCl}}$+$^{2}\mathbf{S}_{\mathbf{2}}$) in Quartet Spin State

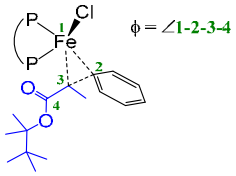

	TS Type[b]	ΔH [a]	ΔG[a]	ΔΔH	ΔΔG	Chirality	Fe-Spin	ϕ	Fe-C	Fe-O[c]
TS1	1	-10.3	6.5	0.0	0.0	*S*	3.35	125	2.32	
TS2	1	-9.3	8.3	1.0	1.8	*R*	3.32	-132	2.31	
TS3	1	-10.0	9.6	0.3	3.1	*S*	3.38	126	2.34	
TS4	1	-7.8	10.4	2.5	3.8	*S*	3.36	124	2.33	
TS5	1	-6.9	10.4	3.4	3.9	*R*	3.35	-133	2.33	
TS6	1	-6.0	11.5	4.3	4.9	*S*	3.35	131	2.35	
TS7	1	-6.8	11.7	3.5	5.1	*S*	3.34	135	2.35	
TS8	1	-5.2	11.8	5.1	5.2	*R*	3.35	-163	2.35	
TS9	1	-6.9	11.7	3.3	5.2	*R*	3.36	-137	2.33	
TS10	1	-4.5	12.4	5.8	5.8	*S*	3.36	124	2.38	
TS11	1	-6.1	12.8	4.2	6.2	*R*	3.42	-133	2.39	
TS6'	1	-4.5	12.8	5.8	6.3	*S*	3.35	125	2.36	
TS12	1	-6.5	12.8	3.8	6.3	*S*	3.37	141	2.36	
TS13	1	-7.7	12.8	2.6	6.3	*R*	3.36	-135	2.33	
TS11'	1	-6.2	12.9	4.1	6.4	*S*	3.40	148	2.37	
TS13'	1	-6.5	13.4	3.8	6.9	*R*	3.41	-121	2.39	
TS14	1	-6.2	13.4	4.1	6.9	*R*	3.44	-132	2.43	
TS15	1	-4.8	13.4	5.4	6.9	*R*	3.40	-140	2.39	
TS16	1	-3.9	13.5	6.4	7.0	*R*	3.35	-86	2.27	2.5
TS15'	1	-4.6	14.3	5.7	7.7	*R*	3.38	-146	2.35	
TS17	1	-5.0	14.7	5.3	8.2	*S*	3.33	61	2.35	
TS18	3	-1.2	15.3	9.1	8.8	*R*	3.69	-41	3.35	
TS14'	1	-3.8	15.6	6.5	9.1	*R*	3.45	-136	2.46	
TS17'	1	-4.2	15.9	6.1	9.4	*S*	3.35	65	2.37	
TS19	3	-2.4	15.9	7.9	9.4	*R*	3.68	88	3.34	
TS20	2	-0.7	16.1	9.6	9.6	*S*	3.70	68	2.97	2.46
TS21	1	-1.4	16.5	8.9	10.0	*S*	3.35	-61	2.42	
TS22	3	0.0	16.6	10.3	10.1	*R*	3.67	61	3.24	
TS23	1	-1.3	16.7	9.0	10.2	*R*	3.46	-67	2.52	
TS24	1	-1.0	16.7	9.3	10.2	*R*	3.36	150	2.39	
TS25	1	-2.1	17.2	8.2	10.7	*R*	3.54	-80	2.64	
TS26	1	-0.9	17.5	9.4	11.0	*R*	3.39	-72	2.42	
TS27	3	-1.7	17.7	8.6	11.2	*R*	3.67	84	3.27	
TS23'	1	-2.0	17.7	8.3	11.2	*R*	3.49	-66	2.55	
TS28	1	-1.0	18.0	9.3	11.4	*R*	3.48	-51	2.55	
TS29	3	1.9	18.2	12.2	11.6	*S*	3.68	-75	3.32	
TS30	2	-1.4	18.2	8.9	11.6	*R*	3.72	-52	3.1	2.39
TS31	1	0.2	18.2	10.5	11.7	*S*	3.49	-64	2.69	
TS32	1	0.0	18.4	10.3	11.8	*S*	3.35	-67	2.42	
TS33	3	3.3	18.5	13.6	11.9	*R*	3.66	112	3.4	
TS34	3	1.9	18.5	12.2	12.0	*R*	3.67	80	3.33	
TS35	1	-1.0	18.7	9.3	12.2	*S*	3.40	-71	2.52	
TS36	1	1.5	19.5	11.8	13.0	*R*	3.53	60	2.75	
TS37	1	-0.1	19.6	10.2	13.1	*S*	3.56	-65	2.78	

TS38	1	-0.9	20.1	9.4	13.6	*S*	3.44	-61	2.61	
TS39	1	2.0	20.3	12.3	13.8	*S*	3.39	14	2.51	
TS40	3	2.0	20.3	12.3	13.8	*R*	3.51	70	2.71	
TS41	1	1.6	20.7	11.9	14.2	*S*	3.47	-74	2.6	
TS42	2	5.2	22.9	15.5	16.4	*R*	3.68	55	2.84	2.27
TS43	1	1.9	23.0	12.2	16.5	*S*	3.33	81	2.24	
TS44	1	5.4	26.6	15.7	20.1	*S*	3.32	-79	2.34	
TS45	4	12.9	31.2	23.2	24.6	*R*	2.31	-55	2.96	2.2
TS46	4	15.1	32.5	25.4	26.0	*R*	2.43	-79	3.54	
TS45'	4	12.1	33.6	22.4	27.0	*R*	2.30	-53	2.96	
TS47	4	14.1	33.8	24.4	27.2	*S*	2.41	90	3.45	
TS48	4	18.4	37.8	28.7	31.3	*S*	2.28	-54	2.99	2.03

[a] The energies (kcal/mol) are with respect to separated ^{5}**2**$_{PhCl}$ and ^{2}**S**$_{2}$. Energy of lowest energy TS1 with respect to lowest energy **I1-**^{4}**3**$_{PhClR}$ intermediate (activation barrier) is 8.8 (10.2) kcal/mol (ΔG(ΔH)). [b] TS type is defined in Figure 14. For Type1 reaction occurs through Fe^{III} species ^{4}**3**$_{PhClR}$ (^{4}**TS-3**$_{PhClR}$**-1**$_{Cl}$) and for Type 2 through ^{4}**3**$_{PhClRo}$ (^{4}**TS-3**$_{PhClRo}$**-1**$_{Cl}$). In Type 3 and Type 4 reaction occur by interaction of radical species ^{2}**S**$_{2}$ with quintet Fe^{II}, ^{5}**2**$_{PhCl}$ (^{4}**TS-2**$_{PhCl}$**-1**$_{Cl}$) and ^{2}**S**$_{2}$ with triplet Fe^{II}, ^{3}**2**$_{PhCl}$ (^{4}**TS-2**$_{PhCl}$**-1**$_{Cl}$) respectively. [c] Value is given only when O-atom is near to Fe-atom.

Table 8b. Energy of TSs[a] for C-C Bond Formation in Doublet and Sextet Spin State (from ^{4}**3**$_{PhClR}$ or ^{5}**2**$_{PhCl}$/^{3}**2**$_{PhCl}$ + ^{2}**S**$_{2}$)

	TS[b] Type	ΔH	ΔG	Fe-Spin
^{6}**TS1-2**$_{PhCl}$**-1**$_{Cl}$	3	3.0	20.4	3.72
^{6}**TS2-2**$_{PhCl}$**-1**$_{Cl}$	3	3.5	20.9	3.73
^{2}**TS1-3**$_{PhClR}$**-1**$_{Cl}$	1	11.5	31.4	1.15
^{2}**TS2-3**$_{PhClR}$**-1**$_{Cl}$	1	11.9	32.2	1.14

[a] The energy are with respect to separated **2**$_{PhCl}$ and **S**$_{2}$. [b] TS type is defined in Figure 14.

The inner-sphere mechanism is favorable if the reaction occurs from ^{5}**2**$_{PhCl}$, leading to an Fe^{III} species through the C–Fe bond formation. The free energy profile for this process is shown in Figure 13 (left). In this case, the activation free energy barrier for Fe–C bond formation is only 8.2 kcal/mol. The resulting Fe^{III} complex, ^{4}**3**$_{PhClR}$, is 2.3 kcal/mol lower than ^{5}**2**$_{PhCl}$ species. Then, the C–C bond formation occurs in the quartet spin state, leading the product (**P**$_{1}$) and Fe^{I} species (^{4}**1**$_{Cl}$) is regenerated (Figure 13). The lowest energy TS (^{4}**TS1-3**$_{PhClR}$**-1**$_{Cl}$) has an activation barrier of 8.8 kcal/mol. TSs of the outer-sphere mechanism show relatively higher energy than ^{4}**TS1-3**$_{PhClR}$**-1**$_{Cl}$ (Figure 14). The quartet spin state TSs were used as the initial guess structures to locate analogs doublet and sextet TSs. It is important to note that sextet TSs involve the outer-sphere mechanism, while the TSs in doublet state proceed through the inner-sphere mechanism. Both sextet and doublet TSs are however relatively higher in energy, and therefore they do not contribute to the overall rate of the C–C bond formation.

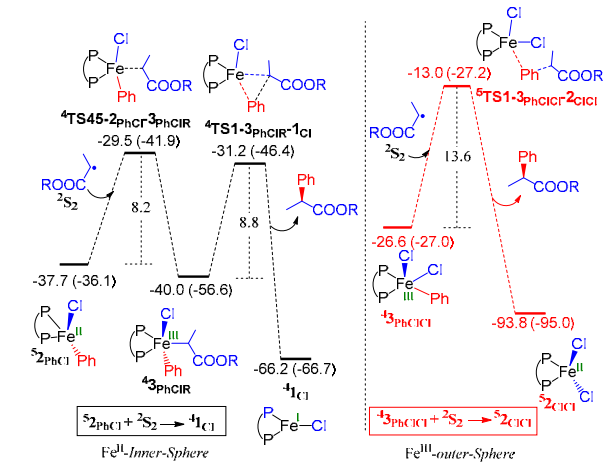

Figure 13. C–C bond formation from Fe^{II} (^{5}**2**$_{PhCl}$) and Fe^{III} (^{5}**3**$_{PhClCl}$) species. The energies [ΔG(ΔH)] are with respect to ^{4}**1**$_{Cl}$.

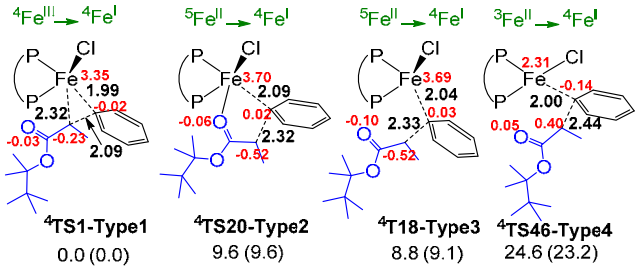

Figure 14. Four types of TSs for C–C coupling reaction between **2**$_{PhCl}$ and **S**$_2$ in quartet spin state. The Type1 TS involves reaction through ^{4}**3**$_{PhClR}$ (inner-sphere). In Type2 TS, carbonyl-oxygen atom of ester interacts with Fe-center. Type3 involves reaction between quintet ^{5}**2**$_{PhCl}$ and ^{2}**S**$_2$ and Type4 involves reaction between triplet ^{3}**2**$_{PhCl}$ and ^{2}**S**$_2$ through outer-sphere mechanism. Distances are given in Å. Mulliken spin densities on atoms involved in reaction coordinate is shown in red. The relative energies [ΔΔG (ΔΔH)] are given in kcal/mol.

The activation barrier for C–C coupling from ^{5}**2**$_{PhPh}$ complex through ^{4}**3**$_{PhPhR}$ is 11.5 kcal/mol. However, it is important to note that the activation barrier for biphenyl formation is 10.5 kcal/mol, and which is 1.0 kcal/mol lower than the activation barrier for the cross-coupling product formation. Therefore, the targeted cross-coupling process would not be formed, while the biphenyl byproduct would be obtained from ^{5}**2**$_{PhPh}$. In order to avoid the biphenyl formation, the concentration of the Grignard reagent must be lower to prevent the formation of ^{5}**2**$_{PhPh}$ (*vide supra*). This can be achieved experimentally by slow addition of the Grignard reagent into the reaction mixture.[5]

Then, the author has studied the C–C coupling through Fe^{III} species, which is discussed in the *in-cage*-mechanism of Nakamura and co-workers (Scheme 2).[5] The two possible Fe^{III} species for the C–C coupling are $\mathbf{3_{PhPhCl}}$ and $\mathbf{3_{PhClCl}}$. The activation barrier for C–C coupling from $^{4}\mathbf{3_{PhClCl}}$ (13.5 kcal/mol) and $^{4}\mathbf{3_{PhPhCl}}$ (20.6 kcal/mol) is relatively higher than that of Fe^{II} species ($\mathbf{2_{PhCl}}$) (Figure 13). Based on the detailed analysis on the TSs for the C–C bond formation, the author concludes that the C–C coupling occurs from $^{5}\mathbf{2_{PhCl}}$ in an inner-sphere fashion through $^{4}\mathbf{3_{PhClR}}$ (Figure 13).

New proposal for the mechanism. After establishing the mechanism in a broad sense, now the author is in the position to sum-up the mechanism of the full catalytic cycle (Figure 15). The first step of the mechanism is the C–Cl activation, and occurs through an atom transfer mechanism with a barrier of 1.5 kcal/mol, leading to $^{5}\mathbf{2_{ClCl}}$ and $^{2}\mathbf{S_2}$. The active species for this step is a Fe^{I} species ($^{4}\mathbf{1_{Cl}}$).[28] Then, the transmetalation converts $^{5}\mathbf{2_{ClCl}}$ into $^{5}\mathbf{2_{PhCl}}$ with a barrier of 9.9 kcal/mol. Subsequent C–C bond formation takes place as an inner-sphere fashion, where coordination of $^{2}\mathbf{S_2}$ to $^{5}\mathbf{2_{PhCl}}$ giving rise to a Fe^{III} species $^{4}\mathbf{3_{PhClR}}$ in the first step. Then, the reductive elimination occurs with a barrier of 8.8 kcal/mol, leading to the formation of the cross-coupling product ($\mathbf{P_1}$) and regenerate $^{4}\mathbf{1_{Cl}}$.

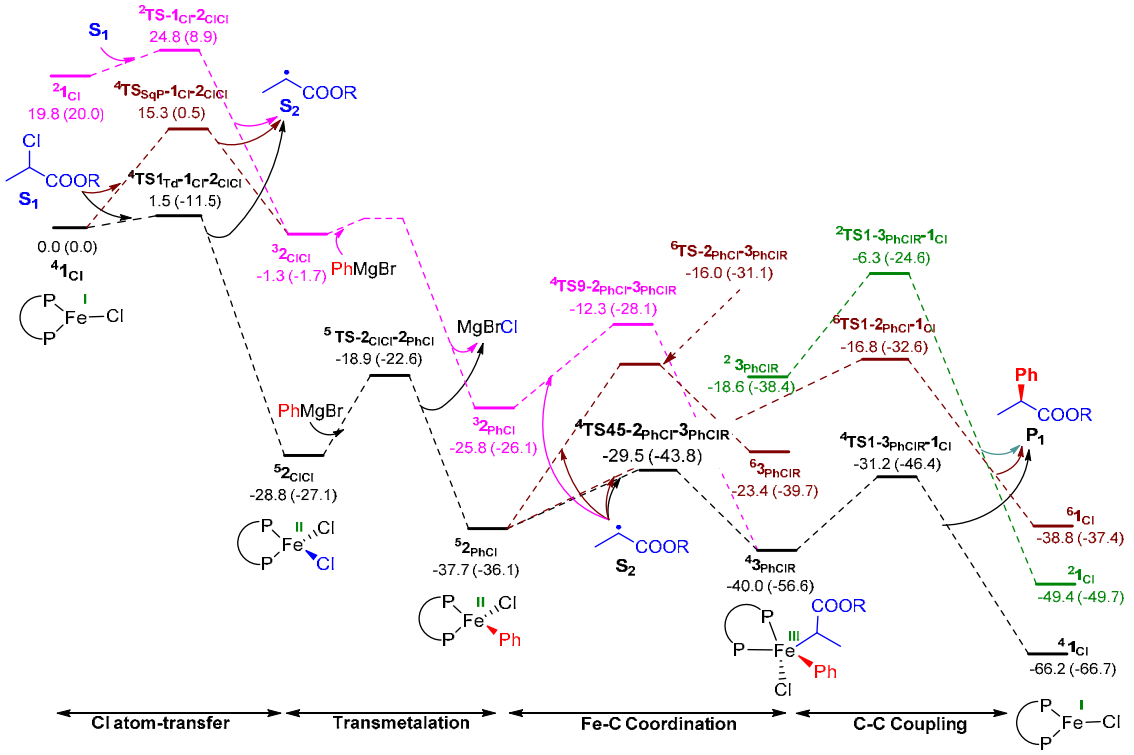

Figure 15. Free energy profile for the favorable reaction pathway ($Fe^{I}/Fe^{II}/Fe^{III}$ pathway). Enthalpies are given in parenthesis.

The mechanistic study suggests that the reaction takes place through the *out-of-cage* mechanism.[5] The C–Cl cleavage by $^{4}\mathbf{1}_{\mathbf{Cl}}$ leads to $\mathbf{S_2}$, which is moved out from the solvent cage of the parent complex, $^{5}\mathbf{2}_{\mathbf{ClCl}}$. Then, radical species $\mathbf{S_2}$ reacts with other available $^{5}\mathbf{2}_{\mathbf{PhCl}}$ species in the reaction mixture.[29] In the meantime, transmetalation of $^{5}\mathbf{2}_{\mathbf{ClCl}}$ to $^{5}\mathbf{2}_{\mathbf{PhCl}}$ can occur. Lower concentration of the Grignard reagent reduces the possibility of $^{5}\mathbf{2}_{\mathbf{PhPh}}$ formation and its reaction with $^{2}\mathbf{S}_{2}$, which in turn reduces the possibility of $\mathbf{3}_{\mathbf{PhPhCl}}$, $\mathbf{3}_{\mathbf{PhPhR}}$, and subsequent byproduct (biphenyl) formation.

It is important to note that the $Fe^{II}/Fe^{III}/Fe^{I}$ (*out-of-cage*) mechanism, shown in Scheme 2, operate before Fe^{I} species formation. This is due to much high energy barrier for the C–Cl activation step from Fe^{II} species ($^{5}\mathbf{2}_{\mathbf{PhCl}}$ and $^{5}\mathbf{2}_{\mathbf{PhPh}}$). Also, the Fe^{II}/Fe^{III} (*in-cage*) mechanism does not operate due to the high energy barrier for C–Cl activation and C–C coupling step.

Origin of the Enantioselectivity. Calculated activation free energy barrier for the C–Cl activation from Fe^{I} species ($^{4}\mathbf{1}_{\mathbf{Cl}}$) is 1.5 kcal/mol, leading to the *S* form of the substrate. While the *R* form of the substrate formation is 2.2 kcal/mol (Table 5). Due to the small activation barrier for C–Cl activation and the small energy difference between two diastereomeric TSs, the kinetic resolution of the substrate is less likely, which is in agreement with experimental observations.

The TS for C-C bond formation is enantioselectivity determining step.[30] As the author has already discussed in the previous sections, the C–C bond formation occurs as the inner-sphere mechanism (through Fe^{III} intermediate, $^{4}\mathbf{3}_{\mathbf{PhClR}}$). Among the different TSs for the C–C bond formation, only Type 1 ^{4}TSs contribute to the reaction (Table 9). $^{4}\mathbf{TS1\text{-}3}_{\mathbf{PhClR}}\mathbf{\text{-}1}_{\mathbf{Cl}}$-*S* contributes to the major *S* form of the product (95%) formation, while $^{4}\mathbf{TS2\text{-}3}_{\mathbf{PhClR}}\mathbf{\text{-}1}_{\mathbf{Cl}}$-*R* gives rise to the minor *R* form of the product (5%) (Figure 16). Contribution from other TSs is too small for the overall rate of the reaction. The computed enantiomeric ratio 95:5 is in good agreement with the experimentally reported ratio (90:10). Enantiomeric ratio calculation from enthalpy also gives similar results (88:12) (Table 9). Similar conclusions can be made with the M06 (96:4), TPSSh (94:6), and B97D (96:4) functionals (Table 10).

Table 9. Low Energy[a] TSs for the C–C Coupling Step and their Probability of Contribution on the Basis of Free Energy to the Reaction Enantioselectivity[b]

^{4}**TS-3$_{PhClR}$-1$_{Cl}$**	ΔΔH	ΔΔG	Product Chirality	Existence Probability (%)	
				H	G
TS1	0.0	0.0	*S*	54.6	94.6
TS2	1.0	1.8	*R*	10.1	4.5
TS3	0.3	3.1	*S*	32.9	0.5
TS4	2.5	3.8	*S*	0.8	0.2
TS5	3.4	3.9	*R*	0.2	0.1
TS6	4.3	4.9	*S*	0	0
TS7	3.5	5.1	*S*	0.1	0
TS8	5.1	5.2	*R*	0	0
TS9	3.3	5.2	*R*	0.2	0
TS10	5.8	5.8	*S*	0	0

[a] TSs lower than 6.0 kcal/mol Gibbs free energy are given here. For all TSs see Table S14 in SI. [b] Enantiomeric ratio: H = 88:12; G = 95:5.

Table 10. Five Low Energy[a] TSs for the C–C Coupling Step and their Probability of Contribution at Different Level of Theory

^{4}**TS-3$_{PhClR}$-1$_{Cl}$**	B3LYP-D3BJ/BS1		B3LYP-D3BJ/BS2		M06/BS2		TPSSh/BS2		B97D/BS2	
	ΔΔH	ΔΔG	ΔΔH	ΔΔG	ΔΔH	ΔΔG	ΔΔH	ΔΔG	ΔΔH	ΔΔG
TS1	0.0	0.0	0.0	0.0	0.0	0.0	0.0	0.0	0.0	0.0
TS2	0.7	1.5	1.0	1.8	1.3	2.1	0.9	1.7	1.2	2.0
TS3	0.3	3.0	0.3	3.1	0.3	3.1	0.8	3.6	0.7	3.5
TS4	2.3	3.7	2.5	3.8	2.6	4.0	2.0	3.3	2.1	3.5
TS5	3.2	3.6	3.4	3.9	2.5	2.9	3.1	3.5	2.8	3.2
%*er* (H) [b]	83.9 : 16.1		89.6 : 10.4[c]		92.8 : 7.2		85.2 : 14.8		90.5 : 9.5	
%*er* (G) [b]	92.5 : 7.5		95.3 : 4.7		96.5 : 3.5		94.4 : 5.6		96.3 : 3.7	

[a] All energies are obtained using PCM (implicit salvation model) with THF as solvent. The energies are obtained using geometry optimized at PCM_{THF}/B3LYP-D3BJ/BS1 level of theory. [b] The enantioselectivity is calculated using five TSs only. First three TSs mainly contribute to enantioselectivity (both on the basis of enthalpy and Gibbs free energy). *er* = enantiomeric ratio. [c] Results are slightly different from Table 1 as the author has taken only five TSs here for *er* calculation.

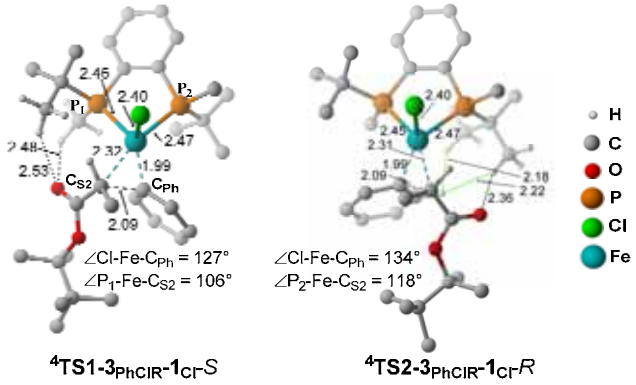

Figure 16. Optimized geometry of lowest energy TSs leading to *S* and *R* forms of the products. H-atoms are omitted for clarity. Distances are given in Å and angle is given in degree.

In the two lowest energy TSs giving rise to the major (**TS1**) and minor products (**TS2**), both methyl and bulky –OR group of the radical species is away from the phosphine and chloride ligand (Figure 16). Both of these TSs have the non-covalent interactions between the carbonyl oxygen and C–H hydrogens of the phosphine ligand. These two features are absent in the relatively high energy TSs (Figure 17). Among low energy diastereomeric TSs, **TS1** has extra C-H…O interaction. The other interactions are similar in two TSs. The weak interactions in these two TSs are further confirmed by analysis of noncovalent interactions (using NCIPlot program) and topological analysis of electron densities (using Multiwfn program) (See Figure 18 and Table 11).[31,32] The TS leading to the minor product have close contact between hydrogen-atoms of phenyl ligand and *tert*-butyl group of phosphine ligand, which may contribute to destabilizing **TS2**. Hence, increasing the bulk of *tert*-butyl group or introducing slightly bulky aromatic ligand (and keeping the C-H…O interactions) may further improve the enantioselectivity.

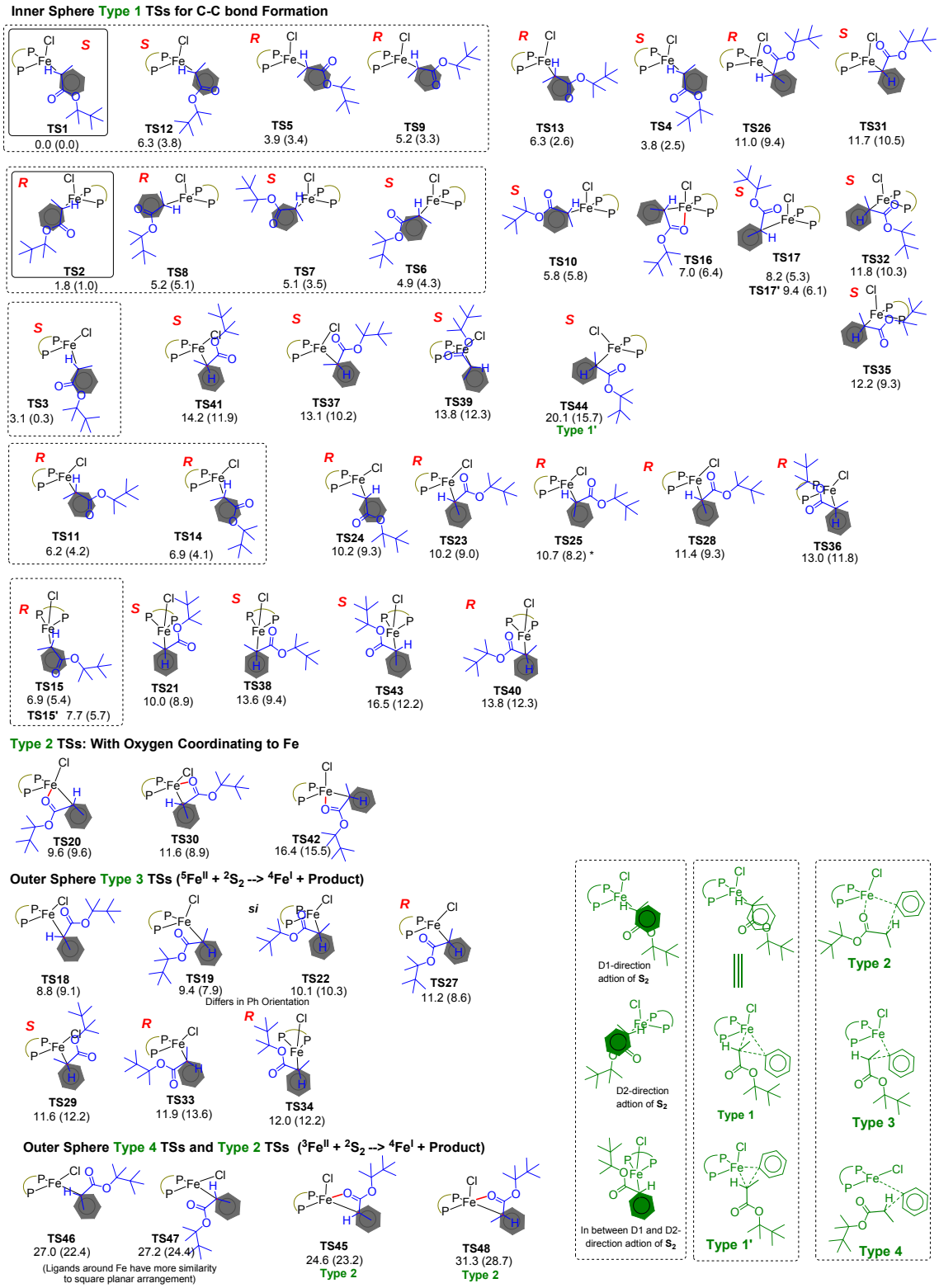

Figure 17. Different conformational TSs optimized for C–C coupling reaction. Structures in green describe TS type. Stereochemistry of corresponding product is given in red for inner-sphere-mechanism (TS Type 1).

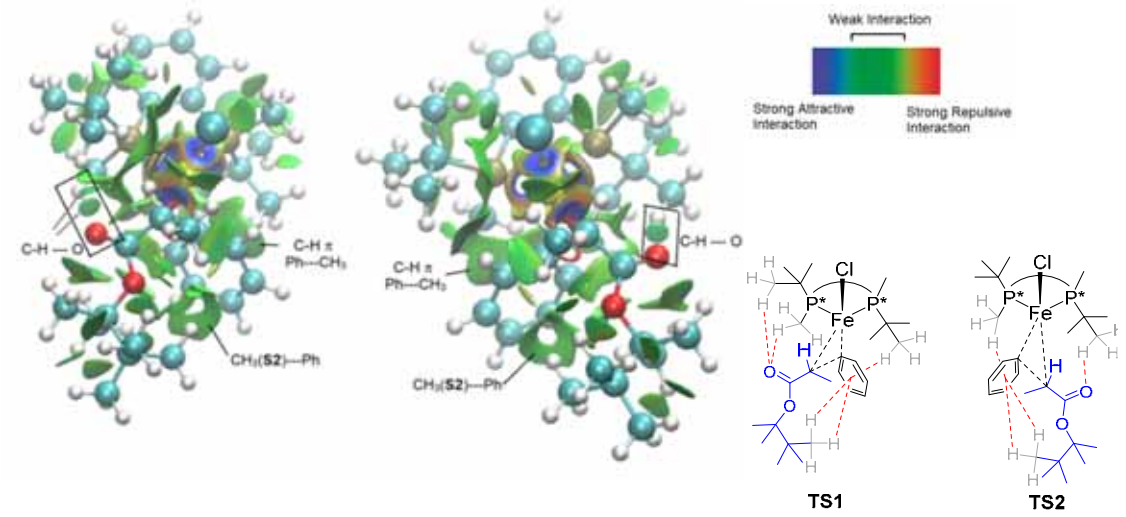

TS1 **TS2**

(a) (b)

Figure 18. (a) NCI plot for two lowest energy TSs (**TS1** and **TS2**) for C–C coupling at PCM_{THF}/B3LYP-D3BJ/BS1 level of theory. (b) The important weak interactions shown in simplified form.

Table 11. Atoms In Molecule (AIM) Analysis[31a] (bond critical point) of Lowest Energy Diastereomeric TSs for C–C Coupling at PCM_{THF}/B3LYP-D3BJ/BS1 Level of Theory for Interaction Between Radical $\mathbf{S_2}$, Phenyl Ligand and Fe(BenzP*)

bcp No.	Bond Critical Point (bcp)	TS1		TS2	
		$\rho \times 10^{-2}$	$\nabla^2\rho$	$\rho \times 10^{-2}$	$\nabla^2\rho$
1	Fe---C(Ph)	-3.512	0.162	-3.574	0.158
2	Fe---C(S2)	-0. 226	0.167	-0.298	0.164
3	C(Ph)---C(S2)	-2.298	0.023	-2.291	0.023
4	O---H-C	0.100	0.033	0.076	0.040
5	O---H-C	0.078	0.031		
6		0.046	0.008		
7	C-H($\mathbf{S_2}$)---Ph	0.094	0.017	0.106	0.020
8		0.049	0.009	0.084	0.016
9		0.139	0.029	0.077	0.014
10	Ph---H-C (Me/tertButyl)	0.129	0.028	0.126	0.021
11				0.070	0.014

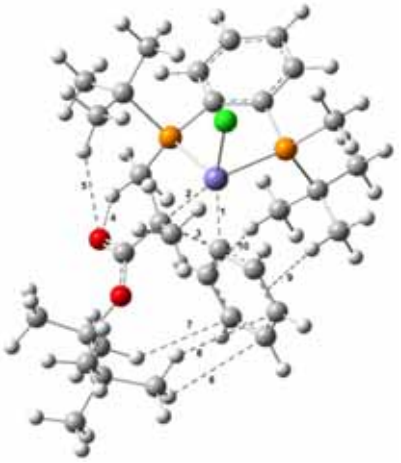

Figure showing bcp No.

Note: Bond paths are shown as dashed lines for clear representation for TS1. $\nabla^2\rho$ = Laplacian of electron density, ρ = electron density.

Energy decomposition analysis (EDA). The author has used EDA to further rationalize the origin of the enantioselectivity.[33] For this purpose, the key TSs leading to major (*S*) and minor (*R*) products, namely ^{4}**TS1-3$_{PhClR}$-1$_{Cl}$** and ^{4}**TS2-3$_{PhClR}$-1$_{Cl}$**, were used. The optimized TS geometries are divided into two fragments **A** and **B**, and their energies (without ZPE) are calculated. Deformation energy (E_{def}) is the difference in energies of separated fragments in TS and optimized fragment [**A**(0) and **B**(0)] energy. The difference in the potential energy of each fragment in two TSs gives ΔE_{def}. The interaction energy is the difference in energies of TS and energies of separated fragments in TS. The difference in interaction energies of two TS gives interaction energy (ΔE_{int}).

According to EDA, deformation energy contributes more to the energy difference between ^{4}**TS1-3$_{PhClR}$-1$_{Cl}$** and ^{4}**TS2-3$_{PhClR}$-1$_{Cl}$**, which is 1.6 kcal/mol (Table 12). Deformation of **A** (1.4 kcal/mol) is higher than **B** (0.2 kcal/mol). Therefore, the author argues that deformation of **A** is the main contributor for the $\Delta\Delta E$, where steric interaction between *tert*-butyl group and phenyl group would lead to greater distortion in ^{4}**TS2-3$_{PhClR}$-1$_{Cl}$**.

Table 12. EDA of Lowest Energy Diastereomeric TSs (TS1-*S* and TS2-*R*). Energies are in kcal/mol.

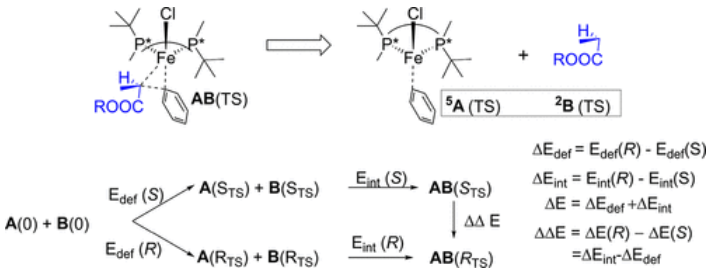

^{4}TS-3$_{PhClR}$-1$_{Cl}$	ΔΔE	ΔE_{def-A}	ΔE_{def-B}	ΔE_{Int}
^{5}A + ^{2}B	1.2	1.6	0.2	-0.6

Conclusions

The mechanism of chiral bisphosphine/iron-catalyzed enantioselective cross-coupling reaction is rationalized using DFT and MC-AFIR methods. Computed mechanism of the full catalytic cycle consists of (a) C–Cl activation, (b) transmetalation, (c) metal-radical coordination and (d) C–C coupling (Figure 19). The calculations suggest that both iron(I) (^{4}**1$_{Ph}$**) and iron(II) (^{5}**2$_{PhPh}$**) complexes can be generated through the reaction between Fe(acac)$_2$, BenzP*, and the Grignard reagent. The iron(I) (^{4}**1$_{Cl}$**) species is most likely involved in the C–Cl activation, whereas iron(II) (^{5}**2$_{PhCl}$** or ^{5}**2$_{PhPh}$**) species (previously proposed active species[12]) would not contribute for the C–Cl activation once the reactive iron(I) species is generated. The C–C bond formation occurs through the reaction between iron(II) (^{5}**2$_{PhCl}$**) and the radical species (^{2}**S$_2$**) through an inner-sphere mechanism, and is the selectivity-determining step of the mechanism. The author has found that slow addition of Grignard reagent in experiments reduces the possibility of byproduct biphenyl formation by suppressing the formation of diaryliron(II) intermediate. The EDA analysis shows that deformations in catalyst mainly contribute to the origin of the enantioselectivity. This study provided important mechanistic insights into iron-catalyzed cross-coupling reactions and is very important for the development of iron-based catalysts for highly stereoselective synthetic organic transformations.

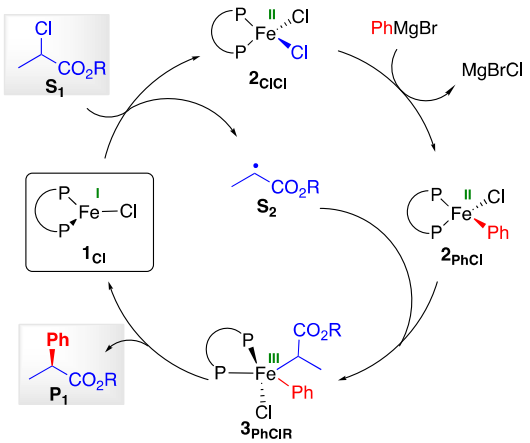

Figure 19. The $Fe^{I}/Fe^{II}/Fe^{III}$ pathway for Fe-catalyzed enantioselective cross-coupling reaction.

ABBREVIATIONS

TS, Transition State; AFIR, Artificial Force Induced Reaction; PES, Potential Energy Surface; Density Functional Theory, DFT; Energy Decomposition Analysis, EDA.

Experimental section

To a mixture of $FeCl_2$ (16.6 mg, 0.13 mmol) and BenzP* (32.7 mg, 0.12 mmol), Et_2O (1.0 ml) and EtOH (1.0 ml) were added, and the mixture was stirred at 50 ºC for 3h. After filtration, the filtrate was condensed and recrystallized from Et_2O to afford the iron complex (32.2 mg, 66% yield). Single crystals suitable for crystallography were obtained by recrystallization from Et_2O and pentane solution at −15 °C. IR (neat) 2958, 2949, 2868, 1576, 1473, 1464, 1448, 1427, 1414, 1395, 1368, 1305, 1293, 1167, 1109, 1057, 1019, 941, 879, 811, 762, 737, 713, 660, 587, 502, 497, 485 cm^{-1}; ^1H NMR (*d*-THF, 392 MHz) δ 7.71, 10.85, 13.02, 102.98; Anal. calcd for $C_{16}H_{28}Cl_2FeP_2$ C, 46.98; H, 6.90, found C, 46.35; H, 6.77.

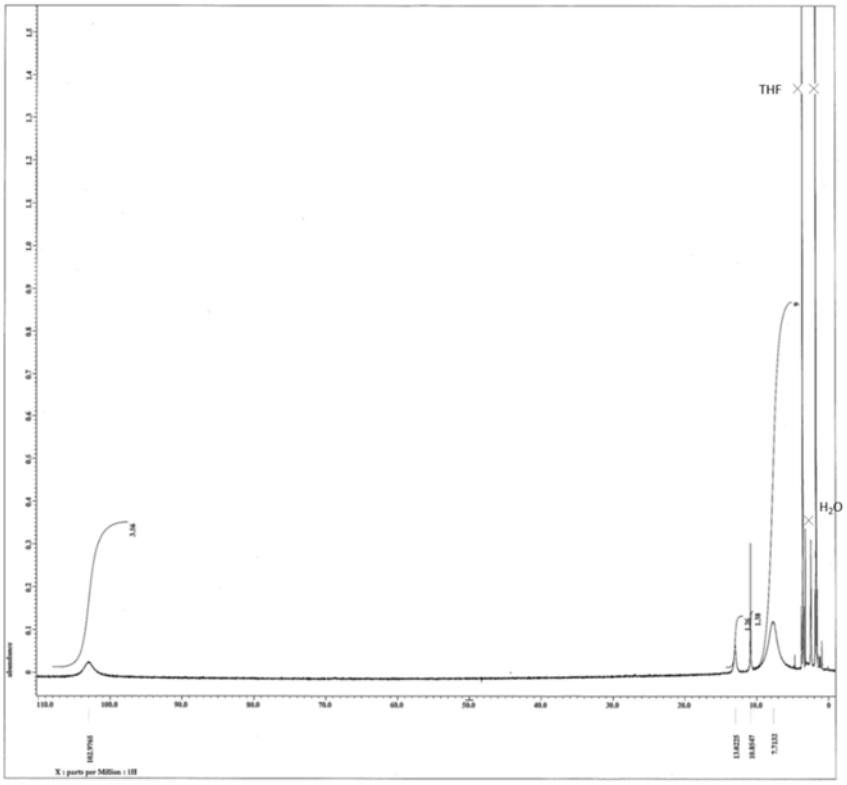

Figure 20a. ^1H NMR spectrum of $FeCl_2$(BenzP*).

X-ray Crystallographic analysis of $FeCl_2$(BenzP*) (2_{ClCl})

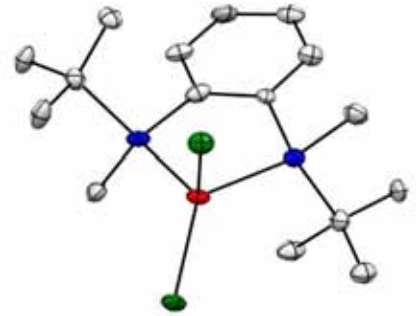

Figure 20b. Molecular structure of $FeCl_2$(BenzP*) with thermal ellipsoids set at 50% probability. Hydrogen atoms were omitted for clarity. C: grey; P: blue; Fe: red; Cl: green.

Table 13. Crystallographic Data for $FeCl_2$(BenzP*).

Molecular Formula	$C_{16}H_{28}Cl_2FeP_2$
Formula Weight	409.07
Crystal Dimensions	0.03 × 0.01 × 0.01 mm^3
Crystal Color	colorless
Crystal System	*monoclinic*
Space Group	*P 21*
a (Å)	10.9038(13)
b (Å)	12.1325(14)
c (Å)	15.4052(19)
α (°)	90
β (°)	90.710(6)
γ (°)	90
Cell Volume ($Å^3$)	2037.8(4)
Z Value	4
F (000)	856
Temperature (K)	*50(2)*
Radiation	synchrotron radiation SPring-8 BL02B1 (λ = 0.7022 Å)
2θmax (°)	27.127
Total Number of Reflections	9289
Number of Unique Reflections	8577
Number of Variables	397
Reflection/Parameter Ratio	23.40
Residuals: R_1 (I>2.00σ(I))	0.0855
Residuals: *R* (All reflections)	0.0936
Residuals: wR_2 (All reflections)	0.2385
Goodness of Fit	1.087
Max Shift/Error	<0.001

Single-crystal X-ray diffraction experiments of $FeCl_2$(BenzP*) were carried out with synchrotron radiation at beamline BL02B1 of SPring-8 (Hyogo, Japan).[34] The crystallographic data are summarized in Table 13. The structures were solved by the direct

methods and refined by the full-matrix least-squares techniques against F^2 with SHELXL-2016.[35] The non-hydrogen atoms were refined anisotropically. Hydrogen atoms were refined using the riding model. The crystallographic data were deposited at the Cambridge Crystallographic Data Centre (CCDC) with the supplementary publication numbers of CCDC-1564354. The data can be obtained free of charge from the CCDC, via www.ccdc.cam.ac.uk/data_request/cif.

References and Notes

[1] (a) Beller, M.; Bolm, C. Transition Metals for Organic Synthesis, Vol. 1; Wiley-VCH: Weinheim, 2004. (b) De Meijere, A.; Diederich, F. Metal-Catalyzed Cross-Coupling Reactions, Vol. 1; Wiley-VCH: Weinheim, 2004. (c) Frisch, A. C.; Beller, M. *Angew. Chem., Int. Ed.* **2005**, *44*, 674–688.

[2] (a) Uozumi, Y. In Comprehensive Chirality; Shibasaki, M., Ed.; Carreira, E. M., Yamamoto, H., Eds.-in-Chief; Elsevier: Oxford, 2012; Vol. 4, p 18. (b) Sarli, V. In Stereoselective Synthesis of Drug and Natural Products; Andrushko, V., Andrushko, N., Eds.; John Wiley and Sons, Inc.: Hoboken, NJ, 2013; Vol. 1, p 369. Enantioconvergent asymmetric couplings of achiral secondary alkyl Grignard and zinc reagents are described in ref 2a. (c) Taylor, B. L. H.; Jarvo, E. R. *Synlett* **2011**, 2761–2765. (d) Swift, E. C.; Jarvo, E. R. *Tetrahedron* **2013**, *69*, 5799–5817. Stereospecific asymmetric cross couplings are reviewed in refs 2c and 2d. (e) Cherney, A. H.; Kadunce, N. T.; Reisman, S. E. *Chem. Rev.* **2015**, *115*, 9587–9652. (f) Chiral Fe-Catalysts: Gopalaiah, K. *Chem. Rev.* **2013**, *113*, 3248–3296.

[3] (a) See: http://www.nobelprize.org/nobel_prizes/chemistry/laureates/2010/. (b) Seechurn, C. C. C. J.; Kitching, M. O.; Colacot, T. J.; Snieckus, V. *Angew. Chem., Int. Ed.* **2012**, *51*, 5062–5085.

[4] Su, B.; Cao, Z.-C., Shi, Z.-J. *Acc. Chem. Res.* **2015**, *48*, 886−896.

[5] Jin, M.; Adak, L.; Nakamura, M. *J. Am. Chem. Soc.* **2015**, *137*, 7128–7134.

[6] (a) Kharasch, M. S.; Fields, E. K. *J. Am. Chem. Soc.* **1941**, *63*, 2316–2320. (b) Jana, R.; Pathak, T. P.; Sigman, M. S. *Chem. Rev.* **2011**, *111*, 1417–1492.

[7] Bauer, I.; Knölker, H.-J. *Chem. Rev.* **2015**, *115*, 3170–3387.

[8] Przyojski, J. A.; Veggeberg, K. P.; Arman, H. D.; Tonzetich, Z. J. *ACS Catal.* **2015**, *5*, 5938–5946.

[9] (a) Bedford, R. B. *Acc. Chem. Res.* **2015**, *48*, 1485–1493. (b) Cassani, C.; Bergonzini, G.; Wallentin, C.-J. *ACS Catal.* **2016**, *6*, 1640–1648.

[10] (a) Bedford, R. B.; Brenner, P. B.; Carter, E.; Cogswell, P. M.; Haddow, M. F.; Harvey, J. N.; Murphy, D. M.; Nunn, J.; Woodall, C. H. *Angew. Chem., Int. Ed.* **2014**, *53*, 1804–1808. (b) Ren, Q.; Guan, S.; Jiang, F.; Fang, J. *J. Phys. Chem. A* **2013**, *117*, 756–764.

[11] (a) Lefèvre, G.; Jutand, A. *Chem. Eur. J.* **2014**, *20*, 4796–4805. (b) Bekhradnia, A.; Norrby, P.-O. *Dalton Trans.* **2015**, *44*, 3959–3962. (c) Hedström, A.; Lindstedt, E.; Norrby, P.-O. *J. Organomet. Chem.* 2013, *748*, 51–55.

[12] (Fe(+II) ferrate) (a) Sun, C.-L.; Krause, H.; Fürstner, A. *Adv. Synth. Catal.* **2014**, *356*, 1281–1291. (b) Bedford, R. B.; Brenner, P. B.; Carter, E.; Cogswell, P. M.; Haddow, M. F.; Harvey, J. N.; Murphy, D. M.; Nunn, J.; Woodall, C. H. *Angew. Chem., Int. Ed.* **2014**, *53*, 1804–1808. (c) Bauer, G.; Wodrich, M. D.; Scopelliti, R.; Hu, X. *Organometallics* **2015**, *34*, 289–298. (d) Hatakeyama, T.; Hashimoto, T.; Kondo, Y.; Fujiwara, Y.; Seike, H.; Takaya, H.; Tamad, Y.; Ono, T.; Nakamura, M. *J. Am. Chem. Soc.* **2010**, *132*, 10674–10676. (e) Hatakeyama T.; Fujiwara Y.; Okada Y.; Itoh T.; Hashimoto T.; Kawamura S.; Ogata K.; Takaya H.; Nakamura M. *Chem. Lett.* **2011**, *40*, 1030–1032. (f) Daifuku, S. L.; Kneebone, J. L.; Snyder, B. E. R.; Neidig, M. L. *J. Am. Chem. Soc.* **2015**, *137*, 11432–11435. (g) Takaya, H.; Nakajima, S.; Nakagawa, N.; Isozaki, K.; Iwamoto, T.; Imayoshi, R.; Gower, N.; Adak, L.; Hatakeyama, T.; Honma, T.; Takagi, M.; Sunada, Y.; Nagashima, H.; Hashizume, D.; Takahashi, O.; Nakamura, M. *Bull. Chem. Soc. Jpn.* **2015**, *88*, 410–418.

[13] For the mechanism of the formation of Fe^{I} species in cross-coupling reactions, see: (a) Adams, C. J.; Bedford, R. B.; Carter, E.; Gower, N. J.; Haddow, M. F.; Harvey, J. N.; Huwe, M.; Cartes, M. A.; Mansell, S. M.; Mendoza, C.; Murphy, D. M.; Neeve, E. C.; Nunn, J. *J. Am. Chem. Soc.* **2012**, *134*, 10333–10336. (b) Bedford, R. B.; Brenner, P. B.; Carter, E.; Clifton, J.; Cogswell, P. M.; Gower, N. J.; Haddow, M. F.; Harvey, J. N.; Kehl, J. A.; Murphy, D. M.; Neeve, E. C.; Neidig, M. L.; Nunn, J.; Snyder, B. E. R.; Taylor, J. *Organometallics* **2014**, *33*, 5767– 5780 and references cited therein. (c) Guisán-Ceinos, M.; Tato, F.; Buñuel, E.; Calleb, P.; Cárdenas, D. J. *Chem. Sci.* **2013**, *4*, 1098–1104. (d) Bedford R. B.; Carter E.; Cogswell P. M.; Gower N. J.; Haddow M. F.; Harvey J. N.; Murphy D. M.; Neeve E. C.; Nunn J. *Angew. Chem., Int. Ed.* **2013**, *52*, 1285–1288.

[14] (a) Hawrelak, E. J.; Bernskoetter, W. H.; Lobkovsky, E.; Yee, G. T.; Bill, E.; Chirik, P. J. *Inorg. Chem.* **2005**, *44*, 3103–3111. (b) Holland, P. L. *Acc. Chem. Res.* **2015**, *48*, 1696–1702. (c) Sun, Y.; Tang, H.; Chen, K.; Hu, L.; Yao, J.; Shaik, S.; Chen, H. *J. Am. Chem. Soc.* **2016**, *138*, 3715–3730. (d) Shaik, S.; Hirao, H.; Kumar, D. *Acc. Chem. Res.* **2007**, *40* 532–542. (e) Polia, R.; Harvey, J. N. *Chem. Soc. Rev.* **2003**, *32*, 1–8.

[15] Imamoto, T. *Chem. Rec.* **2016**, *6*, 2655–2669.

[16] (a) Sperger, T.; Sanhueza, I. A.; Kalvet, I.; Schoenebeck, F. *Chem. Rev.* **2015**, *115*, 9532–9586. (b) Katayev, D.; Jia, Y.-X.; Sharma, A. K.; Banerjee, D.; Besnard, C.; Sunoj, R. B.; Kündig, E. P. *Chem. Eur. J.* **2013**, *19*, 11916–11927. (c) Sharma, A. K.; Roy, D.; Sunoj, R. B. *Dalton Trans.* **2014**, *43*, 10183–10201.
[17] (a) Maeda, S.; Morokuma, K. *J. Chem. Phys.* **2010**, *132*, 241102. (b) Maeda, S.; Morokuma, K. *J. Chem. Theory Comput.* **2011**, *7*, 2335–2345. (c) Maeda, S.; Morokuma, K. *J. Chem. Theory Comput.* **2012**, *8*, 380–385.
[18] (a) Sameera, W. M. C.; Maeda, S.; Morokuma, K. *Acc. Chem. Res.* **2016**, *49*, 763–773. (b) Sameera, W. M. C.; Sharma, A. K.; Maeda, S.; Morokuma, K. *Chem. Rec.* **2016**, *16*, 2349–2363.
[19] Gaussian 09, Revision A.02: Frisch, M. J.; Trucks, G. W.; Schlegel, H. B.; Scuseria, G. E.; Robb, M. A.;Cheeseman, J. R.; Scalmani, G.; Barone, V.; Mennucci, B.; Petersson, G. A.; Nakatsuji, H.; Caricato, M.; Li, X.; Hratchian, H. P.; Izmaylov, A. F.; Bloino, J.; Zheng, G.; Sonnenberg, J. L.; Hada, M.; Ehara, M.; Toyota, K.; Fukuda, R.; Hasegawa, J.; Ishida, M.; Nakajima, T.; Honda, Y.; Kitao, O.; Nakai, H.; Vreven, T.; Montgomery, J. A., Jr.; Peralta, J. E.; Ogliaro, F.; Bearpark, M.; Heyd, J. J.; Brothers, E.; Kudin, K. N.; Staroverov, V. N.; Kobayashi, R.; Normand, J.; Raghavachari, K.; Rendell, A.; Burant, J. C.; Iyengar, S. S.; Tomasi, J.; Cossi, M.; Rega, N.; Millam, N. J.; Klene, M.; Knox, J. E.; Cross, J. B.; Bakken, V.; Adamo, C.; Jaramillo, J.; Gomperts, R.; Stratmann, R. E.; Yazyev, O.; Austin, A. J.; Cammi, R.; Pomelli, C.; Ochterski, J. W.; Martin, R. L.; Morokuma, K.; Zakrzewski, V. G.; Voth, G. A.; Salvador, P.; Dannenberg, J. J.; Dapprich, S.; Daniels, A. D.; Farkas, Ö.; Foresman, J. B.; Ortiz, J. V.; Cioslowski, J.; Fox, D. J. Gaussian, Inc., Wallingford, CT, 2009.
[20] (a) Lee, C.; Yang, W.; Parr, R. G. *Phys. Rev. B* **1988**, *37*, 785–789. (b) Becke, A. D. *J. Chem. Phys.* **1993**, *98*, 5648–5652. (c) Grimme, S.; Ehrlich, S.; Goerigk, L. *J. Comp. Chem.* **2011**, *32*, 1456–1465.
[21] (a) Fuentealba, P.; Preuss, H.; Stoll, H.; Vonszentpaly, L. *Chem. Phys. Lett.* **1982**, *89*, 418–422. (b) Dunning, T. H., Jr.; Hay, P. J. Modern Theoretical Chemistry; Plenum: New York, 1977; Vol. 3, pp 1−28.
[22] (a) Cossi, M.; Barone, V.; Cammi, R.; Tomasi, *J. Chem. Phys. Lett.* **1996**, *255*, 327–335. (b) Cances, E.; Mennucci, B.; Tomasi, J. *J. Chem. Phys.* **1997**, *107*, 3032. (c) Scalmani, G.; Frisch, M. J. *J. Chem. Phys.* **2010**, *132*, 114110.
[23] (a) Gonzalez, C.; Schlegel, H. B. *J. Chem. Phys.* **1989**, *90*, 2154. (b) Gonzalez, C.; Schlegel, H. B. *J. Phys. Chem.* **1990**, *94*, 5523.
[24] (a) Maeda, S.; Ohno, K.; Morokuma, K. *Phys. Chem. Chem. Phys.* **2013**, *15*, 3683–3701. (b) Maeda, S.; Taketsugu, T.; Ohno, K.; Morokuma, K. *J. Am. Chem. Soc.* **2015**, *137*, 3433–3445. (c) Ohno, K.; Maeda, S. *Chem. Phys. Lett.* **2004**, *384*, 277–282. (d) Ohno, K.; Maeda, S. *J. Phys. Chem. A* **2006**, *110*, 8933–8941.
[25] (a) Chung, L. W.; Sameera, W. M. C.; Ramozzi, R.; Page, A. J.; Hatanaka, M.; Petrova, G. P.; Harris, T. V.; Li, X.; Ke, Z.; Liu, F.; Li, H.-B.; Ding, L.; Morokuma, K. *Chem. Rev.* **2015**, *115*, 5678–5796. (b) Chung, L. W.; Hirao, H.; Li, X.; Morokuma, K. *Wiley Interdiscip. Rev. Comput. Mol. Sci.* 2012, 2, 327–350.
[26] CYLview, 1.0b; Legault, C. Y., Université de Sherbrooke, 2009 (http://www.cylview.org).
[27] For stepwise reduction of $Fe(acac)_3$ with phenyl Grignard reagents in the absence of phosphine ligands see, ref. 11a and Schoch, R.; Desens, W.; Werner, T. Bauer, M. *Chem. Eur. J.* **2013,** *19*, 15816–15821.
[28] The author suspects that Fe^{I}(BenzP*)Ph ($^{4}\mathbf{1}_{\mathbf{Ph}}$) acts as the active species in the first catalytic conversion of the substrate to the product, which would lead to Fe^{I}(BenzP*)Cl ($^{4}\mathbf{1}_{\mathbf{Cl}}$) species (Scheme 3). Afterwards, $^{4}\mathbf{1}_{\mathbf{Cl}}$ may be the active species for the reaction.
[29] In the study, the author has focused on the product formation, but the comproportionation cannot be ruled out, which will convert the small concentration of Fe^{I} and Fe^{III} to Fe^{II} species. Hence, Fe^{II} species may be available for the reaction with radical species $\mathbf{S_2}$.
[30] The author has explored the TSs for radical addition step and ensuing complex $^{4}\mathbf{3}_{\mathbf{PhClR}}$ thoroughly (>50 conformers each, Tables 6 and 7). Importantly, the lowest energy diastereomeric $^{4}\mathbf{3}_{\mathbf{PhClR}}$ intermediates (**I1** and **I2** in Table 7) leads to lowest energy TS for C-C bond formation, which contribute mainly to enantioselectivity. However, the TSs of C-Fe bond formation leading to these lowest energy diastereomeric $^{4}\mathbf{3}_{\mathbf{PhClR}}$ intermediates (**I1** and **I2** in Table 7) could not be located, and the relaxed PES along C-Fe bond from these intermediates shows TS region is flat, and the process is barrierless. Therefore, the free energy barrier seems to be mainly due to entropy. Further, the lowest energy diastereomeric TSs obtained for C–Fe bond formation are same in energy. Hence, this step is unlikely to be stereoselectivity determining.
[31] (a) Lu T., Chen F. *J. Comp. Chem.* **2012**, *33*, 580–592. (b) Bader, R. F. W. *Chem. Rev.* **1991**, *91*, 893–928.
[32] (a) Johnson, E. R.; Keinan, S.; Mori-Sanchez, P.; Contreras-Garcia, J.; Cohen, A. J.; Yang, W. *J. Am.*

Chem. Soc. **2010**, *132*, 6498–6506. (b) Contreras-Garcia, J.; Johnson, E. R.; Keinan, S.; Chaudret, R.; Piquemal, J-P.; Beratan, D. N.; Yang W. *J. Chem. Theory Comput.* **2011**, *7*, 625–632.

[33] (a) Morokuma, K. *J. Chem. Phys.* **1971**, *55*, 1236. (b) Kitaura, K.; Morokuma, K. *Int. J. Quantum Chem.* **1976**, *10*, 325–340. (c) van Zeist, W. J.; Bickelhaupt, F. M. *Org. Biomol. Chem.* **2010**, *8*, 3118–3127. (d) Legault, C. Y.; Garcia, Y.; Merlic, C. A.; Houk, K. N. *J. Am. Chem. Soc.* **2007**, *129*, 12664–12665.

[34] K. Sugimoto, H. Ohsumi, S. Aoyagi, E. Nishibori, C. Moriyoshi, Y. Kuroiwa, H. Sawa, M. Takata, *AIP Conf. Proc*. **2010**, *1234,* 887–890.

[35] Sheldrick, G. M. *Acta Cryst*. **2015**, *C71,* 3–8.

CONCLUSION

Providing enantiopure medicines is a very important mission of the pharmaceutical companies in order to avoid potential adverse effects caused by the other enantiomer of the medicinal compound. The catalytic enantioselective carbon-carbon bond formation reactions are one of the most powerful methods to provide the enantiopure medicines because simultaneous constructions of molecular framework and chirality are possible. Due to the less toxic and economical nature, iron seems an ideal catalyst for those reactions, but few enantioselective reactions are reported to date.

In this thesis, two types of iron-catalyzed carbon-carbon bond formation reactions, which enables to efficiently prepare chiral bioactive compounds, are described. The enantioselective carbometalation reactions are described in Chapters 1 and 2, Part 1. The iron-catalyzed enantioselective carbometalation reactions of azabicycloalkenes with arylzinc reagents by using chiraphos as a chiral ligand are described in Chapter 1. Epibatidine derivatives are synthesized by using these iron-catalyzed carbometalation reactions, which make it easy to synthesize epibatidine derivatives. The synthesis of C_1 and C_2 symmetric chiraphos derivatives, some of which show higher enantioselectivity than the original chiraphos, are described in Chapter 2.

The enantioselective cross-coupling reactions and related research works are described in Chapters 3–7, Part 2. In Chapter 3, the iron-catalyzed cross-coupling reactions of non-activated chloroalkanes with aryl Grignard reagents are described. Poly-arylated alkanes can be easily prepared from polychloroalkanes by this method, which cannot be achieved by other conditions due to the formation of byproducts. In Chapter 4, the iron-catalyzed cross-coupling reactions of α-bromoacetic acid derivatives with aryl Grignard reagents to give α-arylacetic acid derivatives, which are found in some medicinal compounds (e.g. lumiracoxib and indomethacin), are reported. In Chapter 5, the iron-catalyzed enantioselective cross-coupling reactions of α-chloroesters with aryl Grignard reagents using BenzP* as a chiral ligand are described. The synthesis of dexibuprofen, an enantiopure anti-inflammatory drug, is achieved by this method. The Suzuki-Miyaura variant of the enantioselective cross-coupling reactions is reported in Chapter 6. In sharp contrast to the cross-coupling reactions with aryl Grignard reagents, BenzP* does not induce the enantioselectivity; QuinoxP* is the best ligand for the Suzuki-Miyaura coupling. In Chapter 7, the reaction mechanism of enantioselective cross-coupling reactions is described by the help of DFT and AFIR study, and revealed

that Fe(I), Fe(II), and Fe(III) species are involved in the cross-coupling reactions.

The present thesis describes the development of the iron-catalyzed enantioselective reactions, which are successfully applied to the synthesis of chiral bioactive compounds and their derivatives. These achievements will encourage further investigation of iron-catalyzed enantioselective reactions to synthesize bioactive compounds, and a variety of optically active medicinal compounds will be able to be synthesized by the less toxic iron catalyst, which is of significant importance from the patient protection perspective.

LIST OF PUBLICATION

Thesis title: Development of Iron-Catalyzed Enantioselective Carbon–Carbon Bond Forming Reactions for Efficient Access to Bioactive Compounds and Their Derivatives

PART 1: Iron-Catalyzed Enantioselective Carbometalation Reaction: Access to the Epibatidine Derivatives

Chapter 1

"Iron-catalyzed Enantioselective Carbometalation of Azabicycloalkenes"

Adak, L.; Jin, M.; Saito, S.; Kawabata, T.; Itoh, T.; Ito, S.; Sharma, A. K.; Gower, N. J.; Cogswell, P.; Geldsetzer, J.; Takaya, H.; Isozaki, K.; Nakamura, M. *Chem. Commun.* **2021**, *57*, 6975–6978.

Chapter 2

"Synthesis of Novel C_1 and C_2 Symmetric Chiraphos Derivatives and Their Application in Iron Catalyzed Enantioselective Carbometalation"

Jin, M.; Nakamura, M. *Chem. Lett.* **2013**, *42*, 1035–1037.

PART 2: Iron-Catalyzed Enantioselective Cross-Coupling Reaction: Access to the NSAIDs

Chapter 3

"Cross-Coupling of Non-activated Chloroalkanes with Aryl Grignard Reagents in the Presence of Iron/*N*-Heterocyclic Carbene Catalysts"

Ghorai, S. K.; Jin, M.; Hatakeyama, T.; Nakamura, M. *Org. Lett.* **2012**, *14*, 1066–1069.

Chapter 4

"Iron-catalyzed Chemoselective Cross-Coupling of α-Bromocarboxylic Acid Derivatives with Aryl Grignard Reagents"

Jin, M.; Nakamura, M. *Chem. Lett.* **2011**, *40*, 1012–1014.

Chapter 5

"Iron-Catalyzed Enantioselective Cross-Coupling Reactions of α-Chloroesters with Aryl

Grignard Reagents"
Jin, M.; Adak, L.; Nakamura, M. *J. Am. Chem. Soc.* **2015**, *137*, 7128–7134.

Chapter 6

"Iron-Catalyzed Enantioselective Suzuki-Miyaura Coupling of Racemic Alkyl Bromides"
Iwamoto, T.; Okuzono, C.; Jin, M.; Nakamura, M. *Chem. Commun.* **2019,** *55*, 1128–1131.

Chapter 7

"DFT and AFIR Study on the Mechanism and the Origin of Enantioselectivity in Iron-Catalyzed Cross-Coupling Reactions"
Sharma, A. K.; Sameera, W. M. C.; Adak, L.; Jin, M.; Okuzono, C.; Iwamoto, T.; Kato, M.; Nakamura, M.; Morokuma, K. *J. Am. Chem. Soc.* **2017,** *139*, 16117–16125.

The following publications are not included in this thesis.

[Original papers]

1. Ura, Y.; Jin, M.; Nakajima, K.; Takahashi, T. *Chem. Lett.* **2001**, *30*, 356–357.
2. Iio, Y.; Yamaoka, M.; Jin, M.; Nakamura, Y.; Nishi, T. *Tetrahedron: Asymmetry* **2011**, *22*, 323–328.
3. Hatakeyama, T.; Imayoshi, R.; Yoshimoto, Y.; Ghorai, S. K.; Jin, M.; Takaya, H.; Norisuye, K.; Sohrin, Y.; Nakamura, M. *J. Am. Chem. Soc*. **2012**, *134*, 20262–20265.

[Patent]

1. Onoda, T.; Nakamura, Y.; Yamaoka, M.; Takeda, T.; Sato, N.; Jin, M. Optically active 4,4-di-substituted oxazolidine derivative and method for producing same. U. S. patent 20080108828, May 8, 2008.
2. Ibrahim, P. N.; Jin, M.; Matsuura, S. Synthesis of a compound that modulates kinases. U. S. patent 20160326169, November 10, 2016.

[Review]

1. Nakamura, M.; Iwamoto, T.; Jin. M.; Okuzono, T. *The Chemical Times* **2021**, *259*, 13–19.

ACKNOWLEDGMENT

First and foremost, I would like to express my sincere gratitude to my advisor Prof. Masaharu Nakamura for helpful suggestions, fruitful discussions, and constant encouragement. I would like to thank Mr. Akihiko Miyadera for providing me the opportunity to work on the iron catalysis in organic chemistry in collaboration with the International Research Center for Elements Science, Institute for Chemical Research, Kyoto University.

I am grateful to Prof. Hikaru Takaya, Prof. Takuji Hatakeyama, Prof. Katsuhiro Isozaki, Prof. Takahiro Iwamoto, and all the staff in the Nakamura group for their kind guidance and helpful suggestions. My sincere appreciation goes to Prof. Keiji Morokuma for his kind guidance, suggestions, and discussions on the computational chemistry. I also acknowledge the contribution of Prof. Laksmikanta Adak, Mr. Shota Saito, Mr. Tatsuya Kawabata, Mr. Takuma Itoh, Prof. Shingo Ito, Dr. Nicholas J. Gower, Dr. Jan Geldsetzer, Dr. Paul Cogswell, Dr. Akhilesh K. Sharma, Dr. Sujit K. Ghorai, Ms. Chiemi Okuzono, Dr. W. M. C. Sameera, and Prof. Masako Kato for their excellent experiments and deep discussions. I appreciate all the members of the Nakamura group for their kind support. I also appreciate all the members of the Process Technology Research Laboratories, Daiichi Sankyo, Co., Ltd. for their support and discussions.

My sincere thanks go to Prof. Kouichi Ohe and Prof. Yasujiro Murata for careful reviewing this thesis and suggestive comments.

Last but not least, I would like to appreciate my family: This doctoral work cannot be completed without help and understanding of my wife. The time with my son and daughters always makes me relaxed, which gives me the vitality to work on this study.

Masayoshi Jin